DEVELOPMENT OF BIODEGRADABLE PACKAGING FOR FOOD IRRADIATION APPLICATION

By

CHATURBHUJ KUMAR SAURABH

(LIFE01201104005)

Bhabha Atomic Research Centre, Mumbai

A thesis submitted to the
Board of Studies in Life Science Discipline
In partial fulfilment of requirements
For the degree of

DOCTOR OF PHILOSOPHY

of

HOMI BHABHA NATIONAL INSTITUTE

August, 2015

Homi Bhabha National Institute

Recommendations of the Viva Voce Committee

As members of the Viva Voce Committee, we certify that we have read the dissertation prepared by Mr. Chaturbhuj Kumar Saurabh entitled "Development of biodegradable packaging for food irradiation application" and recommend that it may be accepted as fulfilling the thesis requirement for the award of Degree of Doctor of Philosophy.

Dr. LalitVarshney	**Chairman**	
Dr. Prasad S. Variyar	**Convener** (Guide)	
Dr. V. Sivakumar	**Examiner**	
Dr. P. A. Hassan	**Member**	
Dr. R.N. Jagtap	**Member**	

Final approval and acceptance of this thesis is contingent upon the candidate's submission of the final copies of the thesis to HBNI.

I/We hereby certify that I/we have read this thesis prepared under my/our direction and recommend that it may be accepted as fulfilling the thesis requirement.

Date: 7- AUGUST- 2015

Place: BARC, MUMBAI

Prasad. S. V

Dr. Prasad S. Variyar (Guide)

STATEMENT BY AUTHOR

This dissertation has been submitted in partial fulfilment of requirements for an advanced degree at Homi Bhabha National Institute (HBNI) and is deposited in the Library to be made available to borrowers under rules of the HBNI.

Brief quotations from this dissertation are allowable without special permission, provided that accurate acknowledgement of source is made. Requests for permission for extended quotation from or reproduction of this manuscript in whole or in part may be granted by the Competent Authority of HBNI when in his or her judgment the proposed use of the material is in the interests of scholarship. In all other instances, however, permission must be obtained from the author.

Chaturbhuj Kumar Saurabh

DECLARATION

I, hereby declare that the investigation presented in the thesis has been carried out by me. The work is original and has not been submitted earlier as a whole or in part for a degree / diploma at this or any other Institution / University.

Chaturbhuj Kumar Saurabh

Dedicated to Lord Vasudeva

ACKNOWLEDGEMENT

I am using this opportunity to express my deepest gratitude to my guide Dr. Prasad S Variyar for his valuable guidance, constructive criticism and generous advice throughout the project work. Without his supervision and constant support this project would not have been possible. I would like to express my gratitude to all the members of my doctoral committee namely Dr. A. K. Sharma, Dr. Lalit Varshney, Dr. P. A. Hassan and Dr. R.N. Jagtap for their suggestions and critical evaluation.

It is my pleasure to express sincere thanks to Mr. Sumit Gupta for giving valuable help and suggestions at all stages of work. I am genuinely grateful to all the members of FFACS; Dr. Suchandra Chatterjee, Jyoti Tripathi, Jasraj Vaishnav, Vanshika Adiani, Vivekanand Kumar, Snehal Yeole and Prashant Mishra for their invaluable help and sincere support. I am also sincerely thankful to Dr. Sahayog Jamdar, Dr. Sachin Hajare, Dr. S. Mazumder, Dr. Jitendra Bahadur and Shyam Sunder for helping in carrying out various experiments done in this thesis.

Heartiest thanks are due to Aparajita for her continuous support throughout the project. Special thanks to my friends Bajarangi, Rishabh, Anuj, Rupali, Shatabhisha, Yogita, Umesh and Mahesh for their love and invaluable help.

I am totally indebted to my family for everything. No words of acknowledgment will be sufficient for them.

Chaturbhuj Kumar Saurabh

Contents	Page no.
SYNOPSIS	x-xix
LIST OF FIGURES	xx-xxv
LIST OF TABLES	xxvi-xxix

Homi Bhabha National Institute

Ph. D. PROGRAMME

1. **Name of the Student:** Mr. Chaturbhuj K. Saurabh
2. **Name of the Constituent Institution:** Homi Bhabha National Institute
3. **Enrolment No. :** LIFE 01201104005
4. **Title of the Thesis:** "Development of biodegradable packaging for food irradiation application"

SYNOPSIS

In the past twenty years, the production and use of plastics has increased enormously to about 200 million tons per year worldwide. Packaging constitutes the largest market for plastics, amounting to over 12 million tons per year. Increasing demand for synthetic packaging materials has put tremendous pressure on the environment because of their poor biodegradability and non-renewability. This has led to a search for packaging materials that are biodegradable as well as recyclable. One of the alternatives is the development of packaging material from biopolymers (i.e. protein, polysaccharide and lipid) that are biodegradable, non-toxic and derived from completely renewable resources. Among the biopolymers, polysaccharides are most widely used for preparation of packaging films. Widely studied polysaccharides for edible or biodegradable films are: starch, chitosan, carrageenan, and galactomannans. Amongst these, galactomannan is commonly used as edible coating in packaging industry as it forms very thick aqueous solution at low concentration, is an excellent emulsifier and is non-toxic. Guar gum (GG) is a type of galactomannan, derived from endosperm of an annual legume

plant *Cyamopsis tetragonoloba*. India accounts for 80 percent of world production of GG. It is a hetropolysaccharide of a mannose (i.e. (1-4)-linked β-D-mannopyranose) backbone with galactose side groups ((1-6)-linked α-D-galactopyranose). It is mainly used in paper, food and pharmaceutical industries.

Major limitations in the use of biopolymers as packaging materials are their relatively poor mechanical and barrier properties such as tensile strength, Young's Modulus and water vapor transmission rate as compared to their non-biodegradable counterparts. This has resulted in a greater focus on improving the properties of biopolymer based films to match the commercially available packaging material. Various chemical and physical methods have been used for improving biofilm properties. Among the chemical methods, modification of guar galactomannan with benzamide for preparation of water resistant films has been recently reported (1). Mikkonen et al. (2007) used enzymatic depolymerization for improving mechanical properties of GG film (2). Among the physical methods, gamma irradiation has been widely used for the improvement of mechanical properties of pectin, starch and calcium caseinate edible films by radiation induced cross-linking between polymeric chains. Use of gamma irradiation for GG depolymerization has been previously reported (3). There are several advantages associated with gamma irradiation such as convenience, eco friendly nature of the process and short processing time.

Gamma irradiation could possibly change conformations of polymers in solution. Several investigations have shown that the conformation and morphology of polymer chains affect the physical properties of the polymer. Polymer chain conformation and chain correlation can be estimated by small angle X-ray scattering (SAXS). SAXS arises from the fluctuations of electron density in a mesoscopic length scale (1–100 nm) in a specimen and hence scattering profile contains the information about the size/size distribution and shape of the inhomogeneities.

Another approach for improving the properties of biopolymer based film is to incorporate various additives into it. Each additive individually or along with other additives affects one or more characteristic of the films. Nanoclays are one of the frequently used additives to make nanohybrid

composite films by mixing inorganic nanosize clay with organic polymer. Addition of nanoclay to bio-polymeric matrixes often shows improved mechanical properties. The size range of nanoclay is around 10-100 nm in one or more dimensions and consists of inorganic layered silicates several hundred nanometers long and having layer spacing of few nanometers. Hundreds of such layered platelets are stacked into particles or tactoids. These layered silicates significantly affect the properties of nano-composite films as due to its nano scale size it interacts with matter at the atomic, molecular, or macromolecular level. There are mainly two approaches which are widely used for the dispersion of nanoclay in polymeric matrices: intercalation and exfoliation. Intercalation is described as a moderate penetration of polymeric chain into nanoclay basal spacing which results in slight expansion of interlayer spaces with the shape of layered stack remaining undisturbed. In exfoliation, on the other hand, layered structure of nanoclay loses its shape to form single sheets and thus behaves more like a homogenous mixture with polymeric solution.

Lipids and waxes are other important additives for reducing WVTR because of their hydrophobic components. Beeswax has been successfully applied by several authors to reduce the water vapor permeability of biodegradable films. Incorporation of wax in biopolymers results in formation of either bilayer or emulsion films. It has been proven that emulsion composite films are simpler and feasible to prepare than bilayer films. The effectiveness of beeswax in emulsion films for reducing WVTR is, however, strongly dependent on the presence of emulsifier that posses both hydrophilic and hydrophobic groups, thus reducing the surface tension of the film forming solution. Addition of plasticizer for improving mechanical properties of biodegradable films has been extensively reported. This process increases the percentage elongation of films by forming hydrogen bond with the polymer and reducing polymeric interactions. Polysaccharide based films are commonly plasticized with polyols such as glycerol.

Concentrations of various additives as mentioned above significantly affects mechanical and barrier properties. Optimization of various additives added can therefore lead to better film characteristics.

Response surface methodology (RSM) is an effective tool for optimizing a protocol to achieve the desired response using a combination of independent variables. Basic principle of RSM is to relate product properties of regression equations by mathematical models that describe interrelations between input parameters and properties of products. RSM has been earlier employed by Maran et al. (2013) to understand interactive effects of individual variables on biofilm parameters (4).

Food packaging materials are intended to increase the shelf life of products by providing physical protection and creating proper physicochemical conditions for it. Antimicrobial packaging is a form of active packaging that could extend the shelf-life of product and provides microbial safety for consumers. It reduces or inhibits the growth of pathogenic microorganisms in packed foods and packaging material. Active packaging was successfully used by several authors to increase the shelf life of minimally processed fresh cut fruits. In order to control undesirable microorganisms on food surfaces antimicrobial agents can either be incorporated into polymers for standalone films or dip coated on food products to get the desired effect. The coating can serve as a carrier for antioxidant and/or antimicrobial compounds. Several natural compounds have been proposed for imparting antimicrobial activity in food packaging. Grape pomace, a wine industry waste, due to its significant antioxidant and antimicrobial properties can have potent application in this respect.

The objective of this project was to develop biodegradable films with improved properties for food irradiation application. In view of the very few reports on the use of GG for development of biodegradable films, this material was used as a base material in the present study. Improvement in mechanical properties of GG films was attempted by gamma irradiation and nanoclay incorporation. Efforts were made to lower the water barrier property of the film by optimizing various additives using RSM. Finally, the effect of gamma irradiation on shelf life of pomegranate arils packed in the films incorporated with grape pomace extract was studied. Besides standalone film, an attempt was also made to develop edible coating using aqueous solution of GG containing grape pomace extract for enhanced shelf life of pomegranate arils.

Chapter 1 of the thesis introduces the subject of biopolymer based packaging films with special emphasise on improvement of various properties of biodegradable films. Various methods were proposed in past for the development of films having better characteristics. Among these methods gamma irradiation and/or nanoclay incorporation is one of the most frequently used processes. Based on the review of available literature, it was found that additives play a crucial role in developing films having desirable properties. Several authors have reported the usefulness of RSM to optimize concentration of various additives in film. Purpose of packaging film is to increase the shelf life of packed product. In this context active packaging play a crucial role for longer shelf life of food products. Standalone film and edible coating with antioxidant and antimicrobial components have been effectively used for obtaining higher shelf life of the minimally processed fresh cut fruits. In the light of available literatures, present thesis deals with the development and improvement of GG film and its subsequent application for shelf life extension of minimally processed fruit by irradiation.

Chapter 2 of the thesis describes the materials and experimental methods. GG was purchased from Merck, India Ltd. and other chemicals from Sigma-Aldrich, USA. Irradiation was carried out using a cobalt-60 irradiator (GC 5000, Board of Radiation and Isotope Technology, India) at BARC, Mumbai. GG was purified by ethanol precipitation before using it for film formation. Native GG films were formed by casting 150 mL of GG solution (1% aq. w/v) having glycerol (40% w/w of GG) on 20 cm X 20 cm glass plates. Films were dried at 80°C for 8 h. Obtained films were characterized after conditioning at 50% RH for 7 days. American Society of Testing and Materials (ASTM) standard method D882-10 was used to measure the tensile strength, Young's modulus and percent elongation at break (%E) of films. Puncture strength and WVTR were analyzed by standard protocols. Conformation of GG was analyzed by small angel X-ray scattering (SAXS). Nanoclay (nanofil 116 and cloisite 20A) was exfoliated by stirring its aqueous suspension for 7 days before incorporating into GG film matrices. Basal spacing of nanoclay was analyzed by SAXS and x-ray Diffraction. The surface morphology of GG based nano-composite films were analyzed by Field Emission Gun-Scanning Electron Microscopes.

RSM was used to optimize the concentration of beeswax, tween 80 (emulsifier), nanofil 116 (nanoclay) and glycerol to obtained the film having cling film like properties.

Aqueous ethanol was used to obtain the grape pomace extract by using speed extractor E-914, BUCHI. Nutritional parameters like vitamin content, total phenolic content and antioxidant properties of grape pomace extract were studied according to standard AOAC protocols. Active packaging was developed by incorporating grape pomace extract into RSM optimized films. Pomegranate arils were packed in polystyrene trays using developed active packaging and gamma irradiation was used for shelf life extension of arils. Besides active packaging, edible coating were also developed by dipping arils into aqueous solution of GG and grape pomace extract for obtaining longer shelf life. Sensory quality of arils was assessed by a sensory panel through hedonic testing. Standard methods were used to enumerate microorganisms present in packed samples.

Chapter 3 deals with the results obtained and its subsequent discussion. It has been divided into following subsections.

3.1 Standardization of protocols for film formation from guar gum: Purification of GG was standardized by ethanol precipitation. Optimized conditions for native film formation were 150 mL of 1% aq. w/v GG solution having 40% (w/w of GG) glycerol. Glass plates were found to be most suitable for film casting than teflon. Standard drying conditions for GG film were 80°C for 8 h. Films prepared from unpurified GG demonstrated thickness of 13.66 ± 3.3 μm, tensile strength of 6 ± 1.1 MPa and Young's modulus of 63 ± 12 MPa, while that from purified GG demonstrated an improved tensile strength of 60.5 ± 8.7 MPa and Young's modulus of 162 ± 23 MPa with thickness of 14.33 ± 2.3 μm. Observed improvement in mechanical properties of films might be due to the additional purification step followed in this study, which leads to removal of insoluble impurities from GG. This could lead to a uniform and compact packing of GG polymer chains in the films prepared, resulting in increased tensile strength. Thus, all further work was performed on purified GG.

3.2 Use of gamma irradiation for improving functional and mechanical properties of developed films: This section deals with the effect of gamma irradiation on various properties of the developed films. Mechanical and water vapor barrier properties of biodegradable films prepared from radiation processed GG were investigated. Films prepared from GG irradiated up to 500 Gy demonstrated significantly higher tensile strength as compared to non-irradiated control films. This improvement in tensile strength observed was demonstrated to be due to the ordering of polymer structures as confirmed by small angle X-ray scattering analysis. Exposure to doses higher than 500 Gy, however, resulted in a dose dependent decrease in tensile strength. A dose dependent decrease in puncture strength with no significant differences in the percent elongation was also observed at all the doses studied. Water vapor barrier properties of films improved up to 15% due to radiation processing. Radiation processing at lower doses for improving mechanical and barrier properties of guar based packaging films is demonstrated here for the first time.

3.3 Use of additives for better film properties: GG based nano-composite films were prepared using organically modified (cloisite 20A) and unmodified (nanofil 116) nanoclays. Effect of nanoclay incorporation on mechanical strength, water vapor barrier property, chromatic characteristics and opacity of films was evaluated. Nano-composites were characterized using X-ray scattering and FTIR and their microstructure was investigated using scanning electron microscopy. A nanoclay concentration dependent increase in mechanical strength and reduction in water vapor transmission rate was observed. Films containing nanofil 116 (2.5% w/w GG) and closite 20A (10% w/w GG) demonstrated a 102% and 41% higher tensile strength, respectively, as compared to the control. Lower tensile strength of cloisite 20A containing films was due to its incompatibility with GG. X-ray scattering analysis revealed that interstitial spacing between nanofil 116 and cloisite 20 A sheets increased due to its intercalation by GG polymer resulting in observed improvement in mechanical and barrier properties.

Apart from nanomaterials addition of additives such as beeswax, tween-80, nanofil 116 and glycerol at different concentrations was attempted to improve the mechanical and barrier properties of GG based biodegradable films. Irradiation of beeswax was performed to increase the compatibility between beeswax and GG. Preliminary experiments suggested that incorporation of 50 kGy irradiated beeswax in film resulted in higher mechanical properties and lower barrier property than unirradiated beeswax. Incorporation of tween-80 and nanofil 116 resulted in improved tensile strength while addition of beeswax led to decreased water vapor transmission rate (WVTR) of the films. Flexibility of films improved on addition of glycerol and tween-80. RSM was used to optimize concentrations of various additives to obtain films having desired mechanical and barrier properties. At optimum concentration: tween-80 (0.88%), 50 kGy irradiated beeswax (1.25%), glycerol (13.91%), nanofil 116 (3.07%) w/w of GG, films having tensile strength of 122.1 MPa, Young's modulus of 98.6 GPa and WVTR of 69.2 $g/m^2/d$ were obtained. The corresponding values for the commercially available cling film were 42 ± 6 MPa, 178 ± 32 MPa and 35 ± 5 $g/m^2/d$ respectively. Above mentioned WVTR of cling film was achieved by increasing the thickness of optimized films from 14 µm to 29 µm. This increase in thickness of film resulted in tensile strength of 124 ± 15 MPa, Young's modulus of 96 ± 7 GPa and WVTR of 39 ± 4 $g/m^2/d$. Optimized film were further used for the development of active packaging.

3.4 Development of active packaging films with possible antioxidant and antimicrobial functions: This section deals with the potential application of above developed and optimized film in food packaging. Aqueous ethanol extract of grape pomace was found to be rich in antioxidants and having antimicrobial activity against food pathogens. Its subsequent incorporation in GG film resulted in active packaging without significant changes in mechanical and barrier properties. Pomegranate arils being a highly perishable product were chosen to study the feasibility of the developed films in food packaging. The overall qualities of the samples packed in the developed films were compared to those packed in commercially available cling films. The microbial, sensory and nutritional qualities of both samples were comparable throughout the storage period. Gamma irradiation was further found to enhance the

shelf life of the packed product by 1 month while maintaining its overall quality. Edible coating was also observed to increase the aril's shelf life by 15 days.

Chapter 4 is the concluding chapter of the thesis. This chapter summarizes the finding of the projects and discusses the possible applications.

References

1. Das, Debasis, et al. "New water resistant biomaterial biocide film based on guar gum." Bioresource technology 102.10 (2011): 5878-5883.

2. Mikkonen, Kirsi S., et al. "Effect of polysaccharide structure on mechanical and thermal properties of galactomannan-based films." Biomacromolecules 8.10 (2007): 3198-3205.

3. Gupta, Sumit, et al. "Role of initial apparent viscosity and moisture content on post irradiation rheological properties of guar gum." Food hydrocolloids 23.7 (2009): 1785-1791.

4. Maran, Prakash J., et al. "Development of model for barrier and optical properties of tapioca starch based edible films." Carbohydrate Polymers 92.2 (2013): 1335-1347.

Publications:

a. Published:

1. Saurabh, C. K., Gupta, S., Bahadur, J., Mazumder, S., Variyar, P. S., & Sharma, A. (2013). Radiation dose dependent change in physiochemical, mechanical and barrier properties of guar gum based films. Carbohydrate polymers, 98(2), 1610-1617.

2. Saurabh, C. K., Gupta, S., Bahadur, J., Mazumder, S., Variyar, P. S., & Sharma, A. (2015). Mechanical and barrier properties of guar gum based nano-composite films. Carbohydrate polymers, 124, 77-84.

b. Communicated:

1. Saurabh, C. K., Gupta, S., Bahadur, J., Mazumder, S., Variyar, P. S., & Sharma, A. Improving mechanical & barrier properties of guar gum based biodegradable films: Optimization of additives by Response Surface Methodology.

c. Manuscript under preparation

1. Saurabh, C. K., Gupta, S., Variyar, P. S., & Sharma, A. Shelf life extension of minimally processed pomegranate arils packed in guar gum based active films by gamma irradiation.

2. Saurabh, C. K., Gupta, S., Variyar, P. S., & Sharma, A. Shelf life extension of minimally processed pomegranate arils by dip coating.

Signature of the student: Chatterbhuj

Date: 22-10-2014

Doctoral Committee:

S No	Name	Designation	Signature	Date
1	Prof. Dr. A. K. Sharma	Chairman		24/10/2014
2	Prof. Dr. Prasad S. Variyar	Convener	Prasad.S.V	24/10/14
3	Prof. Dr. LalitVarshney	Member		27/10/2014
4	Prof. Dr. P. A. Hassan	Member		27/10/2014
5	Prof. Dr. R.N. Jagtap	Member		28/10/14

LIST OF FIGURES

LIST OF TABLES

1. Introduction

1.1 Overview

Petrochemical based packaging material has put tremendous pressure on the environment owing to their poor biodegradability and derivability from non renewable natural resources. This has led to a quest for polymers for packaging to address the short comings of conventional plastics. Biopolymers such as polysaccharides, proteins and lipids form a suitable alternative due to their non toxic and biodegradable characteristics and derivability from renewable natural resources. However, the major limitations in the use of biopolymers as packaging materials are their relatively poor mechanical and barrier properties as compared to their non biodegradable counterparts [1, 2, 3]. Various methods have been proposed in past to overcome the limitation of biopolymer based packaging. Gamma irradiation is one of the most widely reported method for the improvement of film characteristics [4]. Another approach which has been frequently reported by several authors is the incorporation of various additives such as nanoclay, wax and plasticizer in biobased film for improved mechanical and barrier properties [5, 6]. However, despite extensive research in this field, the developed biodegradable films still fall short of the industrial benchmark. Therefore further research for the development of biodegradable film is very much needed to achieve wide commercial application.

1.2 Packaging and its objectives

Packaging is used to protect the packed products against physical, chemical, or biological hazards. It has several objectives:

- **Barrier protection -** A barrier against oxygen, carbon dioxide, water vapor, dust, etc., is often required. Permeation is a critical factor in design.
- **Convenience -** Packages can have features which add convenience in distribution, handling, stacking, display, sale, opening, reclosing, use and reuse.
- **Portion control -** Single serving packaging has a precise amount of contents to control usage.

1.3 History of packaging

One of the first packages used the natural materials available at the time were wooden boxes, pottery vases, woven bags, wooden barrels etc. Processed materials were also used to form packages for example, bronze vessels and early glass. The earliest recorded use of paper for packaging dates back to 1035. The use of tinplate for packaging has been documented since the 18^{th} century. The tin canning process was patented in 1810 because of the importance of air tight containers for food preservation. By 1813, the first canned goods were commercially produced. The first corrugated box was produced commercially in 1817. Commercial paper bags were first manufactured in Bristol, England in 1844. Cellophane was commercially used for packaging during late 1950s and early 1960s. Polyethylene films started gaining importance since mid 90's. In 1933 polyethylene film were used to protect submarine telephone cables and later during World War II for radar cables and drug tablet packaging. By 1980, foods and other hot-fill products such as jams packaged in polyethylene terephthalate became popular. Since then packaging has become an integral part of the food we consume.

1.4 Types of packaging

Packaging on a broader term can be divided into three categories: primary, secondary and tertiary. Primary packaging is the main package that holds the product such as food that is being processed. It is the first packaging layer in which the product is contained, hence, forms the most important packaging owing to its immediate contact with the food products. Secondary packaging combines the primary packages into one box. Tertiary packaging combines all of the secondary packages into one pallet.

1.5 Packaging materials

The commonly used packaging materials are: wood, paper, metals, glass, and plastics (Figure 1).

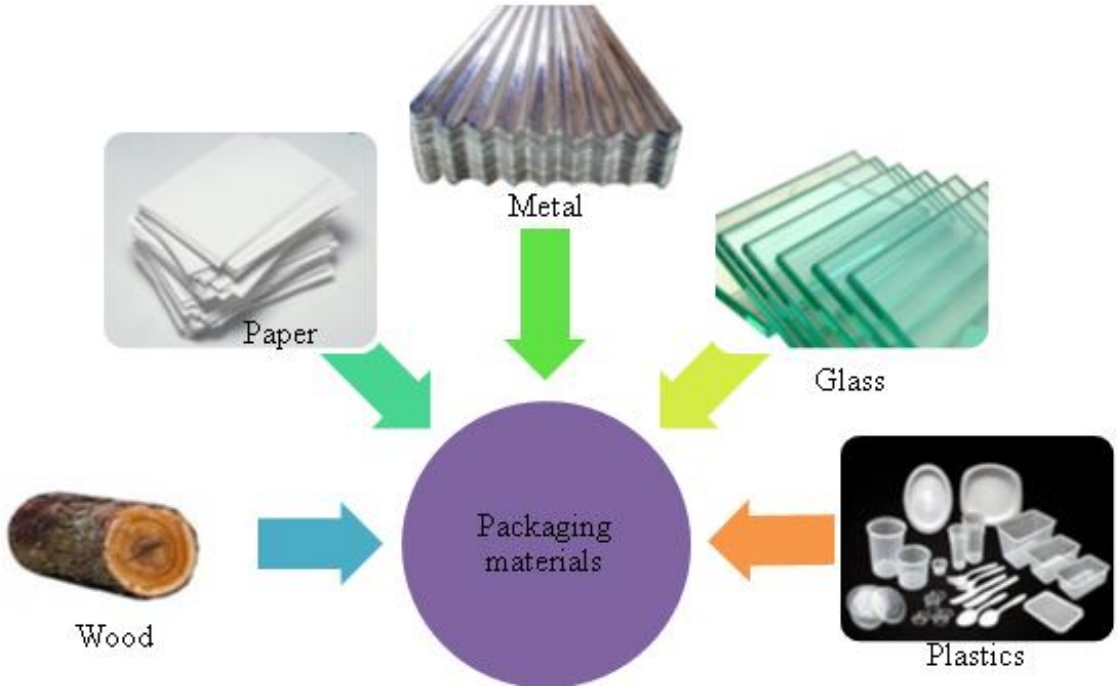

Figure 1: Types of packaging materials.

1.5.1 Wood – It is mostly used for pallets and crates (heavy duty products). Some lidded or hinged boxes are produced for cigars, gifts, tea, cheese etc. Bamboo is emerging as a packaging material. Dell Inc. has developed new compostable packaging materials made from bamboo for laptops. Cork has a long history as a packaging material in wine bottling.

1.5.2 Paper - It is widely used because of low cost, holds its shape, and is easily printable. Commercially available paper is predominantly made from cellulose fiber obtained from pulped wood. However its usage has adverse effects on the environment as it results in deforestation.

1.5.3 Metals - Tin plates and aluminum are the most commonly used metals in packaging industry and are used to make food and drink cans, trays etc. However, due to their heavy weight and limited shapes achievable metals are becoming less popular as packaging material especially when compared to plastics.

1.5.4 Glass - Glass is a popular and useful packaging material due to its inert nature and effective barrier property. The disadvantages of glass are its weight, fragility etc.

1.5.5 Plastics - They are usually synthetic, most commonly derived from petrochemicals and moldable. Due to their relatively low cost, versatility, and imperviousness to water, plastics are used in an enormous and expanding range of food products (Table 1). In developed countries, about a third of plastic is used in packaging. In India 42% of plastic consumption is used in packaging [7]. Common plastic polymers used in packaging are:

1.5.5.1 Polyethylene (PE) - It is the most commonly used plastic. The annual global production of PE is approximately 80 million tones. Its primary use in packaging is to make bags, bottles and films. PE is classified into several different categories based mostly on its density and branching. Important PE for packaging is:

- **Low Density PE -** It is used for manufacturing flexible tubes, film and bottles. It has a low melting point and as a film it has relatively poor oxygen and moisture barrier.
- **High Density PE** - Widely used for bottles and tubs. It has higher melting point and reasonably wide chemical resistance properties.
- **Linear Low Density PE** - Predominantly used as a film or as a sealing layer on multi-laminate materials for bottle seals, sachets, pouches, bags.

1.5.5.2 Polypropylene (PP) - It is a thermoplastic polymer used in a wide variety of applications including packaging and labeling. In 2008, the global market for polypropylene had a volume of 45.1 million metric tons. It is used for developing bottles, jars, cartons and trays.

1.5.5.3 Polyethylene terephthalate (PET) - It has excellent clarity and very high gas and moisture barrier properties and is therefore ideal for carbonated beverages. It is also used for jars, tubes and trays. Its heat resistance property makes it suitable for ovenable trays for ready meals.

1.5.5.4 Polyvinyl chloride - It is the third most widely produced polymer, after polyethylene and polypropylene. It is used for bottles and other non food packaging.

1.5.5.5 Polystyrene - It is a synthetic aromatic polymer made from the monomer styrene. Its uses include protective packaging (such as packing peanuts), containers, lids, bottles, trays, tumblers, and disposable cutlery.

1.5.5.6 Polyvinylidene chloride - It is applied as a water based coating to other plastic films such as biaxially oriented PP and PET. This coating increases the barrier properties of the film, reducing the permeability of the film to oxygen and flavors and thus extending the shelf-life of the food inside the package.

Table 1: Commonly used plastics and their applications in food packaging [8].

Polymer name	Properties	Applications
Low density polyethylene	Flexible, strong, tough, easy to seal and resistant to moisture	Film applications like bread and frozen food bags; flexible lids and squeezable food bottles
High density polyethylene	Resistant to chemical and moisture, stiff, strong, tough and easy to process	Bottles for milk, juices and water; margarine tubs and cereal box liners
Polypropylene	Harder, denser, transparent, resistant to heat and chemicals	Yogurt containers; margarine tubs and microwavable packaging
Polyethylene terephthalate	Low permeability to gases and vapors; good resistant to heat, mineral oils, solvents and acids	Bottles for carbonated drinks; containers; trays and blister packs
Polyvinyl chloride	Stiff, medium strong, transparent material; resistant to chemicals, grease and oil; good flow characteristic and stable electrical properties	Bottles; packaging films and blister packs
Poly styrene	Clear, hard and brittle material; foaming produces an opaque, rigid, light weight material with impact protection and thermal insulation properties	Egg cartons/trays; containers; disposable plastic silverware, lids, cups, plates, bottles and food trays

1.6 Production of plastics

Continuous innovation in plastics has resulted in its increased production by an average of almost 10% every year globally since 1950. From around 1.3 million tons in 1950 the global production of plastics has grown to 230 million tons in 2005 (Figure 2). With continuous growth for more than 50 years, global production in 2012 rose to 288 million tones, 2.8% increase compared to 2011. China remains the leading plastics producer with 23.9%, and the rest of Asia accounts for an additional 20.7%. European production accounts for 20.4% of the world's total production (Figure 3). Packaging applications are the largest application sector for the plastics industry and represent 39.4% of the total plastics demand. Building and construction is the second largest application sector with 20.3% of the total demand (Figure 4).

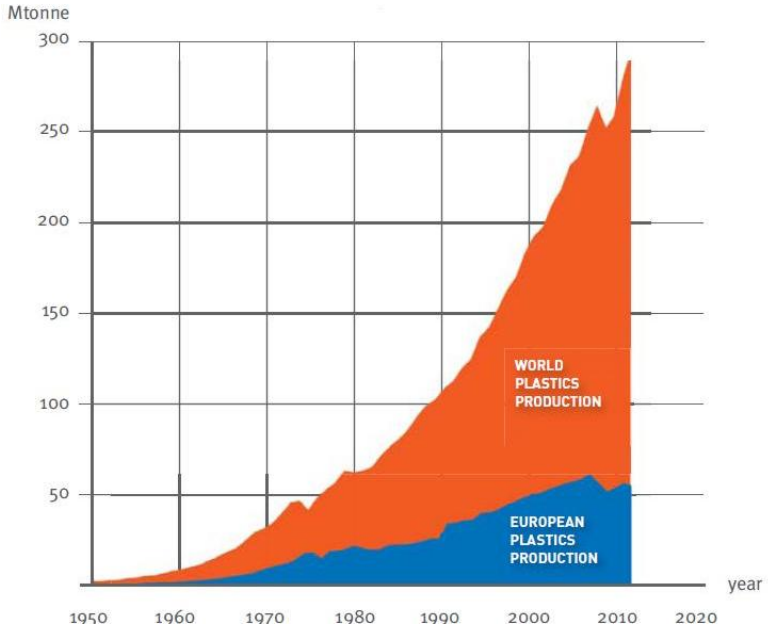

Figure 2: World and European plastic production from 1950 to 2012 (Source: PlasticsEurope (PEMRG) / Consultic).

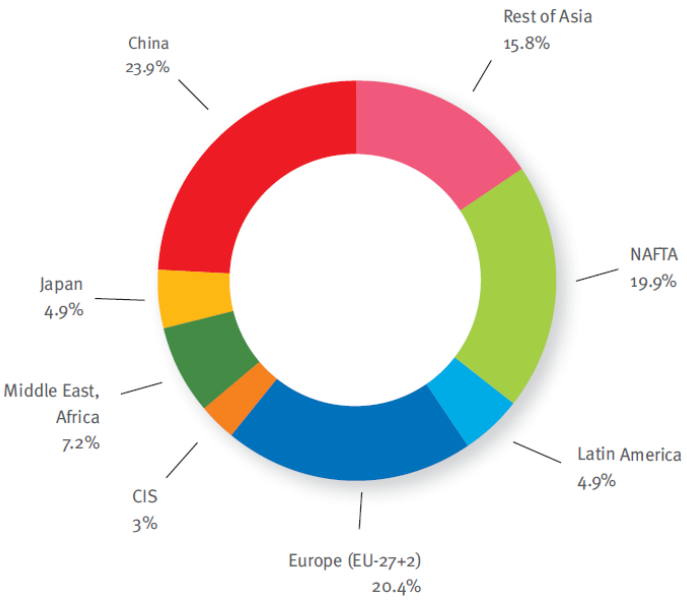

Figure 3: Production of plastics materials world over in 2012 (Source: PlasticsEurope (PEMRG) / Consultic).

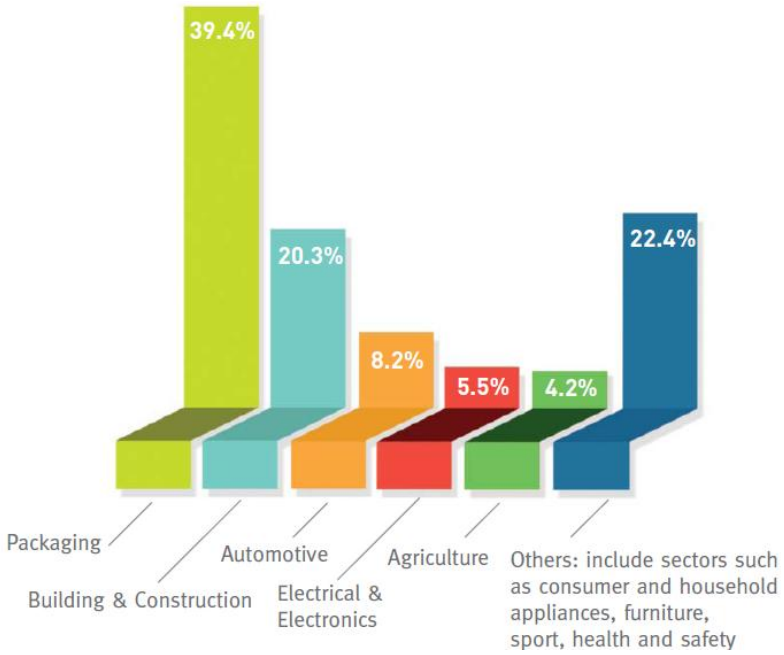

Figure 4: Plastic demand by various sectors, 2012 (Source: PlasticsEurope (PEMRG) / Consultic / ECEBD).

1.7 Concern about packaging plastics

Packaging dominates the waste generated from plastics, accounting for 62.2% of the total. The major hurdle against increased use of plastics is their non-biodegradability and as a result, ever increasing mounting garbage wastes. The accumulation of plastic products in the environment can adversely affect wildlife, wildlife habitat and humans. In 2012, it was estimated that there was approximately 165 million tons of plastic pollution in the world's oceans. Traditional methods for handling post consumer plastic wastes include incineration, recycling and land filling [9]. However there are some apprehensions related to these methods:

1.7.1 Incineration - It is a process that involves the combustion of waste materials. During incineration generated CO_2 adds to the problem of green house effect. Other pollutants such as NO, SO_2, NH_3 etc. discharged into the environment also induce serious problems; particularly causing health hazards like lung cancer, skin diseases, asthma, etc.

1.7.2 Recycling - It provide only a part time solution to long term reduction of plastics. However, during recycling the material lose some of the properties like appearance, chemical resistance, reprocessibility and mechanical characteristics. Recycling of plastics is usually not an economical process in terms of cost and energy required.

1.7.3 Landfill - Waste plastics remain buried for several years, causing ecological pollution. Chlorinated plastic can release harmful chemicals into the surrounding soil, which can then seep into groundwater or other surrounding water sources. This can cause serious harm to the species that drink this water.

Besides these problems plastics also poses some direct grave risk against human health when used in food packaging.

1.8 Food packaging hazards and its prevention

Food packaging materials are intended to increase the shelf life of products by providing physical protection and creating proper physicochemical conditions for it [10]. Currently food packaging market is worth of $250000 million and expected to reach a value of $300000 million by 2019. However, conventional food packaging materials can be source of chemical food contaminants by migration of chemicals from the packaging into the food. According to a recent study by the Food Packaging Forum, 175 chemicals with known hazardous properties are legally used in the production of food contact packaging in U.S. and Europe [11]. Hazardous chemical commonly used in food packaging are:

1.8.1 Biocides - Many biocides like propanol, glutaraldehyde etc used to disinfect surfaces are irritants and sensitizers acting on the skin, eyes and mucous membranes. They can lead to allergic contact dermatitis and asthma.

1.8.2 Bisphenol A (BPA) - It is a key monomer in production of epoxy resins and is the most common form of polycarbonate plastic. In females, fertility and the onset of puberty were affected by BPA. Furthermore, it is carcinogenic and adversely affects male reproductive system.

1.8.3 Phthalates - Mainly used as plasticizers (substances added to plastics to increase their flexibility, transparency, durability, and longevity). It is associated with adverse health effects such as obesity and reduced masculinization in newborn boys.

1.8.4 Polyfluorinated compounds – Fluorosurfactants are commonly present as polyfluorinated compounds in packaging. These compounds greatly reduce surface tension of the films. However, such compounds are corrosive to the skin and eyes and at higher exposures can lead to kidney, testicular and liver cancer.

Various government agencies such as Food and Drug Administration are trying to limit the addition of potentially toxic chemicals in food packaging. Such preventive methods will reduce the health related risk but cannot completely eliminate it. Another approach is the development of biopolymer based biodegradable packaging for foods. Biodegradable plastics are completely safe due to the absence of harmful chemicals or toxins and being biodegradable, they break down into harmless products that get absorbed into the soil.

1.9 Biodegradable plastics

Biodegradable plastics are gaining importance in packaging industry. Demand for biodegradable plastics is expected to reach nearly 525 thousand metric tons (KMT) from the current 269 KMT with a market value exceeding $3400 million by 2019. Two basic classes of biodegradable plastics exist:

- Plastics made from petrochemicals containing biodegradable additives that enhance their degradation. Oxo-biodegradable (ODB) plastic bags are one such example. However, the time needed for OBD plastics to degrade is quite slow and tiny fragments of these plastic may remain in ecosystem. These microscopic plastic fragments tend to enter into food chain and prove to be more lethal than conventional plastic.

- Plastics whose components are derived from renewable biomass sources (bioplastics). Some bioplastics are designed to biodegrade in both under anaerobic and aerobic environments. They are used mainly for disposable items such as fruit, meat and vegetable wrapping.

1.10 Biopolymer based biodegradable plastics for food packaging

Much work in the field of food packaging in present era is focused towards the development of natural biopolymers based packaging. These biopolymers being derived from replenishable resources are biocompatible, biodegradable and are thus ecofriendly [12]. Packaging is the biggest application of biodegradable plastics and is projected to be worth $2,000 million by 2019. These plastics are broadly divided into three classes based on the method of production or their source [13] (Figure 5):

- Polymers produced by chemical synthesis starting from renewable bio based monomers such as polylactic acid.
- Polymers produced by microorganisms such as polyhydroxyalkanoates.
- Polymers directly extracted from vegetal or animal biomass such as polysaccharides and proteins.

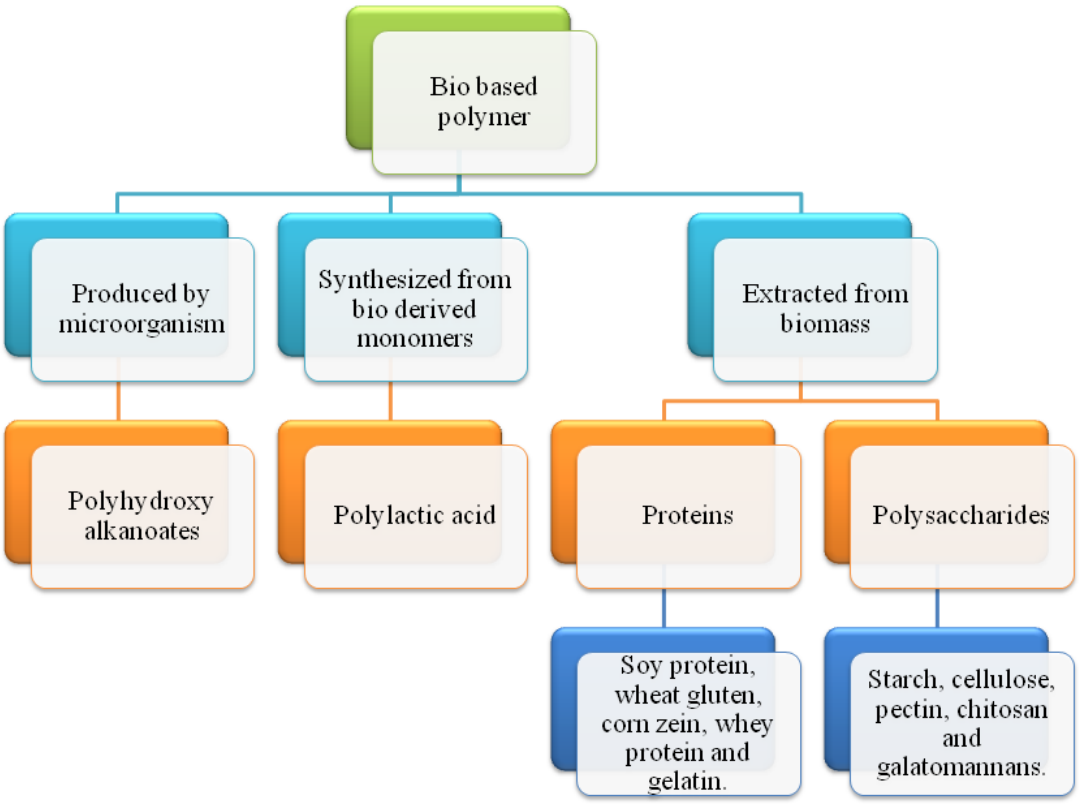

Figure 5: Different classes of biopolymer used for food packaging.

Biomass has been proven to be a cheap source of biopolymer which also has the added advantage in terms of commercialization of bioplastics. Extensive research has been done on proteins and polysaccharides film because they have suitable physico-mechanical properties. Such films also demonstrate adequate gas barrier properties [14] enabling the extension of shelf life of food products without creating anaerobic conditions [15].

1.10.1 Proteins

Proteins cover a broad range of polymeric compounds that provide structure or biological activity in plants and animals. It is made up of amino acids linked together by peptide bonds. Varieties of proteins from different sources have been widely reported for the

production of films, such as plant protein (soy protein, wheat gluten, corn zein and whey protein) and animal protein (gelatin).

1.10.1.1 Soy protein

Soy protein is isolated from soybean. Its film forming ability has been widely reported along with characteristic functional properties such as cohesiveness and adhesiveness [16]. Soy protein isolate is comprised of two major components namely β-conglycinin and glycinin. These globular proteins are commonly referred to as 7S and 11S globulin, respectively. Earlier reports demonstrated that films from 11S fraction were smooth and opaque, whereas those from the 7S fraction were translucent and creased [17]. The protein concentration and pH of film forming solutions are important factors in preparing soy protein based films. For better film properties, soy protein is dissolved in alkaline pH to unfold the protein. The film forming abilities of soy protein incorporating other materials, for example sodium dodecyl sulfate, polylactic acid and enzyme were also studied by various authors [18, 19, 20].

1.10.1.2 Wheat gluten

Gluten found in wheat is composed of the proteins gliadin and glutenin. Numerous studies refer to the film forming properties of wheat gluten proteins. Purified gluten films had twice the tensile strength than that of films from unpurified gluten. Films obtained from glutenin fraction presented higher tensile strength, lower elasticity and water vapor permeability than gliadin films [21]. Effect of chemical, physical and aging treatments on wheat gluten films were also studied earlier [22, 23, 24].

1.10.1.3 Corn zein

Zein is a major storage protein present in the endosperm tissue of corn. Cross-linking between zein molecules had been induced using reagents such as formaldehyde and glutaraldehyde for improved mechanical and barrier properties of the film [25]. Ultraviolet treatment was also used successfully for cross-linking of zein within the film structure [26].

1.10.1.4 Whey protein

Whey protein is a mixture of globular proteins isolated from whey, a by-product of cheese industries. It has been earlier reported that film prepared from whey proteins are elastic [27] and they had good oxygen barrier and moderate moisture permeability [28, 29].

1.10.1.5 Gelatin

Gelatin is a soluble protein obtained by partial hydrolysis of collagen. The molecular weight distribution and amino acid composition are believed to play a key role in the mechanical and barrier properties of the gelatin films [30]. The current trend is to develop biodegradable materials for food packaging by combining gelatin with soy protein isolates [31], konjac glucomannan [32], chitosan [33], plasticizers [34], polyethylene [35], as well as cross-linking agents, such as glutaraldehyde [36].

1.10.2 Polysaccharides

Polysaccharides are polymeric carbohydrate molecules composed of long chains of monosaccharide units bound together by glycosidic linkages. Polysaccharides are more researched biopolymer than proteins in terms of development of biodegradable packaging because of its simple processing and wide availability.

1.10.2.1 Starch

Starch (polymer of glucose) is produced by most green plants to store energy and it consists of linear amylose and branched amylopectin. When starch is treated in an extruder by application of both thermal and mechanical energy, it is converted to a thermoplastic material. Thermoplastic starch has recently been commercialized and used as a packaging material. Various efforts have been taken for the development of starch based films [37, 5].

1.10.2.2 Cellulose

Cellulose is an important structural components of the primary cell wall of plants, a polysaccharide consisting of a linear chain of β (1→4) linked D-glucose units. A number of cellulose derivatives such as carboxymethyl cellulose, methyl cellulose, ethyl cellulose, hydroxypropyl cellulose, hydroxyethyl cellulose and cellulose acetate are used in the preparation of cellulose based films. Cellulose acetate films are most widely used in food packaging than other derivatives, since it has low gas and moisture barrier properties [16].

1.10.2.3 Pectin

Pectin is a structural heteropolysaccharide contained in the primary cell walls of plants. Blends of pectin and starch give strong and flexible films [38]. Laminated films from pectin and chitosan in combination were also earlier prepared [39].

1.10.2.4 Chitosan

It is chemically derived by deacetylation of chitin, an abundant polysaccharide found in shellfish. Chitosan possesses a unique cationic nature relative to other neutral or negatively charged polysaccharides. It has strong antimicrobial properties against fungi, bacteria and viruses [40]. Because of these appealing features various reports exists on chitosan based films [41, 42, 43].

1.10.2.5 Galactomannans

It consists of a mannose backbone with galactose side groups. Based on the mannose to galactose ratio, galactomannans can be classified into four types as shown in Table 2. Galactomannans are commonly used in food industry as stabilizer, thickener and emulsifier. It is a suitable candidate that can be used for the production of biodegradable films owing to its edibility and biodegradability. The greatest advantage of galactomannans is its ability to form very viscous solutions in water at low concentrations that is relatively unaffected by pH, ionic strength and heat processing [44]. These properties make the handling of film forming solution much easier.

Table 2: Types of galactomannan.

Types of galactomannan	Mannose:Galactose
Fenugreek gum	1:1
Guar gum	2:1
Tara gum	3:1
Locust bean gum	4:1

1.10.2.5.1 Galactomannans based films

Among the various sources of galactomannan (Table 2), fenugreek and tara gum are costlier and the performance of their films are also poorer than other two galactomannan based film. One of the first reports using locust bean gum (LBG) characterizes the water vapor permeability of films having different concentrations of polyethylene glycol (PEG) [45]. Another report suggests that the luminous transmittance and total light transmittance of LBG film decreased at higher PEG concentrations [46]. Bozdemir et al. (2003) [47] studied the water vapor permeability of edible films made with LBG and various plasticizers (glycerol, propylene glycol and PEG). Extensive research has been carried out on films made of LBG. However, guar gum is more readily soluble in water than LBG and is a better stabilizer. Guar gum is cheap and not self gelling like LBG; such properties make guar gum a potentially suitable polymer for making biodegradable packaging.

1.11 Guar gum

Guar gum (GG), also called guaran is derived from endosperm of an annual legume plant *Cyamopsis tetragonoloba*. The guar seed consists of three parts: the seed coat (14-17%),

the endosperm (35-42%), and the germ (43-47%) (Figure 6). Seeds are dehusked, milled and screened to obtain the GG.

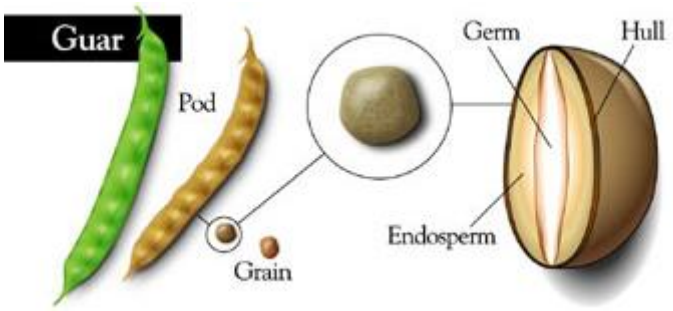

Figure 6: Guar seed structure.

India is the largest producer of GG with about 80% of world production. India's guar seed production increased from 2 to 18 lakh tons during 2005-06 to 2012-13 [48]. It is a hetropolysaccharide of a mannose ((1-4)-linked β-D-mannopyranose) backbone with galactose side groups ((1-6)-linked α-D-galactopyranose) (Figure 7) [49].

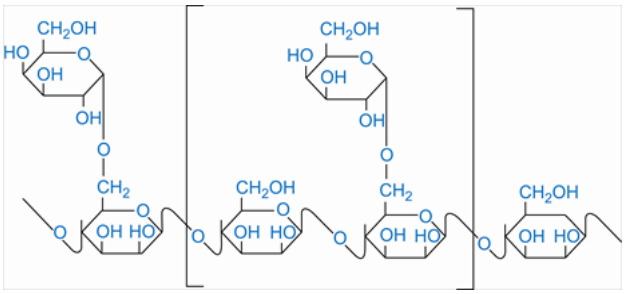

Figure 7: Structure of guar gum.

Various derivatives of GG are available of which commercially important include oxidized GG, sulphated GG, GG formate and GG acrylamide [48].

1.11.1 Application of GG

1.11.1.1 Industrial application

- Paper industry – improved sheet formation, folding and denser surface for printing.
- Explosives industry – as waterproofing agent mixed with ammonium nitrate, nitroglycerin, etc.
- Pharmaceutical industry – as binder or as disintegrator in tablets; main ingredient in some bulk forming laxatives.
- Cosmetics and toiletries industries – thickener in toothpastes, conditioner in shampoos.
- Hydraulic fracturing - Shale oil and gas extraction industries consumes about 90% of GG produced from India and Pakistan because of its multiple functions such as fluid and water loss control, lubrication and cooling of drill bits, shale inhibitor and solids carrier. It has excellent solution rheology, stability, solubility and compatibility with other auxiliaries used in oil well drilling.
- Nanoparticles industry - to produce silver or gold nanoparticles, or to develop innovative delivery mechanisms for drugs in pharmaceutical industry.

1.11.1.2 Food applications

GG has wide application in the food industry.

- Used in frozen foods such as ice creams, soft serves etc. GG works as crystal growth controller, moisture loss controller, freezer burn reducer, syneresis controller, freezing point and thaw separation controller.
- In baked goods, it increases dough yield, gives greater resiliency, and improves texture and shelf life.
- Used in beverages such as cocoa drinks, fruit juices, sugar free and alcoholic beverages where it acts as a suspending agent, maintains viscosity and improves mouth feel.
- In ketchup, barbecue sauces and pickles GG improves free flowing properties of sauce and reduces separation between water and oil phases. It has unique cold water dispersibility, acid resistance and acts as free water binder in salad dressings, sauce, pickles and relishes.
- In dairy products, it thickens milk, yogurt, kefir, and liquid cheese products, and helps maintain homogeneity and texture of ice creams.

Some of the characteristics of GG such as its solubility in cold water and stability at a wide pH range and temperature make the handling of the solution easier during film casting and drying. Thus besides having wide applicability of GG in industry it can also be investigated for the development of food packaging.

1.11.2 GG based packaging

Very few reports exist on development of film from GG. Chemical modification of guar galactomannan with benzamide for preparation of water resistant films have been recently

reported [49]. Mikkonen et al. (2007) [50] used enzymatic depolymerization for improving mechanical properties of GG film. Antimicrobial films were earlier prepared by mixing GG and chitosan [51]. Incorporation of GG in wax film decreased the permeability to oxygen and carbon dioxide [52]. Limited studies has been conducted in past on GG based films leaving much scope for further exploration of this polymer for food packaging.

1.12 Limitation of biopolymer based packaging

There is wide range of biopolymers that are available for manufacturing of food packaging. However various drawbacks associated with such packaging, limits its commercialization as compared to their non biodegradable counterparts. The problems related with biodegradable polymers are threefold: performance, processing, and cost [53]. Major disadvantages are:

Poor mechanical properties – (such as tensile strength) limit its application where packaging films undergo wear and tear.

High moisture sensitivity - Biopolymer films prepared from polysaccharides and protein are strong, but have poor water resistance property than synthetic polymers and thus absorb more moisture, with associated swelling, upon contact with water [54 and 55]. All these contribute to a considerable loss of mechanical properties, which prohibits straightforward use in most applications.

Cost – Poly (lactic acid) is one of the most commercially produced biopolymer for bioplastics; however, its high cost as compared to conventional packaging limits its wide applicability [56].

Others - Brittleness, low heat distortion temperature, and poor resistance to protracted processing operations also strongly limits their applications [57].

1.13 Methods for improving properties of biopolymer based packaging

Various chemical and physical methods have been proposed in past to improve the mechanical and barrier properties of biopolymer based packaging. Frequently used methods are: thermal treatment, mixing of two or more polymer to form composite films, chemical modification of biopolymer, gamma irradiation and incorporation of various additives in films.

1.13.1 Thermal treatment

Protein networks can easily achieve strong intermolecular covalent bonds, close molecular packing and reduced polymer mobility by means of cross-linking using thermal treatment. Most proteins denature when exposed to high temperature thereby exposing the amino acid groups of protein to the solvent [58]. This leads to the cross-linking of protein molecule by formation of disulphide bonds. Variation in heating time and temperature is presumed to influence the degree of cross-linking [59].

Several studies have focused on the improvement of film characteristics by heat induced cross linking. Liu et al. (2004) [60] showed that peanut protein films made from thermally

treated solution (70 °C for 30 min) had improved tensile strength compared to the untreated films. It was earlier reported that heat treatment improved the Young's modulus of whey protein isolate films [61]. Micard et al. (2000) [22] also demonstrated that heat treated wheat gluten films had significantly higher tensile strength than the untreated films.

1.13.2 Composite film

The combination of varying ratios of polysaccharides and/or proteins in the form of blend offers the possibility of manufacturing composite films with improved film properties [62]. Composite films prepared from pectin and fish skin gelatin or soybean flour protein showed increased stiffness and strength and decreased water solubility and water vapor transmission rate than pure pectin film [63]. Tensile elongation of gellan/gelatin composite films increased with increasing gelatin proportion [64]. Wang et al. (2010) [65] demonstrated that mechanical and barrier properties of films were improved by combining whey protein isolate, gelatin and sodium alginate.

1.13.3 Chemical modification

Functional properties of films can also be improved by chemical modification of bio molecules. Several methods of chemical treatment of biopolymers for film formation were earlier studied. Percentage elongation of soy protein based film increased when mildly treated with alkali [66]. Incorporation of each of the cross-linkers (glutaraldehyde and formaldehyde) into the whey protein isolate solution resulted in improved tensile strength and reduced water solubility of the formed films [67]. Calcium mediated cross-

linking of casein reduced the water vapor and gas permeability of sodium caseinate and calcium caseinate films [68].

1.13.4 Irradiation

Irradiation by ionizing radiation is a processing technique which involves exposure of food products to gamma rays, X-rays or electron beam [69]. Being a cold process, it can efficiently used to preserve food, reduce the risk of food borne illness, prevent the spread of invasive pests, delay or eliminate sprouting or ripening without significantly affecting its sensory and nutritional quality. These features make food irradiation one of the most extensive and thoroughly studied methods of food preservation. The non residual feature of ionizing radiation is a significant advantage in minimizing the use of chemicals applied to fruits and vegetables. In 1980, joint expert committee of Food and Agriculture Organization/International Atomic Energy Agency/World Health Organization on food irradiation concluded "The irradiation treatment of any food commodity up to an overall average dose of 10 kGy presents no radiological, microbiological or toxicological hazard" [70]. This joint committee approved the irradiation technology on wholesomeness of food since then it is being commercially practiced in several countries [71]. Only those foods approved under the Food Safety and Standards Authority of India (FSSAI) rules can be irradiated and sold in Indian domestic market (Table 3). Nowadays, the use of this technology to achieve similar results in fresh fruit products is one of the most challenging targets for processors.

Table 3: Items of food permitted for irradiation under Food Safety and Standards Authority of India (FSSAI) rules.

Name of Food	Dose of irradiation (kGy)		Purpose
	Min	Max	
Onion	0.03	0.09	Sprout inhibition
Potato	0.06	0.15	
Shallots	0.03	0.15	
Rice, semolina, whole wheat flour, refined wheat flour, pulses and dried sea food	0.25	1	Insect disinfestations
Raisins, figs and dried dates	0.25	0.75	
Mango	0.25	0.75	Shelf life extension and quarantine treatment
Meat and meat products	2.5	4	Shelf life extension and pathogen control
Fresh sea food	1	3	Shelf life extension
Frozen sea food	4	6	Microbial pathogen control
Spices	6	14	Microbial decontamination

1.13.4.1 Irradiation application in fresh fruits

Fresh cut fruits are highly susceptible to food borne illness. New tools to ensure the safety of fresh cut produce are required and low dose irradiation is one of the most promising methods [72]. There are various reports of radiation processing on shelf-life of fresh fruits (Table 4). Literature survey suggests that fruits were generally irradiated with gamma radiation from a radioisotope source. Irradiation in combination with proper packaging can thus effectively enhance shelf life of perishable fruits hence successfully contributing to food industry.

Table 4: Radiation processing of fruits for shelf-life extension [69].

Species	Irradiation type	Dose (kGy)
Mango	γ-irradiation	1
Papaya	γ-irradiation	0.5
Early season "Rio Red" grapefruit	γ-irradiation	0.07, 0.2, 0.4 and 0.7
Late season "Rio Red" grapefruit	γ-irradiation	0.07, 0.2, 0.4 and 0.7
Fresh Tristar' strawberries	Electron beam	1 and 2
Pineapple	γ-irradiation	0.05, 0.1 and 0.15
Apples (Fuji apple)	γ-irradiation	1.5, 4.5, 5 and 6
Pre climacteric mango	γ-irradiation	0.1 and 0.2
"Gala" apples	γ-irradiation	0.3 and 0.9
Clementine mandarin	X-ray irradiation	0.195 and 0.395

Irradiation is commercially used for shelf-life improvement and quarantine treatment of packed food product. However recent studies have also demonstrated its applicability in improving the properties of biobased film.

1.13.4.2 Gamma irradiation of packaging materials for prepackaged irradiated foods

Radiation processing is used commercially for decontamination of packed food products against bacteria and fungus. However, irradiation may cause leaching of additives or other components of the packaging material into food thus affecting odor, taste, and safety of the irradiated food. Packaging materials irradiated in contact with food are subject to premarket approval by the Food and Drug Administration (Table 5) because

irradiated polymer or adjuvant could migrate into food and affect odor, taste, and safety of the irradiated food [73].

Table 5: Packaging materials used for irradiated prepackaged foods [74].

Packaging Materials	Max Dose [kGy]
Nitrocellulose coated cellophane	10
Glassine paper	10
Wax coated paperboard	10
Polyolefin film	10
Kraft paper	0.5
Polyethylene terephthalate film (basic polymer)	10
Polystyrene film	10
Rubber hydrochloride film	10
Vinylidene chloride-vinyl chloride copolymer film	10
Nylon 11 [polyamide 11]	10
Ethylene vinyl acetate copolymer	30
Vegetable parchment	60
Polyethylene film (basic polymer)	60
Polyethylene terephthalate film	60
Nylon 6 [polyamide 6]	60
Vinyl chloride vinyl acetate copolymer film	60

1.13.4.3 Gamma irradiation of biopolymer based packaging

Exposure of biopolymers to ionizing radiation can cause conformational changes, breaking of covalent bonds, formation of free radicals, and recombination and polymerization reactions. As a result, irradiation of biopolymer leads to either cross linking or molecular degradation [75] resulting in changes in the mechanical and barrier properties of the film. There are several advantages associated with radiation processing such as convenience, eco friendly nature of the process [76] and short processing time.

Various reports suggest the use of gamma radiation for improving films characteristics by inducing cross linking of polymeric chains. Gamma irradiation improved the tensile

strength of pectin based biodegradable film [4]. Radiation technology was successfully used to induce the cross linking between starch and LBG for improved functional properties of starch based film [77]. Mechanical and barrier properties of soy and whey protein based films were improved by gamma irradiation [78]. Furthermore, Micard et al. (2000) [22] reported that gamma irradiated gluten films had increased WVP, increased tensile strength, and decreased elongation.

Further, gamma irradiation can also bring about conformational changes in the polymers in solution form. Several investigations have shown that the conformation and morphology of polymer chains affect the physical properties of the polymer which in turn alter the film characteristics [79]. Polymer chain conformation and chain correlation can be estimated by small angle X-ray scattering [80]. However, no such report exists on effect of radiation processing on biopolymer conformation and its subsequent film properties. Therefore further studies in this area can lead to development of biodegradable packaging with improved characteristics.

1.13.5 Additives

Apart from the above methods applied for improving mechanical properties of films, additives are commonly used for this purpose. These are substances that are added in small amounts in films to improve, strengthen or otherwise alter its properties. Usually additives are incorporated up to 50% by weight of the polymer. Most frequently used additives in food packaging are plasticizers, nanoclays, wax and lipids, surfactants and antimicrobial agents.

1.13.5.1 Plasticizers

The council of the IUPAC (International Union of Pure and Applied Chemistry) defined a plasticizer as "a substance or material incorporated in a material (usually a plastic or elastomer) to increase its flexibility, workability, or distensibility". Its primary role is to improve the flexibility and processability of polymers by lowering the glass transition temperature (Tg). The low molecular size of a plasticizer allows it to occupy intermolecular spaces between polymeric chains thus increasing the flexibility by restricting the formation of hydrogen bond between the chains [81]. Esters of phthalic acid usually carboxylic acid esters with linear or branched aliphatic alcohols of moderate chain lengths (predominantly C6–C11) constitute more than 85% of the total plasticizer consumption [81]. In relation to the classic plasticizers, the phthalate esters, adipates, citrates besides acid esters, alkane dicarboxylic, glycols and phosphates are used [82].

1.13.5.1.1 Plasticizers for biopolymer based films

Variety of plasticizers has been previously used for the improvement of flexibility of biofilms (Table 6). However, water is the most effective plasticizer for hydrocolloid based films [83] because it is a key solvent for natural biopolymer. The plasticization action of water molecules on biopolymers has been widely reported in the literature [84, 85].

Table 6: Plasticizers used in different types of biodegradable films [81].

Types of biopolymer	System of application	Plasticizers
Polysaccharide based films	Carrageenan edible films	glycerol and water
	Potato starch	glycerol
	Maize starch	glycerol, sorbitol and water
	Starch/gelatine	glycerol, sorbitol and sucrose
	Corn starch	glycerol, sorbitol and ethanolamine
	Chitosan	glucerol, sorbitol and urea
	Cellulose	residual xylan acetate
	Alginate/pectin	glycerol
Protein based films	Zein	oleic and linoleic acids
	Caseinate/pullulan	water and sorbitol
	Wheat gluten	glycerine
	Feather keratin	glycerol
	Whey protein	glycerol and sorbitol

In addition to water, other commonly used plasticizers are polyols, mono-, di- and oligosaccharides. Polyols are found to be particularly effective for plasticizing hydrophilic polymers [86]. Glycerol is a highly hygroscopic molecule generally added to the film forming solutions to prevent film brittleness [87]. Recent studies have demonstrated glycerol as an effective plasticizer for biodegradable films [83, 88 and 89].

1.13.5.2 Nanoclays

Nanoclays are other commonly used additive in packaging industry. These are nanoparticles of layered mineral silicates and have size ranging up to 100 nm in at least one dimension [90]. Montmorillonite (MMT), a typical example of nanoclay, consists of several hundred nanometers long inorganic layered silicates having layer spacing of few

nanometers and hundreds of such layered platelets stacked into particles or tactoids [91]. Chemically, MMT consists of two silicate tetrahedral sheets sandwiching an octahedral sheet of either magnesium or aluminum hydroxide (Figure 8) [92].

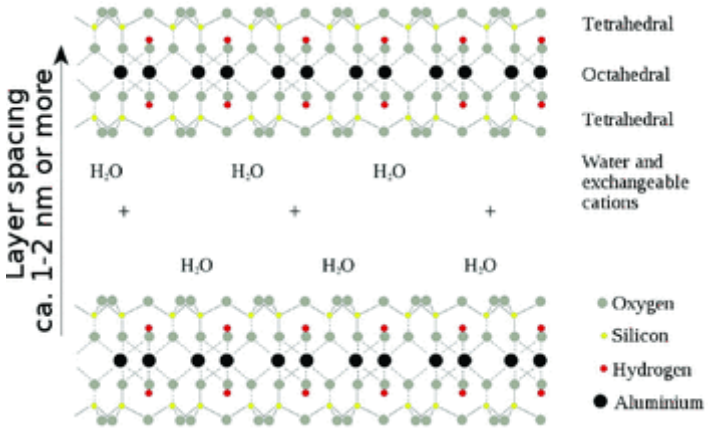

Figure 8: Structure of montmorrilonite clay [91].

Table 7 demonstrates the two classes of nanoclays which are frequently used for the development of polymer based nanoclay films.

Table 7: Types of nanomaterials employed in development of biodegradable films [93].

Inorganic	Organic (Edible)
Nano clays (layered silicates) • Montmorillonite (MMT)	Chitosan Chitin or chitosan nanostructures
Carbon nanotubes • Single-wall nanotube (SWNT) • Multiwall nanotubes (MWNT)	Cellulose • Cellulose nanoreinforcements (CNRs) • Cellulose nano-whiskers • Cellulose nanofibers (CNF)
Silica nanoparticles • Silicon dioxide nano particles	Starch • Starch nanocrystals (SNCs)

1.13.5.2.1 Types of nanocomposites

Incorporation of clay into polymer results in a class of hybrid materials composed of organic polymer and nanoscale clay fillers defined as nanocomposites [94]. Nanoclay when mixed with polymer, results in three types of composites. Commonly formed composites are tactoid, intercalated, and exfoliated structures (Figure 9). In tactoids, complete clay particles are dispersed within the clay matrix and silicate layers does not separate. Such mixture of polymer and nanoclay are microscale composites and clay only serves as conventional filler [10]. Intercalation and exfoliation produce two ideal nanoscale composites. Intercalation is described as a moderate penetration of polymeric chain into nanoclay basal spacing which results in slight expansion of interlayer spaces but the shape of layered stack remains undisturbed. In exfoliation nanoclay's layered structure loses its shape into single sheets and form more like homogenous mixture with polymeric solution [91]. Tactoids hamper the mechanical characteristics of nanocomposite based films due to its microscopic size. Intercalation or exfoliation on the other hand provides an interaction between polymer chains and layered sheet at nanoscale resulting in better film forming properties.

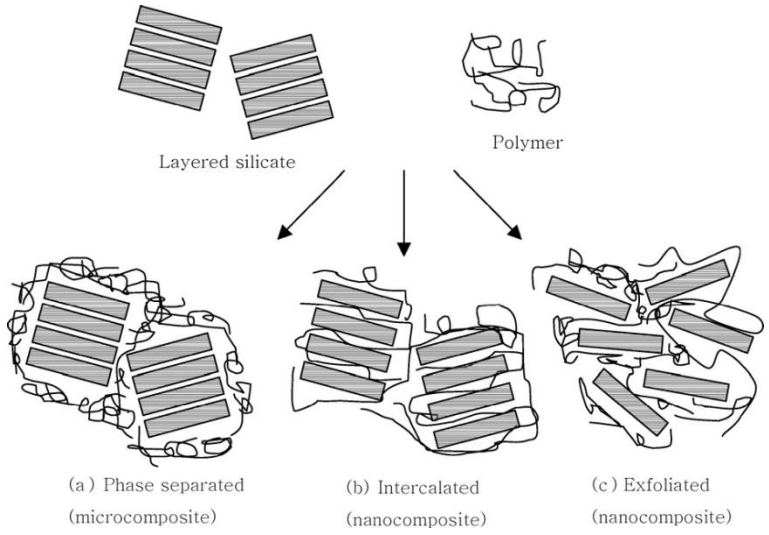

Figure 9: Types of composite structure of polymer layered silicate clay materials [95].

1.13.5.2.2 Nanocomposites in packaging

Incorporation of small percentage of nanoclay into polymer results in large scale improvement in the mechanical and physical properties including increased modulus, strength, gas barrier and water barrier properties (Table 8). This has imparted significant attention to polymer clay nanocomposite films in the recent era of food packaging.

Table 8: Different types of nanocomposites and effect of incorporation of nanoclay on functional properties of biopolymer [96].

Biopolymer	Nanofiller	Improvements
Agar	MMT	Tensile strength
Stach	MMT	Tensile strength
	Carbon nanotubes	Water vapor barrier property
	Na+MMT	Tensile strength
Cellulose	Tourmaline	Tensile strength
Pectin	MMT	Water vapor barrier property
Carrageenan	Mica	Water vapor barrier property
Soy protein	MMT	Tensile strength
		Water vapor barrier property
Wheat protein	MMT	Tensile strength
Bovine gelatin	MMT	Water vapor barrier property
Fish gelatin	MMT	Tensile strength
		Water vapor barrier property
Whey Protein	MMT	Water vapor barrier property
		Antibacterial property

Literature data demonstrates that nanoclay layered silicates significantly affect the properties of nanocomposite films because of its high aspect ratio which possibly provide greater energy transfer from one phase (polymer) to another phase (silicate layer) [97] and also due to its nanoscale size it interacts with matter at atomic, molecular or macromolecular level [98]. It was also observed that loading of nanoclay in polymer matrices induced tortuous path in film resulting in improved barrier properties of nanocompoites (Figure 10 A & B).

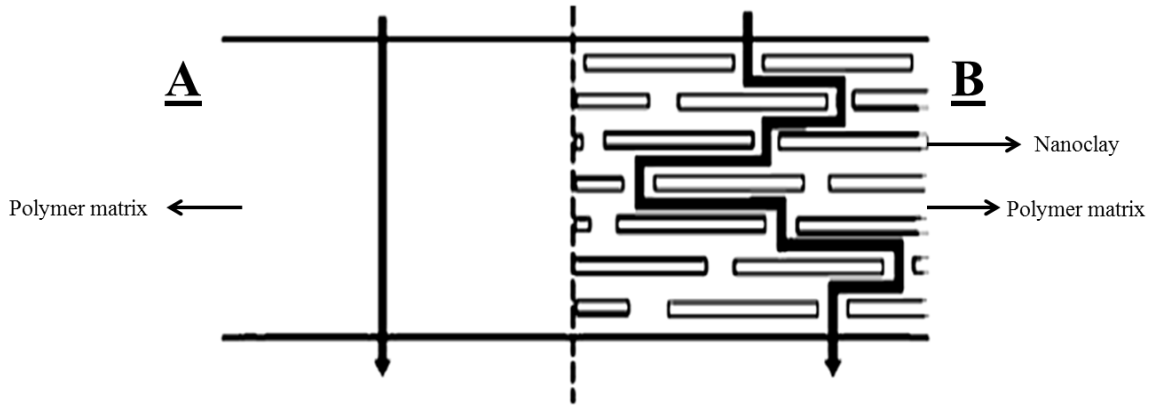

Figure 10: (A) Penetration of water molecule in pure polymer matrix (B) Tortuous path created by incorporation of nanoclay in polymer matrix.

1.13.5.3 Wax and lipids

Lipids may be broadly defined as hydrophobic, small and naturally occurring molecules that include fats, waxes, sterols, fat soluble vitamins and others. Lipid and wax based films exhibit poor mechanical properties because of their lack of cohesive structural integrity [99]. Therefore films are usually prepared by mixing lipids or waxes with protein or polysaccharide. Such films contain polymer for structural integrity and waxes or lipids for imparting hydrophobic character thus exploiting the advantages of each component to develop film having superior moisture barrier and mechanical properties (Table 9) [100]. Beeswax and paraffin wax are some of the frequently used waxes to prevent moisture loss from fruits and vegetables [38]. Paraffin wax, a byproduct of petroleum industry, however, contains some undesired chemicals [101]. Therefore, beeswax being edible and non toxic is a suitable additive for food packaging to improve water vapor barrier properties of films.

Table 9: Some examples of applications of lipid/wax based composite films on fruits and vegetables [102].

Commodity	Coating material	Primary functions
Apple (fresh-cut)	Polysaccharide/lipid bilayer	O_2/CO_2 barrier, gloss
	Wax, shellac	O_2/CO_2 barrier
	Whey protein isolate, beeswax emulsion	O_2 barrier
	Whey protein isolate, wax	O_2 barrier
Green bell pepper	Lipid based	$O_2/CO_2/H_2O$ barrier
Mango fruit	Wax, shellac, zein, cellulose derivative	$O_2/CO_2/H_2O$ barrier
Peach	Wax, carboxy methyl cellulose	H_2O barrier
Plum	Hydroxypropylmethyl cellulose/lipid composite	$O_2/CO_2/H_2O$ barrier

1.13.5.3.1 Beeswax

Beeswax is a natural wax produced in the bee hive and mainly composed of esters of fatty acids and various long chain alcohols. India is the leading producer of beeswax. It has been successfully used by several authors to reduce the water vapor permeability of biodegradable films. Addition of beeswax decreased the water vapor permeability and solubility of whey protein emulsion films [103]. Beeswax also imparted plasticizing effect on the soy protein isolate based films [104]. Similar effects were observed by Han et al. (2006) [105] after incorporating beeswax in pea starch based edible films

Incorporation of wax in biopolymer resulted in either bilayer or emulsion films [106]. It is known that emulsion films are easier and feasible than bilayer films in terms of

preparation procedures [107]. However, the effectiveness of emulsion films in improving water vapor barrier property is strongly dependent on the presence of surfactant [108]. Surfactants posses hydrophilic and hydrophobic groups simultaneously, thus reducing the surface tension of the film forming solution [109].

1.13.5.4 Surfactants

Variety of surfactants has been used by several authors to develop biodegradable packaging (Table 10). Surfactants with higher hydrophilic/lipophilic balance (HLB) value allow a greater association of their hydrophilic fraction with the hydrophilic film matrix, which may reduce the amount of water binding sites of polymer while the hydrophobic fraction may act as a barrier for water vapor [110]. There are very few reports on the effect of tween 80 on wax composite films, however, it can be a good surfactant for food packaging owing to its high HLB value (>10), edibility and non toxicity. Tween 80 has been used by Brandelero et al. (2012) [111] for prevention of phase separation between thermoplastic starch and poly (butylene adipate co-terephthalate) and soybean oil. Tween 80 also enhanced the hydrophobicity of the gelatinized starch plus carnauba wax [112].

Table 10: Surfactants used for the development of biobased film.

Surfactant	Polymer	Reference
Lecithin or yucca extract	Gelatin based edible films	134
Tween 80, Span 80	Chitosan film	135
Tween 20, Span 80, soy lecithin	Potato starch	136
Sucrose ester	Tapioca starch/dHG	137
Stearoyl-2-lactil-sodium lactate, sucrose ester	Polysaccharides and/or lipids	138
Span 20	Soyabean protein isolate	139

1.13.5.5 Antimicrobial agents

To control undesirable microorganisms on foods, antimicrobial compounds can be incorporated in to food packaging materials. Antimicrobial packaging is a promising form of active packaging to improve safety and shelf-life of food products. There are wide range of antimicrobial agents for food packaging such as weak organic acids, enzymes like lysozyme, nisin etc. (Table 11) [1]. However, literature survey suggests that plant extracts such as grape fruit seed extract target wide range of microorganism unlike other antimicrobial agents (Table 11).

Table 11: Examples of films incorporated with antimicrobials that are used for food packaging [119].

Antimicrobials	Polymer/carrier	Main target microorganisms
Organic acids/anhydrides: Propionic, benzoic, sorbic, acetic, lactic and malic	Edible films, EVA, LLDPE	Molds
Enzymes: Lysozyme, glucose oxidase	Cellulose acetate, PS, Edible films	Gram positive bacteria
Spices: Cinnamic, caffeic,	Nylon/PE, cellulose	Molds, yeast,
Plant extracts: bamboo powder, rheum palmatum, coptis chinesis extracts and grapefruit seed extract, hinokitiol	LDPE, cellulose	Mold, yeast and bacteria

1.13.5.5.1 Grape pomace

Grape (except for orange) is the world's largest fruit crop, cultivated mainly as *Vitis vinifera* for wine production [120]. Grape pomace consists of the grape skins and seeds and is the main by-product of wine industry. It consists of bioactive metabolites of polyphenolic nature (Figure 11) [121]. Many studies have highlighted that the flavanoids and polyphenols content of grape pomace are beneficial for human health [122, 123]. In particular, skins are rich in anthocyanins, a group of polyphenols well known for their useful properties [124]. Therefore, extract from grape pomace is being used as a food additive in several countries. It also possesses wide spectrum antimicrobial activity against food borne pathogens such as *Staphylococcus aureus, Escherichia coli, Listeria species etc.* [121, 125].

Water being the most widely used solvent for biodegradable packaging, grape aqueous extract can be useful in imparting inherent antimicrobial properties to the films. Further, the antimicrobial activity of grape extract is reported to be stable even at higher temperatures. As a result, grape extract is expected to retain its antimicrobial activity, even when subjected to high temperatures during the process of film extrusion [1].

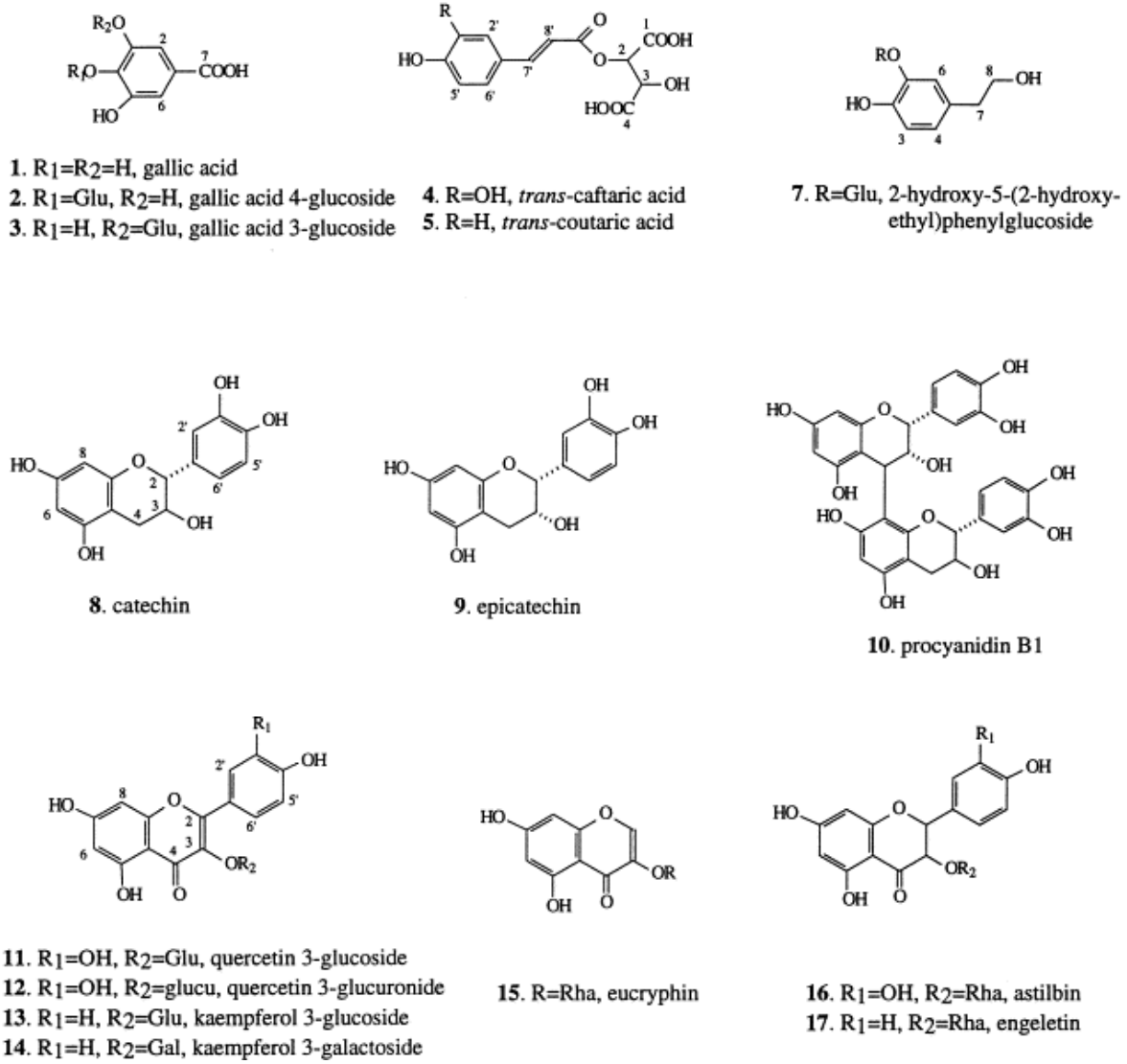

Figure 11: Chemical structures of polyphenols from grape pomace [122].

Literature survey suggests that grape pomace extract is a cheap source of polyphenols and antimicrobial agents. In spite of these properties of grape pomace extract, very few reports exist on development of biodegradable active food packaging incorporating this extract. Grape seed extract incorporated pea starch films reduced the bacterial growth on pork loins infected with *Brochothrix thermosphacta* [126]. Starch based film biodegradability rate was reduced by winery bio waste as compared to pure starch film [127]. Pomace extract based films with different types of biopolymer demonstrated antimicrobial activity against food pathogens [128]. Thus incorporation of pomace extract in to various other biopolymers and applying the resultant films for improving the shelf-life of variety of packed food products appears promising.

1.14 Optimization of various film additives

Various additives, as discussed above, alone or along with other additives alter or improve one or more packaging film properties. Effectiveness of these additives will however depend on its optimum concentration in films. Hence, the concentration of different additives in film needs to be optimized to get the desired result. Various tools are available for optimization such as Response Surface Methodology (RSM), Plackett–Burman Design, Robust Parameter Design etc. RSM is one of the most frequently used tools for the process optimization because it is easy to estimate and apply.

1.14.1 Response Surface Methodology (RSM)

This method was introduced by G. E. P. Box and K. B. Wilson in 1951. RSM has been reported to be an effective tool for optimizing a process when the independent variables

(additives) have a combined effect on the desired response (film properties in the present case) [129]. The basic principle of RSM is to relate product properties of regression equations that describe interrelations between input parameters and properties of products [130]. In order to understand better, the individual and interactive effects of variables on biofilm parameters, RSM was earlier used by several authors (Table 12). Two experimental design of RSM which are frequently used for optimizing variables in biopolymer based films are Box Behnken design and central composite design. Optimization of different biopolymer content in composite films, pH, drying and storage conditions for better film properties by RSM has been reported earlier as shown in table 10.

Table 12: Optimized variables for different biofilms by Response Surface Methodology.

Polymer	**Optimized variables**	**References**
Wheat gluten	Cellulose nanofibrils, glycerol and sodium dodecyl sulfate	[131]
Methyl cellulose	Pediocin and zinc oxide nanoparticles	[132]
Chitosan	Temperature, relative humidity and storage period	[133]
Whey protein isolate	pH and corn oil	[134]
Tapioca starch	Tapioca starch, glycerol, agar and span 80	[109]
Poly(vinyl alcohol)/cornstarch	Amylase and glycerol	[135]
Starch	Stearic acid glycerol	[136]
Tapioca starch	Glycerol and chitosan	[137]
Poly(vinyl alcohol)/starch blended plastic resin	Glycerol and ethylene acrylic acid	[130]
Soy protein isolate	Temperature and relative humidity	[138]

1.15 Edible coating

Besides standalone film as discussed above, edible coating is another form of packaging which enhances the quality of food products, protecting them from physical, chemical and microbiological deterioration [41] being an effective carrier of nutraceuticals and antimicrobial agents. Edible coating, an integral part of food product, is a thin layer of edible material (generally regarded as safe) applied to the product surface in addition to or as a replacement for natural protective waxy coatings and to provide a barrier to moisture, oxygen, and solute movement for the food [139]. They are applied directly on the food surface by dipping, spraying, or brushing to create a modified atmosphere.

The main purpose of the development and improvement of standalone film or edible coating is to protect the packed food products. Beside packaging, irradiation has also been extensively used for the shelf-life extension of food products.

1.15.1 Edible coating for fresh fruits

Fruits are highly perishable as they contain 80 to 90% water by weight. In addition, fresh fruits get easily contaminated leading to spoilage and other biochemical deteriorations such as browning, off flavor development, and texture breakdown thereby reducing consumer acceptability [140]. Edible coatings provide an additional protective coating to fresh produce and an alternative to modified atmosphere storage. This has led to extensive work on development of edible coatings for fruits (Table 13). One major advantage of using edible films and coatings is that several active ingredients can be incorporated into

the polymer matrix which can be consumed with the food. Thus apart from enhancing safety it provides additional nutritional and sensory attributes to the product [140].

Table 13: Edible coating used for different fruits [140].

Coating material	Composition	Fruit
Semperfresh™	Sucrose esters, short chain unsaturated fatty acid esters, sodium salts of CMC, mono and diglycerides	Apple and banana
Prolong	Sucrose fatty acid esters, sodium CMC, mono and diglycerides	Mango and pear
Tal Prolong	Sucrose fatty acid esters, sodium CMC, mono and diglycerides	Mango
Nature seal™	Cellulose	Mango and pome fruit
Chitosan	Tween 80	Strawberry, apple, pear, plum, peach, lichi, cucumber and bell pepper
Nutri save	N,O carboxyl methyl chitosan	Apple, pear and pomegranate
Brilloshine	Sucrose esters and wax	Apple, avocado, citrus and melon
Nu coatFlo and Ban seel	Sucrose esters of fatty acids and sodium salt of CMC	Apple, banana, cucumber, guava, melon, peach and plum
Citrashine	Sucrose ester and wax	Mandarins
Casein	Calcium caseinate	Bell pepper

1.16 Fresh cut fruit-Pomegranate arils

Pomegranate (*Punica granatum*) is an exotic fruit bearing deciduous shrub. Aril is the specialized outgrowth from the funiculus (attachment point of the seed) that covers or is attached to the seed. India ranks first in the world with respect to pomegranate cultivation area (0.125 million ha) and production (1.14 million tonnes) [141]. Removal of pomegranate cuticle to obtain the arils is a tedious process. Therefore, marketing of pomegranate arils in 'ready to eat' form would be a convenient and desirable alternative to the consumption of the whole fruit [142]. Pomegranate aril as a minimally processed

product is highly prone to microbial contamination because of removal of thick protective cuticle.

1.16.1 Edible coatings for pomegranate arils

Edible coating of arils is an effective way to increase its shelf-life. Romero et al. (2013) [143] demonstrated that aloe vera gel coating maintained the quality and safety of pomegranate arils. It was also reported that chitosan coating inhibited bacterial and fungal growth on the surface of arils [144]. Edible starch based coating including *Nigella sativa* oil greatly reduced softening of pomegranate arils, weight loss and percent of browning index, loss of vitamin C, loss of anthocyanin content and delayed microbial decay [145]. The effect of carboxy methyl cellulose and gelatin based edible coating as a carrier of essential oils (lavender, lemon grass and peppermint) and ultraviolet light on quality of pomegranate arils was studied by Salama et al. (2012) [146]. Honey solution dip treatments extended the fresh like quality of minimally processed arils by delaying quality loss, microbial development, and pigment changes [147].

1.17 Scope of the work: Aims and objective

Plastics are the most commonly used material used for food packaging. However, conventional plastics owing to their origin from petroleum source impose threat to environment. Biopolymer based biodegradable films can be a suitable alternative for such packaging. Various biopolymer based films have been documented by researcher but their inherent properties are not comparable to the commercially available counterparts hence lack commercial applications. Guar gum can be a suitable polymer in this regard due to

its edibility, renewability and aqueous solution forming properties. In light of available information, principal aim of this thesis was the development and improvement of biodegradable packaging and its subsequent application for food packaging to reduce or eliminate usage of petroleum based plastics (Figure 12).

The detailed objective of the project is listed below:

- Development of biodegradable packaging films using biopolymer.
- Use of gamma radiation, nanomaterials and other additives such as beeswax for improving functional and mechanical properties of biodegradable films.
- Development of active packaging films with possible antioxidant and antimicrobial functions.
- Potential technological applications with a focus on radiation processed food.

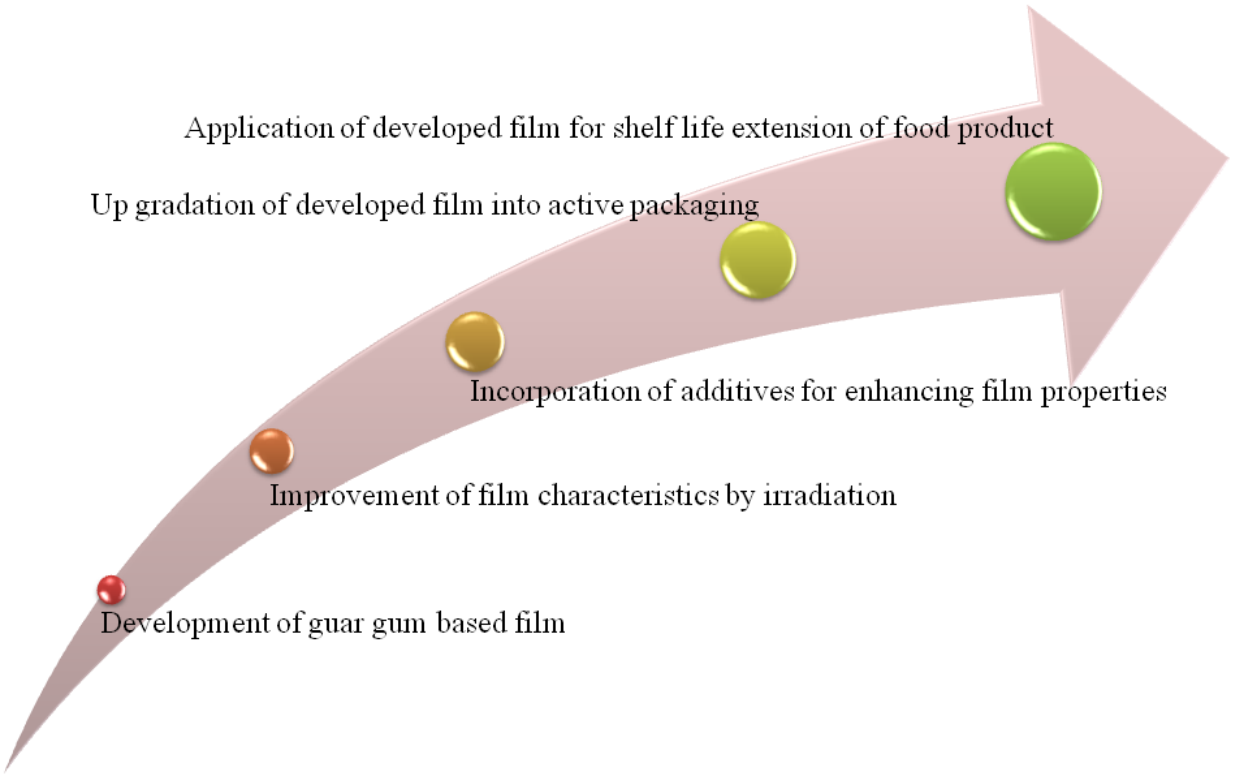

Figure 12: Flow chart of the project.

2. Materials and Methods

2.1 Preparation and characterization of non-irradiated and irradiated GG films

2.1.1 Purification

2.5 gm of GG (Merck, India ltd.) was dissolved in 250 mL of distilled water by using shear mixer (Omni mixer, Sorvall, U.S.A.) at a speed corresponding to the position of the knob at 2 for 2 min. Solution thus obtained was kept overnight on magnetic stirrer at room temperature (25 ± 2°C). Resulting solution was centrifuged at 8600 g for 30 min for removal of insoluble impurities and high molecular weight fractions of GG. Ethanol was added to the supernatant in a ratio of 2:1 for precipitation of GG. The suspension was kept overnight and the precipitate obtained was freeze dried under room temperature using Scanvac Coolsafe 55-4 Pro to obtain purified dry GG powder. Yield of the purified GG was 60% (w/w).

2.1.2 Irradiation of GG

Purified GG was subjected to radiation processing as a dried powder and as 1% (w/v) aqueous solution using a ^{60}Co gamma irradiator (GC-5000, BRIT, India) having a dose rate of 4.1 kGy/h. In the powder form, GG was subjected to varying doses (0.25, 0.5, 0.75, 1, 5, 10, 25 and 50 kGy) while aqueous solution was exposed to doses of 0.1, 0.2, 0.5, 1, 2, 3, 4 and 5 kGy.

2.1.3 Viscosity average molecular weight of GG by Ostwald viscometer

Viscosity average molecular weight of GG post irradiation (powder form and aqueous form) was measured usinga Ostwald's viscometer at constant temperature of 24 ± 1 °C. A 0.1% w/v aqueous solution was prepared from control and irradiated GG and specific viscosity (η_{sp}) was obtained using following equation:

$[\eta_{sp}] = \frac{t-t_0}{t_0}$

t = flow time of a polymer solution through viscometer

t_o = flow time of the pure solvent through the same viscometer

Intrinsic viscosity (η) was then calculated from η_{sp}using following equation.

$[\eta] = [\eta_{sp}]/c$

c = polymer concentration

Viscosity average molecular weight (M_v) was calculated from η [148].

$[\eta] = KM_v^a$

K and *a* are the parameters that depend on the solvent-polymer pair. The *a* and *K* values used for guar galactomannan were 0.72 and 5.13×10^{-4} respectively [149].

2.1.4 Molecular weight and polydispersity index analysis by gel permeation chromatography

Number average molecular weight (M_n), weight average molecular weight (M_w) and polydispersity index (PDI) (M_w/M_n) were determined by gel permeation chromatography (GPC) on a HPLC system (Ultimate 3000, Dionex corporation, Germany) equipped with a 5u Biobasic SEC-1000 column (300 mm length × 4.6 mm I.D.; Thermo scientific, UK) and having a differential refractive index detector (RI-101, Shodex corporation, USA). The mobile phase was deionized water (Millipore, Bedford, MA) and the flow rate was fixed at 0.6 mL/min. All GG samples (irradiated and control) were injected (20 µL) as their aqueous solutions at concentrations of

0.2% (w/v) which were centrifuged at 15000 g for 15 min prior to analysis. The column was calibrated using pullulan standards ranging from molecular weights of 6000 to 2,560,000 Da. Pullulan standards were analyzed using similar HPLC conditions described above.

Number average molecular weight (M_n) was calculated by following equation.

$$M_n = \sum\left(\frac{N_i}{\sum N_i} \times M_i\right)$$

Where N_i = detector response at a particular time

$\sum N_i$ = Total detector response

M_i = Molecular weight at given time

Weight average molecular weight was calculated by following equation

$$M_w = \sum\left(\frac{Ai \times Mi}{\sum Ai}\right)$$

Where $A_i = N_i \times M_i$

Based on M_n and M_w, PDI was calculated using equation given below

$$PDI = \frac{M_w}{M_n}$$

2.1.5 Determination of galactose to mannose ratio by HPLC

Control and irradiated GG samples were hydrolyzed with 1 N sulphuric acid at 90 ºC for 5 h. After hydrolysis, samples were neutralized using barium hydroxide and the

barium sulfate precipitates thus formed were removed by centrifugation at 15000 g for 10 min. Supernatants were freeze dried and dried powder obtained was dissolved (1% w/v) in 70:30::acetonitrile:water and filtered through 45 µm filter prior to analysis. Samples were then analyzed using HPLC system (Quaternary gradient pump, PU-2089 plus, Jasco, Japan) equipped with High Q silica base amino column (Hi Q SIL NH_2, KYA TECH Corporation, Japan) with column dimension 4.6 mm I.D. × 250 mm L and refractive index detector ((RI-2031 plus, Jasco, Japan). The mobile phase was 80:20::acetonitrile:water with a flow rate of 1 mL min^{-1}. 100 µL of all GG samples were injected. Standard curves for both galactose and mannose were made from 0.25 mg to 1 mg using similar HPLC conditions described above. Linear regression equations for both standards were then obtained.Galactose and mannose content in the hydrolyzed GG samples was calculated using linear regression equations obtained above and the G/M ratio was determined.

2.1.6 Film preparation

1.5 g of GG (irradiated and control) was added into 150 mL water along with 0.5 mL of glycerol (Sigma Aldrich, USA) (40 % w/w of GG) as plasticizer and kept overnight at room temperature (25 ± 2°C) on magnetic stirrer. Solution thus obtained was centrifuged at 950 g for 15 min for the removal of air bubbles. 150 mL of the solution was poured and spread evenly onto the surface of a glass plate (21 cm × 21 cm), having a removable boundary made up of insulating tape. Plates were then dried in an oven at 80 °C for 8 h. Dried GG films were conditioned at 50 % relative humidity at room temperature (25 ± 2°C) for 7 days. After conditioning, films were pealed and subjected to physical and mechanical analysis. Additionally, films were also prepared

form irradiated aqueous GG solution by directly adding glycerol (40% w/w of GG) in to the solution and then further processed as detailed above. In another set of experiments, films were also prepared from unpurified native GG in the same manner as above. Regression equation for mannose was $y=192.65x-1074.5$, $R^2=0.9905$, and for galactose was $y=251.07x-19969$, $R^2=0.9941$, where y was peak area and x was amount in µg.

2.1.7 Irradiation of GG films

GG films prepared from control samples were also directly subjected to irradiation processing (1, 5, 10, 25, 50 and 100 kGy) at room temperature in ^{60}Co gamma irradiator (GC-5000, BRIT, India) having a dose rate of 4.1 kGy/hr. The treated films were conditioned as mentioned above (section 2.1.6) prior to analysis of their physical and barrier properties.

2.1.8 Analysis of physical and mechanical property

GG films were cut into strips of dimension 2 cm × 15 cm. A micrometer (103–131, Mitutoyo, Japan) was used to determine film thickness. Measurements were randomly taken at three different locations on each film strip. The mean value of thickness of each strip was used to calculate tensile strength andYoung's modulus. Mechanical properties of films were analyzed using a Texture analyzer (TA.HD Plus, Stable Micro Systems). The American Society of Testing and Materials (ASTM) standard method D882-10 was used to measure the tensile strength, Young's modulus and percent elongation at break of the films. Puncture strength of films (5 cm × 2 cm) were determined by 2 mm needle probe having test speed of 30 mm/min.Water vapor

transmission rate (WVTR) of GG films were determined by using round cups having 100 mL volume capacities and having 120 cm^2 mouth area. It was filled with 60 mL of distilled water and sealed with GG film using adhesive tapes. The whole assembly was then kept in a desiccator at 25 ± 2 ºC. A RH gradient of 87% was used and maintained by using aqueous solution of H_2SO_4. The mass of water lost from the cup was monitored as a function of time, and the WVTR was calculated from the steady state region of a graph of time v/s water loss.

Color of films were determined using a colorimeter (CM-3600d Konica Minolta sensing Inc., Japan) by measuring *L** (lightness), *a** (−green, +red) and *b** (−blue, +yellow) values. Instrument was calibrated using a white tile supplied along with the equipment. Source used was D65 with observer set at 10 degrees. Opacity is a measure of the extent of light passing through any material. Opacity of films was determined using Hunter lab method. The relationship between reflectance of each sample on standard black tile and the reflectance on standard white tile was determined using an equation as given below:

$$\text{Opacity} = (Y_b/Y_w) \times 100$$

2.1.9 Small angle X-rays scattering (SAXS) measurements

SAXS measurements were performed on the aqueous solution of the control, 500 Gy and 50 kGy dose treated polymer at a lab based SAXS setup using CuKα source. Size of the incident photon beam on the sample was 0.4 mm diameter. The SAXS detector was mounted at a sample-to-detector distance of 1.07 m, correspondingto a q-range of 0.1–2.5 nm^{-1}. The magnitude of the scattering wavevector, q equals:

$q = 2 \sin\theta/\lambda = q/2\pi$

where 2θ is the scattering angle and λ=0.154 nm the wave length used.

2.1.10 FTIR analysis

Spectra of GG films were scanned in the range of 4000–600 cm^{-1} on a FTIR (FT/IR 4100, Jasco) spectrometer using an ATR assembly. Films were directly pressed on ATR assembly and spectra were recorded. 40 scans were taken for each film sample.

2.1.11 Thermogravimetric Analysis (TGA)

TGA of the films was carried out using a Diamond TG/DTA (PERKIN ELMER,USA) analyzer. The experiment was carried out under an argon atmosphere (40 cm^3min^{-1}). The samples were heated from 40 °C to 605 °C at a rate of 10 °Cmin^{-1}.

2.2 Preparation and characterization of GG based nanocomposite films

2.2.1 Dispersion of nanoclay

Cloisite 20A is a natural MMT modified with a quaternary ammonium salt while nanofil 116 is an inorganic nano-dispersible layered silicate based on a refined natural bentonite. Both the clays were obtained as a gift sample from Southern Clay Products, Inc., US. Rockwood Additives Ltd., UK. Different dilutions of aqueous nanoclay suspensions (0.01, 0.025, 0.05, 0.075, 0.1 and 0.2 % w/v of distilled water) were prepared and then separately kept on a magnetic stirrer for 7 days at low temperature (5 ± 0.5 ºC) to avoid microbial contamination. After 7 days of mixing, obtained

nanoclay suspension was centrifuged at 1700 g for 10 min at 10 ºC to pellet out nanoclay tactoids.

2.2.2 Nanocomposite film preparation

1.5 gm of purified controlGG was added into 150 mL of dispersed nanoclay suspension along with 0.6 g of glycerol (40% w/w of GG) as plasticizer and kept overnight at room temperature (25 ± 2 °C) on a magnetic stirrer. The resultant suspension was then further processed as detailed in section 2.1.6. Amount of nanoclay on w/w basis w.r.t. GG was 1, 2.5, 5, 7.5, 10, 15 and 20 %. In another set of experiment nanocomposite films were prepared from 500 Gy irradiated GG.

2.2.3 Irradiation of nanocomposite films

GG based films incorporated with 2.5% nanofil 116 or 10% cloisite 20A were subjected to gamma irradiation (1, 5, 10, 25, 50 and 100 kGy) at room temperature in ^{60}Co gamma irradiator (GC-5000, BRIT, India, dose rate 4.1 kGyhr^{-1}). The treated films were conditioned as mentioned above (section 2.1.6) prior to analysis of their physical and barrier properties.

2.2.4 Characterization of nanocomposite film

Method as detailed in section 2.1.8, 2.1.10 and 2.1.11 was followed.

2.2.5 X-rays scattering measurements

SAXS measurements were performed on the cloisite 20A composite films (films were 4 times folded) and powder cloisite 20A using a lab based SAXS setup as detailed in

section 2.1.9. Interlayer distance (d or d-spacing) between clay layers was estimated from:

$d = 2\pi/q$

X-ray powder diffraction (XRD) measurements were performed on nanofil 116 powder andnanofil 116 composite films (films were 4 times folded). XRD patterns were obtained on a Philips PW-1820 powder diffractometer using CuKα radiation. The X-ray tube rating was maintained at 30 kV and 20 mA. The goniometer was calibrated for correct zero position using silicon standard. Interlayer distance between clay layers can be estimated from Bragg's equation[150]:

$d = \lambda / (2\sin(\theta))$

2.2.6 Field Emission Gun-Scanning Electron Microscopes (FEG-SEM)

The surface morphology of nanocomposite films was analyzed by FEG-SEM. The scanning electron micrographs were taken with a JSM-7600F instrument (Joel, Japan). A sputter coater was used to precoat conductive gold onto the films surface before observing the microstructure at 25 kV.

2.3 Preparation and characterization of GG based emulsion films

2.3.1 Irradiation of beeswax

Refined yellow beeswax was purchased from Sigma Aldrich, USA. Beeswax were subjected to gamma irradiation (5, 25, 50 and 100 kGy) at room temperature, using a ^{60}Co gamma irradiator (GC-5000, BRIT, India) having dose rate of 3.6 $kGyhr^{-1}$.

2.3.2 Neutral lipid composition of beeswax

Beeswax (control and irradiated) was dissolved in distilled chloroform (10 % w/v). 15 µL of solution thus obtained was loaded onto silica gel 60 TLC (Kieselgel 60, Merck, Germany). Neutral lipids were analyzed using a mobile phase consisting of petroleum ether (b.p. 60-70 °C): diethyl ether: acetic acid (90:10:1). The individual lipid class was identified from reported R_f values as well as by comparison with R_f values of co-chromatographed standard compounds [151]. The separated spots were visualized by exposing the plate to iodine vapor and the relative area of the individual spots was quantified on a TLC-densitometer (CS9301PC, Shimadzu, Japan).

2.3.3 Intrinsic viscosity of beeswax by Ostwald viscometer

Intrinsic viscosity of beeswax (control and irradiated) was measured using Ostwald's viscometer at constant temperature of 24 ± 1 °C. Beeswax was dissolved in distilled chloroform (2% w/v) and its intrinsic viscosity was obtained by using equations described in section 2.1.3.

2.3.4 Fourier transform infrared spectroscopy (FTIR) analysis of beeswax

Spectra of control as well as irradiated solid beeswax was scanned in the range of 4000–650 cm^{-1} on a FTIR (FT/IR 4100, Jasco) spectrometer. ATR assembly was used for obtaining FTIR spectra. Samples were directly pressed on ATR assembly and spectra were recorded. 40 scans were taken for each film sample.

2.3.5 Experimental design

Results of Response Surface Methodology (RSM) experiments were analyzed by Design-Expert 8.0.1 software (Stat-Ease Inc., U.S.A.). A full rotatable ($k < 6$) Central Composite Design (CCD) was adopted for the present study. In CCD each independent variables was varied over 5 levels: plus and minus alpha (axial points), plus and minus 1 (factorial points) and the center point. The total number of test runs needed for this design was 30. Three duplicates were included at the centre of the design. Center point concentration of nanoclay, glycerol, beeswax and tween 80 were 5, 20, 1.25 and 0.75 (w/w of GG) for present experimental design (Table 14). Two set of RSM was conducted one with control beeswax and the other with 50 kGy irradiated beeswax with other additives remaining the same. Coded and actual values of independent variables and their responses are shown in Table 14. Beeswax (control or 50kGy irradiated), nanofil 116 (suspension as detailed in section 2.2.1), tween 80 and glycerol were independent variables and tensile strength, Young's modulus, percent elongation, puncture strength and WVTR were response parameters in this experimental design. The lowest and highest levels of independent variables investigated were chosen based on results from preliminary tests.

Table 14: Experimental design as rotatable Central Composite Design.

Std	Run	Beeswax (% w/w GG) (control or 50 kGy irradiated)	Tween 80 (%w/w GG)	Glycerol (%w/w GG)	Nanofil 116 (%w/w GG)
1	15	0.63 (-1)	0.63 (-1)	10 (-1)	2.5 (-1)
2	19	1.88 (1)	0.63 (-1)	10 (-1)	2.5 (-1)
3	22	0.63 (-1)	0.88 (1)	10 (-1)	2.5 (-1)
4	12	1.88 (1)	0.88 (1)	10 (-1)	2.5 (-1)
5	1	0.63 (-1)	0.63 (-1)	30 (1)	2.5 (-1)
6	29	1.88 (1)	0.63 (-1)	30 (1)	2.5 (-1)
7	23	0.63 (-1)	0.88 (1)	30 (1)	2.5 (-1)
8	8	1.88 (1)	0.88 (1)	30 (1)	2.5 (-1)
9	10	0.63 (-1)	0.63 (-1)	10 (-1)	7.5 (1)
10	21	1.88 (1)	0.63 (-1)	10 (-1)	7.5 (1)
11	9	0.63 (-1)	0.88 (1)	10 (-1)	7.5 (1)
12	20	1.88 (1)	0.88 (1)	10 (-1)	7.5 (1)
13	26	0.63 (-1)	0.63 (-1)	30 (1)	7.5 (1)
14	17	1.88 (1)	0.63 (-1)	30 (1)	7.5 (1)
15	27	0.63 (-1)	0.88 (1)	30 (1)	7.5 (1)
16	11	1.88 (1)	0.88 (1)	30 (1)	7.5 (1)
17	24	0 (-2)	0.75 (0)	20 (0)	5 (0)
18	4	2.5 (2)	0.75 (0)	20 (0)	5 (0)
19	5	1.25 (0)	0.5 (-2)	20 (0)	5 (0)
20	6	1.25 (0)	1 (2)	20 (0)	5 (0)
21	3	1.25 (0)	0.75 (0)	0 (-2)	5 (0)
22	7	1.25 (0)	0.75 (0)	40 (2)	5 (0)
23	28	1.25 (0)	0.75 (0)	20 (0)	0 (-2)
24	13	1.25 (0)	0.75 (0)	20 (0)	10 (2)
25	16	1.25 (0)	0.75 (0)	20 (0)	5 (0)
26	2	1.25 (0)	0.75 (0)	20 (0)	5 (0)
27	30	1.25 (0)	0.75 (0)	20 (0)	5 (0)
28	25	1.25 (0)	0.75 (0)	20 (0)	5 (0)
29	14	1.25 (0)	0.75 (0)	20 (0)	5 (0)
30	18	1.25 (0)	0.75 (0)	20 (0)	5 (0)

Actual values for various independent variables are shown while their values in coded form are given in bracket.

2.3.6 Preparation of GG based emulsion film

Purified GG (1.5 g) was added into 150 mL of dispersed nanofil 116 suspension (as detailed in section 2.2.1) along with glycerol, beeswax (control or 50 kGy irradiated) and tween 80 and resulting solution was kept overnight at room temperature (25 ± 2 °C) on magnetic stirrer. Thus the amount of nanoclay on w/w basis with respect to GG was 2.5, 5, 7.5 and 10%. Amount of various additives such as glycerol, beeswax

(control or 50 kGy irradiated), nanofil 116 and tween 80 were according to RSM experimental design detailed in table 14. Solution thus obtained was heated at 80 °C for 1 h while continuous stirring to melt the beeswax. Later, 150 mL of solution (while hot) was poured and spread evenly onto surface of glass plate (21 cm × 21 cm), having removable boundary made up of insulating tape. For drying, plates were immediately kept in pre-warmed oven at 80 °C for 8 h. Further conditioning of films was done as described in section 2.1.6. Two types of films were prepared; one with control beeswax and the other one with 50 kGy irradiated beeswax.

2.3.7 Characterization of emulsion films

Method as detailed in section 2.1.8, 2.1.10 and 2.1.11 was followed.

2.4 Preparation and characterization of GG based active films

2.4.1 Preparation of grape pomace

Red wine grapes (Shiraz variety), was chosen for the present study. Grapes were harvested at optimum maturity from vineyards located at Narayangaon, Maharashtra. Samples were brought to laboratory within twelve hours of harvesting. Pomace preparation was carried out essentially as per procedure detailed earlier [152]. In brief, berries (2 kg) were crushed and pH of the resultant must was adjusted to 3.5 using tartaric acid. To the must was then added 50 ppm potassium metabisulfite ($K_2S_2O_5$). After 2 h the must was inoculated with 1% yeast (*Saccharomyces cerevisiae*) inoculum and fermentation was carried out at 25 ± 1 °C. During fermentation flasks were shaken twice a day and cotton plug was removed for a while to facilitate CO_2 removal. After completion of fermentation (200 h) seeds and skins (pomace) were

separated from wine by straining through muslin. The residue designated as grape pomace was freeze dried and stored at -20°C till further use.

2.4.2 Batch extraction and concentration

10 g of dried grape pomace was powered for 30 sec using a high speed homogenizer (B400, Buchi, Switzerland). Extraction of pomace powder thus obtained was carried out using pressurized solvent extractor (Speed Extractor E-914, BUCHI, Switzerland). 2 g of pomace powder was taken in a thimble (Whatman filter paper 42) and then placed in 40 mL extraction cell. The powder was extracted at 70 °C using 60% aqueous ethanol (100 bar, flow rate of 10 mL/ min) using 2 cycles. First cycle had a heat up time of 3 min followed by 5 min holding time at 70 °C and 100 bar and then 5 min discharge time. Second cycle had heat up, holding and discharge time of 1, 5 and 5 min respectively. Finally, samples were flushed for 2 min by solvent and then by N_2 gas for 3 min. Obtained extract was concentrated by using rotavapor (Rotavapor R-114, BUCHI, Switzerland) and stored at -20 °C till further use.

2.4.3 Analysis of grape pomace extracts

Pomace extract were analyzed for total phenolic content by Folins-ciocalteu method and antioxidant capacity by DPPH and FRAP assay using standard methods described previously [153]. Forty times diluted extract samples were used for Folin's, DPPH and FRAP assay.

2.4.3.1 Total phenolic Content

The diluted sample (100 µL)was mixed with 250 µL of Folins-ciocalteu reagent and 6% sodium carbonate solution. After 30 min of incubation O.D. was taken at 725 nm.Gallic acid (GA) standard curve was obtained in concentration range of 5-20 µg mL^{-1} using same procedure as above and total phenolics were represented as mg GA equivalents (GAE) g^{-1} of grape pomace.

2.4.3.2 DPPH assay

100 µL of diluted extract was mixed with 1 mL of 105 µM solution of DPPH. Mixture was then incubated for 20 min in dark and O.D. was taken at 520 nm. Trolox standard curve was obtained in concentration range of 1-10µg mL^{-1} and total antioxidant capacity was expressed as mg trolox equivalents (TE) g^{-1} of pomace.

2.4.3.3 FRAP assay

In 200 µL diluted sample, 800 µL of phosphate buffer (0.2 M, 7.2 pH) along with 500 µL of 1% potassium ferricyanide ($K_3[Fe(CN)_6]$) was added. Resulting mixture was incubated in dark for 20 min at 50 °C. After incubation 500 µL of 10 % solution of trichloro acetic acid (TCA) was added in solution. In 500 µL of obtained mixture 500 µL of distilled water and 100 µL of 0.1% $FeCl_3$ was added. O.D. was taken at 700 nm after incubation of 10 min in dark. Trolox standard curve was obtained in range of 15-70 µg and results expressed as mg trolox equivalents (TE) g^{-1} of pomace.

2.4.3.5 Total flavanoid content

The $AlCl_3$ method reported by Luximon-Ramma et al. was used for determination of total flavonoid content [154]. To aliquots of 1.5 mL of extract was added equal volume of a solution of 2% AlCl3.6H_2O (2 g in 100 mL water). The mixture was vigorously shaken, and absorbance was read at 367.5 nm after 10 min of incubation. Flavonoid content was expressed as mg quercitin equivalent (QE) g^{-1} of pomace.

2.4.3.6 Total anthocyanin content

Total anthocyanin content (TAC) of diluted extract (1/100 (v/v) with 1% (v/v) of HCl) was measured at 520 nm [155]. TAC was calculated as mg malvidin-3-glucoside L^{-1} equivalents. Standard curve of malvidin-3-glucoside was prepared in concentration range of 0.0375 to 5 μg mL^{-1}. TAC in the extract was calculated using a linear regression equation obtained from standard curve.

2.4.3.7 Ascorbic acid content:

Total vitamin C content of pomace was estimated in accordance with standard AOAC official titrimetric method [156]. Ethanolic extract of pomace was appropriately diluted with 20% metaphosphoric acid and the obtained solution was titrated with 2,6 dichlorophenol indophenols (DCPIP). The end point of the reaction was detected by appearance of pink color by excess of the dye in the solution. The same process was followed for standard ascorbic acid solutions of known concentration (0.1–0.0015 %). Ascorbic acid content was expressed as mg/100 g of pomace.

2.4.4 Preparation of RSM optimized active films

Different amounts of grape pomace extract (0.5, 1, 2.5, 5 and 7.5 % w/w of GG) was added along with 3.5 g of GG in 350 mL nanofil 116 suspension. RSM optimized active films were prepared (as detailed in section 2.3.6) having 50 kGy irradiated beeswax (1.21%), 87.5% tween 80, 3.07 % nanofil 116 and 13.91 % glycerol (w/w of GG). In another set of experiment RSM optimized films were prepared having similar additives concentration as mentioned above but without grape pomace.

2.4.5 Irradiation of RSM optimized active films

Active films were subjected to gamma irradiation (0.5, 1, 2.5, 5 and 7.5 kGy) at room temperature, using a ^{60}Co gamma irradiator (GC-5000, BRIT, India) having dose rate of 3.6 kGy/hr. Irradiated films were conditioned before characterization as per procedure detailed in section 2.1.6.

2.4.6 Characterization of active films

2.4.6.1 Mechanical and barrier properties of active films

Mechanical and barrier properties of control and irradiated active films were measure according to the procedure detailed in section 2.1.8.

2.4.6.2 Total anthocyanin, phenolic, antioxidant, ascorbic acid and flavanoid content

50 mg film was dissolved in 5 mL water. Obtained solution was further analysed for total anthocyanin, phenolic, antioxidant, flavanoid and ascorbic acid content (as described in section 2.4.3).

2.4.6.3 Antimicrobial activity of active films

Antimicrobial activity of films was tested qualitatively by inhibition zone method and quantitatively by viable cell count method. In qualitative method, five different food pathogenic bacteria including *Staphylococcus aureus*, *Salmonella typhimurium*, *Escherichia coli*, *Bacillus subtilis* and *Bacillus cereus* were used for testing the antimicrobial activity of the films. Film samples were punched to make disks (diameter =6 mm), and the antimicrobial activity was determined using an agar diffusion assay (disk test). The plates were examined for possible clear zones after incubation at 37 °C for 2 days. The clear zone that forms around the film disk on the agar plate was recorded as a measure of inhibition against the microbial species.

The quantitative measure of the antimicrobial activity of the films was determined using a viable cell count method on the test pathogenic bacteria. 250 mg of films amples were placed in individual sterile flasks to be used for microbial inhibition. All five pathogenic strains were separately grown in nutrient broth and incubated aerobically for 16 h at 37 °C. Each strain was diluted with broth to (1.0-2.5) × 10^6 colony forming units per millilitre ($CFUmL^{-1}$). Then, 100 mL of the inoculum was aseptically added to each of the flasks containing the sample films. For each type of

bacteria, an inoculum of cell suspension in a flask with no film sample was used as a control. The flasks were placed on an orbital shaker and rotated at 50 rpm and 37 °C. Aliquots of 0.1 mL of cell suspension were periodically taken from the flasks, diluted serially with 0.9% saline solution, and plated in duplicate on Plate Count Agar (PCA). The plates were incubated in an aerobic chamber for 2 days at 37 °C. The number of colonies on eachplate was counted and reported as CFU per millilitre.

2.5 Packing of food product for irradiation application

2.5.1 Arils packaging

Fresh local market samples of pomegranate (Bhagwa variety) were washed manually with tap water, bruised or damaged items removed and healthy fresh fruits were selected. Fruits were carefully cut at the equatorial zone with sharpened sterile stainless steel knives and the arils were manually removed. Handpicked healthy arils were packed (40 g) into polystyrene trays (inner dimensions: 9 cm × 9 cm × 2.5 cm). The trays were then over-wrapped all around with cling film (Klin wrap, Flexo Film Wraps Ltd., India). In one set of experiment, trays were packed with RSM optimized films (as in section 2.4.4) and in other set, trays were packed with optimized active films having 5% grape pomace extract (as in section 2.4.4).

2.5.2 Irradiation and storage of arils

Packaged samples were subjected to various radiation doses (0.5, 1.0, 1.5, 2.0 and 2.5 kGy) as described in section 2.4.5. Irradiated samples were stored in the dark at 10 ± 0.5 °C. Non-irradiated samples served as control samples during the entire storage

period. Three replicates were prepared for each dose, storage day and types of packaging. The samples were examined on 0, 4, 8, 12 and 16 days after packaging.

2.5.3 Analysis of head space gas composition

O_2 and CO_2 content of each packed tray was analyzed using a gas chromatograph (GC 2010, Shimadzu Corporation, Japan). The GC was equipped with split/splitless injector, a molecular sieve column (length 30 m, 0.35 I.D., RT-Msieve 5A, Restek Corporation, USA) and a thermal conductivity detector (TCD) detector. Injection port temperature was 35 ºC. Initial column temperature was kept 30 ºC for 5 min and then raised at rate of 0.167 $^{o}Cs^{-1}$ to 100 ºC. The column was further held at 100 ºC for 5 min with the TCD current and temperature maintained at 90 mA and 110 ºC, respectively. Sampling was done by inserting a hypodermic needle into the packed trays. A 0.1 mL of headspace sample was extracted and injected into the GC at a split ratio of 5. Only O_2 and N_2 could be evaluated on the column used in the study. Based on observed O_2 and N_2 concentrations in the package headspace, actual concentrations of O_2 and CO_2 ($\%O_2$ and $\%CO_2$) were calculated using following equations:

$$\% O_2 = (\text{Observed } \%O_2 / \text{Observed } \%N_2) \times 78.084$$

$$\%CO_2 = 100 - [(\text{Observed}\%O_2/\text{Observed}\%N_2) \times 78.084 + 78.084]$$

(Atmospheric composition of N_2 taken as 78.084%)

2.5.4 Analysis of arils for quality

2.5.4.1 Moisture loss

For measurement of water loss through packaging film, each tray was weighed at regular intervals of 24 h. Further, moisture loss was calculated cumulatively by comparing the weights of trays subsequent to packing of the arils immediately and at various storage times. Results were expressed as a percentage of weight loss [157].

2.5.4.2 Microbial analysis

Standard methods were used to enumerate microorganisms present in minimally processed pomegranate aril at each sampling time [158]. Mesophilic bacterial counts were carried out in triplicate for each single tray using plate count agar (PCA) and the pour plate method [158]. Arils sample (25 g) from each tray were and taken in stomacher bag containing 225 mL sterile physiological saline within a laminar. The sample was homogenized in a stomacher instrument at 260 rpm for 1 min. After appropriate serial dilutions, the samples were pour plated on PCA. The colonies were counted after 24 h of incubation at 37°C. Total yeast and mold counts were performed with the pour plate method using potato dextrose agar supplemented with 0.1% tartaric acid to maintain pH of the media at 3.5. Plates were incubated at 37°C for 48 h before counting. Microbial counts were expressed as $\log_{10}$ $CFUg^{-1}$ of arils. Each analysis was performed in triplicate.

2.5.4.3 Sensory analysis

Arils (non-irradiated and irradiated) were analyzed by the panellist in different sessions. 10 g of samples were served in white trays numbered randomly to the sensory panel. Sensory analysis at all doses was carried out by hedonic test employing a sensory panel of 15 members (7 women and 8 men). All panellists had previous experience in carrying out sensory analysis of similar food products. Hedonic test was carried out using a 9-point scale with 1, dislike extremely or not characteristic of the product and 9, like extremely or very characteristic of the product [159]. Parameters evaluated were color, aroma, texture, taste and overall acceptability. To determine the acceptability of the samples at different storage points, packaging and treatment (radiation processing) all the parameters analyzed were compared with fresh control samples on each day. The scores given for all the attributes for each sample were tabulated. Next, the mean value was calculated for each attribute of a sample, representing the panel's judgment about the sensory quality of the product and significant difference was found by analysis of variance (ANOVA).

2.5.4.4 Determination of arils color

Color of the arils was measured by a colorimeter (as detailed in section 2.1.8). Nine arils were selected randomly from each packaged tray at different storage period for 20 days.

2.5.4.5 Texture analysis

The texture analysis for the sample was performed using a Texture Analyzer (TA. HD. Plus, Stable Micro Systems) [160]. Twelve grams of arils were weighed into a 28

cm^2 metal plate and were crushed using a 5-cm diameter cylindrical probe. Maximum force (N) was measured and expressed as firmness. Speed of 5 mm/s and penetration distance of 7 mm were used.

2.5.4.6 Analysis of arils juice quality

Arils were crushed using mortar and pestle followed by muslin cloth filtration to obtain the juice. Total soluble sugars and pH of juice were directly measured. The juice was then centrifuged at 10500 g for 5 min at RT. The supernatant was used for analysis of anthocyanin, phenolic, antioxidant, ascorbic and flavanoid content as described earlier (section 2.4.3).

2.6 Development of edible coating

2.6.1 Dip treatment

0.5% (w/v) aqueous GG solution was prepared having 40% (w/w of GG) glycerol concentration. In the above solution different amounts (0.2% and 0.5% aqueous w/v) of grape pomace extract were added. In each of the 500 mL of mixture (having 0.2% and 0.5% pomace extract) thus obtained, 100 g of fresh pomegranate arils (section 2.5.1) were dipped for 2 min with continuous stirring. After dipping, arils were left in tray to dry under laminar flow for 1 h. Arils were then packed by using active film as detailed in section 2.5.1 and stored at 10°C. In the present study, arils dipped in water prior to packaging acted as control samples during the entire storage period. Three replicates were prepared for each dip treatment and storage day. The samples were examined on 0, 2, 4, 6 and 8 days after packaging.

2.6.2 Analysis of head space gas composition

Method as detailed in section 2.5.3 was followed.

2.6.3 Analysis of arils for quality

The different parameters analyzed and the methods followed are described in section 2.5.4.

2.7 Statistical analysis

Analysis of variance (ANOVA) ($p < 0.05$) and multiple comparisons of means were carried out using Duncan's multiple range test applying DSAASTAT ver. 1.101 software by Andrea Onofri. Three samples were taken for every treatment and each sample was further analyzed in triplicate.

3. Results and discussion

3.1 Standardization of protocols for film formation from guar gum

Very few reports exist in literature on GG based film. The methodologies reported for development of the films are not consistent. Methodology for preparation of GG based film such as concentration of GG solution to be used, volume of casting solution, drying temperature, drying time and relative humidity during conditioning of the film was thus optimized.

3.1.1 Optimization of GG content and drying conditions for film preparation

Aqueous GG solutions at different concentrations (7.5, 10 and 12.5 gL^{-1}) and volumes (100, 150 and 200 mL) were prepared. Among the different concentrations used higher concentration (12.5 gL^{-1}aqueous solution) resulted in incomplete dissolution of GG in water and a non-homogenous drying of the films. Further experiments were therefore conducted on GG solutions having concentrations of either 7.5 or 10 gL^{-1}. Glycerol concentration was kept 40 percent w/w of GG in film forming solution as it was earlier reported in literature to impart best mechanical properties [50].

Films formed from 100 mL of GG solution irrespective of its concentration had low thickness of 5 ± 1 µm as compared to films prepared with 150 and 200 mL of GG solution having a thickness of 8 ± 1 and 12 ± 2 µm, respectively. At this volume (100 mL) inability to peel film off from casting base was encountered and hence further experiments were performed using 150 and 200 mL of GG solutions. Different drying temperatures (70, 80 and 90 ^{o}C) and duration (8 and 10 h) of drying were also optimized.

A full factorial experiment was conducted on above conditions for optimization of film forming protocols and results obtained are shown in Table 15.

Films prepared with 7.5 gL^{-1} solutions using either 150 or 200 mL solution had a thickness of 8 ± 2 µm, while thickness of films prepared with 10 gL^{-1} solution was 15 ± 3 µm. Further, films prepared with higher concentration (10 gL^{-1}) of GG demonstrated better physical properties as compared to films formed using lower concentration (7.5 gL^{-1}) of GG. Maximum tensile strength and Young's modulus obtained with 7.5 gL^{-1} solution was 39 ± 5 MPa and 166 ± 26 MPa, respectively, while corresponding values for these properties were 58 ± 7 MPa and 180 ± 23 MPa, respectively for films prepared with 10 gL^{-1} solutions (Table 15). It was observed that with increase in volume no statistically significant ($p < 0.05$) improvement in film characteristics was observed at either of the concentrations studied (Table 15). Thus, 150 mL of 10 gL^{-1} GG solution was found to be optimum for film formation that is 0.34 mL of solution per cm^2 of casting plates. A significant ($p < 0.05$) effect of drying temperatures on resulting film properties was observed. Maximum tensile strength of 58 ± 7 MPa was observed for films dried at 80 °C for 8 h (Table 15). Therefore, these drying conditions were finally chosen for film preparation.

Table 15: Effect of GG concentration, volume and drying conditions (temperature and duration) on film properties.

Guar gum		Drying condition		Tensile strength (MPa)	Young's modulus (MPa)	Puncture strength (N)	Percent elongation	WVTR ($g/m^2/d$)
Concentration (aqueous w/v)	Volume (mL)	Temperature (^0C)	Duration (h)					
0.75%	150	70	8	33 ± 3	161 ± 26	0.9 ± 0.1	15 ± 3.2	215 ± 34
			10	38 ± 7	154 ± 14	1.0 ± 0.1	14 ± 2.8	208 ± 20
		80	8	34 ± 5	160 ± 19	1.0 ± 0.1	13 ± 2.1	210 ± 18
			10	32 ± 6	152 ± 24	1.1 ± 0.1	15 ± 3.2	209 ± 23
		90	8	27 ± 3	156 ± 25	0.8 ± 0.1	16 ± 3.6	212 ± 38
			10	29 ± 4	147 ± 27	0.9 ± 0.1	17 ± 3.7	201 ± 42
	200	70	8	NA	NA	NA	NA	NA
			10	NA	NA	NA	NA	NA
		80	8	36 ± 3	159 ± 14	1.1 ± 0.1	15 ± 3.8	161 ± 21
			10	39 ± 5	166 ± 26	1.2 ± 0.1	13 ± 4.5	178 ± 28
		90	8	37 ± 4	170 ± 17	1.2 ± 0.1	14 ± 4.9	180 ± 29
			10	31 ± 7	177 ± 19	1.1 ± 0.1	12 ± 3.1	191 ± 32
1%	**150**	70	8	39 ± 9	153 ± 22	1.5 ± 0.3	19 ± 7.1	173 ± 25
			10	48 ± 11	168 ± 29	1.6 ± 0.3	18 ± 6.3	188 ± 31
		80	**8**	**58 ± 7**	**180 ± 23**	**1.7 ± 0.2**	**17 ± 4.5**	**168 ± 24**
			10	56 ± 6	190 ± 27	1.6 ± 0.2	16 ± 4.1	170 ± 21
		90	8	47 ± 5	199 ± 22	1.5 ± 0.2	15 ± 3.9	175 ± 28
			10	43 ± 8	212 ± 32	1.4 ± 0.1	14 ± 3.3	165 ± 23
	200	70	8	NA	NA	NA	NA	NA
			10	NA	NA	NA	NA	NA
		80	8	41 ± 8	172 ± 36	1.9 ± 0.3	21 ± 6.2	165 ± 23
			10	44 ± 4	188 ± 31	1.8 ± 0.3	20 ± 5.8	169 ± 27
		90	8	49 ± 9	194 ± 24	1.7 ± 0.2	19 ± 5.3	179 ± 30
			10	55 ± 12	222 ± 20	1.6 ± 0.2	18 ± 6.1	188 ± 38

3.1.2 Effect of GG purification on mechanical and barrier properties of films

In order to study the effect of purification step on film forming properties of GG films were casted as per optimized procedure (10 gL^{-1}, 150 mL, 80 °C, 8 h in section 3.1.1) using purified and unpurified GG. Purification step had no significant ($p < 0.05$) effect on thickness of film. Thickness of films prepared with purified GG was found to be 14 ± 2 μm as compared to the films prepared with unpurified GG with thickness of 15 ± 3 μm. However, purification had a significant ($p < 0.05$) influence on other physical properties

of films. Films prepared from unpurified GG demonstrated tensile strength of 6 ± 1 MPa, Young's modulus of 63 ± 12 MPa and percent elongation of 9 ± 2 %. The corresponding value for films prepared with purified GG was 60 ± 7 MPa, 179 ± 27 MPa and 15 ± 4 %, respectively (Table 16). It could be clearly observed from the data that purification resulted in ten time increase in tensile strength of films. A substantial improvement in characteristics of films observed here might be due to the fact that purification leads to removal of insoluble impurities from GG. It was previously reported that, impurities mainly consists of high molecular weight macromolecules, proteins and arabinose and glucose residues [161]. Purification could have lead to a uniform and compact packing of GG polymer chains in the films prepared, resulting in increased physical properties. Thus, all further work was performed on purified GG.

Table 16: Physical properties of films made up of purified and unpurified GG.

Guar gum	Tensile strength (MPa)	Young's modulus (MPa)	Puncture strength (N)	Percent elongation	WVTR ($g/m^2/d$)
Unpufiried	6 ± 1^b	63 ± 12^b	1.1 ± 0.2^b	9 ± 2^b	190 ± 22^a
Purified	60 ± 7^a	179 ± 27^a	1.7 ± 0.3^a	15 ± 4^a	171 ± 28^a

Any two means in the same column followed by the same letter are not significantly ($p > 0.05$) different.

3.1.3 Effect of different casting plates on film characteristics

Teflon and glass plates have been widely used as casting surface because dried films could be easily peeled off (stripped) from these plates [162, 163]. Hence these plates were used in this study. Films prepared using both Teflon and glass plates were further analyzed to study the effect of casting plates on properties of GG based films. No

statistically significant difference ($p < 0.05$) in physical properties was observed in films casted on either of the two plates. However, film casted on glass plates was more transparent than film casted on Teflon plates (Figure 13 A & B). This was due to the rough surface of Teflon resulting in opaque films. Therefore glass was chosen as a casting surface for films.

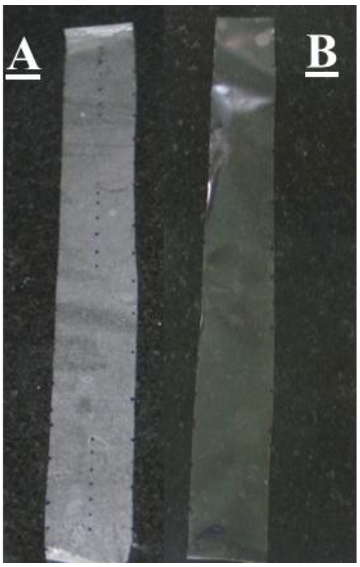

Figure 13: GG based film casted on (A) Teflon plates (B) Glass plates.

3.1.4 Effect of viscosity of GG solution on film characteristics

Commercially, different viscosity grades of GG are available. Films were casted by using 2000, 5000 and 7000 cP (centipiose) grade GG and further analyzed to determine the effect of various viscosity grade GG on film's functional properties. It was observed that change in viscosity did not have any significant effect ($p < 0.05$) on mechanical and barrier characteristics of biodegradable films (Table 17).

Table 17: Effect of various film properties by using different viscosity grade GG.

Viscosity grade GG (cP)	Tensile strength (MPa)	Young's modulus (MPa)	Puncture strength (N)	Percent elongation	WVTR ($g/m^2/d$)
2000	59 ± 5^a	188 ± 32^a	1.4 ± 0.2^a	21 ± 4^a	168 ± 19^a
5000	61 ± 7^a	196 ± 34^a	1.7 ± 0.3^a	18 ± 3^a	174 ± 23^a
7000	63 ± 4^a	201 ± 29^a	1.6 ± 0.3^a	17 ± 3^a	180 ± 21^a

Any two means in the same column followed by the same letter are not significantly ($p > 0.05$) different.

3.1.5 Storage effects on mechanical and barrier properties of GG film

GG films were stored at room temperature (25 ± 2 °C) and at 50% RH. Periodically films were characterized to study the effect of storage on its mechanical and barrier properties. GG films demonstrated excellent storage stability up to 100 days without loosing its various physical properties (Table 18). Time dependent decrease in mechanical characteristics of film was observed thereafter. Observed reduction in film properties might be due to degradation of GG matrices.

Table 18: Effect of storage on physical properties of GG based films.

Storage (days)	Tensile strength (MPa)	Young's Modulus (MPa)	Puncture strength (N)	Percent elongation	WVTR ($g/m^2/d$)
0	66 ± 7^{a}	155 ± 27^{a}	1.5 ± 0.3^{a}	14 ± 2.8^{a}	175 ± 21^{a}
50	65 ± 5^{a}	148 ± 26^{a}	1.6 ± 0.3^{a}	15 ± 3.2^{a}	153 ± 24^{a}
100	$\mathbf{60 \pm 6^{ab}}$	$\mathbf{130 \pm 15^{a}}$	$\mathbf{1.7 \pm 0.2^{a}}$	$\mathbf{16 \pm 3.6^{a}}$	$\mathbf{161 \pm 20^{a}}$
150	51 ± 4^{bc}	128 ± 14^{a}	1.6 ± 0.2^{a}	14 ± 3.7^{ab}	162 ± 26^{a}
200	45 ± 3^{c}	103 ± 11^{b}	1.5 ± 0.2^{a}	12 ± 3.3^{ab}	154 ± 19^{a}
250	37 ± 5^{d}	85 ± 16^{b}	1.4 ± 0.1^{a}	10 ± 2.1^{b}	199 ± 18^{a}

Any two means in the same column followed by the same letter are not significantly ($p > 0.05$) different.

3.1.6 Effect of water content on mechanical and barrier properties of GG based film

Water is a key solvent for natural biopolymer it also acts as an effective plasticizer for hydrocolloid based films [83]. As GG is highly hygroscopic, an effort was made to understand the effect of water content on film properties.

3.1.6.1 Conditioning of films at different relative humidity and its characterization

GG based films were conditioned at different RH (0%, 25%, 50%, 75% and 100%) for 7 days to alter the water content in films before its investigation. It was observed that tensile strength and Young's modulus decreased while percent elongation increased in a RH dependent manner (Table 19). This might be due to increase in water content of film with increase in RH. Thus, the plasticizing ability of water on GG films was demonstrated. Rachtanapun et al., (2012) [164] also observed similar relation between

RH and tensile strength of chitosan films. Increase in plasticizer (water) content decreases tensile strength and increases percent elongation. The plasticizer molecules are known to affect polymer interaction, decreasing intermolecular attraction and thus increasing polymer mobility [165].

Table 19: Mechanical and barrier properties of GG based film conditioned at different RH.

Relative humidity	Tensile strength (MPa)	Young's modulus (MPa)	Puncture strength (N)	Percent elongation	WVTR ($g/m^2/d$)
0	81 ± 20^{a}	280 ± 41^{a}	1.3 ± 0.2^{a}	10 ± 1^{b}	164 ± 23^{a}
25	70 ± 13^{ab}	220 ± 33^{ab}	1.6 ± 0.2^{a}	13 ± 6^{ab}	155 ± 29^{a}
50	56 ± 6^{b}	180 ± 31^{b}	1.7 ± 0.3^{a}	17 ± 8^{ab}	170 ± 23^{a}
75	50 ± 7^{b}	140 ± 28^{bc}	1.4 ± 0.1^{a}	21 ± 7^{a}	177 ± 31^{a}
100	40 ± 5^{b}	102 ± 23^{c}	1.5 ± 0.1^{a}	24 ± 6^{a}	180 ± 33^{a}

Any two means in the same column followed by the same letter are not significantly ($p > 0.05$) different.

In the present study, 50% RH was chosen for conditioning due to the ease of handling of such film. Lower humidity (0% and 25% RH) resulted in brittle film, while higher RH (75% and 100% RH) leads to poor mechanical strength of the (Table 19).

Optimized protocol for GG based film formation was graphically presented below:

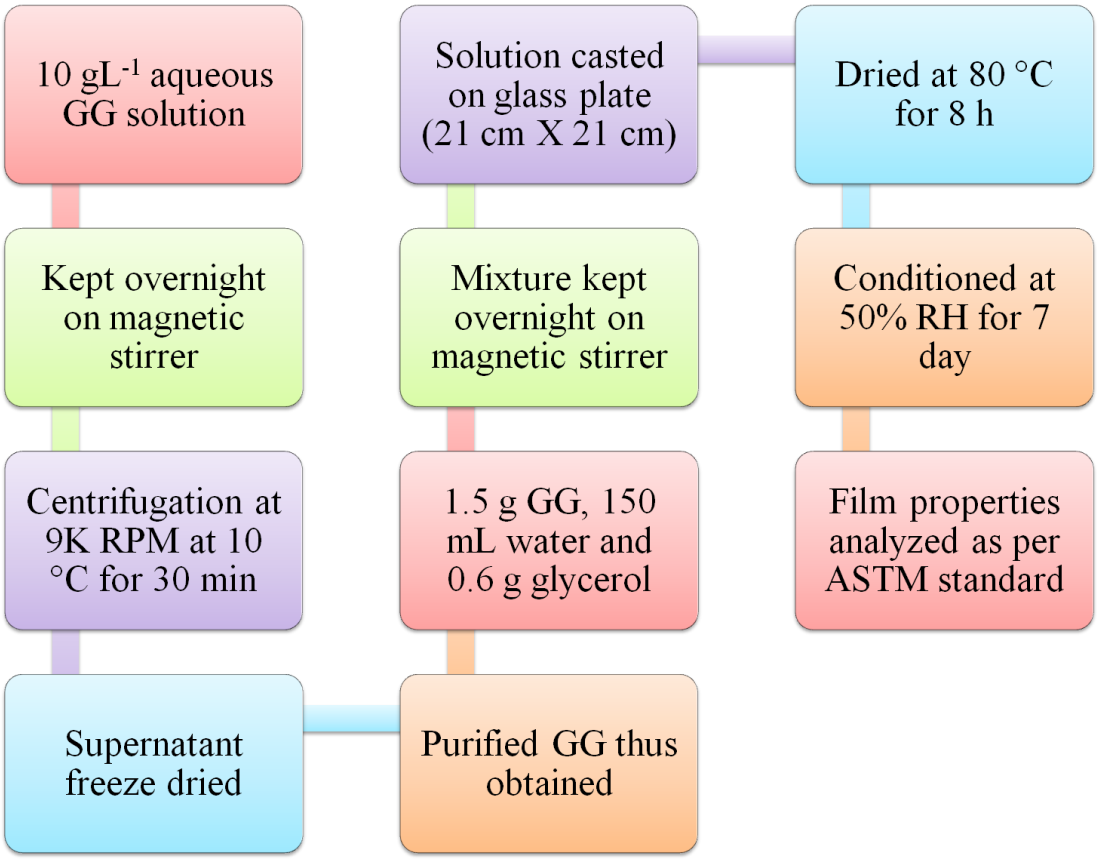

Standardization of GG concentration and volume along with drying temperature and time was thus performed to obtain film having excellent characteristics. Effect of purification, casting plates, viscosity, and storage period on GG based film's properties was also investigated. Additionally, effect of water content on film characteristics was also studied by conditioning of film at different relative humidity. Further enhancement in mechanical and barrier properties of film prepared from standard protocol employing gamma irradiation was attempted after performing above mentioned basic investigations.

3.2 Use of gamma irradiation for improving functional and mechanical properties of developed films

Films prepared using biopolymers have low mechanical strength and high water vapor permeability as compared to their commercial synthetic counterparts. Thus improving mechanical and barrier properties of biopolymer based film is currently an active area of research. Several reports are available in literatures demonstrating use of γ-irradiation for improving physical property of biopolymer based films. However to the best of our knowledge no reports are available on effect of radiation processing on mechanical and barrier properties of GG films.

3.2.1 Effect of γ-irradiation on viscosity average molecular weight of GG

Figure 14 demonstrates the effect of gamma irradiation on viscosity average molecular weight (M_v) of GG in its powder and solution form. Radiation processing of GG as dried powder and as aqueous solution (1%) resulted in significant ($p < 0.05$) reduction in its intrinsic viscosity (η_{sp}) and viscosity average molecular weight (M_v). Control GG had intrinsic viscosity (η_{sp}) of 2.95 and viscosity average molecular weight (M_v) of 4.09×10^6 Da. Irradiation of GG powder resulted in a non-linear decrease in M_v (Figure 14 A). GG irradiation resulted in rapid decrease in M_v up to 2 kGy followed by a much slower decrease at higher doses. M_v of GG reduced to 1.5×10^6 Da and 4.9×10^5 Da at 2 and 50 kGy, respectively (Figure 14 A). Similar results were obtained by Jumel et al. (1996) [166] during radiation processing of GG. However, irradiation of GG solution resulted in a much rapid decrease in M_v as compared to irradiated GG powder (Figure 14 A & B).

M_v of GG when irradiated in solution form reduced to 6.56×10^4 Da at a dose of 2 kGy. In present no significant effect of irradiation beyond a dose of 50 kGy on viscosity average molecular weight of GG powder was observed.

Observed rapid rate of degradation of GG when irradiated in solution form as compared to irradiation in powder form has been explained by Gupta et al. (2009) [167] wherein it was stated that in solution form the degradation of sample is due to a cumulative effect of OH radical formed by water radiolysis and gamma irradiation whereas in powder form the degradation is mainly due to the direct effect.

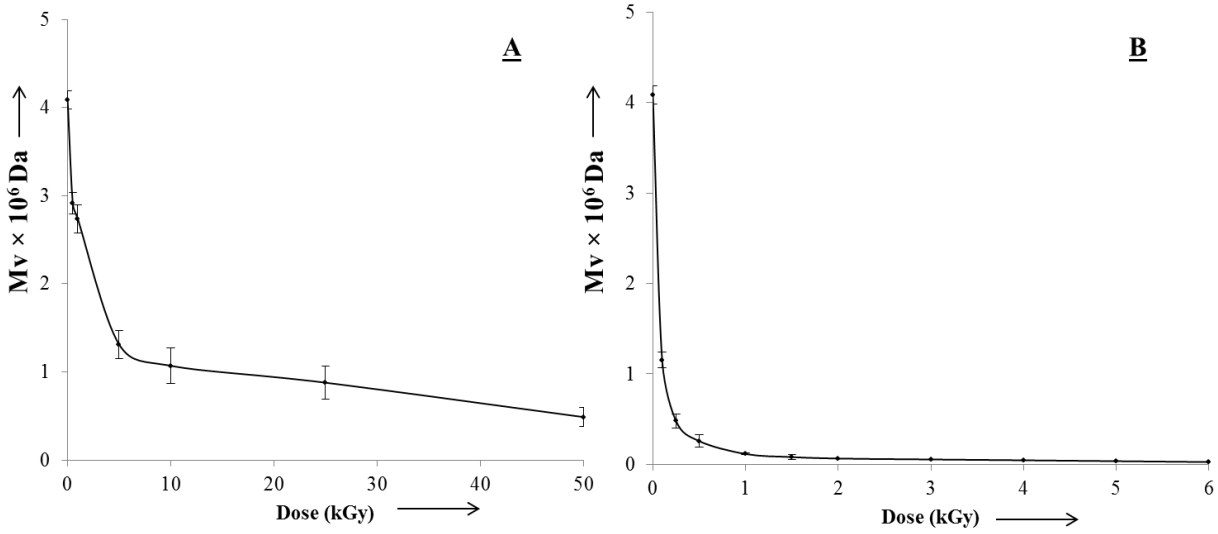

Figure 14: Effect of gamma irradiation on viscosity average molecular weight (M_v) of GG (A) Powder form (B) Solution form.

3.2.2 Effect of γ-irradiation on weight average molecular weight of GG

GG samples were further analyzed using gel permeation chromatography (GPC) to further analyze effect of radiation processing on their weight average molecular weight

(M_w). GPC chromatogram for the control GG showed a single peak corresponding to M_w of 4×10^6 Da (Figure 15 A). In earlier studies on GG, M_w was reported to be 2.7×10^6 Da by Jumel et al. (1996) [166]. Hence results obtained are in accordance with published data.

In GG samples irradiated in powder form, two peaks (Peak 1 and 2) were observed in GPC chromatograms for doses up to 1 kGy (Figure 15 B). Peak 1 and 2 had M_w of 4.6×10^6 and 2.5×10^6 Da, respectively. M_w of these peaks was comparable to that of control GG. At low doses (up to 1 kGy) of irradiation a disruption of supramolecular structures of GG polymer rather than depolymerization as reported by Jumel et al. (1996) [166] could possibly explain the two peaks observed in GPC chromatograms. A third peak (Peak 3) having a M_w 2×10^5 Da was also observed in GPC chromatograms beyond the irradiation dose of 1 kGy (Figure 15 C). Appearance of this peak in the chromatogram could be attributed to the formation of depolymerized polymer as a result of gamma radiation.

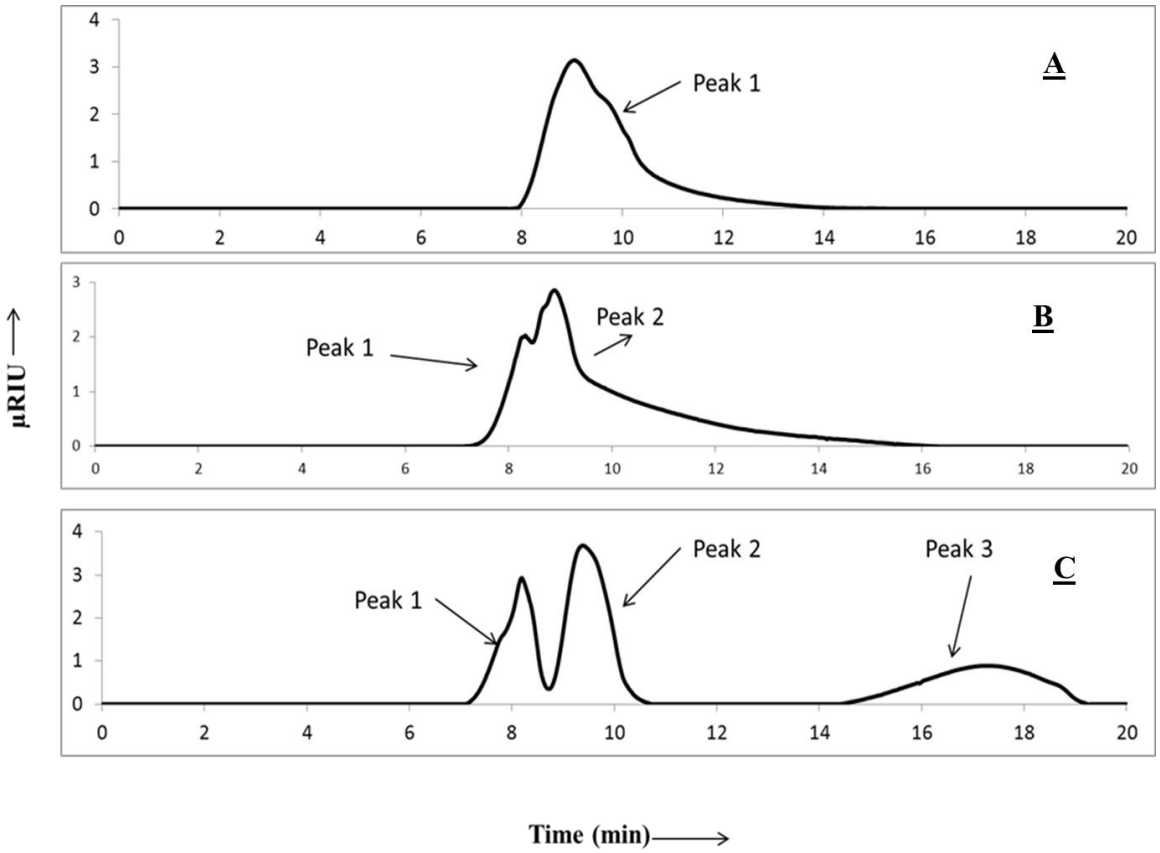

Figure 15: A representative gel permeation chromatogram (GPC) of irradiated powder GG samples (A) Control non-irradiated GG (B) GG irradiated to a dose of 1 kGy (C) GG irradiated to a dose of 50 kGy.

Variation in relative area percent of all three peaks in GPC chromatogram for GG irradiation in powder form is shown in figure 16. Radiation processing of GG powder up to a dose of 5 kGy resulted in significant ($p < 0.05$) increase in relative area of peak 2 with corresponding decrease in area of peak 1 (Figure 16). However, beyond radiation dose of 5 kGy a significant ($p < 0.05$) dose dependent increase in relative area percent of peak 3 with a decrease in peak 1 and 2 was observed (Figure 16).

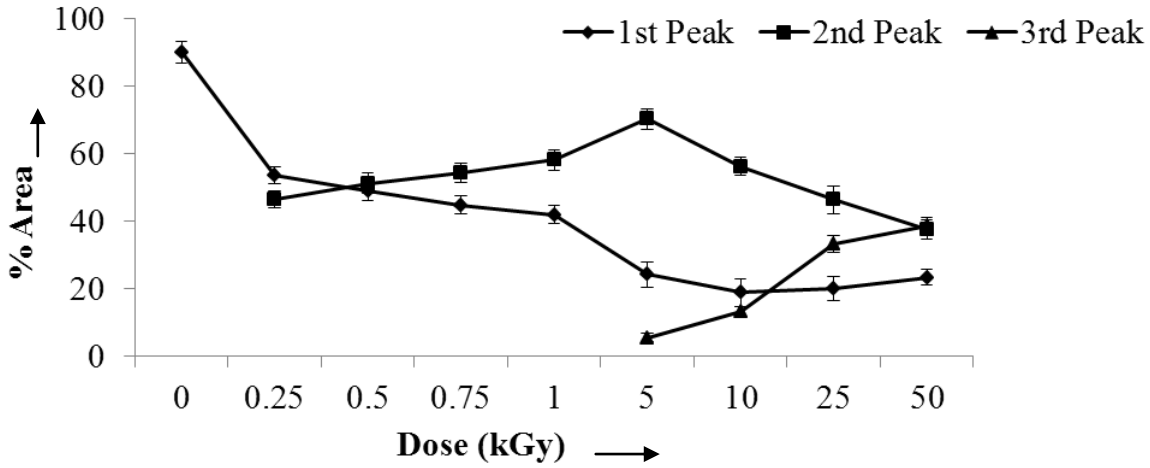

Figure 16: Variation of relative percent area of peaks observed in gel permeation chromatography (GPC) of powdered GG with radiation dose.

Results obtained for GPC analysis of GG irradiation in solution form is shown in Figure 17. Two peaks (peak 1 and 2) having M_w of 4.6×10^6 and 2.1×10^6 Da, respectively were observed at a dose of 200 Gy. Furthermore, a peak 3 of depolymerized fraction having Mw of 1.8×10^5 Da was observed in samples irradiated to a dose of 500 Gy and higher (Figure 17). A radiation dose dependent decrease in area of peak 1 and 2 with corresponding increase in area of peak 3 was observed (Figure 18).

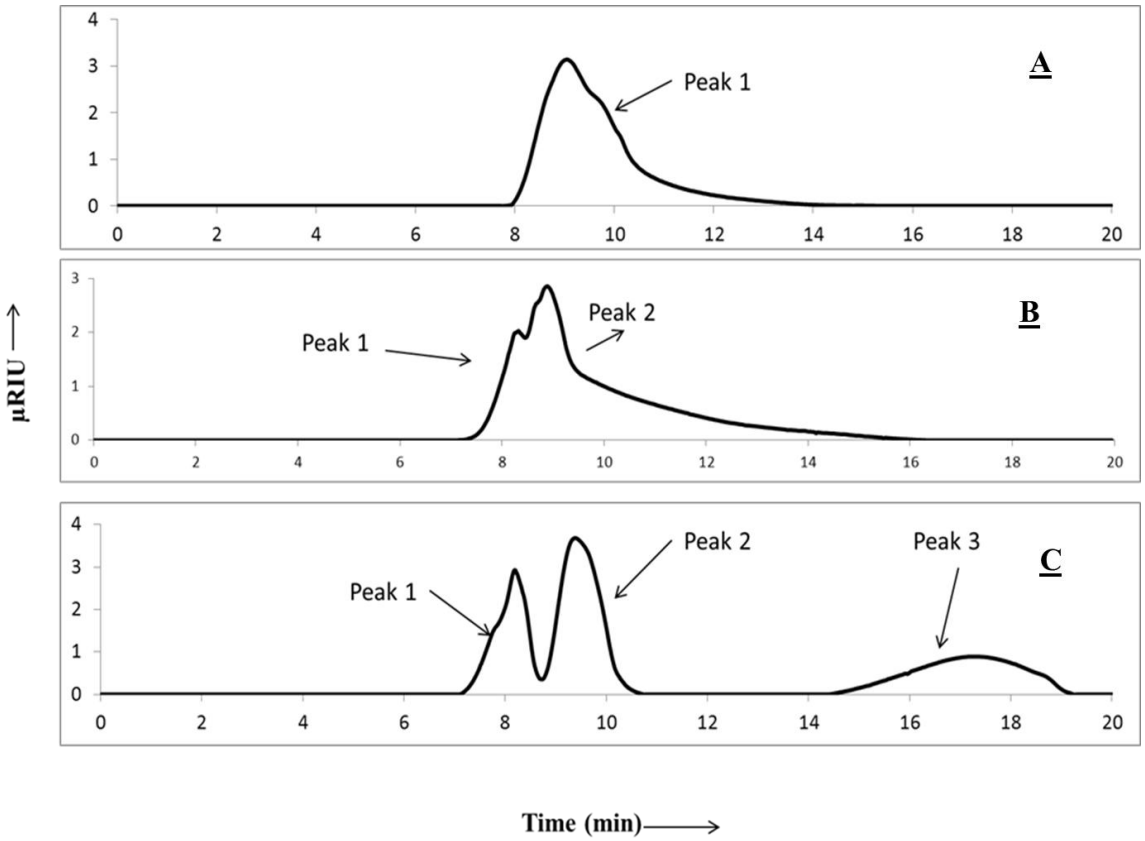

Figure 17: A representative gel permeation chromatogram (GPC) of irradiated aqueous GG solution samples (A) Control non-irradiated GG (B) GG irradiated to a dose of 200 Gy (C) GG irradiated to a dose of 500 Gy.

In accordance with the obtained viscosity data (section 3.2.1) a much higher rate of degradation of GG was observed for radiation processing carried out in solution form. A significantly ($p < 0.05$) higher content of depolymerized fraction was observed in samples irradiated in solution form as compared to samples irradiated in powder form. Samples irradiated in solution form had 78 percent depolymerized fraction (Figure 18) even at a dose of 5 kGy, whereas samples irradiated in powder form only had 40 percent depolymerized fraction even at a dose of 50 kGy (Figure 16). Results from both viscosity

as well as gel permeation chromatography suggested a gradual degradation of GG during irradiation. Similar results for radiation induced degradation of GG were earlier reported by Gupta et al. (2009) [167].

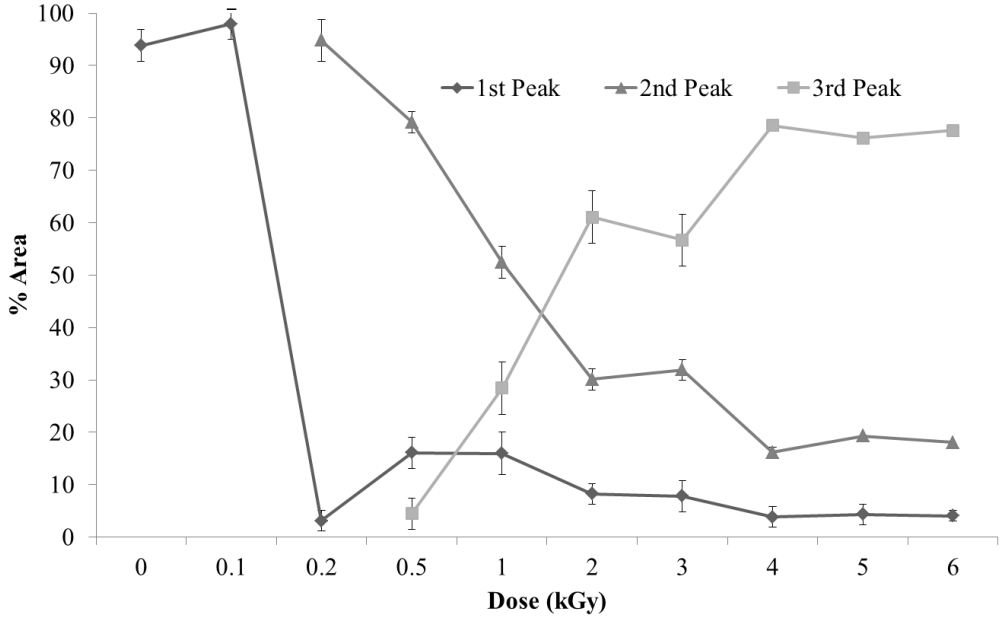

Figure 18: Variation of relative percent area of peaks observed in gel permeation chromatography (GPC) of GG solution with radiation dose.

3.2.3 Effect of γ-irradiation on polydispersity index

Polydispersity index (PDI) is a measure of molecular weight distribution of any polymer sample. In the present work PDI was calculated for control and irradiated GG samples in powder and solution form. A radiation dose dependent increase in PDI of both GG samples was observed (Figure 19 A & B). PDI of control GG was 1.05 which increased to

1.16 at 1 kGy and 1.29 at 50 kGy for irradiated GG powder (Figure 19 A). However, PDI of irradiated aqueous GG was 1.33 at 1 kGy and 3.42 at 6 kGy (Figure 19 B). Jumel et al. (1996) [166] have also reported a wide molecular weight distribution of irradiated GG samples as compared to controls. Increase in PDI with irradiation dose could possibly be explained by random phenomenon of radiation induced degradation of GG polymer. Higher PDI of aqueous GG might be due to higher rate and extent of degradation in GG solution than GG powder as a result of irradiation.

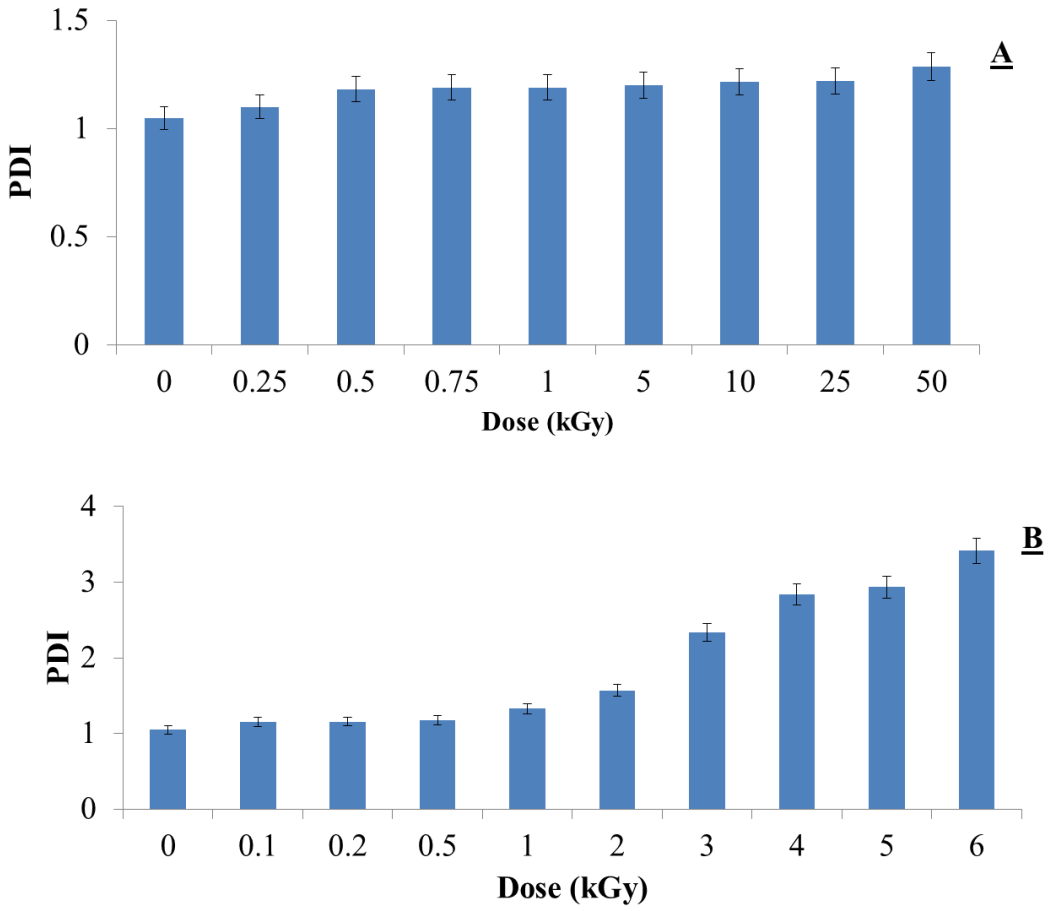

Figure 19: Polydispersity index of (A) irradiated GG powder (B) irradiated GG solution.

3.2.4 Effect of irradiation on mannose to galactose (M/G) ratio of GG

M/G ratio is an important parameter determining the physicochemical properties of films. In the present study, M/G ratio of control and irradiated GG powder was found to be 1.6:1 (Figure 20) which is in accordance with results reported previously by Cunha et al. (2005) [168]. Similarly, no statistically significant ($p < 0.05$) differences were observed in M/G ratio of aqueous GG samples due to radiation processing in the present study. M/G ratio of galactomannans significantly affects the mechanical properties of the films. For e.g. films prepared from the locust bean gum (M/G ratio of approximately 3.33) were stronger and more flexible than films prepared from control GG (M/G ratio of approximately 1.67) [50].

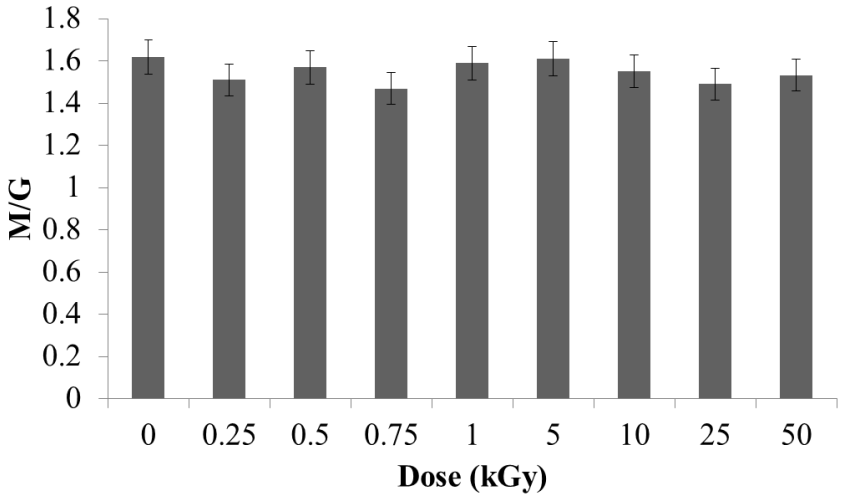

Figure 20: Mannose to galactose ratio of different irradiated GG powder samples.

3.2.5 Effect of gamma irradiation on physicochemical characteristics of GG based films

3.2.5.1 Effect of radiation on tensile strength of films

Tensile strength is the maximum stress that a material can withstand while being stretched or pulled before failing or breaking. Effect of radiation processing on tensile strength of GG films (prepared from control and irradiated samples) was studied. Control film had a tensile strength of 60.5 ± 8.7 MPa. Radiation processing of GG powder was found to have a significant ($p < 0.05$) effect on the tensile strength of GG films (Table 20). Dose dependent rapid decrease in tensile strength was observed for GG irradiation in solution form (Table 21). Tensile strength of film made from GG irradiated (2 kGy) in solution form reduced to 6 ± 1.2 MPa. This poor film characteristics was a result of radiation induced extensive degradation of aqueous GG as already confirmed from GPC data (Figure 17). Interestingly, for GG irradiation in powder form, an increase in tensile strength to 80.2 ± 13.9 MPa up to a dose of 500 Gy with dose dependent decrease, thereafter, was observed (Table 20). The tensile strength of GG films reduced to 7.8 ± 2.5 MPa at a dose of 50 kGy. Kim et al. (2008) [77] reported an increase in tensile strength by 27.5% of starch and locust bean gum based composite films at irradiation dose of 3 kGy. An increased tensile strength for starch based plastics sheets at irradiation dose of 30-70 kGy with a dose dependent decrease at higher doses (> 70 kGy) was also reported by Zhai et al. (2003) [169]. For pectin based films, an increase in tensile strength by 31.2 % at a dose of 10 kGy with a decrease at higher doses was reported earlier [170]. Improved tensile strength due to irradiation in previous studies was attributed to radiation

induced cross-linking of polymers, while reduction in tensile strength at higher doses was reported to have occurred due to radiation induced degradation of polymers [171]. An increase in tensile strength of GG based films due to enzymatic de-polymerization because of increased solubility and better orientation of short chain polymer was previously reported [50]. Surprisingly, no increase in tensile strength was observed due to radiation processing in the present study. This might be due to the fact that radiation induced de-polymerization resulted in different molecular weight distributions as compared to enzymatic de-polymerization. Dose dependent increase in PDI was observed in the present study thus suggesting a wide molecular weight distribution of irradiated GG samples. Further, even at a high radiation dose of 50 kGy presence of higher Mw fractions was demonstrated by GPC studies (Figure 15 C). Due to the presence of higher Mw fractions and wide molecular weight distribution, a restriction in the ordering of polymer chains is expected that could possibly decrease tensile strength.

Table 20: Effect of gamma irradiation on mechanical and barrier properties as well as color co-ordinates of GG films. Films prepared from irradiated GG powder.

Dose (kGy)	Tensile strength (MPa)	Young's Modulus (MPa)	Puncture strength (N)	% elongation	WVTR ($gm/m^2/day$)	L* (black to white)	a* (green to magenta)	b*(blue to yellow)	Opacity (%)
0	60.5 ± 8.7^{bc}	162 ± 23^{a}	2.3 ± 0.2^{a}	13.9 ± 4.5^{b}	190 ± 10^{ab}	97.7 ± 0.8^{a}	0.8 ± 0.2^{c}	1 ± 0.1^{d}	12.9 ± 0.2^{d}
0.25	71.4 ± 10.6^{ab}	151 ± 39^{a}	1.93 ± 0.2^{b}	22.8 ± 3.8^{a}	186.9 ± 8.3^{abc}	94.4 ± 0.8^{d}	2.3 ± 0.3^{a}	1.9 ± 0.2^{f}	15.2 ± 0.5^{a}
0.5	80.2 ± 13.9^{a}	158 ± 16^{a}	1.8 ± 0.2^{b}	18.6 ± 1.9^{ab}	192.5 ± 12^{ab}	94.4 ± 0.9^{d}	1.6 ± 0.3^{b}	1.7 ± 0.2^{f}	13.4 ± 0.5^{cd}
0.75	58.6 ± 7.8^{bc}	149 ± 11^{a}	1.69 ± 0.1^{b}	19.4 ± 2.5^{ab}	195.7 ± 12^{ab}	96.1 ± 0.7^{bc}	0.1 ± 0.01^{ef}	$0.2 \pm .04^{b}$	13.3 ± 0.5^{cd}
1	55 ± 6.2^{c}	154 ± 19^{a}	1.6 ± 0.3^{b}	14.7 ± 1.2^{b}	184 ± 7.5^{abc}	97.2 ± 0.6^{ab}	$.03 \pm .02^{ef}$	$0.3 \pm .04^{b}$	12.9 ± 0.3^{d}
5	26.7 ± 5.3^{d}	65 ± 19^{b}	1.7 ± 0.3^{b}	18.4 ± 2.4^{ab}	170 ± 4.4^{cd}	98.3 ± 0.8^{a}	0.2 ± 0.1^{de}	0.7 ± 0.1^{c}	13.2 ± 0.7^{cd}
10	22.4 ± 3.8^{de}	63 ± 11^{b}	1.2 ± 0.1^{c}	19.1 ± 3.3^{ab}	175.6 ± 8^{bcd}	94.8 ± 0.7^{cd}	0.1 ± 0.04^{f}	0.9 ± 0.04^{a}	14.3 ± 0.3^{b}
25	19.32 ± 4.5^{de}	49 ± 12^{b}	1.0 ± 0.2^{c}	16.1 ± 1.6^{b}	177.5 ± 9^{bcd}	96 ± 0.7^{bc}	0.42 ± 0.04^{d}	0.8 ± 0.1^{c}	13.9 ± 0.3^{bc}
50	7.8 ± 2.5^{e}	35 ± 11^{b}	0.8 ± 0.2^{c}	7.8 ± 2.5^{c}	160.6 ± 5.2^{d}	96.1 ± 0.6^{bc}	0.7 ± 0.2^{c}	1.4 ± 0.1^{e}	13.8 ± 0.4^{bc}

Any two means in the same column followed by the same letter are not significantly ($p > 0.05$) different.

Interestingly, at a lower irradiation dose of 500 Gy, a 32.6 percent increase in tensile strength was observed (Table 20). These changes could possibly be due to conformational change in GG particle structure. Conformation of control and irradiated (500 Gy and 50 kGy) GG was analyzed by small angle X-ray scattering. The SAXS profiles of control and different dose treated polymer are shown in Figure 21. In the present case, the interpretation the SAXS scattering data is based on the analysis of the scattering curve, which showed the dependence of the scattering intensity, *I*, on the scattering wave vector *q*. The scattered intensity as a function of q for the three solutions (Figure 21), shows a power law behavior [$I(q) \sim q^{-d}$]. The slope of the linear region in log $I(q)$ v/s log q plot gives the value of the exponent d, the dimensionality of the scattering object. Typically, the exponent $d = 2$ is exhibited by Gaussian chains in case of polymer. The scattering

curve for the control polymer and 50 kGy treated polymer show a q^{-2} dependence in the experimental q range. However, for the 500 Gy dose treated polymer, in addition to the q^{-2} dependence a prominent peak at high q was also observed (Figure 21). This prominent peak probably arises due to correlations of short length scales, with the inter-chain correlation length, $\xi=2\pi/q^*$ (where q^* is the peak position). The peak position was found to be 1.74 nm^{-1}. The correlation length ξ was calculated as 3.6 nm. The scattering profile for control and 50 kGy treated polymer is modeled by assuming Gaussian coiled chain, the formula used for (equation 1):

$$Igc(q) = \frac{2\left[\exp(-q^2 R_g{}^2) - 1 + q^2 R_g{}^2\right]}{q^4 R_g{}^4} \qquad (1)$$

where R_g is the typical chain length of the polymer.

To account the ordering of polymer treated up to 500 Gy, a hard sphere structure factor $S(\varphi, r_{hs})$ was taken into account where φ is the local packing fraction of the polymer and $2r_{hs}$ is the typical correlation length [172]. The scattering intensity for the 500 Gy treated polymer can be written as:

$I(q) = Igc(q) \times S(\varphi, r_{hs})$

It is evident from figure 21 that above discussed model fit the data quite satisfactorily. The typical chain length R_g for the all the specimens was found to be ~ 20 nm. The correlation length $2r_{hs}$ was found to be 3.2 nm which is approximately same as that estimated from the peak position (ξ). The local packing fraction of the chain was found to be 0.22. Thus, it is clear from the SAXS analysis that the conformation of the GG

polymer chain does not undergo modification under different radiation doses under the present probed length scale. However, for lower dose of 500 Gy, the ordering of the chains occurs with typical correlation length of 3.6 nm and local packing fraction of 0.22. Thus the possibility of ordering of chains resulting in better orientation of GG polymers during film formation and increased tensile strength at lower dose up to 500 Gy is suggested.

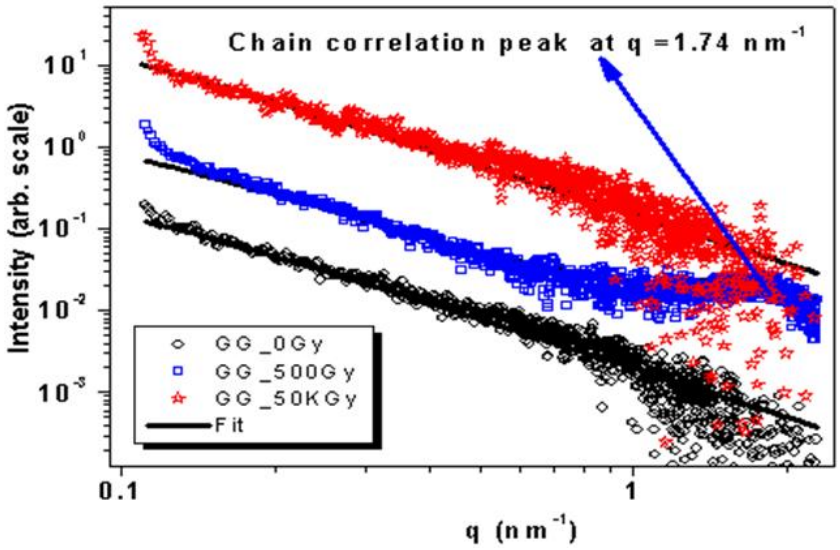

Figure 21: The small angle X-ray scattering (SAXS) profiles of the control and irradiated (500 Gy, 50 kGy) GG.

Table 21: Effect of gamma irradiation on mechanical and barrier properties as well as color co-ordinates of GG films. Films prepared from irradiated GG solution.

Dose (kGy)	Tensile strength (MPa)	Young's Modulus (MPa)	Puncture strength (N)	% elongation	WVTR ($gm/m^2/day$)	L* (black to white)	a* (green to magenta)	b*(blue to yellow)	Opacity (%)
0	60.5 ± 8.7^{a}	162 ± 23^{a}	2.3 ± 0.2^{a}	13.9 ± 4.5^{ab}	190 ± 10^{a}	97.7 ± 0.8^{a}	0.8 ± 0.2^{b}	-1 ± 0.1^{a}	12.9 ± 0.2^{b}
0.1	34.4 ± 3.1^{b}	119 ± 14^{b}	1.6 ± 0.1^{b}	15.5 ± 0.5^{ab}	113.5 ± 6.4^{bc}	95.4 ± 0.8^{b}	1.1 ± 0.3^{ab}	-1.7 ± 0.2^{b}	13.2 ± 0.5^{b}
0.2	20.4 ± 3.4^{c}	80 ± 11^{c}	0.7 ± 0.1^{c}	17.4 ± 2.2^{ab}	117 ± 1.4^{b}	94.4 ± 0.9^{bc}	1.2 ± 0.3^{ab}	-1.9 ± 0.2^{b}	13.4 ± 0.5^{b}
0.5	18 ± 2.8^{cd}	56 ± 6^{d}	0.8 ± 0.1^{c}	18 ± 1.0^{a}	113.8 ± 4.1^{bc}	93.1 ± 0.7^{cd}	1.1 ± 0.1^{ab}	$-2.2 \pm .04^{c}$	14.3 ± 0.5^{ab}
1	10.5 ± 1.6^{d}	40 ± 5^{e}	1 ± 0.0^{c}	18.2 ± 0.4^{a}	110.7 ± 5.2^{bc}	92.3 ± 0.6^{d}	$1.3 \pm .02^{a}$	$-2.3 \pm .04^{c}$	14.9 ± 0.3^{ab}
2	6 ± 1.2^{e}	23 ± 3^{f}	0.8 ± 0.2^{c}	10.9 ± 6.9^{b}	104.4 ± 4.2^{c}	92.2 ± 0.8^{d}	0.9 ± 0.1^{b}	-2.7 ± 0.1^{d}	15.2 ± 0.7^{a}

Any two means in the same column followed by the same letter are not significantly ($p > 0.05$) different.

GG films prepared from control samples were also directly subjected to irradiation processing and its impact on their tensile strength is shown in Table 22**.** No significant ($p < 0.05$) impact on tensile strength was observed due to radiation processing up to a dose of 25 kGy. Beyond this dose the tensile strength showed a dose dependent decrease (Table 22). Overall it can be concluded that maximum rate of degradation was observed by radiation processing of aqueous GG followed by powdered GG and then of irradiated GG films.

Table 22: Effect of irradiation on mechanical and barrier properties as well as color co-ordinates of GG films. Films prepared from control GG and irradiated thereafter.

Dose (kGy)	Tensile strength (MPa)	Young's Modulus (MPa)	Puncture strength (N)	% elongation	WVTR ($gm/m^2/day$)	L* (black to white)	a* (green to magenta)	b*(blue to yellow)	Opacity (%)
0	60.5 ± 8.7^{a}	162 ± 23^{a}	2.3 ± 0.2^{a}	13.9 ± 4.5^{ab}	190 ± 10^{a}	97.2 ± 0.6^{a}	0.6 ± 0.2^{a}	-1.1 ± 0.2^{e}	12.9 ± 0.2^{d}
1	51.9 ± 1.1^{a}	158 ± 33^{a}	2.1 ± 0.1^{a}	12 ± 3.9^{ab}	190.8 ± 11.1^{a}	95 ± 0.6^{b}	$.02 \pm .01^{e}$	0.3 ± 0.1^{b}	13.8 ± 0.4^{ab}
5	55.9 ± 4.5^{a}	177 ± 36^{a}	2.3 ± 0.2^{a}	12.3 ± 5.5^{ab}	188.3 ± 8^{a}	94.7 ± 0.4^{b}	0.4 ± 0.1^{bc}	-0.7 ± 0.1^{d}	13.3 ± 0.3^{cd}
10	51.8 ± 5.2^{a}	148 ± 25^{ab}	2 ± 0.3^{ab}	15 ± 0.9^{ab}	185.6 ± 6.2^{ab}	94.8 ± 0.8^{b}	0.2 ± 0.1^{de}	$.04 \pm .02^{c}$	13.5 ± 0.2^{bc}
25	58.5 ± 3.8^{a}	166 ± 29^{a}	1.6 ± 0.3^{bc}	18.5 ± 5.1^{a}	192.9 ± 3.8^{a}	93.7 ± 0.4^{bc}	0.3 ± 0.1^{cd}	$0.3 \pm .01^{b}$	14.2 ± 0.3^{a}
50	43.1 ± 1.2^{b}	151 ± 29^{ab}	1.4 ± 0.3^{c}	9.3 ± 1.7^{b}	183.9 ± 4.7^{ab}	93 ± 0.4^{c}	0.5 ± 0.1^{ab}	$-.01 \pm .01^{c}$	13.2 ± 0.1^{cd}
100	40.9 ± 5.3^{b}	101 ± 20^{b}	0.9 ± 0.1^{d}	17.5 ± 3.6^{a}	181 ± 6.5^{ab}	93.3 ± 1^{c}	0.7 ± 0.1^{f}	3.1 ± 0.2^{a}	14.1 ± 0.2^{a}

Any two means in the same column followed by the same letter are not significantly ($p > 0.05$) different.

3.2.5.2 Effect of radiation on Young's modulus of films

Young's modulus is a measure of stiffness of any sample. Films prepared with irradiated GG powder demonstrated no statistically significant ($p < 0.05$) difference in Young's modulus up to a dose of 1 kGy, nevertheless, a dose dependent decrease was noted thereafter (Table 20). A decrease in Young's modulus signifies a reduction in stiffness of films i.e. films prepared become more amenable to deformation. On the other hand, high susceptibility of aqueous GG towards radiation treatment resulted in significant ($p < 0.05$) decrease in Young's modulus even at 100 Gy (Table 21).

However, films prepared with control GG and irradiated thereafter demonstrated no significant ($p < 0.05$) impact on Young's modulus due to radiation processing up to a dose of 50 kGy. Beyond this dose, the Young's modulus showed a dose dependent

decrease (Table 22). This decrease was however significantly ($p < 0.05$) lower as compared to films prepared from irradiated GG.

3.2.5.3 Effect of radiation treatment on puncture strength and percent elongation of films

Puncture strength of films is a measure of the force required to penetrate the films. Effect of radiation on puncture strength of films was hence evaluated. Puncture strength of control GG films was 2.3 ± 0.2 N. A radiation dose dependent decrease in puncture strength of films prepared from irradiated GG powder was observed (Table 20). Puncture strength reduced to 1.2 ± 0.1 N at 10 kGy, and thereafter to 0.8 ± 0.2 N at 50 kGy. Similarly, puncture strength of films prepared from irradiated GG solution reduced to 0.7 ± 0.1 N at a dose of 200 Gy (Table 21). Films prepared from control GG and subjected to irradiation processing demonstrated no significant change in puncture strength up to a dose of 10 kGy; however it decreased to 1.6 ± 0.3 N and 0.9 ± 0.1 N at 25 kGy and 100 kGy respectively (Table 22).

Percent elongation indicates the flexibility of films. The films prepared from control GG demonstrated 13.9 ± 4.5 percent elongation. In a previous study by Mikkonen et al. (2007) [50] percent elongation of GG films was reported to be 40 percent. In the present study, GG was purified to remove all insoluble impurities before film preparation. This might have resulted in decreased percent elongation. No trend was observed on the percent elongation of films prepared from irradiated GG powder, GG solution and for GG films subjected directly to irradiation (Table 20, 21 & 22). Similar results were also found

for percent elongation by Zhai et al. (2003) [169], for irradiation of starch based plastic film. Thus, our results are in concurrence with earlier studies.

3.2.5.4 Effect of radiation treatment on WVTR of films

The GG films developed in the present study are intended to be used for food packaging purposes. The moisture content of the food sample is often effected by the WVTR of the packaging material. Hence, studying the effect of gamma irradiation on WVTR of developed films becomes an important parameter. Films with high WVTR can lead to excessive drying of the packaged samples thereby decreasing its shelf life. WVTR of control GG films was 190 ± 10 gm/m^2/day. Aydinli et al. (2004) [46] found WVTR for locust bean gum plasticized with PEG 200 and PEG 1000 to be 251 gm/m^2/day and 136 gm/m^2/day respectively. In present study radiation significantly ($p < 0.05$) affected the WVTR of films. Films made from irradiated GG powder had WVTR of 160.6 ± 5.2 gm/m^2/day at 50 kGy (Table 20). Thus an enhanced barrier to water vapor in GG films prepared from GG powder irradiated at higher doses with no significant ($p < 0.05$) effect at doses less than 1 kGy was observed. However, a pronounced effect was observed in irradiated GG solution on film WVTR. WVTR of film formed from 2 kGy treated GG solution decreased to 45% as compared to control film (Table 21). These results are in good agreement with Kim et al. (2008) [77] who concluded that radiation treatment of biomaterials may result in more compact structure (because of lower molecular weight fragments) and could help natural polymers to overcome their hydrophilic character. Therefore it can be concluded that gamma radiation induced extensive degradation of GG solution as compared to GG powder was responsible for lower WVTR of film prepared

from irradiated GG solutions. No significant effect of radiation was observed on the WVTR of films prepared from non-irradiated GG and subjected to irradiation processing thereafter (Table 22).

3.2.5.5 Color and opacity

Color is an important aspect for packaging films. Values for color coordinates i.e. *L**, *a** and *b** are shown in Table 20, 21 & 22. No noteworthy differences were obtained in *L** values for films prepared with irradiated GG powder (Table 20). Films prepared with GG irradiated at lower doses up to 500 Gy demonstrated slightly higher *a** values as compared to control films indicating increased redness of films. However at higher doses beyond 500 Gy *a** values were comparable to that of control. No particular trend was obtained in *b** values for films prepared with irradiated GG powder (Table 20). Films prepared from irradiated GG solution demonstrated decrease in *L** and *b** values whereas *a** remained constant with irradiation doses (Table 21). For films prepared with control GG and subjected to radiation processing thereafter a significant dose dependent reduction in *L** and *a** values were observed (Table 22). At very high dose of 100 kGy increased b* values was observed. Increase in *b** values indicate increase yellowness of films. Jo et al. (2005) [170] also reported similar results for irradiated pectin and gelatin based films i.e. with dose decrease in *L** and *a** values and increase in *b** values.

Opacity indicates degree to which light is not allowed to pass through. Opacity of packaging films is important as it affect the packaged products visibility to consumers. A significantly higher opacity was observed in all three samples of GG based film as

compared to control samples (Table 20, 21 & 22). Observed increase in opacity might be due to increased darkness or redness in irradiated samples. Although, significant variance was observed instrumentally in color and opacity of samples after irradiation visual differences were negligible to be discerned by naked eye.

3.2.5.6 FTIR analysis of GG based films

To compare the changes in chemical structure of films prepared from control GG, irradiated powder GG, irradiated aqueous GG and gamma irradiated control GG films FTIR spectra were recorded (Figure 22 A, B & C). It was observed that irradiation had no effect on appearance or disappearance of peaks of FTIR spectra. Gupta et al. (2009) [167] demonstrated similar results wherein no change in FTIR spectrum of control and irradiated GG was observed. Thus above results clearly demonstrate that radiation processing causes no major functional group transformations but only random free radical chain scission in GG.

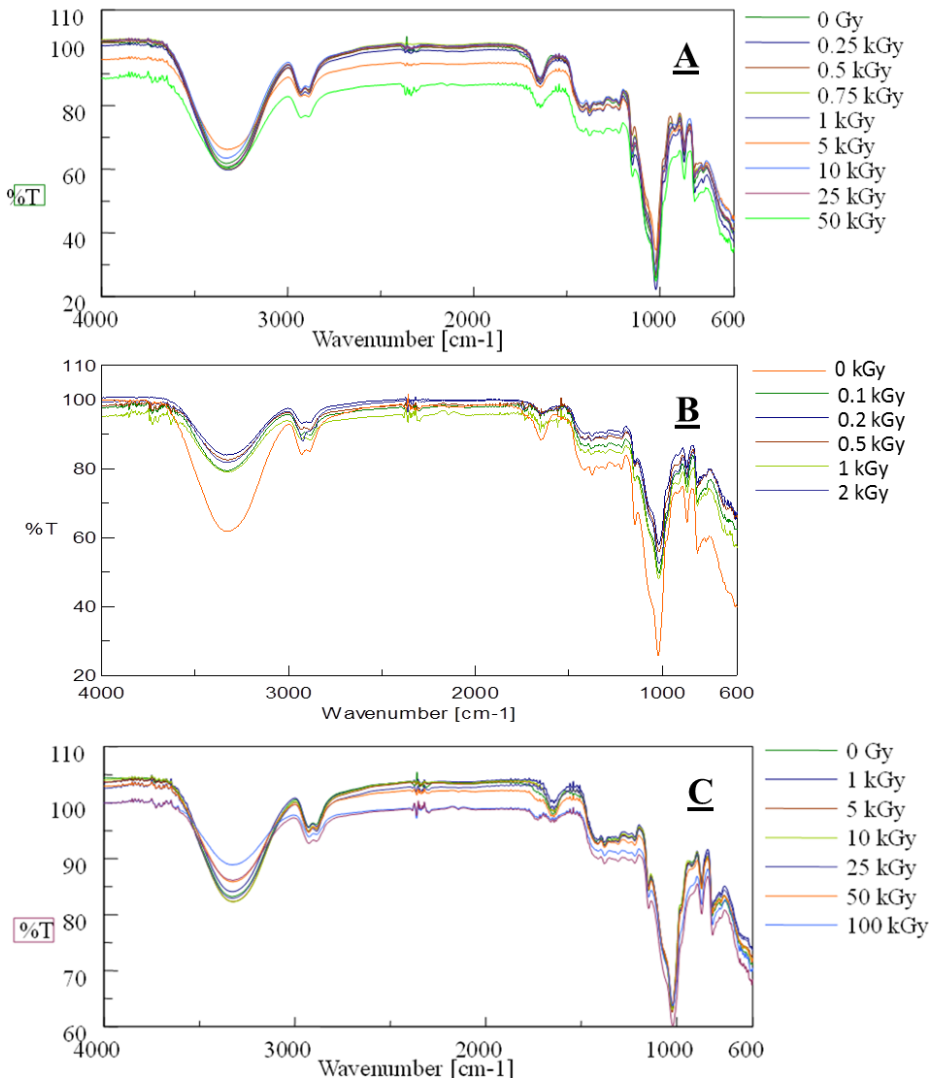

Figure 22: FTIR profiles of GG films (A) Films prepared from irradiated GG powder (B) Films prepared from irradiated GG solution (C) Control GG films then subjected to irradiation.

3.2.5.7 TGA analysis

Thermal stability of films was analyzed by superimposition of TGA profiles. TGA curves for films prepared from control GG, 500 Gy irradiated powder GG and 2 kGy irradiated aqueous GG as well as 100 kGy irradiated film prepared from control GG are shown in figure 9. Mass loss below 110 °C was mainly ascribed to water loss. At 110 °C, percent weight loss of control GG film, powder irradiated GG film, solution irradiated GG film and irradiated GG film were 7.5%, 9.3%, 11.1% and 11% respectively. Lowest weight loss of control GG film was due to radiation induced degradation of GG which might result in low water retention capacity of films at higher temperature. All film samples demonstrated two step decomposition patterns. The first step started at 275 °C which resulted in major weight loss of the samples this could be attributed to the formation of volatile disintegrated products [173]. The second step began at 320 °C which mainly caused by the thermal decomposition of the GG along with glycerol and the products were mainly composed of small molecular carbon and hydrocarbon [173]. Parvin et al. (2011) [173] demonstrated that irradiation decreased the rate of thermal degradation due to radiation induced cross-linking of films. However, in present study reduction in molecular weight occurred due to gamma irradiation as confirmed by GPC there by explaining the ineffectiveness of irradiation on thermal degradability of films.

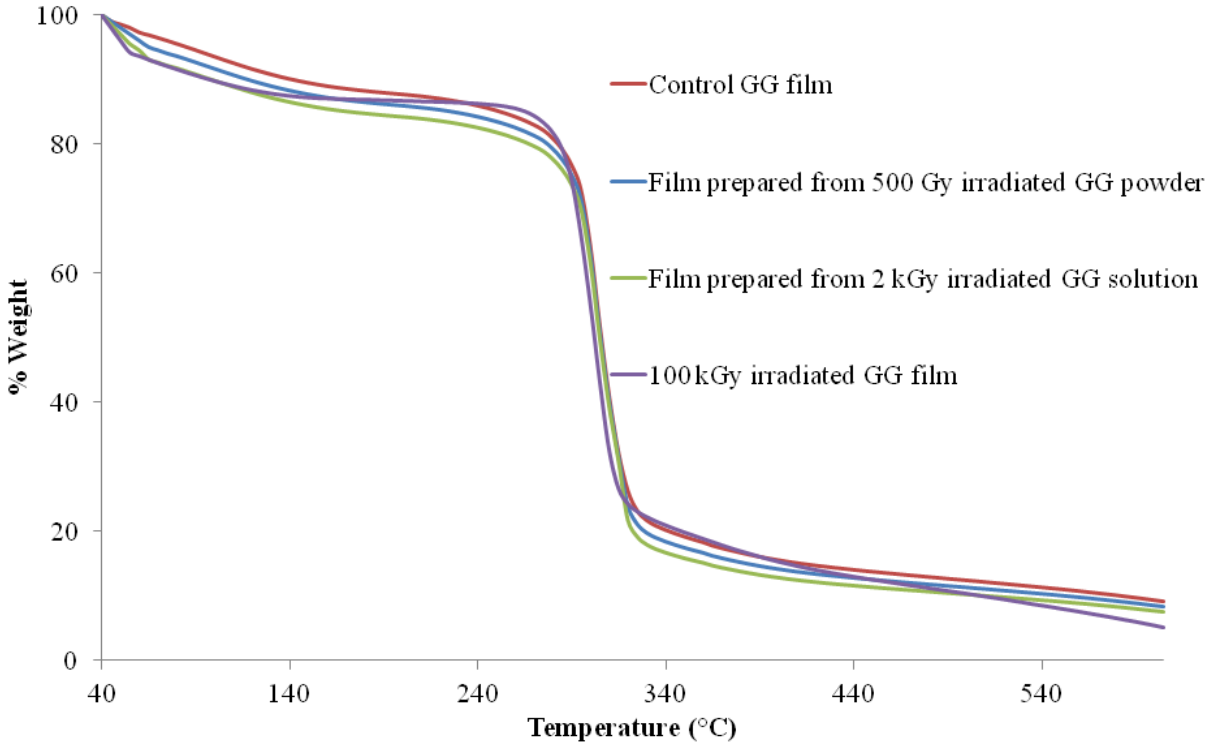

Figure 23: Thermal behavior of GG based films.

Radiation significantly affected the mechanical and barrier properties of GG based films. It was observed that gamma irradiation was more effective on GG solution than on GG powder in terms of reduction of molecular weight and various film characteristics. However, GG films were found to be highly resistant against change in its mechanical and barrier properties when subjected to irradiation. Subsequent to analyzing the effect of radiation treatment of various forms of GG (powder, solution and film) on its film properties, further improvement in film functional properties was attempted by incorporation and optimization of various additives.

3.3 Use of additives for better film properties

In the earlier section (3.2.5.1) it was observed that a low dose (500 Gy) of gamma radiation resulted in 33 percent improvement in tensile strength of GG films. No significant ($p < 0.05$) influence on the water vapor transmission of the films was however noted with a water vapor transmission rate (WVTR) of 190 ± 10 g/m^2/day. In contrast, commercial plastic films widely used for packaging of food products generally have a WVTR in range of 30-40 g/m^2/day. It was therefore of interest to reduce the WVTR of GG films. Several reports exist in literature on the use of nanoclays and beeswax for improving mechanical and barrier properties of biopolymer based films. To the best of our knowledge no reports exists on the effect of addition of these additives (beeswax and nanoclays) on mechanical and barrier properties of GG based films. The effect of incorporation of nanoclays and beeswax on properties of GG based film therefore further investigated.

3.3.1 Effect of nanoclay type and content on mechanical and barrier properties of GG based films

GG based nanocomposite films were prepared using organically modified (cloisite 20A) and unmodified (nanofil 116) nanoclays. Cloisite 20A is a natural MMT modified with a quaternary ammonium salt while nanofil 116 is an inorganic nano-dispersible layered silicate based on a refined natural bentonite. Effect of incorporation of both the types of nanoclay on the mechanical strength, water vapor barrier property, chromatic characteristics and opacity of films was evaluated.

3.3.1.1 Effect on tensile strength and Young's modulus

Thickness of native GG films was found to be 15.2 ± 2.3 μm. No significant ($p < 0.05$) effect was observed on thickness of films due to addition of nanoclays. Rhim et al. (2006) [174] also reported no significant change in thickness between chitosan based nanocomposite film and neat chitosan film.

Table 23 and 24 demonstrates the effect of addition of nanoclay on tensile strength and Young's modulus of the films. A significant ($p < 0.05$) concentration dependent increase in tensile strength and Young's modulus as compared to control GG films was observed due to incorporation of both nanoclays i.e. nanofil 116 (Table 23) and cloisite 20A (Table 24). Nanocomposites prepared by incorporating nanofil 116 demonstrated highest tensile strength and Young's modulus at a concentration of 2.5%, while the best mechanical properties for cloisite 20A containing films was observed at a concentration of 10%. Nanofil 116 incorporation (2.5%) resulted in films with tensile strength of 113 ± 20 MPa and Young's modulus of 11 ± 0.8 GPa (Table 23) while these values for cloisite 20A (10%) containing films were 79 ± 8 MPa and 1.8 ± 0.2 GPa, respectively (Table 24). Control films had a tensile strength of 56 ± 7 MPa and Young's modulus of 0.2 ± 0.1 GPa (Table 23). This observed improvement in mechanical properties of nanocomposites could be due to the nano level interactions of clay with the polymer matrix resulting in greater possibility of energy transfer from polymer to clay layered silicates [97]. Improved mechanical properties of biodegradable films by formation of clay nanocomposites were previously reported for several polymers such as polyethylacrylate

[175], starch [176, 5,177], pectin [178] and agar [179]. Thus our results are in agreement with already published literature data.

Incorporation of either of the nanoclay beyond concentration of 10% in films resulted in a significant ($p < 0.05$) reduction in mechanical properties as compared to the control films (Table 23 & 24). Negative impact of clay loading in films at higher concentration (> 10%) is mainly attributed to agglomeration of clay particles resulting in formation of stacked clays without complete dispersion through the polymer matrix. This leads to non-homogenous distribution of clay in the film thus forming cracks and reduction in mechanical strength [180].

In the present study, the maximum increase in tensile strength as compared to control film was 102% for 2.5% nanofil 116 films and 41% for 10% cloisite containing films (Table 23 & 24). In previous studies, a 31.5% increase for agar based 10% cloisite Na^+ clay nanocomposite films [179] and 88% increase for 3% pectin based natural MMT films [178] was reported. Thus, in the present study a higher improvement in tensile strength as compared to previous reports was observed, especially in case of nanofil 116 (natural MMT). This might be due to the better compatibility between GG and nanofil 116. Another reason for observed results in present work might be due to mild treatment (stirring for seven days) that was given for intercalation. However, in previous studies high shear mixing and ultrasonication was used [179, 178]. It is known that parallel sheet of nanoclay can break under high shear mixing as well as ultrasound [181, 182]. This could lead to the reduction in aspect ratio of nanoclay that could negatively affect the mechanical properties of films.

It was also noted that mechanical properties of films prepared by incorporating nanofil 116 at concentrations of 2.5% and above were significantly ($p < 0.05$) superior as compared to films prepared with cloisite 20A (Table 23 & 24) at similar concentrations. This might be due to the hydrophobic nature of the two tallow groups of cloisite 20A resulting in its uneven dispersion in hydrophilic GG polymeric matrices compared to nanofil 116. Mangiacapra et al. (2006) [178] have also demonstrated better physical properties of apple peel pectin based nanocomposites employing hydrophilic natural sodium MMT in comparison to organically (hydrophobic) modified clay.

Thus in present study, incorporation of nanofil 116 was found to be more effective for improved GG based film characteristics than cloisite 20A. An attempt was made to further improve physical characteristics of film by synergistic effect of nanofil 116 along with 500 Gy irradiated GG powder which induces ordering of chains. Films prepared from 500 Gy irradiated GG powder incorporated with 2.5% of nanofil 116 demonstrated a tensile strength of 98 ± 11 MPa, Young's modulus of 9 ± 1 GPa, and WVTR of 140 ± 19 g/m^2/ d. Surprisingly, the prepared nanocomposites demonstrated poor properties as compared to film prepared from control GG having 2.5% of nanofil 116 (Table 23). Observed results might be due to improper intercalation of GG chains into layered silicates brought about by a ordering of polymer chains and a consequent coiled structure at nanometer scale thus restricting its entry into layer spacing of nanofil 116.

Table 23: Physical properties of GG based nanofil 116 composites.

Nanofil116 (w/w GG)	Tensile strength (MPa)	Young's Modulus (GPa)	Puncture strength (N)	% elongation	WVTR (g/m^2/ d)	L*	a*	b*	Opacity (%)
0%	56 ± 7^{b}	0.2 ± 0.1^{f}	1.8 ± 0.3^{a}	17 ± 5.5^{a}	170 ± 23^{a}	98.7 ± 0.6^{a}	0.6 ± 0.2^{a}	1.1 ± 0.2^{bc}	12.9 ± 0.2^{cd}
1%	56 ± 12^{b}	0.6 ± 0.4^{d}	1.5 ± 0.3^{ab}	15 ± 4.5^{a}	153 ± 21^{ab}	98 ± 0.3^{a}	-0.5 ± 0.1^{b}	0.8 ± 0.1^{c}	12.1 ± 0.6^{d}
2.5%	113 ± 20^{a}	11 ± 0.8^{a}	1.6 ± 0.3^{ab}	11 ± 3^{a}	128 ± 19^{bc}	97.9 ± 0.7^{a}	-0.6 ± 0.1^{b}	1 ± 0.1^{bc}	12.4 ± 0.7^{cd}
5%	91 ± 13^{a}	9.5 ± 0.8^{b}	1.7 ± 0.3^{ab}	18 ± 4^{a}	112 ± 10^{c}	95.3 ± 0.8^{b}	-1.2 ± 0.2^{c}	1.3 ± 0.2^{b}	12.4 ± 0.9^{cd}
7.5%	98 ± 17^{a}	9.7 ± 0.2^{b}	1.7 ± 0.2^{a}	13 ± 3^{a}	104 ± 16^{c}	94.8 ± 0.9^{b}	-1.5 ± 0.3^{c}	1.4 ± 0.2^{b}	13.5 ± 0.8^{bc}
10%	94 ± 14^{a}	7.5 ± 0.5^{c}	1.9 ± 0.3^{a}	16 ± 5.5^{a}	102 ± 13^{c}	90.6 ± 0.6^{c}	-2.2 ± 0.3^{d}	1.9 ± 0.3^{a}	14.5 ± 0.4^{ab}
20%	36 ± 9^{b}	1.7 ± 0.3^{e}	1.2 ± 0.3^{b}	13 ± 3^{a}	109 ± 12^{c}	89.7 ± 0.5^{c}	-2.4 ± 0.3^{d}	2.1 ± 0.4^{a}	14.8 ± 1^{a}

Any two means in the same column followed by the same letter are not significantly ($p > 0.05$) different.

Table 24: Physical properties of GG based cloisite 20A composites.

Cloisite 20A (w/wGG)	Tensile strength (MPa)	Young's modulus (GPa)	Puncture strength (N)	% elongation	WVTR (g/m^2/ d)	L*	a*	b*	Opacity (%)
0%	56 ± 7^{c}	0.2 ± 0.1^{d}	1.8 ± 0.3^{a}	17 ± 5.5^{a}	170 ± 23^{a}	98.7 ± 0.6^{a}	0.6 ± 0.2^{a}	1.1 ± 0.2^{bc}	12.9 ± 0.2^{bc}
1%	53 ± 11^{c}	0.6 ± 0.1^{c}	1.4 ± 0.2^{ab}	16 ± 3.5^{a}	157 ± 10^{a}	98.9 ± 0.3^{a}	-0.2 ± 0.1^{b}	0.9 ± 0.1^{c}	12.3 ± 0.4^{c}
2.5%	62 ± 10^{bc}	0.7 ± 0.1^{c}	1.6 ± 0.1^{ab}	16 ± 5^{a}	132 ± 10^{b}	98.4 ± 0.7^{a}	-0.7 ± 0.2^{c}	1 ± 0.1^{bc}	12.6 ± 0.7^{c}
5%	67 ± 12^{abc}	1.2 ± 0.3^{b}	1.7 ± 0.3^{ab}	13.5 ± 5^{a}	125 ± 9^{b}	95.7 ± 0.8^{b}	-0.9 ± 0.2^{cd}	1.1 ± 0.2^{bc}	12.8 ± 0.9^{c}
7.5%	77 ± 8^{ab}	1.5 ± 0.2^{b}	1.8 ± 0.1^{a}	17 ± 3.5^{a}	121 ± 9^{b}	94.2 ± 0.6^{c}	-1.2 ± 0.3^{d}	1.3 ± 0.2^{b}	13.4 ± 0.7^{abc}
10%	79 ± 8^{a}	1.8 ± 0.2^{a}	1.6 ± 0.2^{ab}	16 ± 3^{a}	124 ± 9^{b}	91.8 ± 0.6^{d}	-1.9 ± 0.3^{e}	1.7 ± 0.3^{a}	14.1 ± 0.7^{ab}
20%	25 ± 2^{d}	1.2 ± 0.1^{b}	1.2 ± 0.3^{b}	21.5 ± 4.5^{a}	129 ± 8^{b}	90.9 ± 0.9^{d}	-2.3 ± 0.2^{e}	1.9 ± 0.1^{a}	14.6 ± 0.9^{a}

Any two means in the same column followed by the same letter are not significantly ($p > 0.05$) different.

3.3.1.2 Effect on puncture strength and percent elongation

Puncture strength of control film was 1.8 ± 0.3 N. A significant ($p < 0.05$) reduction (33%) in puncture strength as compared to control was observed in films incorporated with 20% of either nanoclays (Table 23 & 24). Nanoclay concentration (up to 10%) had no significant ($p < 0.05$) effect on the puncture strength (Table 23 & 24). The reduction in puncture strength concentration above 10% might be due to agglomeration of nanoclays. Very few studies have been conducted in the past to determine the effect of nanoclay concentration on puncture strength of films. Nascimento et al. (2012) [183] also found that addition of organoclay reduced the puncture strength of mesocarp flour of passion fruit (*Passifloraedulis*) based films.

The control films showed a percent elongation of 17 ± 5.5. No significant change ($p < 0.05$) was observed in percent elongation of the films due to incorporation of nanoclays (Table 23 & 24). Chrissafis et al. (2007) [184] reported only 8% increase in percent elongation when cloisite 20A was added in poly ε-caprolactone film due to plasticizing effect of the MMT's organic modifier. Thus the results presented in this study are in agreement with previous reports.

3.3.1.3 X-ray scattering

SAXS patterns of cloisite 20A powder and GG-cloisite 20A (2.5%, 10%, and 20% w/w GG) nanocomposite films are shown in Figure 24A. Cloisite 20A powder showed a signature peak at q of 2.48. The d-spacing of cloisite 20A corresponding to this peak was calculated to be 2.53 nm. This was slightly higher than the reported d-spacing value of

2.48 nm [185]. However, SAXS pattern of GG-cloisite 20A nanocomposites showed a signature peak at q of 1.62 which corresponds to d-spacing 3.88 nm. Higher basal spacing of GG-cloisite 20A nanocomposites was due to 7 days of stirring of cloisite 20A. XRD patterns of nanofil 116 powder and GG-nanofil 116 (2.5%, 10%, and 20% w/w GG) nanocomposite films are shown in Figure 24B. Nanofil 116 powder showed a diffraction peak at a 2θ angle of 7.06°. The d-spacing of nanofil 116 corresponding to the diffraction peak was calculated to be 1.25 nm. This was in agreement with the d-spacing value of 1.25 nm as reported earlier [186]. After seven days of dispersion, a 2θ angle of 4.8 corresponding to a d-spacing of 1.81 nm was noted for nanofil 116 composite. Thus, it is evident from the above results that basal spacing in nanoclays increased after seven days of stirring. Increased basal spacing resulted in a greater intercalation of nanoclays by GG polymer thus resulting in increased mechanical properties of nanocomposites as compared to control. Similar results were also observed by Rhim (2011) [179] for agar based cloisite Na^{+}clay composite films. In spite of higher basal spacing of cloisite 20A than nanofil 116, mechanical properties of cloisite 20A composite films were inferior to nanofil 116 containing films. This might be due to the organophilic modification of closite 20A which renders it incompatible with hydrophilic GG.

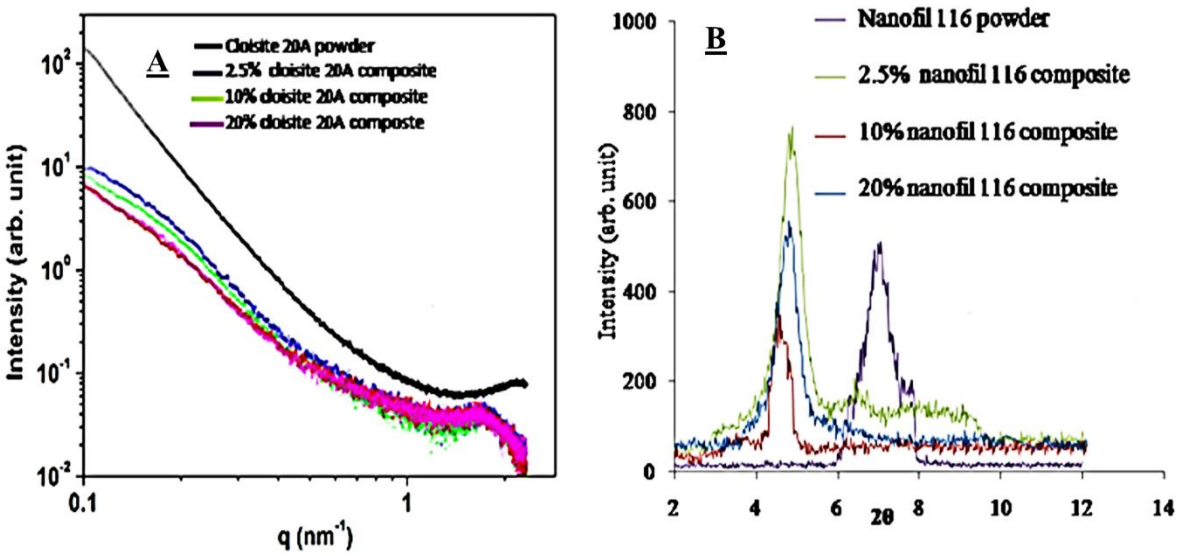

Figure 24: X-ray scattering profiles (A) SAXS patterns of cloisite 20A powder and GG-cloisite 20A nanocomposites (B) XRD patterns of nanofil 116 powder and GG-nanofil 116 nanocomposites.

3.3.1.4 Effect of irradiation on mechanical properties of nanocomposite films

Radiation processing significantly improved the mechanical properties of native GG films (section 3.2.5). Hence, the effect of gamma irradiation on nanocomposite films was of particular interest. In the present study, maximum tensile strength and Young's modulus was observed for nanocomposites prepared with 2.5% nanofil 116 and 10% cloisite 20A. Thus, further work on radiation processing of nanocomposites was performed on these films. Tensile strength of nanofil 116 composite films showed resistance against radiation up to 25 kGy with a significant ($p < 0.05$) dose dependent decrease thereafter (Table 25). Films incorporated with cloisite 20A, on the other hand, were found to be more radiation sensitive and unstable beyond a dose of 5 kGy (Table 26). We had earlier demonstrated

that GG films were stable up to a radiation dose of 25 kGy (section 3.2.5). Interestingly, a radiation dependent increase in Young's modulus of nanofil 116 composite films was observed up to a dose of 25 kGy with a dose dependent decrease thereafter (Table 25). Young's modulus increased from 11 ± 0.8 GPa in the control to 15.3 ± 1 GPa at 25 kGy which however reduced to 5 ± 1.1 GPa at 100 kGy. The observed enhancement in Young's modulus might be due to greater dispersion of nanoclay in the polymer matrices with radiation dose as reported earlier for polylactide based nanocomposite films by Zaidi et al. (2013) [187]. Surprisingly, no significant ($p < 0.05$) change in Young's modulus was observed for cloisite 20A films up to a dose of 100 kGy (Table 26). Table 25 also demonstrates the effect of gamma irradiation on percent elongation of the nanocomposite films. No effect of radiation processing on percent elongation was observed for nanofil 116 containing films. Puncture strength demonstrated stability up to radiation dose of 10 kGy with dose dependent decrease thereafter. In case of cloisite 20A containing films, a reduction in percent elongation beyond 50 kGy was observed while its puncture strength remained stable only up to 5 kGy (Table 26).

The above data, thus, clearly demonstrated that radiation enhanced Young's modulus while other properties of nanofil 116 containing films remained constant as compared to cloisite 20A films. In a previous work on radiation treatment of starch and unmodified MMT it was observed that clay particles stimulated the formation of radicals and also prolonged life time of radicals which favored cross-linking between starch molecules. Radiation processing of starch-unmodified MMT nanocomposites led to increased gel formation thus confirming cross-linking. Starch based nanocomposites were stable under

radiation up to a dose of 30 kGy with degradation observed thereafter [176]. Similarly, radiation processing (30 kGy) resulted in increased film strength of polylactic acid and MMT nanocomposites [188].

However, several authors have reported an increased rate of degradation of nanocomposites prepared with organically modified clay (OMMT) as compared to pristine polymerdue to radiation processing. Touati et al. (2007) [189] reported that polypropylene (PP)/OMMT nanocomposites undergo much faster degradation as compared to pristine PP due to radiation processing. These authors suggested that organically modified clay particles act as oxidation catalysts leading to the degradation of the polymer. Similar result was observed by Qin et al. (2005) [190] wherein the rate of photo-oxidative degradation of PP/MMT nanocomposites was much faster than that of pure PP when exposed to ultraviolet radiation.

Thus it can again be concluded that unmodified clay nanocomposites (prepared using nanofil 116) demonstrated significantly better radiation stability as compared to those prepared with organically modified clay (cloisite 20A). Organically modified clay particles (cloisite 20A) might have produced significantly higher number of carbon centered radicals due to radiation processing as compared to unmodified clay (nanofil 116) leading to greater degradation of GG polymer. To the best of our knowledge, no reports are available on comparative effect of modified and unmodified clays on polymers during radiation processing. Therefore, direct literature comparisons could not be obtained.

Table 25: Effect of irradiation on physical properties of GG based 2.5% nanofil 116 composites.

Dose (kGy)	Tensile strength (MPa)	Young's modulus (GPa)	Puncture strength (N)	% elongation	WVTR ($g/m^2/d$)	L*	a*	b*	Opacity (%)
0	113 ± 20^{a}	11 ± 0.8^{b}	1.6 ± 0.3^{ab}	11 ± 3^{a}	128 ± 19^{a}	97.9 ± 0.7^{a}	-0.6 ± 0.1^{a}	1 ± 0.1^{e}	12.4 ± 0.7^{b}
1	108 ± 13^{a}	12 ± 1^{b}	1.7 ± 0.1^{a}	15 ± 2^{a}	132 ± 10^{a}	97.3 ± 0.7^{a}	-0.7 ± 0.1^{a}	1.2 ± 0.1^{e}	12.4 ± 0.7^{b}
5	98 ± 10^{a}	13.3 ± 0.7^{ab}	1.4 ± 0.2^{abc}	14.5 ± 4.5^{a}	115 ± 13^{a}	97 ± 0.6^{a}	-1.3 ± 0.2^{b}	1.4 ± 0.1^{d}	12.6 ± 0.7^{b}
10	94 ± 11^{a}	14.1 ± 3.8^{ab}	1.5 ± 0.3^{ab}	13.5 ± 2^{a}	113 ± 13^{a}	96.8 ± 0.8^{ab}	-1.8 ± 0.3^{c}	2.4 ± 0.3^{c}	12.9 ± 0.6^{b}
25	91 ± 10^{a}	15.3 ± 1^{a}	1.3 ± 0.1^{bc}	13 ± 3.5^{a}	108 ± 15^{a}	95.7 ± 0.7^{bc}	-2.1 ± 0.2^{c}	3.8 ± 0.3^{b}	13.4 ± 0.4^{b}
50	40 ± 6^{b}	6 ± 1.1^{c}	1.1 ± 0.1^{cd}	12 ± 2^{a}	124 ± 12^{a}	95 ± 0.5^{cd}	-2.6 ± 0.4^{d}	4.3 ± 0.5^{ab}	14.2 ± 0.2^{a}
100	32 ± 3^{b}	5 ± 1.1^{c}	0.9 ± 0.1^{d}	11 ± 2^{a}	121 ± 9^{a}	94.3 ± 0.9^{d}	-3.4 ± 0.4^{e}	5.4 ± 1^{a}	14.7 ± 0.3^{a}

Any two means in the same column followed by the same letter are not significantly ($p > 0.05$) different.

Table 26: Effect of irradiation on physical properties of GG based 10% cloisite 20A composites.

Dose (kGy)	Tensile strength (MPa)	Young's modulus (GPa)	Puncture strength (N)	% elongation	WVTR ($g/m^2/d$)	L*	a*	b*	Opacity (%)
0	79 ± 8^{a}	1.8 ± 0.2^{a}	1.6 ± 0.2^{a}	16 ± 3^{a}	124 ± 9^{a}	91.8 ± 0.6^{a}	-1.9 ± 0.3^{a}	1.7 ± 0.3^{e}	14.1 ± 0.7^{c}
1	76 ± 11^{a}	1.9 ± 0.2^{a}	1.6 ± 0.3^{a}	19 ± 4^{a}	116 ± 9^{a}	91.6 ± 0.3^{ab}	-2.2 ± 0.7^{a}	2.1 ± 0.5^{e}	14 ± 0.6^{c}
5	64 ± 8^{a}	1.7 ± 0.2^{a}	1.5 ± 0.2^{ab}	15 ± 3^{a}	115 ± 14^{a}	91 ± 0.4^{abc}	-2.8 ± 0.5^{ab}	2.9 ± 0.7^{de}	14.6 ± 0.3^{bc}
10	46 ± 10^{b}	2.4 ± 0.4^{a}	1.2 ± 0.1^{bc}	15 ± 2^{a}	112 ± 7^{a}	90.6 ± 0.2^{bc}	-3.6 ± 0.4^{bc}	3.9 ± 0.8^{cd}	14.8 ± 0.8^{bc}
25	32 ± 7^{bc}	1.7 ± 0.1^{a}	1 ± 0.2^{c}	14 ± 2^{ab}	116 ± 8^{a}	90.1 ± 0.9^{cd}	-4.7 ± 0.6^{c}	5.1 ± 0.6^{c}	15.3 ± 0.9^{abc}
50	23 ± 10^{cd}	2 ± 0.4^{a}	0.5 ± 0.1^{d}	14 ± 4^{ab}	113 ± 13^{a}	89.4 ± 0.7^{d}	-5.9 ± 0.8^{d}	6.8 ± 1^{b}	15.9 ± 1^{ab}
100	15 ± 6^{d}	2.1 ± 0.1^{a}	0.4 ± 0.1^{d}	10 ± 2^{b}	113 ± 7^{a}	$89.2\pm.6^{d}$	-7.3 ± 1^{e}	8.5 ± 1^{a}	16.3 ± 0.5^{a}

Any two means in the same column followed by the same letter are not significantly ($p > 0.05$) different.

3.3.1.5 WVTR of control and irradiated nanocomposite films

Table 23 and 24 demonstrates the effect of nanoclay on WVTR of nanocomposite films. WVTR of nanocomposites prepared with either of nanoclays demonstrated a significant ($p < 0.05$) decrease as compared to control GG based films up to concentrations of 2.5%. However, no further reduction in WVTR at higher concentrations (> 2.5%) was observed. A reduction was noted in WVTR from 170 ± 23 g/m^2/day in control films to 128 ± 19 and 132 ± 10 g/m^2/day for 2.5% nanofil 116 and cloisite 20A films, respectively (Table 23 & 24). Irradiation of nanocomposite films had no significant ($p < 0.05$) effect on its WVTR (Table 25 & 26). It is known that the layered structure of nanoclays obstruct transmission of water vapor through the film matrix and thus delay the diffusion of water vapor due to tortuosity [191]. Thus, an optimum concentration of 2.5% nanofil 116 yielded a nanocomposite film that had a lower WVTR besides highest tensile strength and Young's modulus among both the clays studied. Incompatibility of cloisite 20A with GG could explain the higher WVTR of films containing cloisite 20A as compared to nanofil 116.

3.3.1.6 FEG-SEM of GG based nanocomposite

In order to understand microstructure of the developed films FEG-SEM analysis was carried out. Surface morphology of control GG films was observed to be homogeneous and smooth (Figure 25A). As observed from the results obtained in the present study, the best mechanical properties were obtained at a concentration of 2.5% and 10% for nanofil 116 and cloisite 20A respectively. Further, addition of either of the clays up to 10% resulted in films having better mechanical properties than control films. However, higher

concentration of nanoclay (20%) resulted in decreased mechanical properties of nanocomposite films (Table 23 & 24). FEG-SEM analysis showed that at lower concentration of 2.5% nanofil 116 containing films had homogeneous and smooth surface like control film (Figure 25B). However, surface morphology of cloisite 20A (10%) containing films was not smooth and few nanoclay clumps were clearly observed (Figure 25C).

At higher concentration of 20% presence of large amount of nanoclay clumps in nanofil 116 and cloisite 20A films can be clearly seen (Figure 25 D & E). This agglomeration of clay particles at higher concentrations resulted in reduced mechanical strength of nanocomposites. It was also observed that at a concentration of 20%, cloisite 20A containing films had larger clumps and patches as compared to nanofil 116 incorporated films (Figure 25 D & E). This further proves incompatibility of organomodified clay (closite 20A) with the GG. Better mechanical properties of nanofil 116 composite films as compared to cloisite 20A composite films observed in the present study could thus be explained.

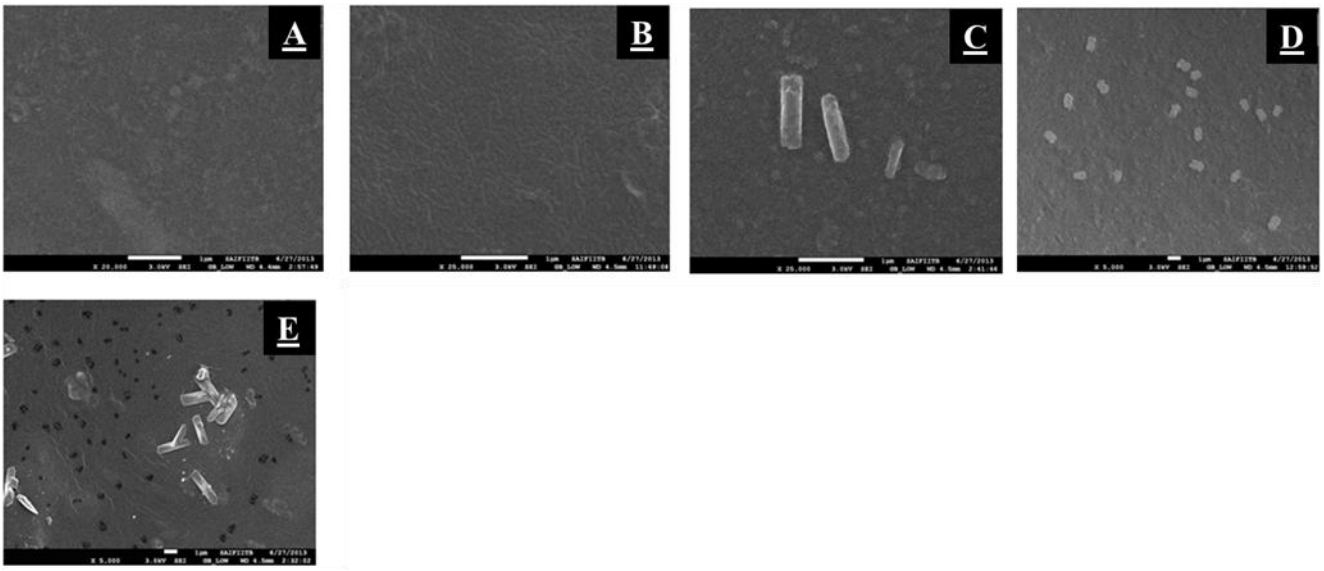

Figure 25: FEG-SEM images of GG based films (A) control GG film (×20000) (B) 2.5% nanofil 116 composite (×25000) (C) 10% cloisite 20A composite (×20000) (D) 20% nanofil 116 composite (×5000) (E) 20% cloisite 20A composite (×5000).

3.3.1.7 Color and opacity

Values for color coordinates of GG based nanocomposite films are shown in Table 23, 24, 25 and 26. *L**, *a** and *b** values of control films was 98.7 ± 0.6, 0.6 ± 0.2 and 1.1 ± 0.2 respectively. It was observed that *L** and *a** values reduced significantly ($p < 0.05$) on nanoclay concentration dependent manner. However, a concentration dependent increase in *b** values was observed. Reduction in *L** and *a** values indicates increased darkness and greenness of the films respectively, while increase in *b** values signify increased yellowness of films. Similar results were also observed for chitosan based nanocomposite films by Rhim et al. (2006) [174]. Thus, the results obtained in the present study are in accordance with already published literature data. Radiation dose dependent decrease in

*L** and *a** values with corresponding increase in *b** values was also observed for nanocomposite films (Table 25 & 26). We had earlier demonstrated similar results for films prepared with only GG (section 3.2.5.5).

Nanoclay concentration or radiation dose dependent increase in opacity was observed in GG based nanocomposite films (Table 23, 24, 25 & 26). Opacity of control GG film was 12.9 ± 0.2 which increased to 14.5 ± 0.4 and 14.1 ± 0.7 for 10% nanofil 116 and cloisite 20 A containing film, respectively (Table 23 & 24). Observed increase in opacity might be due to increased darkness or color of the GG based films. Although, significant ($p < 0.05$) variance was observed instrumentally in color and opacity of samples after incorporation of nanoclay, visual differences were negligible to be discerned by naked eye.

3.3.1.8 FTIR

Change in chemical structure of control (without nanaoclays), irradiated and non-irradiated nanocomposite GG films was determined by comparison of FTIR spectra. A superimposable FTIR spectrum of control as well as nanocomposite GG films was obtained suggesting that addition of nanoclays or radiation processing had no major functional group transformations (Figure 26 A & B). Small shifts in peak due to phosphorous stretching (P-O-P) in plane bands between 1025 cm^{-1} to 870 cm^{-1} could be observed in nanocomposite films due to presence of nanoclays.

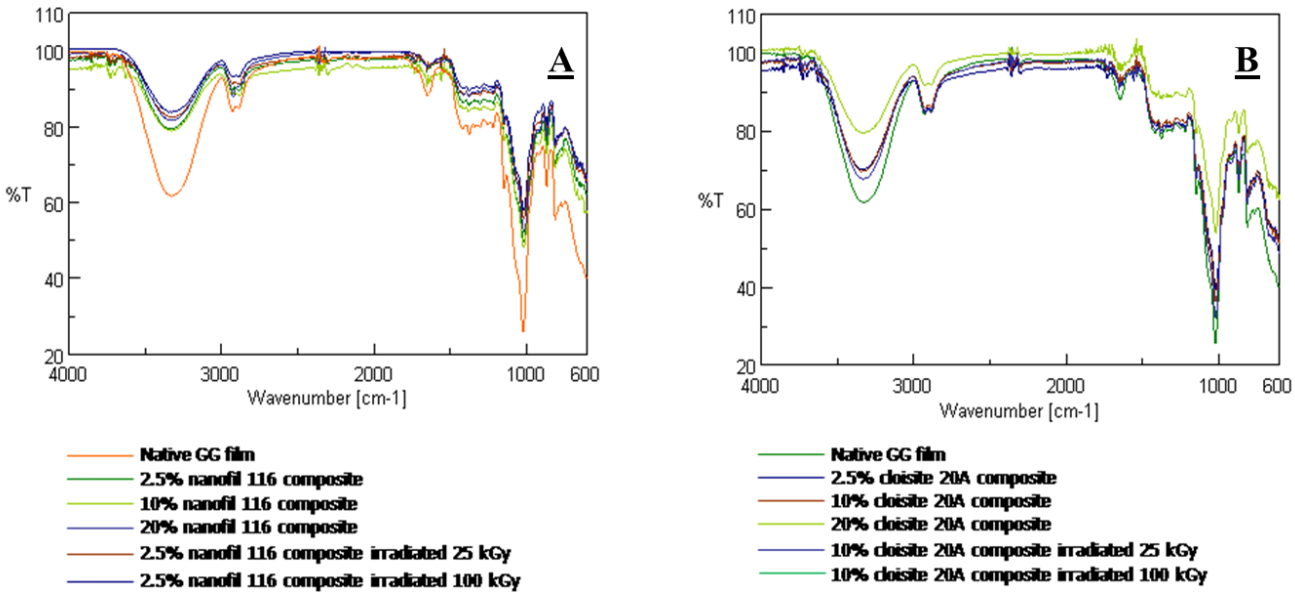

Figure 26: FTIR spectra (A) control GG films, and irradiated and non-irradiated GG-nanofil 116 nanocomposite films (B) control GG films, and irradiated and non-irradiated GG-cloisite 20A nanocomposite films.

3.3.1.9 TGA analysis of nanocomposites

TGA results of non-irradiated and irradiated GG/clay composite films in the temperature range from 40 to 600 °C are shown in Figure 27. The weight loss below 110 °C was due to removal of water in form of vapors. Maximum weight loss was observed for native GG films.This might be attributed to the nanoclay acting as barrier to the water vapors. All the film samples demonstrated two step decomposition patterns. As discussed earlier (section 3.2.5.7), the first degradation step started at 275 °C and second step began at 320 °C for control GG film (Figure 27). Addition of nanoclays resulted in improved thermal stability of GG based nanocomposites. First degradation step started at 295 °C and the second step started at 325 °C. Chiou et al. (2007) [192] also demonstrated that

starch/cloisite Na+ nanocomposite had improved thermal stability than samples without nanoclay.

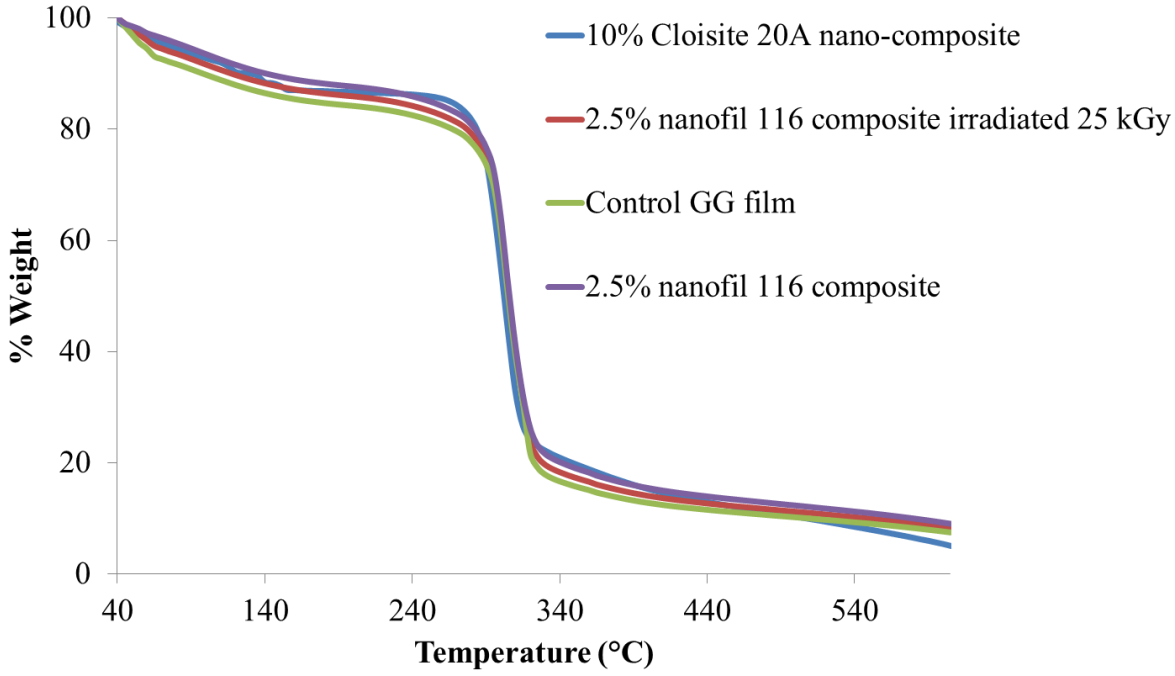

Figure 27: Thermal behavior of GG based nanocomposites.

3.3.2 Addition of various additives for the improvement of mechanical & barrier properties of GG based films

The developed nanocomposite films (nanofil 116; 2.5 percent) had WVTR of 128 ± 19 g/m^2/d (Table 23), while commercially available PVC stretch wrap films that are widely used for food packaging applications have a WVTR of 35 ± 5 g/m^2/d. Therefore, an attempt was made to reduce water vapor permeability of GG based nanocomposite films by incorporation of beeswax. Tween 80 was used to improve compatibility between beeswax and GG. RSM has been frequently used by several authors for optimizing

concentration of various additives to obtain films with desired properties. In the current investigation, beeswax, tween 80, nanofil 116 and glycerol were used as additives and their optimum concentration in GG film was determined using RSM.

3.3.2.1 Incorporation of various film additives

3.3.2.2 RSM analysis

Results obtained for various individual responses of the experimental design are shown in Table 14 and 27. Statistical analysis using ANOVA showed that the models generated by RSM were significant ($p < 0.05$) while lack of fit was insignificant ($p > 0.05$). Further, signal to noise ratio (S/N) of all models were above 4 indicating sufficient data to navigate designed space (Table 28). Coefficients for predicted regression models and coefficient of determination (R^2) are shown in Table 29. High values for R^2 also suggest that the models are good fit. Analysis of concentrations of various additives on different film properties was done by using generated model.

Table 27: Observed responses of Response Surface Methodology films prepared from GG.

Std	Run	Tensile strength (MPa)	Young's Modulus (GPa)	Percent elongation (%)	WVTR ($g/m^2/d$)	Puncture strength (N)
1	15	119	68	2.45	83.6	1.72
2	19	33	62	3.21	118.8	1.53
3	22	104	58	2.88	84.1	1.41
4	12	22	55	3.01	115.2	1.58
5	1	77	44	14.56	91.3	1.75
6	29	27	38	3.03	121.4	2.03
7	23	72	49	14.52	90.1	2.29
8	8	23	37	3.66	117.8	1.96
9	10	69	60	2.54	82.3	1.45
10	21	28	53	2.71	115.2	2.08
11	9	85	53	2.97	84	1.81
12	20	16	49	2.91	116.8	1.79
13	26	51	40	13.68	90.2	1.33
14	17	14	30	4.38	119.4	1.88
15	27	50	39	14.73	92.7	1.94
16	11	19	31	4.89	120.9	1.62
17	24	98	40	7.84	105	1.79
18	4	17	26	2.32	150.9	1.63
19	5	42	73	7.77	102.5	1.49
20	6	45	61	9.55	104.5	1.55
21	3	79	85	0.86	105.2	1.82
22	7	29	49	9.19	116	2.08
23	28	34	55	8.64	109.7	1.97
24	13	48	50	9.08	90.1	2.21
25	16	69	72	8.22	92.8	1.85
26	2	54	83	9.56	98.6	1.94
27	30	64	73	7.99	90.6	1.79
28	25	56	75	9.19	94.2	2.01
29	14	64	80	7.99	97.3	1.99
30	18	59	77	8.46	90.5	1.58

Table 28: Significance statistics, p values and signal to noise ratio (S/N) of Response Surface Methodology predicted models.

Response	Model			Residual			S/N
	Sum of squares	df	p-value	Sum of squares	df	p-value	
Tensile strength	20791.45	14	< 0.0001	1673.92	15	0.0501	13.544
Young's modulus	7622.33	14	< 0.0001	411.17	15	0.2678	16.072
Percent elongation	468.39	14	< 0.0001	21.56	15	0.0562	18.510
Puncture strength	1.22	14	0.0309	0.48	15	0.3926	6.789
WVTR	6618.72	14	< 0.0001	591.59	15	0.0517	15.137

Table 29: Coefficients of fitted polynomial representing relationship between response and process variable and R^2 values.

Coefficients	Tensile strength	Young's modulus	Percent elongation	Puncture strength	WVTR
Intercept	61	76.67	8.57	1.86	94
A-beeswax	-25.29[a]	-3.5[a]	-2.15[a]	0.02	14.12[a]
B-tween 80	-0.88	-2	0.27	0.03	0.14
C-glycerol	-10.13[a]	-9.25[a]	2.81[a]	0.08[a]	2.73
D-nanofil 116	-4.88[a]	-2.75[a]	0.09	0.01	-1.67
AB	-1.06	0.13	-0.05	-0.11[a]	-0.48
AC	6.94[a]	-1	-2.66[a]	-0.03	-1.05
AD	5.56	-0.13	0.15	0.06	-0.06
BC	1.06	2	0.08	0.06	-0.06
BD	2.69	0.125	0.09	0.01	0.95
CD	0.94	0	0.15	-0.13[a]	0.38
A^2	-0.62	-12.08[a]	-1.02[a]	-0.05	7.19[a]
B^2	-4.12	-3.58[a]	-0.13	-0.09[a]	1.08
C^2	-1.49	-3.58[a]	-1.04[a]	0.01	2.86[a]
D^2	-4.74[a]	-7.21[a]	-0.08	0.05	0.18
R^2	0.93	0.95	0.96	0.72	0.92

[a] Significant terms at $p < 0.05$.

3.3.2.3 Tensile strength

The thickness of films varied between 12 to 20 µm. At higher concentration of beeswax (1.25% ≤) thickness increased due to the formation of beeswax crystal.

The tensile strength varied between 14 to 119 MPa (Table 27). All four additives significantly ($p < 0.05$) affected the tensile strength of films (Figure 28 A & B). Addition of nanoclay up to 2.5% led to significant ($p < 0.05$) increase in tensile strength of films with concentration dependent decrease thereafter (Figure 28A). Incorporation of 2.5% of nanofil 116 in film resulted in tensile strength of 60 MPa as compared to films without nanoclay that had a tensile strength of 49 MPa while other additives were at their respective center point concentration. This improvement in mechanical properties of nanoclay composites has been earlier proposed to be due to the nano-level interactions of clay with the polymer matrix [97]. Negative impact of clay loading in films at higher concentration is mainly because of agglomeration of clay particles as has already been reported by Chang et al. (2003) [180].

The effect of addition of beeswax and tween 80 on the tensile strength is depicted in Figure 28B. It was observed that the tensile strength decreased rapidly with an increase in beeswax concentration. Tensile strength decreased from 86 MPa at a beeswax concentration of 0.63% to 35 MPa when beeswax was increased to 1.88%, while concentrations of others additives were at their respective center point. Soazo et al. (2011) [6] also reported that addition of beeswax significantly reduced tensile strength of whey protein emulsion films. Navarro-Tarazaga et al. (2008) [193] had earlier explained that

the negative effect of beeswax addition in hydroxypropyl methylcellulose (HPMC) films was caused by the disruption of the HPMC continuous matrix, thus, resulting in the development of a heterogeneous film structure and a consequent decrease in tensile strength. Beeswax induced heterogeneity was also observed in the present study. At low concentration of beeswax (0.63%), films were as smooth and homogenous as GG films without beeswax (Figure 29A). However as the beeswax concentration increases films become more and more heterogeneous with emulsion and crystal formation at 1.25% and 1.88% respectively due to lack of its compatibility with GG (Figure 29 B & C).

Tween 80 can be used for oil in water application due to its high HLB (Hydrophilic Lipophilic Balance) value (15) [194]. Thus it was used as an emulsifier for improving miscibility of beeswax in aqueous GG. Required range of HLB values for oil in water emulsion for beeswax has been reported to be 10-16 [195]. Tween 80 concentration dependent increase in tensile strength was observed up to 0.75% (Figure 28B). This might be due to the better compatibility between beeswax and GG film matrix assisted by tween 80. However, tensile strength decreased with further increase in tween 80 concentration. Thus at 0.63% (w/w of GG) of tween 80, tensile strength was 58 MPa that increased to 64 MPa and then decreased to 53 MPa at 0.75% and 0.88% respectively while concentrations of beeswax, glycerol and nanofil 116 were maintained at their center point. Brandelero et al. (2010) [110] demonstrated that addition of tween 80 (2 g of tween 80 per 100 g starch/poly butylene adipateco-terephthalate (PBAT)) in cassava thermoplastic starch and PBAT blend films lowered tensile strength. This was due to the interaction between starch and surfactant which increased the free volume between the starch chains.

Addition of glycerol, irrespective of the presence of other additive, significantly reduced tensile strength due to its plasticizing effect (Figure 28A). Tensile strength decreases from 70 to 49 MPa with increase in glycerol concentration from 10% to 30%. Glycerol facilitates the movement of polymeric chains, imparting increased film flexibility thus reducing tensile strength [196].

3.3.2.4 Young's modulus

Lowest and highest values of Young's modulus were 26 GPa and 85 GPa respectively in present study (Table 27). Effect of nanofil 116 and glycerol on Young's modulus of GG films is demonstrated in Figure 28C. Young's modulus increased from 53 to 77 GPa on increasing nanoclay concentration from 0% to 5% and then decreased to a value of 67 GPa at 7.5% of nanoclay. Observed improvement in Young's modulus of nanocomposites might be due to the nano level interactions between clay and GG film matrix resulting in greater possibility of energy transfer from GG to clay layered silicates [97]. However, due to formation of nanoclay tactoids Young's modulus decreased at higher concentration of nanofil 116. In case of glycerol, a concentration dependent decreased in Young's modulus was observed irrespective of the concentration of other additives, due to increase in film flexibility and thus reduced rigidity (Figure 28C). Young's modulus decreased from 82 to 64 GPa with increase in concentration of glycerol from 10% to 30%. Effect of beeswax and tween 80 addition on Young's modulus is shown in figure 28D. Young's modulus increased with beeswax concentration up to 1.25% irrespective of concentrations of other additives. Young's modulus increased from 68 to 77 GPa and then reduced to 61 GPa when beeswax concentration increased from 0.63% to 1.25% and then to 1.88%, at center

point concentration of other additives. It was earlier demonstrated that incorporation of beeswax in pea starch films resulted in decreased tensile strength and increased Young's modulus [197]. This might be due to the fact that hydrophobicity of beeswax resulted in decreased water affinity and consequently increased stiffness of film [6, 104]. Further increase in beeswax concentration beyond 1.25% resulted in reduced Young's modulus due to crystal formation thus increasing the heterogeneity of films (Figure 29C). Young's modulus decreased with increased tween 80 concentrations irrespective of presence of other additives (Figure 28D). This might be due to tween 80 induced increase in the free volume of film matrices [110]. Young's modulus decreased from 75 to 69 GPa when tween 80 concentration increased from 0.63 to 0.88%.

3.3.2.5 Percent elongation

Table 27 demonstrates the effect of incorporation of additives on percent elongation of films. Percent elongation varied between 0.86% and 14.73% depending on the concentration of various additives (Figure 28 E & F). Glycerol concentration dependent increase in percent elongation of GG film was observed. Increase in glycerol concentration from 10 to 30 % resulted in increase in percent elongation from 5 to 10 (Figure 28E). Beeswax on the other hand had inverse effect on percent elongation of films. Percent elongation decreased from 10 to 5 % when the concentration of beeswax increased from 0.63 to 1.88 % (Figure 28F). This might be due to increase in hydrophobicity of film matrix resulting in non-homogenous and poor elastic films. However addition of tween 80 slightly improved the percent elongation in presence of other additives (Figure 28F). This could be due to better compatibility between beeswax

and GG induced by tween 80. At tween 80 concentrations of 0.63% and 0.88% percent elongation was 8.2% and 9.1% respectively. On the contrary, Brandelero et al. (2010) [110] demonstrated tween 80 dependent decrease in film flexibility due to the effect of surfactant on free volume of polymeric matrices. Incorporation of nanoclay, however had no effect on the percent elongation of film (Figure 28E).

3.3.2.6 Puncture strength

Puncture strength values ranged from 1.33 N to 2.29 N (Tables 27). Puncture strength was not significantly affected by beeswax or tween 80 (Figure 28H). However, puncture strength slightly increased from 1.89 to 1.91 N with increase in nanoclay concentration from 2.5 to 7.5 % (Figure 28G). Similarly with increase in glycerol percentage from 10 to 30 % puncture strength increased from 1.79 to 1.96 N (Figure 28G).

3.3.2.7 WVTR

WVTR of films varied between 82.3 to 150.9 $g/m^2/d$ (Table27). Incorporation of 0.63% of beeswax resulted in a significant ($p < 0.05$) reduction in WVTR of the films as compared to films without beeswax (Figure 28I). This might be due to the introduction of hydrophobicity in film by beeswax. However, further increase in beeswax concentration resulted in increase in WVTR due to the formation of crystals that induce cracks and holes within and on the surface of the films (Figure 29C). WVTR decreased from 101 to 85 $g/m^2/d$ due to increase in beeswax concentration from 0 to 0.63 %, however, an increase in WVTR was observed to 115 $g/m^2/d$ on further increasing beeswax

concentration to 1.88%. Tween 80, however, had no significant effects on WVTR (Figure 28I).

Nanofil 116 concentration dependent decrease in WVTR was observed (Figure 28J). WVTR reduced from 100 to 91 g/m^2/d with increase in nanofil 116 concentrations from 0 to 7.5% respectively. Increase in glycerol concentration demonstrated an increase in WVTR of the films (Figure 28J). WVTR increases from 94 to 100 g/m^2/d at glycerol concentration of 10% and 30% respectively. Similar results were observed by Chillo et al. (2008) [137] for tapioca starch-based film. Arvanitoyannis et al. (1998) [33] attributed this increase in WVTR might be due to the plasticizing effect of glycerol, resulting in reduced polymer packaging density.

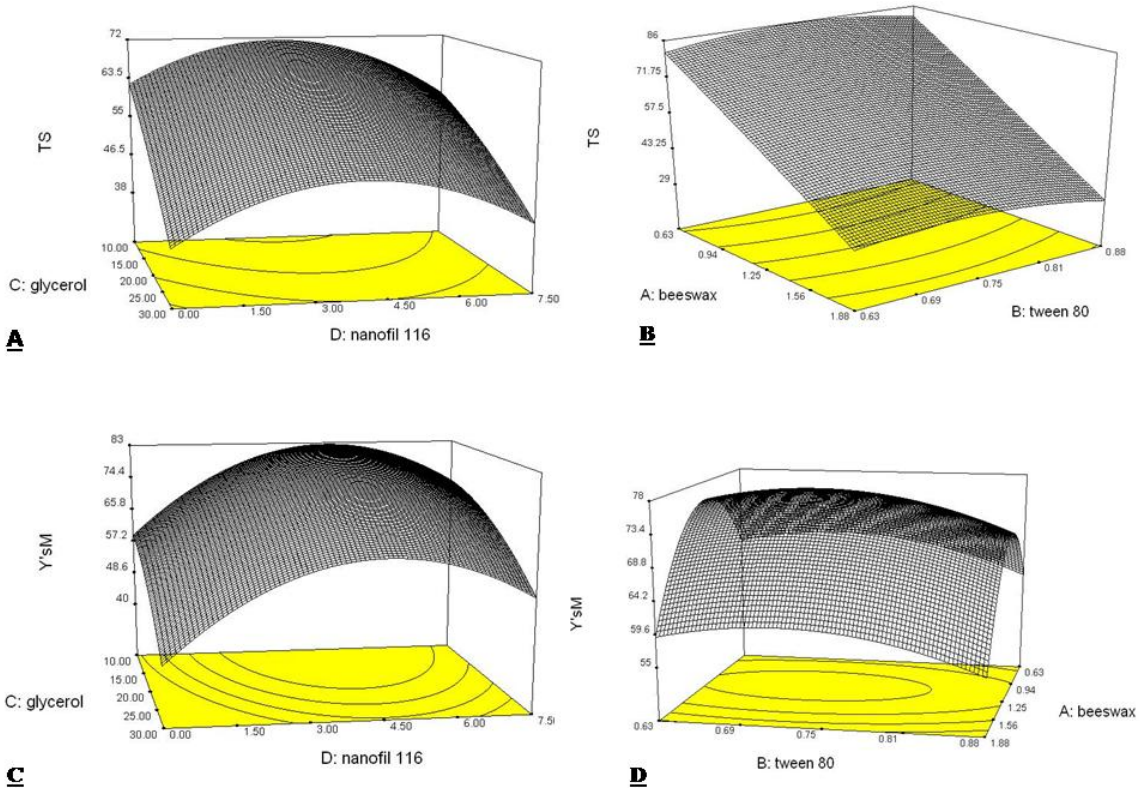

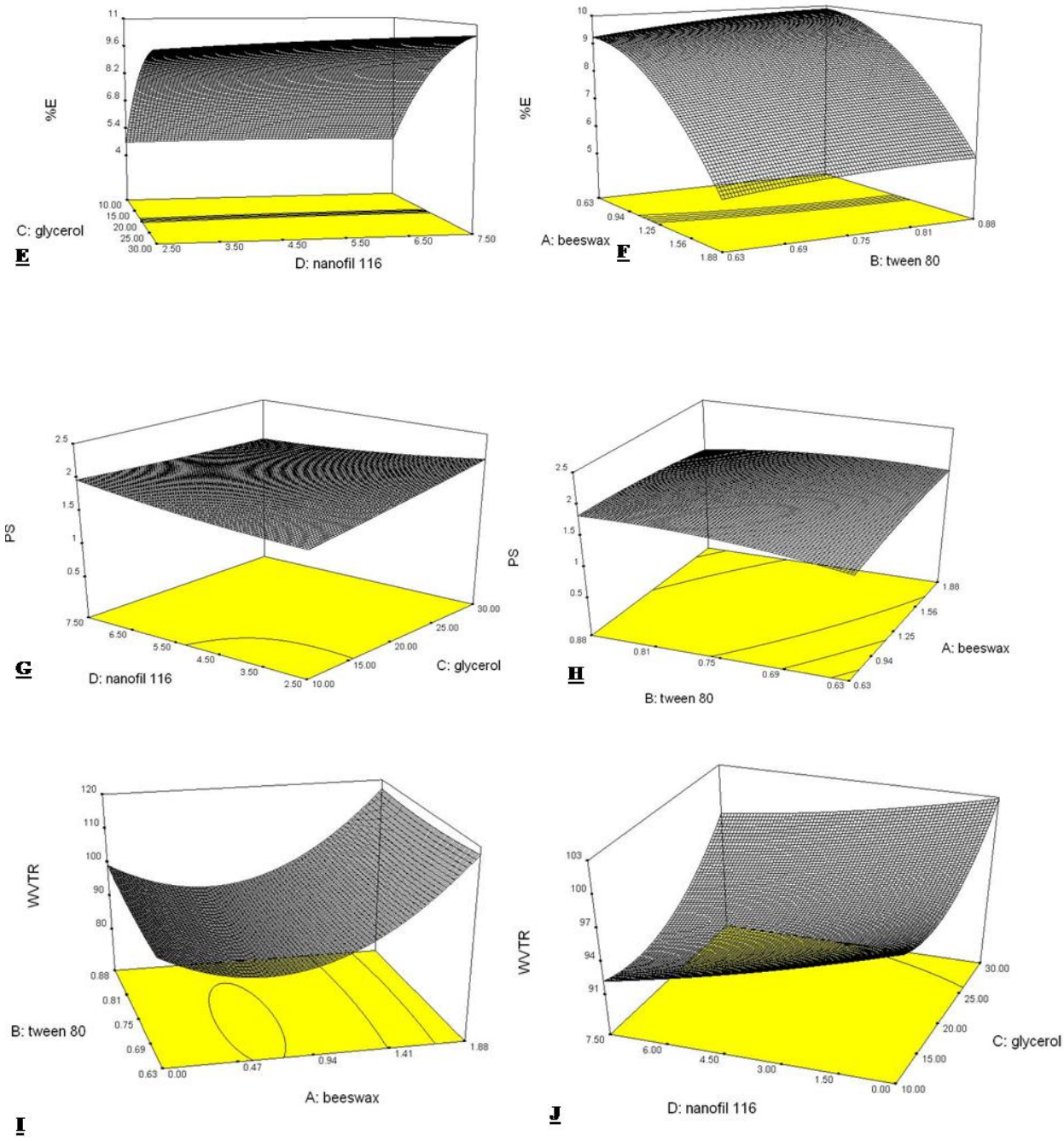

Figure 28: Response surface curves (A) Tensile strength *V/s* nanoclay and glycerol at center point of beeswax and tween 80 (B) Tensile strength *V/s* beeswax and tween 80 at center point of nanoclay and glycerol (C) Young's modulus *V/s* nanoclay and glycerol at center point of beeswax and tween 80 (D) Young's modulus *V/s* beeswax and tween 80 at

center point of nanoclay and glycerol (E) %E *V/s* nanoclay and glycerol at center point of beeswax and tween 80 (F) %E *V/s* beeswax and tween 80 at center point of nanoclay and glycerol (G) Puncture strength *V/s* nanoclay and glycerol at center point of beeswax and tween 80 (H) Puncture strength *V/s* beeswax and tween 80 at center point of nanoclay and glycerol (I) WVTR *V/s* beeswax and tween 80 at center point of nanoclay and glycerol (J) WVTR *V/s* nanoclay and glycerol at center point of beeswax and tween 80.

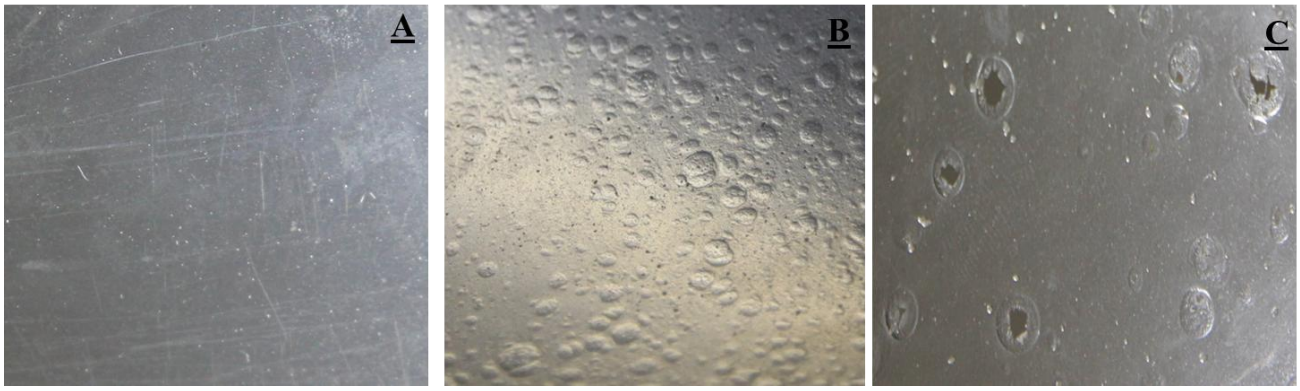

Figure 29: SLR Images of GG film prepared with different concentrations of beeswax while other additives at their respective center point concentration (A) 0.63% beeswax (B) 1.25% beeswax (C) 1.88% beeswax.

3.3.2.8 Optimization and verification of results

Criteria set for optimization of parameters and solutions obtained are given in Table 30. RSM suggested solution was used for validation of models generated. Predicted and actual value of tensile strength was 104 and 98.1 MPa, Young's modulus was 68.3 and 63.6 GPa and WVTR was 89.36 and 88.9 $g/m^2/d$ respectively for solution shown in Table

30. Close agreement between actual and predicted values indicate suitability of model generated. The optimized film demonstrated significant ($p < 0.05$) higher Young's modulus and tensile strength as compared to cling wrap film which had a Young's modulus of 0.12 ± 0.02 GPa and tensile strength of 42 ± 7 MPa. However, developed film still had very high WVTR than cling film which had a WVTR of 35 ± 5 g/m^2/d. Therefore further attempt was made to decrease WVTR of the developed films.

Table 30: Criteria for various factors and responses for process optimization and corresponding optimized solutions obtained.

	Criteria	**Solution**
Beeswax (w/w guar gum)	minimize	0.63
Tween 80 (w/w guar gum)	minimize	0.63
Glycerol (w/w guar gum)	minimize	11.87
Nanofil 116 (w/w guar gum)	minimize	2.5
Tensile strength (MPa)	maximize	98.1[b] (104)[a]
Young's modulus (GPa)	maximize	63.6[b] (68.3)[a]
Percent elongation (%)	maximize	4.8[b] (4.38)[a]
WVTR	minimize	88.9[b] (89.36)[a]
Puncture strength (N)	maximize	1.8[b] (1.54)[a]
Desirability		**0.92**

[a]Predicted values for solutions.[b]Actual values.

Incorporation of beeswax into films was found to result in significant ($p < 0.05$) decrease in the WVTR of the films. A concentration dependent decrease in WVTR was observed

with increase in beeswax concentration up to 0.63%. Poor compatibility between beeswax and GG was the limiting factor for incorporation of higher amount of wax into films. Emulsifier improved the compatibility but only to a certain extent as shown in the present study. It was earlier reported that radiation technology may also serve as a tool for enhancing compatibility [198]. Therefore improving the compatibility between beeswax and GG by irradiation of beeswax was explored.

3.3.3 Effect of irradiation on beeswax

Radiolytic breakdown of lipids on exposure to ionizing radiation has been reported in literature. Gamma irradiation could therefore possibly alter physicochemical quality of beeswax. Hence, prior to incorporation of gamma irradiated beeswax into films, the effect of irradiation on intrinsic viscosity and lipid content of beeswax was investigated.

3.3.3.1 Effect of irradiation on intrinsic viscosity of beeswax

Reduction in molecular weight of beeswax due to irradiation can be evaluated by measuring the intrinsic viscosity of beeswax. Decrease in molecular weight could facilitate incorporation of higher amount of beeswax in GG films. It was observed that up to 25 kGy there was no significant reduction in intrinsic viscosity of beeswax. Baggio et al. (2005) [199] earlier demonstrated that there were no significant effects of gamma irradiation (up to 25 kGy) on physiochemical properties of beeswax. However, further radiation processing decreased intrinsic viscosity of beeswax from 5.7 ± 0.5 in the control to 3.9 ± 0.3 at 50 kGy and 2.8 ± 0.2 at 100 kGy (Table 31). Significant reduction in

intrinsic viscosity might be due to radiation induced degradation of beeswax which could possibly facilitate better compatibility.

Table 31: Effect of irradiation on intrinsic viscosity of beeswax.

Irradiation of beeswax	Intrinsic viscosity (×100)
control	5.7 ± 0.5^{a}
5 kGy	5.4 ± 0.4^{a}
25 kGy	4.8 ± 0.4^{a}
50 kGy	3.9 ± 0.3^{b}
100 kGy	2.8 ± 0.2^{c}

Any two means in the same column followed by the same letter are not significantly ($p > 0.05$) different.

3.3.3.2 Effect of irradiation on lipid content of beeswax

Lipids are a group of naturally occurring hydrophobic molecules that include fats and waxes. It was earlier reported that the nature of lipid and its content affect the water vapor permeability of films [200]. In current work effect of irradiation on lipid composition of beeswax was analyzed by thin layer chromatography (TLC). Figure 30 depicts the TLC chromatograms of lipid species in the control and irradiated beeswax. Wax esters (R_f= 0.9), alkenyl diacylglycerols (R_f= 0.64), fatty acids (R_f= 0.19) and fatty alcohols (R_f= 0.14) were identified as one of the major lipid constituents.

TLC densitometry analysis revealed a radiation dose dependent decrease for wax ester and alkenyl diacylglycerols with a corresponding increase in fatty acids and fatty alcohols (Table 32). Free radical mediated radiolysis of wax ester and alkenyl diacylglycerols releasing fatty acids and fatty alcohols might be the reason behind decrease in wax ester and alkenyl diacylglycerols and consequent increase in fatty acids and fatty alcohols.

Similar hypothesis was proposed by Banerjee et al. (2014) [201] wherein radiolysis of membrane lipids in irradiated cabbage led to a decrease in triacylglycerol content with a subsequent increase in free fatty acids. Wax ester and alkenyl diacylglycerols are more non-polar than fatty acids and fatty alcohols. Therefore, it can be inferred from above result that irradiation reduces the non-polarity of beeswax which could also facilitate the compatibility between beeswax and GG.

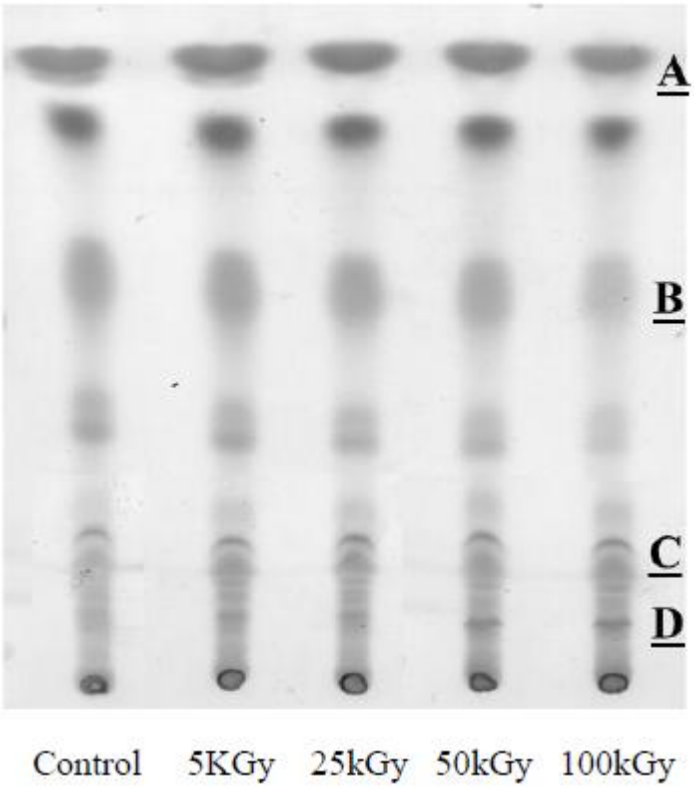

Figure 30: Effect of irradiation on lipid composition of beeswax (A) Wax esters (B) Alkenyl diacylglycerols (C) Fatty acids (D) Fatty alcohols.

Table 32: Effect of irradiation on lipid composition of beeswax.

Irradiation of beeswax (kGy)	Wax ester (% decrease)	Alkenyl diacylglycerols (% decrease)	Fatty acids (% increase)	Fatty alcohols (% increase)
control	NA	NA	NA	NA
5	4.1 ± 0.3^{d}	7.6 ± 0.9^{d}	4.4 ± 0.6^{d}	8.1 ± 0.8^{d}
25	5.1 ± 0.5^{c}	10.7 ± 1^{c}	16.1 ± 1.8^{c}	17.8 ± 2.1^{c}
50	10.7 ± 1.1^{b}	16.7 ± 1.4^{b}	31.4 ± 3.9^{b}	26.2 ± 2.4^{b}
100	17.5 ± 2.4^{a}	36.1 ± 2.9^{a}	44.4 ± 4.1^{a}	76.1 ± 6.3^{a}

Any two means in the same column followed by the same letter are not significantly ($p > 0.05$) different.

3.3.4 Effect of incorporation of irradiated beeswax on mechanical and barrier properties of GG films

Irradiation resulted in increased percentage of fatty acids and fatty alcohols (Table 32). Addition of fatty acid and fatty alcohol in whey protein emulsion is reported to decrease WVTR of prepared films [202]. Increase in polarity and decrease in intrinsic viscosity of beeswax on irradiation could attribute better compatibility of beeswax with GG. Hence, the effect of incorporation of irradiated beeswax on various properties of the films was further studied. GG based films were prepared using 40% glycerol, 1% tween 80 and different concentrations of irradiated and control beeswax (0, 0.5, 1, 1.5, 2 and 2.5%). Incorporation of 0.5% of control beeswax showed no significant ($p < 0.05$) change in tensile strength of the films whereas increased Young's modulus was observed at this concentration (Table 33 & 34). The hydrophobicity of beeswax decreases water affinity of the film, thereby reducing water content and increasing the stiffness of the films [6, 104]. The WVTR of control films significantly decreased from 168 ± 21 to 92 ± 9 g/m^2/d

at 0.5% beeswax (Table 35). Further loading of control beeswax (≥ 1%) demonstrated no significant ($p < 0.05$) change in WVTR whereas reduction in mechanical properties was observed (Table 33, 34 & 35). At higher concentration, control beeswax was found to form crystals thereby reducing the homogeneity of GG film.

Incorporation of irradiated beeswax upto 25 kGy demonstrated no significant ($p < 0.05$) improvement in mechanical and barrier properties of the films as compared to control beeswax incorporated film (Table 33, 34 & 35). However, incorporation of 1% of 50 kGy irradiated beeswax resulted in films having WVTR of 77 ± 6 $g/m^2/d$ (Table 35).

This might be due to radiation induced compatibility between beeswax and GG. However, further loading of 50 kGy beeswax resulted in films having poor film characteristics. When 2% beeswax was loaded emulsion formation was observed whereas for 2.5% crystal formation was introduced. Higher doses of radiation (100 kGy) enabled even higher loading of beeswax (> 1%) without any crystal formation but there was no significant ($p < 0.05$) change in mechanical and WVTR properties of film as compared to 50 kGy beeswax incorporated films at similar concentration (Table 35).

Table 33: Effect of irradiated beeswax on tensile strength (MPa) of GG films.

Beeswax (% w/w GG)	control	5 kGy	25 kGy	50 kGy	100 kGy
0	55 ± 7^{a}	55 ± 7^{a}	55 ± 7^{a}	55 ± 7^{a}	55 ± 7^{a}
0.5	56 ± 9^{a}	58 ± 6^{a}	53 ± 4^{a}	56 ± 6^{a}	56 ± 6^{a}
1	40 ± 6^{b}	38 ± 5^{b}	41 ± 4^{b}	58 ± 9^{a}	57 ± 8^{a}
1.5	31 ± 4^{bc}	30 ± 4^{bc}	32 ± 6^{bc}	40 ± 6^{b}	59 ± 5^{a}
2	25 ± 3^{c}	23 ± 3^{c}	24 ± 5^{c}	35 ± 5^{b}	50 ± 6^{a}
2.5	27 ± 8^{c}	25 ± 6^{c}	29 ± 5^{c}	30 ± 4^{b}	39 ± 4^{b}

Any two means in the same column followed by the same letter are not significantly ($p > 0.05$) different.

Table 34: Effect of irradiated beeswax on Young's modulus (MPa) of GG films.

Beeswax (% w/w GG)	control	5 kGy	25 kGy	50 kGy	100 kGy
0	196 ± 26^{b}	196 ± 26^{b}	196 ± 26^{b}	196 ± 26^{c}	196 ± 26^{c}
0.5	254 ± 31^{a}	262 ± 28^{a}	249 ± 19^{a}	277 ± 21^{b}	296 ± 24^{b}
1	160 ± 22^{b}	150 ± 30^{b}	162 ± 18^{b}	352 ± 32^{a}	385 ± 25^{a}
1.5	83 ± 18^{c}	94 ± 11^{c}	85 ± 12^{c}	220 ± 40^{bc}	359 ± 28^{a}
2	70 ± 7^{c}	65 ± 9^{d}	61 ± 13^{d}	140 ± 22^{d}	283 ± 17^{b}
2.5	68 ± 13^{c}	63 ± 8^{d}	55 ± 14^{d}	98 ± 15^{e}	119 ± 20^{d}

Any two means in the same column followed by the same letter are not significantly ($p > 0.05$) different.

Table 35: Effect of incorporation of irradiated beeswax on WVTR ($g/m^2/d$) of GG films.

Beeswax (% w/w GG)	control	5 kGy	25 kGy	50 kGy	100 kGy
0	168 ± 21^{a}	168 ± 21^{a}	168 ± 21^{a}	168 ± 21^{a}	168 ± 21^{a}
0.5	92 ± 9^{d}	90 ± 16^{c}	93 ± 8^{c}	83 ± 14^{c}	91 ± 8^{bc}
1	93 ± 10^{cd}	103 ± 21^{bc}	107 ± 14^{bc}	77 ± 6^{c}	73 ± 12^{c}
1.5	115 ± 18^{bcd}	110 ± 12^{bc}	$112 \pm 9b^{c}$	92 ± 9^{bc}	81 ± 15^{bc}
2	120 ± 19^{bc}	118 ± 13^{bc}	119 ± 16^{bc}	109 ± 12^{b}	101 ± 18^{bc}
2.5	132 ± 11^{b}	129 ± 22^{b}	122 ± 7^{b}	112 ± 13^{b}	106 ± 13^{b}

Any two means in the same column followed by the same letter are not significantly ($p > 0.05$) different.

Above results demonstrated the effectiveness of 50 kGy irradiated beeswax for better mechanical and barrier properties of GG based films. Therefore further RSM analysis was performed by using 50 kGy beeswax for the development of film with the desired properties.

3.3.5 Optimization of irradiated beeswax, glycerol, nanoclay and tween 80 in GG film for improved film properties

Standardization of additives such as 50 kGy irradiated beeswax, tween 80, nanofil 116 and glycerol at different concentrations was attempted by RSM to improve the mechanical and barrier properties of GG based biodegradable films.

3.3.5.1 Generation of RSM model

Results obtained for various individual responses of the experimental design are shown in Tables 14 & 36. Fitting of the data to various models (linear, interactive, quadratic and cubic) were carried out to obtain the regression equations. The fit summary of the output suggested quadratic model for all responses. Statistical analysis by ANOVA showed that the models generated by RSM were significant ($p < 0.05$) while lack of fit was insignificant ($p > 0.05$). Further signal to noise ratio (S/N) of all models were above 4 indicating sufficient data to navigate designed space (Table 37). Coefficients for predicted regression models and coefficient of determination (R^2) are shown in Table 38. High values for R^2 also suggest that the models to be of good fit. Analysis of concentrations of various additives on different film properties was done by using generated model.

Table 36: Observed responses of Response Surface Methodology films prepared from GG.

Std	Tensile strength (MPa)	Young's Modulus (GPa)	Percent elongation	WVTR ($g/m^2/d$)	Puncture strength (N)
1	121	98	2.45	69	1.7
2	123	72	1.56	73	1.53
3	134	978	2.03	69	1.31
4	132	115	2.54	70	1
5	107	78	12.65	76	1.57
6	87	98	13	76	2.03
7	102	79	11.98	75	2.29
8	93	117	10.79	73	1.96
9	79	94	2.88	67	1.45
10	68	63	2.97	70	2.48
11	125	93	3.2	69	1.8
12	36	59	2.7	71	1.79
13	91	60	13.68	75	1.3
14	34	38	12.62	76	1.78
15	80	56	14.52	77	1.49
16	18	41	14.73	74	1.7
17	98	69	7.84	99	1.72
18	77	46	1.15	101	1.83
19	92	73	11.64	69	1.73
20	105	91	10.13	68	1.09
21	125	128	0.86	70	1.63
22	61	79	17.5	81	1.47
23	54	89	11.38	75	1.4
24	32	50	10.93	75	1.27
25	129	92	11.24	77	1.61
26	113	93	10.9	78	1.55
27	114	93	10.58	76	1.74
28	116	105	10.6	83	1.9
29	133	95	10.64	77	1.31
30	139	97	12.97	76	1.75

Table 37: Significance statistics, p values and signal to noise ratio (S/N) of Response Surface Methodology predicted models.

Response	Model			Residual			S/N
	sum of squares	df	p-value	sum of squares	df	p-value	
Tensile strength	77.24424834	14	0.0002	10.73591	15	0.0548	9.717245
Young's modulus	48.04931992	14	< 0.0001	2.486422	15	0.0931	16.79338
Percent elongation	687.0188133	14	< 0.0001	37.86433	15	0.0719	17.34535
WVTR	1431.068564	14	0.0019	306.3106	15	0.0861	10.43797
Puncture strength	2.115186667	14	0.0325	0.8362	15	0.3383	8.355641

Table 38: Coefficients of fitted polynomial representing relationship betweenresponse and process variable and R^2 values.

Coefficients	Tensile strength (TS) = Sqrt(TS + 20.00)	Young's modulus (Y'sM)=Sqrt(Y'sM)	Percent elongation	WVTR	Puncture strength
Intercept	11.98875574	9.782635416	11.155	77.71905333	1.643333
A-beeswax	-0.640830581	-0.294648401	-0.660833333	0.373284167	0.065833
B-tween 80	0.029947782	0.196971691	-0.0975	-0.312944167	-0.07417
C-glycerol	-0.672578605	-0.522813092	4.871666667	2.74649	0.030833
D-nanofil 116	-0.900140468	-0.808116844	0.391666667	-0.042244167	0.005833
AB	-0.27286136	0.208122439	0.03375	-0.73649125	-0.14
AC	-0.201044378	0.283856752	-0.05625	-0.968565	0.0175
AD	-0.674032496	-0.547981287	-0.0025	-0.07624125	0.12875
BC	-0.176132167	-0.06015695	-0.03375	-0.330545	0.12625
BD	-0.149970323	-0.224423855	0.3325	0.58678875	0.0025
CD	0.027171649	-0.411999065	0.2475	0.37959	-0.2225
A^2	-0.34607987	-0.561247335	-1.858333333	4.394262292	0.063125
B^2	-0.211246584	-0.178980225	-0.260833333	-3.600900208	-0.02813
C^2	-0.304121416	0.083644314	-0.687083333	-1.704575208	0.006875
D^2	-0.959877958	-0.375646267	-0.193333333	-1.850162708	-0.04688
R-Squared	0.877973463	0.950798741	0.947764914	0.823693853	0.716676

[a] Significant terms at $p < 0.05$.

3.3.5.2 Tensile strength

Tensile strength increased up to 2.5% of nanofil 116 incorporation in GG film thereafter it subsequently declined at higher concentration (Figure 31A). At 0% of nanofil 116, tensile strength was 83 MPa and it increased to 122 MPa at nanoclay concentration of 2.5%. Further increase in nanoclay concentration to 7.5% resulted in film having 88 MPa of tensile strength. Observed effect of nanoclay on tensile strength is similar to results already obtained in present study and described in section (3.3.2.3).

Effect of incorporation of irradiated beeswax and tween 80 on tensile strength of GG films is depicted in Figure 31B. It was observed that tensile strength decreased with increase in irradiated beeswax concentration. At 0.63% of beeswax, tensile strength was 128 MPa which reduced to 104 MPa at 1.88% of beeswax. However, more rapid decrease in tensile strength of film was observed when non-irradiated beeswax was incorporated (section 3.3.2.3).

This might be due to radiation induced higher compatibility between beeswax and GG. Variation in tween 80 content was also noted to affect the tensile strength; wherein a concentration dependent increase was observed in tensile strength of the films (Figure 31B). Tensile strength increased from 115 to 122 MPa with increase in tween 80 concentration from 0.63 to 0.88%. However, in previous section (3.3.2.3), a decrease in tensile strength of films at higher concentration of tween 80 was observed. Difference in observation might be due to radiation induced qualitative change in lipid constituents of beeswax. Thus higher amount of tween 80 further facilitate the compatibility of beeswax

with GG. Addition of glycerol, irrespective of the presence of any additive, significantly reduces the tensile strength due to its plasticizing effect (Figure 31A). At 10% glycerol concentration tensile strength was 132 MPa and at 30% of glycerol percentage tensile strength decreased to a value of 104 MPa.

3.3.5.3 Young's modulus

Similar to the results obtained in section (3.3.2.4) Young's modulus of the films was noted to increase with an increase in nanofil 116 concentration up to 2.5% thereafter it decreased in a nanoclay concentration dependent manner (Figure 31C). Young's modulus increased from 97 to 103 GPa with increase in nanofil 116 concentration from 0 to 2.5 %. Further increase in nanoclay concentration (7.5%) resulted in film having Young's modulus of 76 GPa. Effect of beeswax (50 kGy) and tween 80 addition on Young's modulus is illustrated in figure 31D. Young's modulus increased with beeswax (50 kGy) concentration up to 1.25%. Further increase in irradiated beeswax concentration resulted in reduced Young's modulus. At 0.63% of beeswax Young's modulus was 90 GPa and at 1.25% it increased to a value of 96 GPa. Further increase in beeswax percentage to 1.88% resulted in decrease in Young's modulus to 82 GPa. Increase in Young's modulus was observed in tween 80 concentration dependent manner. Young's modulus increased from 89 to 96 GPa with increase in tween 80 concentration from 0.63 to 0.88 %. RSM analysis of non-irradiated beeswax in the present study (section 3.3.2.4), however, showed a decrease in Young's modulus with an increase in tween 80 concentrations. Difference in observation was might be due to the better compatibility between irradiated beeswax and GG facilitated by tween 80 resulting in an increased in Young's modulus of films.

Young's modulus decreased from 107 to 89 GPa with increase in amount of glycerol from 10 to 30 % in GG based film (Figure 31C).

3.3.5.4 Percent elongation

Percent elongation strongly depends on glycerol content because of its plasticizing ability (Figure 31E). Percent elongation increased from 5.6 to 15.3 % at glycerol percentage of 10 and 30 % respectively. Incorporation of irradiated beeswax improved the flexibility of the films. At 0.63% percent elongation was 9.9%. Use of irradiated beeswax (50 kGy) at a concentration of 1.25% resulted in increase in percent elongation to 11.2% (Figure 31F). On the other hand, incorporation of non-irradiated beeswax demonstrated decrease in percent elongation of film (section 3.3.2.5). The difference in observation could be a result of radiation induced lowering in intrinsic viscosity and change in lipid profile of irradiated wax as discussed in section 3.3.3. According to Callegarin et al. (1997) [203] lipids are normally used to increase the elasticity of polymeric films thereby supporting our results. Percent elongation decreases with further increase in amount of irradiated beeswax. However, tween 80 and nanofil 116 had no effect on percent elongation (Figure 31 E & F).

3.3.5.5 Puncture strength

Puncture strength was not significantly affected by addition of irradiated beeswax (50 kGy), glycerol, tween 80 and nanofil 116 (Figure 31 G & H).

3.3.5.6 WVTR

Additives had distinct effects on WVTR. WVTR decreases with increase in beeswax (50 kGy) concentration up to 1.25% (Figure 31I). However, WVTR increases on further increase in beeswax content. Similarly, WVTR increases with tween 80 concentration up to 0.75% then decreases gradually with increase in concentration of tween 80 in films (Figure 31I). According to Villalobos et al. (2006) [204] and Andreuccetti et al. (2011) [205] water vapor permeability of film increases when surfactant/hydrocolloid ratio is not adequate. Increase in nanofil 116 concentration from 5 to 10 % reduced the WVTR from 76 to 69 g/m^2/d, whereas, increase in glycerol concentration resulted in increased WVTR of films (Figure 31J).

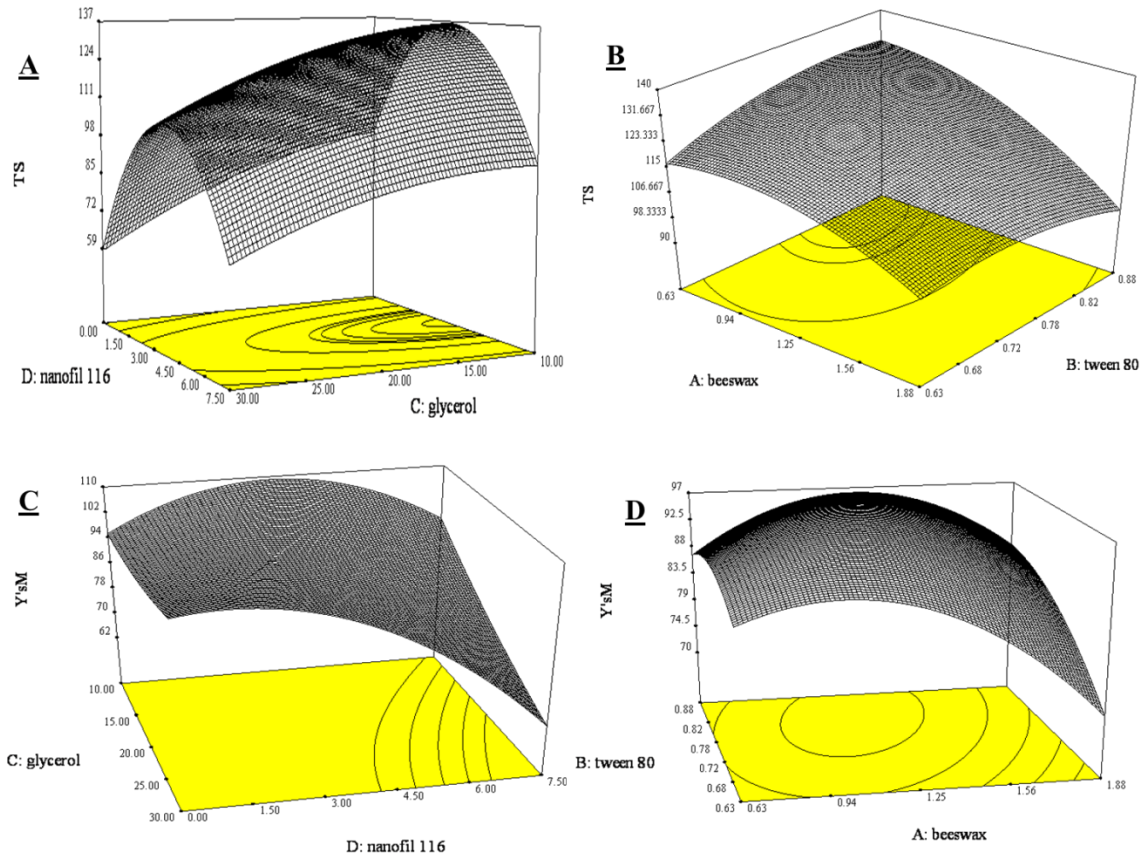

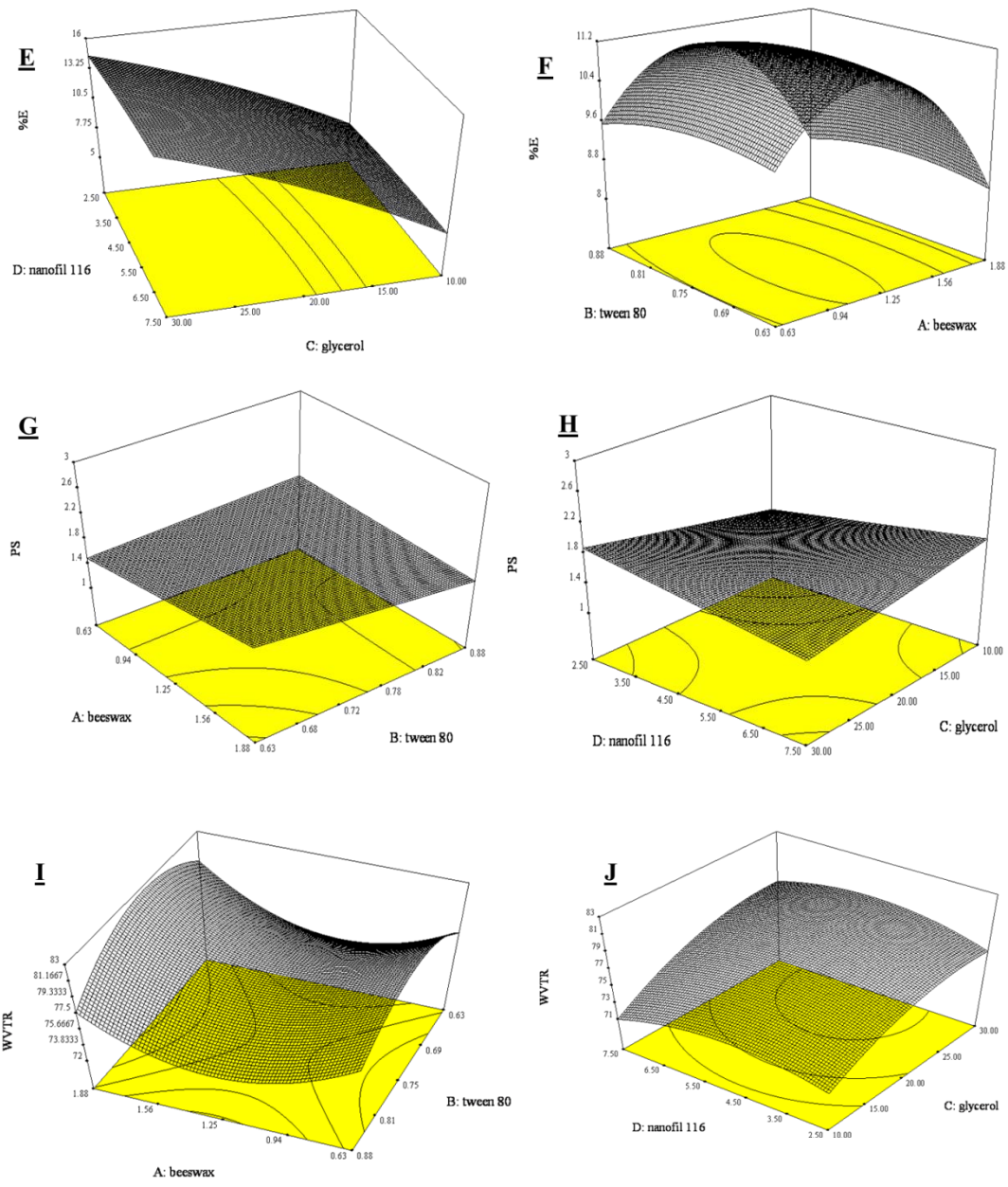

Figure 31: Response surface curves when 50 kGy irradiated beeswax was used along with other additives (A) Tensile strength *V/s* nanoclay and glycerol at center point of beeswax and tween 80 (B) Tensile strength *V/s* beeswax and tween 80 at center point of nanoclay and glycerol (C) Young's modulus *V/s* nanoclay and glycerol at center point of beeswax

and tween 80 (D) Young's modulus *V/s* beeswax and tween 80 at center point of nanoclay and glycerol (E) %E *V/s* nanoclay and glycerol at center point of beeswax and tween 80 (F) %E *V/s* beeswax and tween 80 at center point of nanoclay and glycerol (G) Puncture strength *V/s* beeswax and tween 80 at center point of nanoclay and glycerol (H) Puncture strength *V/s* nanoclay and glycerol at center point of beeswax and tween 80 (I) WVTR *V/s* beeswax and tween 80 at center point of nanoclay and glycerol (J) WVTR *V/s* nanoclay and glycerol at center point of beeswax and tween 80.

RSM analysis thus demonstrated that incorporation of irradiated (50 kGy) beeswax had a different effect on various film properties as compared to non-irradiated beeswax. This might be due to radiation induced changes in intrinsic viscosity as well as content of wax esters, alkenyl diacylglycerols, fatty acids and fatty alcohols of beeswax. Incorporation of beeswax irradiated with a dose of 50 kGy was found to significantly ($p < 0.05$) decrease the WVTR of the films while maintaining the other properties.

3.3.5.7 Optimization and verification of results

Various film additives were optimized for achieving desired mechanical properties. Criteria set for optimization of parameters and solutions obtained are given in table 39. RSM suggested solution was used for validation of models generated. Predicted and actual values of parameters for solution are shown in Table 39. Close agreement between actual and predicted values indicate suitability of model generated (Table 39).

Table 39: Criteria for various factors and responses for process optimization and corresponding optimized solutions obtained.

	Criteria	Solution
Beeswax (w/w GG)	in range	1.21
Tween 80 (w/w GG)	in range	0.88
Glycerol (w/w GG)	in range	13.91
Nanofil 116 (w/w GG)	in range	3.07
Tensile strength (MPa)	maximize	128[b] (135)[a]
Young's modulus (GPa)	maximize	103[b] (111)[a]
Percent elongation (%)	maximize	6.5[b] (7.1)[a]
WVTR	minimize	69[b] (70.4)[a]
Puncture strength (N)	maximize	1.52[b] (1.67)[a]
Desirability		**0.809706**

[a]Predicted values for solutions.[b]Actual values.

It is clearly evident from results that optimized film having irradiated (50 kGy) beeswax had superior mechanical and barrier properties as compared to optimized film having non-irradiated beeswax (Table 30 & 39). Therefore further analysis was carried out on RSM optimized film containing irradiated beeswax.

3.3.5.8 Color analysis

RSM optimized film had an opacity of 14.46% while it's *L**, *a** and *b** value were 97.6, -1.09 and 2.21 respectively. Native GG films had color co-ordinates of 97.7, 0.8 and 1.0 for *L**, *a** and *b** respectively while its opacity was 12.9% (section 3.2.5.5). Although a significant variation was observed instrumentally with respect to color and opacity between optimized and native films, visual differences were negligible to be discerned by naked eye.

3.3.5.9 FTIR

Changes in chemical structure were determined by comparison of FTIR spectra of native GG based films, optimized RSM film with irradiated beeswax and irradiated (50 kGy) beeswax (Figure 32). Comparison of FTIR spectrum suggested that addition of beeswax resulted in appearance of three new peaks in RSM optimized film as compared to native GG film (Figure 32A). Incorporation of irradiated (50 kGy) beeswax gave new peaks at 1735.62 ± 1.2, 2917.97 ± 1.1 and 2850.88 ± 0.8 cm^{-1} in RSM optimized films. Similarly, these three distinct peaks were observed in FTIR spectrum of irradiated beeswax at 1735.62 ± 1.2, 2915.14 ± 0.9 and 2848.03 ± 1.1 cm^{-1} (Figure 32 B & C). Peak at 1735.62 cm^{-1} was observed due to C=O stretching of aldehydes (Figure 32B). Whereas peaks at 2915.14 ± 0.9 and 2848.03 ± 1.1 cm^{-1} were due to symmetric stretching of CH bond in alkanes and CH stretching of aldehydes, respectively.

There was no shifting observed in peak at 1735.62 ± 1.2 $cm^{-1}$of optimized film as compared to irradiated beeswax (Figure 32B). However, a significant ($p < 0.05$) shifting was observed in other two peaks in RSM optimized films as compared to irradiated beeswax. Significant ($p < 0.05$) shifting in these two peaks suggested that alkanes and aldehydes of irradiated beeswax interact with GG thus resulting better compatibility and reduction in water vapor permeability.

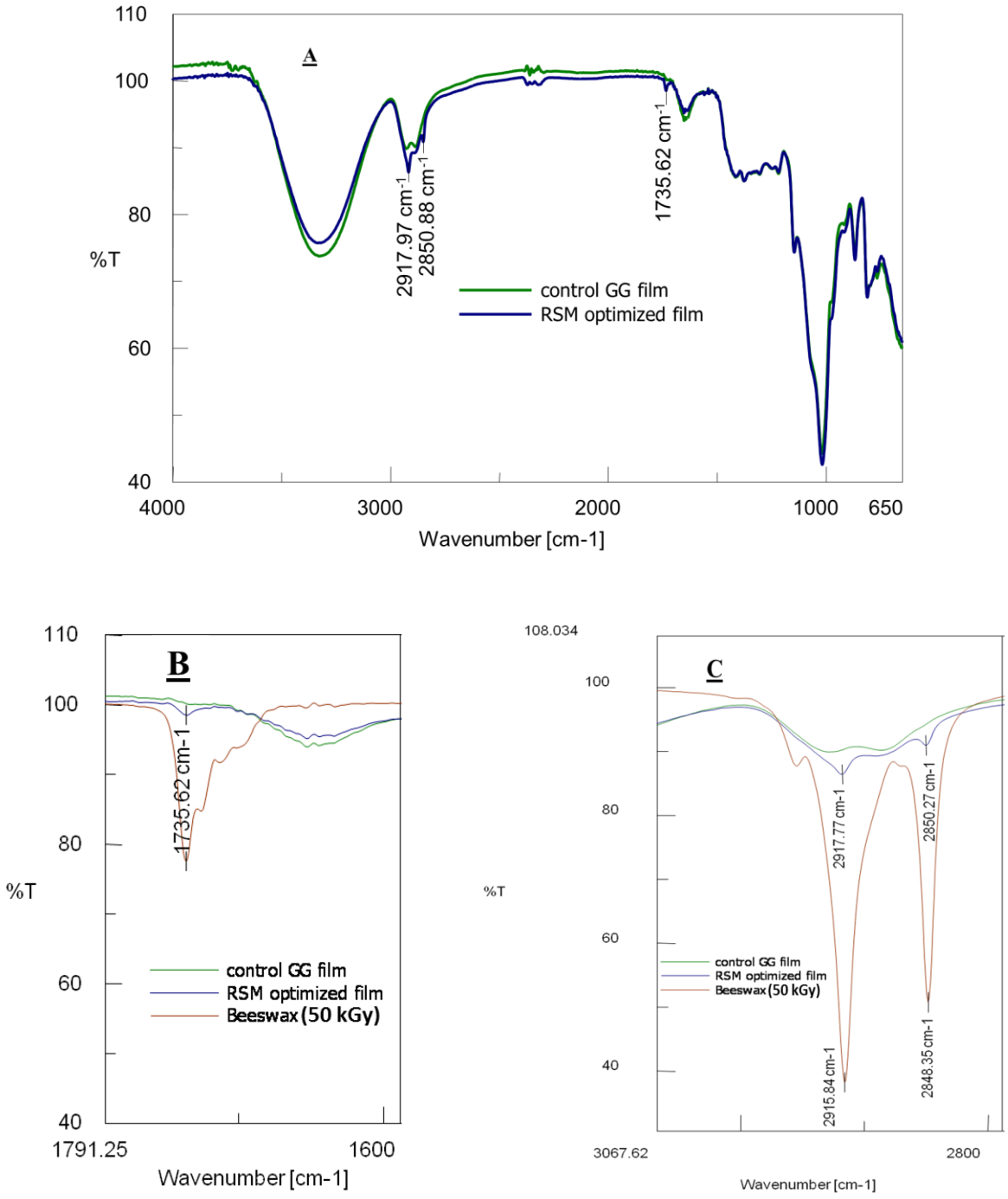

Figure 32: FTIR spectra: (A) Native GG films and optimized film (B) 50 kGy irradiated beeswax, control GG film and optimized film (C) 50 kGy irradiated beeswax, control GG film and optimized film.

3.3.5.10 TGA analysis of RSM optimized film

TGA curves for control GG film and RSM optimized film with irradiated beeswax are shown in Figure 33. Mass loss below 110 °C was mainly ascribed to water loss. At 110 °C, percent weight loss of control GG film and optimized film was 7.4% and 6.6% respectively. Differences in percent weight loss were due to low moisture content of optimized film because of beeswax [206]. High water retention capacity of native film was also responsible for the extra initial weight loss [207]. Both samples demonstrated two step decomposition patterns. As discussed earlier (section 3.2.5.7) first degradation step started at 275 °C and second step begun at 320 °C for control GG film, however, for optimized film degradation steps started at 285 °C and 325 °C respectively (Figure 33). This indicates that additives increased the thermal stability of RSM optimized film.

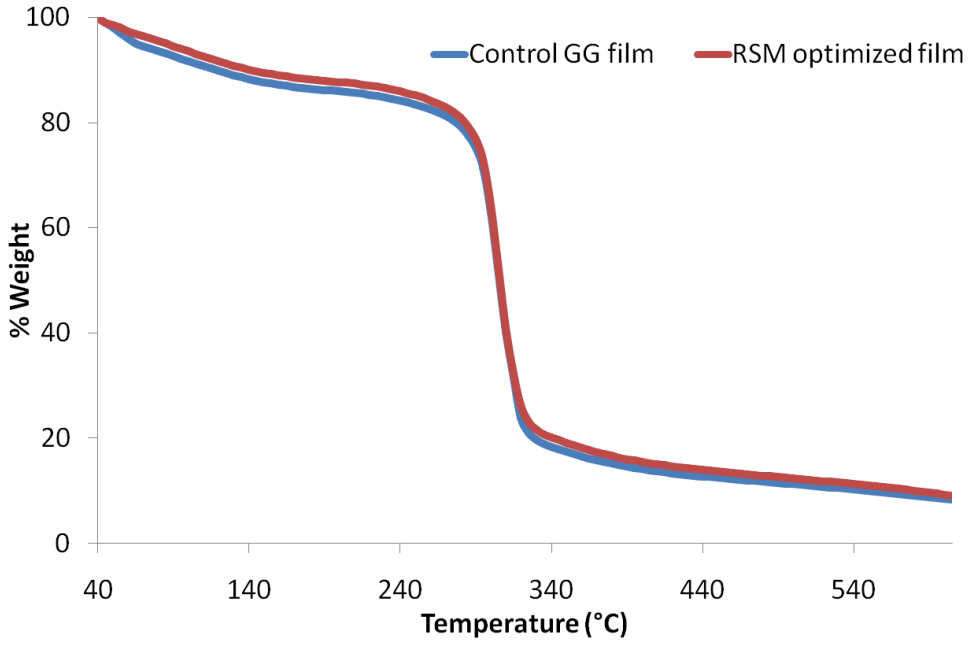

Figure 33: Thermal behavior of control GG film and optimized film.

3.3.6 Inter-comparison of mechanical and barrier properties of GG film and cling films

The films thus developed by optimizing different additives and processing conditions are intended to be used for packing fresh cut fruits and vegetables. Cling wrap films are widely used for preserving a variety of fresh fruits and vegetables in supermarkets. Packaging in this form has the advantage that it preserves moisture and aroma in foods wrapped in it and keeps it fresh. They are the most widely used materials for wrapping in supermarkets because they have good clarity and thus are effective for display. The mechanical and barrier properties of RSM optimized film was hence compared with the commercially available cling film. It was observed that tensile strength and Young's modulus of developed film was superior to cling film (Table 40). However, WVTR of cling film was 35 ± 5 g/m^2/d and that of optimized film having thickness of 14 µm was 69 ± 12 g/m^2/d. Therefore, to further lower the WVTR, thickness of optimized film was increased to 29 µm by increasing volume of casting solution. The films thus developed did not affect its mechanical properties while WVTR decreased to 39 ± 4 g/m^2/d which was equivalent to the cling film.

Table 40: Physical properties of developed film and commercially available cling film.

Physical Properties	Cling film (12 µm)	RSM Optimized Film (14 µm)	RSM Optimized Film (29 µm)
Tensile strength (MPa)	42 ± 7	128 ± 18	122 ± 18
Young's Modulus (GPa)	0.12 ± 0.02	103 ± 8	99 ± 8
WVTR (g/m^2/d)	35 ± 5	69 ± 12	39 ± 4

Any two means in the same column followed by the same letter are not significantly ($p > 0.05$) different.

Thus it was clearly demonstrated that additives significantly affected various properties of GG based film. By optimizing the concentration of various additives (1.21% 50 kGy irradiated beeswax, 0.88% tween 80, 13.91% glycerol and 3.07% nanofil 116) and increasing the film thickness to 29 µm, films having properties equivalent to commercially available cling film were developed.

3.4 Development of active packaging films with possible antioxidant and antimicrobial functions

The optimized film developed in previous section had superior mechanical strength and water vapor barrier properties comparable to commercial cling films. The next objective of the project was to develop active films possessing antimicrobial properties. To the best of our knowledge no report exists on the use of GG based active film for shelf life improvement of minimally processed food products. A wide range of antimicrobial agents are used for development of active food packaging such as weak organic acids, enzymes like lysozyme, nisin etc. Additionally, fruit extracts are also known to target wide range of microorganism. Grape pomace, a waste of wine industry, is a rich source of polyphenols and antimicrobial agents [124]. In the present study grape pomace was therefore used to develop active films with antimicrobial and antioxidant activities.

3.4.1 Bioactive constituents of grape pomace extract

Grapes pomace is reported to contain significant amount of anthocyanins, flavanoids and polyphenols. These constituents impart antioxidant and antimicrobial properties to grape pomace extract. Total anthocyanin and flavonoid content of the extract was found to be 181.61 ± 20.1 mg/100 g and 73.26 ± 6 mg CE/g (Catechin equivalent g^{-1}) of pomace respectively (Table 41) which was comparable to that previous reported earlier by Sousa et al. (2014) [208] and Butkhup et al. (2010) [209]. Total phenolic content in the extract was however found to be lower (41.38 ± 4.3 mg GAE/g) (Table 41), when compared to literature value of 74.75 mg GAE/g reported for Cabernet Sauvignon grape varieties

[210]. Fruits are also known to be rich source of vitamins. The vitamin C content in the extract was found to be 42 ± 3 mg of ascorbic acid/100g of pomace (Table 41). Fresh fruits are also known to possess significant antioxidant activity. In present study DPPH radical scavenging activity was 120 ± 12 mg TE/g of pomace, while the Fe^{3+}-reducing powers of grape pomace extract was found to be 30.56 ± 3.2 mg TE/g of pomace (Table 41). Quantitative differences in various chemical constituents as well as bioactivities were observed between present study and published literature. This might be due to difference in variety of grapes and process of extraction used by authors.

Table 41: Bioactive constituents in grape pomace extract.

Chemical constituents	**Quantity in grape pomace**
Total anthocyanins	181.61 ± 20.1 (mg/100g)
Total phenolic content	41.38 ± 4.3 (mg GAE/g)
Total flavanoid	73.26 ± 6 (mg QE/g)
Ascorbic acid	42 ± 3 (mg/100g)
FRAP	30.56 ± 3.2 (mg TE/g)
DPPH	120 ± 12 (mg TE/g)

3.4.2 Effect of incorporation of grape pomace on mechanical and barrier properties of films

Incorporation of pomace extract up to 5% (w/w of GG) resulted in no significant ($p < 0.05$) effect on the characteristics of the developed RSM optimized film (Table 40 and

42). However, further loading of extract resulted in poor film properties which might be due to introduction of non-homogeneity in films by grape pomace. Film incorporated with 5% of pomace extract had a tensile strength of 108 ± 12 MPa which reduced to 80 ± 10 MPa at 7.5% of pomace concentration. Thus 5% pomace extract incorporated optimized film were used further.

Table 42: Physical properties of films incorporated with grape pomace extract.

Grape pomace extract (% w/w of GG)	Tensile strength (MPa)	Young's Modulus (GPa)	WVTR ($g/m^2/d$)
Control	122 ± 18^{a}	99 ± 8^{a}	39 ± 4^{b}
0.5	123 ± 15^{a}	101 ± 10^{a}	38 ± 5^{b}
1	119 ± 15^{a}	95 ± 9^{a}	40 ± 4^{b}
2.5	112 ± 9^{a}	91 ± 8^{a}	41 ± 5^{b}
5	108 ± 12^{a}	88 ± 9^{a}	44 ± 6^{ab}
7.5	80 ± 10^{b}	70 ± 6^{b}	53 ± 7^{a}

Any two means in the same column followed by the same letter are not significantly ($p > 0.05$) different.

3.4.3 Effect of radiation treatment on physical properties of films

Food products are pre-packed prior to gamma irradiation for extending their shelf life. Thus there is a need to analyze the effect of radiation treatment on mechanical and barrier properties of packaging films. It was observed that up to 5 kGy of irradiation, films incorporated with 5% pomace extract showed no significant ($p < 0.05$) change in film characteristics (Table 43) as compared to control film. However, at higher doses (7.5 kGy), a decrease in functional properties was noted (Table 43). A 5% pomace incorporated film when irradiated at 5 kGy resulted in film having tensile strength of 88 ±

12 MPa, Young's modulus of 73 ± 8 GPa and WVTR of 53 ± 4 g/m^2/d. However, with increase in irradiation to a dose of 7.5 kGy resulted in film with tensile strength of 77 ± 8 MPa, Young's modulus of 65 ± 5 GPa and WVTR of 60 ± 7 g/m^2/d. Previous report on irradiation of starch/PVA-based film incorporated with *Acacia catechu* extract have shown significant decrease in tensile strength as compared to non-irradiated films beyond a dose of 2 kGy [211]. Films developed in present study were found to have a considerably higher radiation resistance as compared to those reported literature data. Thus the presently developed films can be successfully employed for packing of food that is meant for radiation processing.

Table 43: Effect of gamma irradiation on mechanical and barrier properties of RSM optimized film having 5% grape pomace extract.

Dose (kGy)	Tensile strength (MPa)	Young's Modulus (GPa)	WVTR (g/m^2/d)
Control	108 ± 12^a	88 ± 9^a	44 ± 6^b
0.5	103 ± 15^a	84 ± 10^a	46 ± 5^b
1	97 ± 11^a	80 ± 8^a	49± 4^b
2.5	92 ± 9^{ab}	76 ± 7^{ab}	51 ± 5^{ab}
5	88 ± 12^{ab}	73 ± 8^{ab}	53 ± 4^{ab}
7.5	77 ± 8^b	65 ± 5^b	60 ± 7^a

Any two means in the same column followed by the same letter are not significantly ($p > 0.05$) different.

3.4.4 Characterization of extract incorporated film

Developed film (5% grape pomace extract w/w of GG) was further analyzed to determine its antioxidant activity and antimicrobial property since these properties actively helps in extending the shelf life of packed agricultural produce.

3.4.4.1 Antioxidant activity of the developed film

Table 44 shows the content of various classes of bioactive compounds and their antioxidant activity in the developed active films. Total phenolic content of active film was 1.6 ± 0.3 mg GAE/g of film. The phenolic content estimated in the present study was much lower than that reported in literature. For example, chitosan film formulated with grape seed extract (10 g of oil per liter of film forming solution) had a phenolic content of 76 mg GAE/g of film [212]. Low amount of phenolics present in developed active films was due to addition of small quantity of grape pomace extract per liter of the film forming solution (0.5 g/L). It was also noted that irradiation up to 5 kGy resulted in no significant ($p < 0.05$) change in bioactive compounds present in the active film.

Table 44: Content of various classes of bioactive compounds and their antioxidant activity in GG based active film.

Chemical constituents	Quantity in GG based film
Total anthocyanins	6.8 ± 1.2 (mg/100g)
Total phenolic content	1.6 ± 0.3 (mg GAE/g)
Total flavanoid	2.6 ± 0.1 (mg QE/g)
Ascorbic acid	1.6 ± 0.2 (mg/100g)
FRAP	1.1 ± 0.2 (mg TE/g)
DPPH	4.5 ± 0.5 (mg TE/g)

3.4.4.2 Antimicrobial activity of the developed film

Antimicrobial activity of films was tested qualitatively and quantitatively by inhibition zone method and a viable cell count method respectively. Five different food pathogenic bacteria including *Staphylococcus aureus, Salmonella typhimurium, Escherichia coli, Bacillus subtilis and Bacillus cereus* were used. Table 45 shows the diameter (cm) of inhibition zone developed against different pathogenic strains and log cycle decrease in bacterial population due to incorporation of the active films. The highest inhibition of 3.6 ± 0.3 log cycle decrease was noted against *E. coli* while no inhibition was observed against *B. subtilis*. *B. subtilis* was thus found to be resistant to the active film. *B. cereus* was however susceptible towards the bioactive compounds present in the developed film (Table 45). Both *Bacillus* strains demonstrated different susceptibility towards active film this might be due to different types of antibiotic resistant plasmid present in both the strains [213]. Similar results were also obtained by viable cell count method (Table 45). Largest zone of inhibition with a diameter of 1.3 ± 0.2 cm was observed for *E. coli*. The antimicrobial activity of the developed film could be attributed to the different bioactive constituents present (Table 45). Radiation treatment up to a dose of 5 kGy showed no significant ($p < 0.05$) change in antimicrobial activity (quantitative or qualitative) of film. Similar result was observed for polyamide coated LDPE film with active compounds (sorbic acid, carvacrol, thymol and rosemary oleoresin) wherein the antimicrobial activity of the films was found to get retained when exposed to 1–3 kGy [214].

Table 45: Antimicrobial activity of developed active film.

Microrganism	Zone of inhibition (cm)	Log cycle decrease
E. coli	1.3 ± 0.2	3.6 ± 0.3
S. aureus	1.2 ± 0.2	3.3 ± 0.3
B. cereus	1.1 ± 0.1	2.9 ± 0.2
S. typhimurium	0.9 ± 0.1	2.1 ± 0.1
B. subtilis	0	0

Thus GG based active film with high antimicrobial activity can be used for food irradiation application up to a dose of 5 kGy. This was further demonstrated using fruit samples wherein minimally processed pomegranate arils was packed in RSM optimized active (5% pomace extract) film for shelf life extension.

3.4.5 Effect of irradiation and type of packaging on quality of pomegranate arils

Pomegranate arils were packed in both RSM optimized (section 3.3.6) and active films currently developed as well as in commercial cling wrap films and irradiated prior to storage to determine the effect of packaging and radiation treatment on its shelf life.

3.4.5.1 Microbial analysis

Gamma irradiation is known to be an effective tool for food hygieneization reducing both bacterial and fungal population in food products. Effect of irradiation (0.5, 1, 1.5, 2 and 2.5 kGy) on microbial load was analyzed at different storage points. A dose dependent decrease in bacterial and fungal population was noted irrespective of packaging. In all the three packaging (cling film, RSM optimized film and active film) dose of 2 and 2.5 kGy

dose was found to substantially reduce microbial population throughout the storage period with maximum reduction of 1.5 log cycles was noted immediately after irradiation at both the doses (Figure 34). Interestingly no fungal colonies were detected at these doses. Similar results have been reported for irradiated lettuce [215] and other vegetables [216]. Khattak et al. (2005) [217] reported that fungal colonies were eliminated on cucumber and cabbage when treated with doses higher than 2 kGy. Thus, results obtained in the present study are in agreement with that reported previously by other researchers. Sensory acceptability of 2 kGy irradiated arils was higher than 2.5 kGy irradiated arils due to radiation induced softness of fruits at 2.5 kGy. Therefore, 2 kGy was found to be the optimum dose required for maintenance of microbial safety during storage of ready to eat pomegranate arils.

A significant ($p \leq 0.05$) increase in bacterial load during storage was observed in the non-irradiated samples; the counts reached higher than 10^7 CFU/g on 8^{th} day of storage in all packaging which is beyond the acceptable limit (10^7 CFU/g) prescribed for fresh cut vegetables and fruits (Figure 34 A). In samples irradiated at 2 kGy the mesophilic counts were well below the acceptable limits only up to 8 days for cling and optimized films, however, for active film arils were microbiologically safe up to 12 days at 2 kGy (Figure 34B & 35). Longer shelf life of arils packed in active films could be attributed to the antimicrobial activity of films which reduces the chances of contamination of the arils through packaging during storage. A survey performed by the WHO (1995) indicated that almost 25% of the food-borne outbreaks could be traced back to recontamination. One of the possible routes of recontamination is through primary packaging because it is in direct

contact with the food products. Moreover, Reij et al. (2004) [218] stated that seams and seals of packaging film can cause micro-leaks that may allow access of a variety of microorganisms, including pathogens to packed food. For the safety of packaged irradiated foods it is essential to ensure a reliable heat seal by using transversely curved heat sealing bars otherwise it may lead to microbial recontamination [219, 220]. However, developed active film minimizes the chance of recontamination through it owing to its antimicrobial properties. Appendini et al. (2002) [119] also proposed that self-sterilized or sanitized antimicrobial packaging materials prominently reduce the chance of recontamination of processed products. Similarly Hotchkiss et al. (1997) [221] proposed that self-sterilizing abilities of the packages due to their own antimicrobial effectiveness simplified the aseptic packaging process. This in turn extends the shelf-life of minimally processed fruits.

The response of yeast and mould count of arils packed using different packaging materials against 2 kGy of radiation doses is shown in figure 34D. Total fungal count of control samples wrapped in cling film was 0.9 ± 0.13 cfu/g at day 0 which increased to a value of 2.79 ± 0.21 cfu/g at the end of day 8. No fungi were detected in pomegranate arils when packed in any film immediately after irradiation, however, it reached to value of 1.72 ± 0.16 cfu/g with the storage period of 8 days when cling packaging film was used. The fungal population in samples packed with active films was significantly ($p < 0.05$) lower than those packed using cling or optimized films (Figure 34 C & D).

Thus based on microbial analysis an optimum shelf life of 8 days was achieved when arils were irradiated at 2 kGy and packed with cling or optimized films, however, active

packaging along with irradiation (2 kGy) resulted in shelf life improvement of 12 days. Hence, further analysis of irradiated and non-irradiated arils packed in active or cling film was performed for evaluation of different packaging on arils quality.

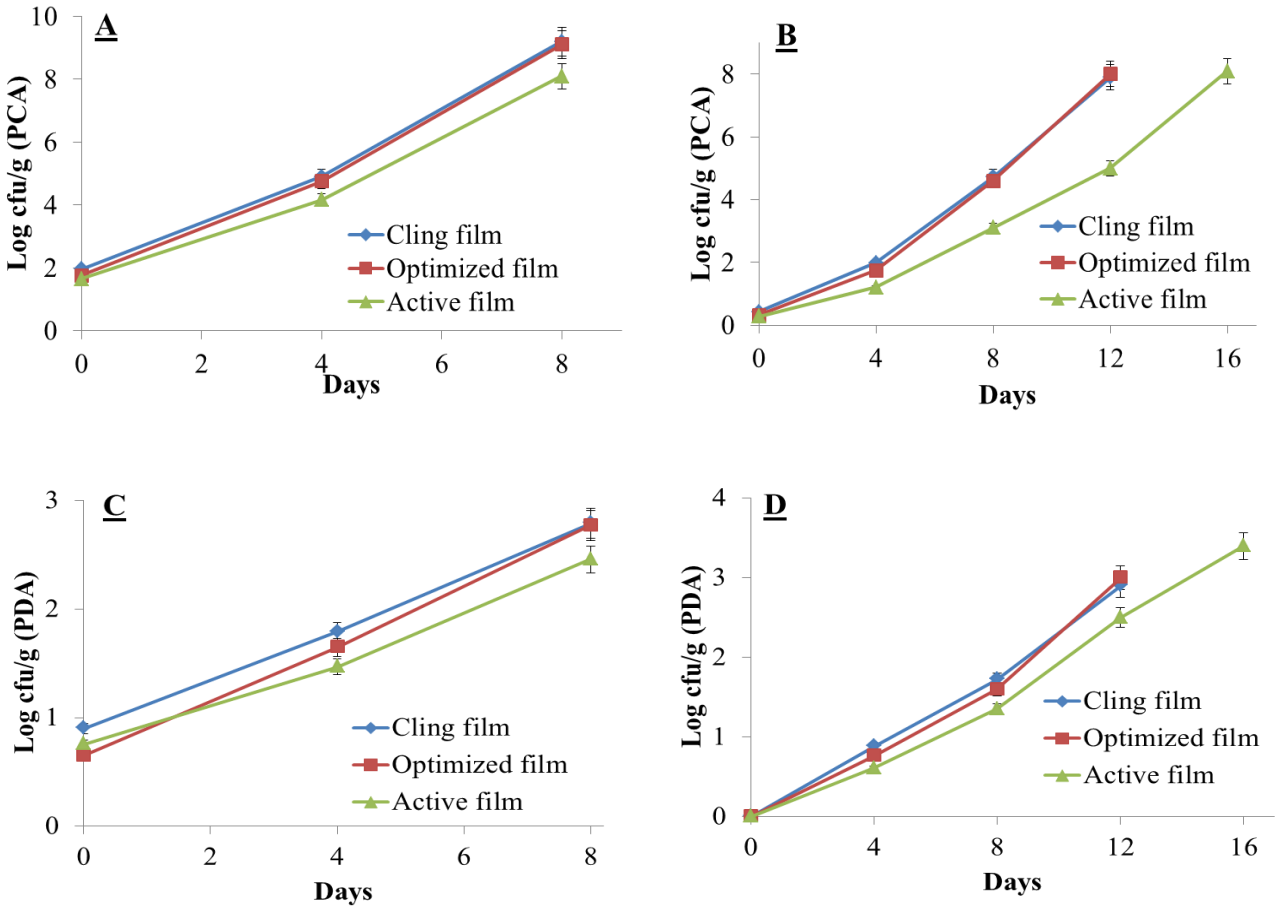

Figure 34: Effect of irradiation and packaging on (A) Bacterial count of control arils (B) Bacterial count of arils irradiated at 2 kGy (C) Fungal count of control arils (D) Fungal count of arils irradiated at 2 kGy.

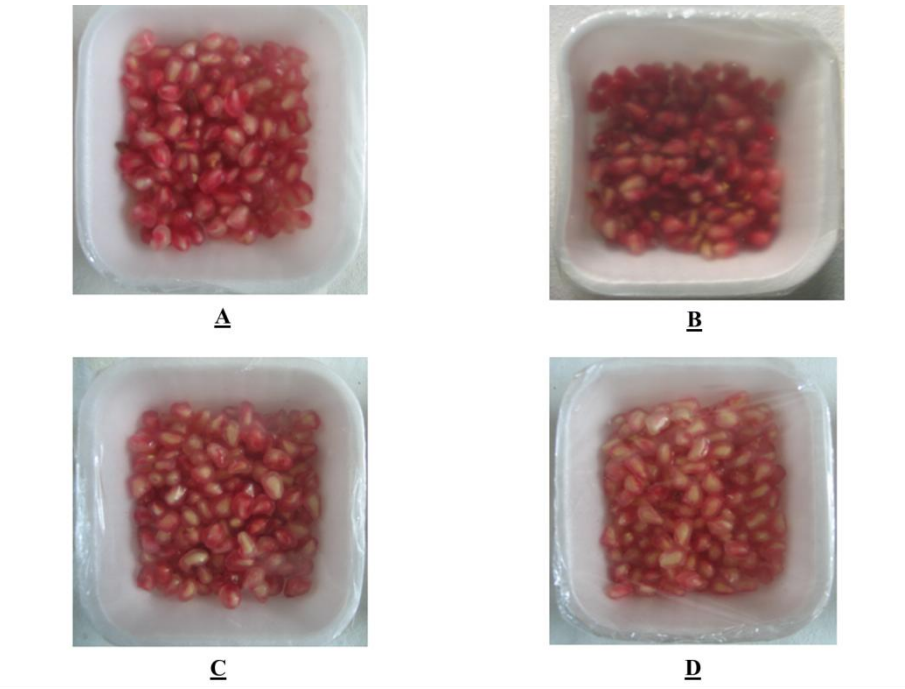

Figure 35: Pomegranate arils packed in active film (A) Control, day 0 (B) Control, day 12 (C) Irradiated, day 0 (D) Irradiated, day 12.

3.4.5.2 Sensory analysis

Sensory quality of control and irradiated samples were analyzed by hedonic scores. Sensory attributes of control and 2 kGy irradiated pomegranate arils is given in table 46. Sensory quality of non-irradiated sample packed in either of the packaging was found to deteriorate within 4 days of storage owing to the blackening of the arils. However, no such observation was made by sensory panel for irradiated samples during the entire storage. No significant ($p < 0.05$) difference in the aroma quality of samples was observed between control and irradiated sample immediately after irradiation. The irradiated samples were found to maintain the aroma quality throughout the storage period of 12 days when packed in active film and 8 days for cling wrapped samples. No difference was

observed in the texture quality between control and irradiated samples throughout the storage period. Sensory analysis of control samples was not performed beyond day 4 because they were microbiologically unsafe. The taste quality of irradiated samples packed in active film was maintained up to a storage period of 12 days. However, taste quality of cling wrapped samples was maintained only up to 8 days. Results from hedonic testing demonstrated that the overall quality of the control samples lowered gradually with storage whereas the irradiated samples received good overall sensory scores throughout the storage period irrespective of packaging used.

Table 46: Effect of radiation treatment and storage on sensory quality of arils packed in (A) Active film (B) Cling film.

A

Days	Dose	Color	Texture	Taste	Aroma	Overall acceptability
0	control	7.1 ± 1.1^a	6.8 ± 0.4^a	7.9 ± 0.8^a	6.0 ± 1.0^a	7.6 ± 0.9^a
	2 kGy	7.3 ± 0.6^a	6.6 ± 0.7^a	7.7 ± 1.1^a	6.5 ± 0.6^a	7.3 ± 0.8^a
4	control	7.2 ± 0.4^a	6.3 ± 0.5^a	7.5 ± 0.3^a	6 ± 0.7^a	6.5 ± 0.6^a
	2 kGy	7.1 ± 1.1^a	6.5 ± 0.8^a	7.4 ± 0.7^a	6.1 ± 0.4^a	6.9 ± 0.9^a
8	control	NA	NA	NA	NA	NA
	2 kGy	6.9 ± 0.8^a	6.3 ± 0.9^a	7.1 ± 0.7^a	6.0 ± 0.8^a	6.8 ± 0.7^a
12	control	NA	NA	NA	NA	NA
	2 kGy	6.7 ± 0.7^a	6.2 ± 0.8^a	6.7 ± 0.6^a	6.0 ± 0.6^a	6.5 ± 0.3^a

B

Days	Dose	Color	Texture	Taste	Aroma	Overall acceptability
0	control	7.2 ± 1.2^a	6.7 ± 0.5^a	7.7 ± 0.9^a	6.0 ± 1.0^a	7.7 ± 0.8^a
	2 kGy	7.3 ± 0.5^a	6.6 ± 0.7^a	7.6 ± 1.3^a	6.4 ± 0.6^a	7.4 ± 1.1^a
4	control	7.0 ± 0.8^a	6.2 ± 0.5^a	7.4 ± 0.7^a	6.1 ± 0.6^a	6.7 ± 0.8^a
	2 kGy	7.2 ± 1.2^a	6.7 ± 0.9^a	7.2 ± 0.7^a	6.3 ± 0.5^a	6.8 ± 0.9^a
8	control	NA	NA	NA	NA	NA
	2 kGy	7.1 ± 0.6^a	6.4 ± 0.7^a	7.0 ± 0.7^a	6.2± 0.8^a	6.6 ± 0.7^a

Any two means in the same column followed by the same letter are not significantly ($p > 0.05$) different.

3.4.5.3 Color

Appearance forms important criteria in determining consumer's acceptability. Figure 36 represents the effect of irradiation and storage on L^* values of pomegranate arils. L^* values decreased significantly ($p < 0.05$) for both control samples due to blackening of arils at tips. It decreased from 63 ± 5 at day 0 to 45 ± 3 at the end of 12th day when packed

in active film. Interestingly, luminosity (L^*) of irradiated (2 kGy) arils packaged in both films remained statistically ($p < 0.05$) constant during storage and the visual quality was acceptable at the end of storage. The instrumental data thus support the sensory scores obtained by hedonic testing. Active packaging followed by gamma irradiation can thus maintain the visual quality of the samples for a period of 12 days.

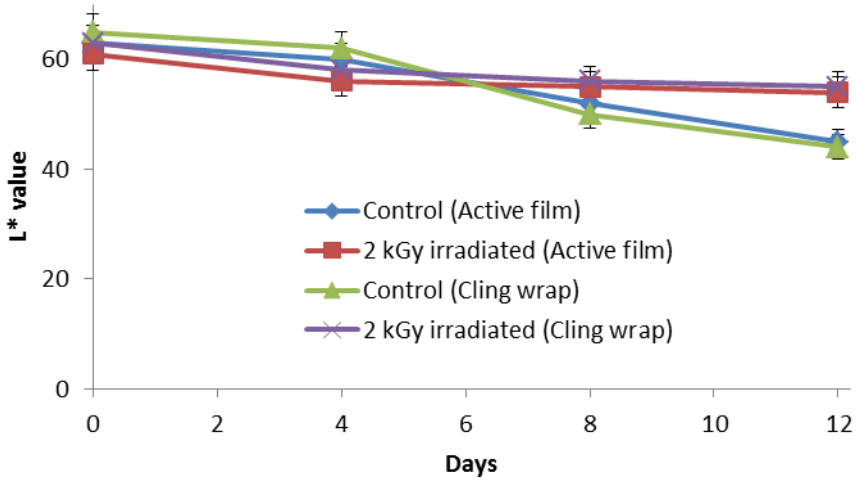

Figure 36: Effect of irradiation and storage on L^* value of arils packed in active film.

3.4.5.4 Headspace gases

Headspace gas composition forms an important aspect in the storage of minimally processed fruits and vegetables. A high O_2 percentage often leads to greater unfavorable reactions like browning while a lower O_2 level leads to the growth of anaerobic bacteria, consequently, maintenance of optimum balance between O_2 and CO_2 level is very crucial. O_2 level less than 2% is known to support the growth of anaerobic bacteria like *Clostridium botulinum* and microaerophilic bacteria like *Listeria spp.* and lactic acid bacteria [222].

In the present study, significant ($p < 0.05$) effect of irradiation and storage period on the headspace composition of both the gases was observed. CO_2 and O_2 percentage remained constant for non-irradiated samples (packed in active or cling film) throughout the storage period i.e. 1.8 ± 0.1 % and 20.1 ± 1 % respectively (Figure 37). However, irrespective of packaging a significant decrease in O_2 and an increase in CO_2 percentage were noted immediately after irradiation compared to O_2 and CO_2 percentage of non-irradiated sample. The lowest O_2 content observed was 16.5 ± 1.2 % and highest CO_2 percentage was 5 ± 0.29 % immediately after irradiation for samples packed in active film. This might be due to rapid increase in respiration rate due to rise in cellular activity after irradiation induced stress response. On further storage, the O_2 content gradually increased to 19.5 ± 1.6 % and CO_2 content decreased to a value of 2 ± 0.15 % thus reaching the level as in the control on day 8 and then remained constant throughout the storage period. A similar observation in irradiated mushroom resulting from reduction in metabolic activity during storage has been demonstrated. Elevated CO_2 levels have been shown to extend lag phase and thus slow the propagation of bacteria [223]. The enhanced CO_2 levels during the initial storage period in the irradiated samples may thus aid in slowing down microbial growth and thus improving shelf life compared to the control samples. The maintenance of constant O_2 and CO_2 level beyond storage of period of 8 days may be due to attainment of equilibrium condition between package headspace and atmosphere with time. A similar observation was also noted earlier in irradiated minimally processed ash gourd [224]. The headspace gas composition was therefore found to be suitable for storage of minimally processed pomegranate arils. However, O_2 and CO_2 percentage of

cling wrapped irradiated sample was lower and higher respectively, than arils packed in active film throughout the storage period (Figure 37). This might be due to higher gaseous permeability of GG based active film.

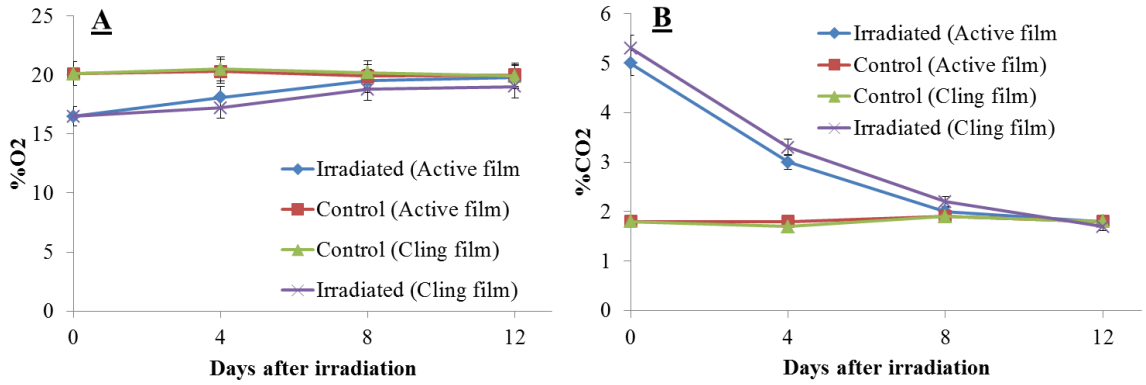

Figure 37: Effect of irradiation on headspace gas composition of arils packed in active films or cling film (A) O_2% (B) CO_2%.

3.4.5.5 Texture analysis

Loss in firmness of fruits often affects consumer acceptability. Therefore texture of minimally processed pomegranate arils was analyzed by a texture analyzer. Figure 38A provides the firmness of both the control and irradiated (2 kGy) samples packed in either of the films. In control samples packed in active film, the firmness increased from 156 ± 10 N at day 0 to 225 ± 12 N at the storage period of 12 days. On the other hand a slight decrease in firmness immediately after irradiation to a value of 135 ± 10 N with further increase in texture thereafter until the end of the storage period was noted. Increased texture during storage may be attributed to moisture loss of arils through the packaging. On the other hand, extent of increase in firmness was significantly ($p < 0.05$) lesser for

samples packaged in cling films as compared to those packed in active films. After storage period of 12 days control samples packed in cling films demonstrated a texture of 198 ± 11 N.

This might be due to higher moisture loss through GG based active films. However, this increase in firmness as determined by the texture analyzer was not perceived by the sensory panellists for arils packed in active or cling film. Similarly, Ayhan et al (2009) [160] observed increase in firmness of RTE pomegranate arils with storage. Thus our results are in accordance with the already published literature data.

3.4.5.6 Moisture loss

Figure 38B shows the percentage of weight losses (%) of minimally processed pomegranate arils as affected by irradiation and storage. There was a significant ($p < 0.05$) weight loss in all the samples during storage. Maximum weight loss of 3.2 ± 0.18 % at the end of 12 days was observed for 2 kGy irradiated arils packed in active film. However, 2 kGy irradiated arils wrapped in cling film resulted in water loss of 2.2 ± 0.2 %. Similarly, Hamid et al (2012) [225] observed a maximum weight loss of 1.38% for 1 kGy irradiated pear fruit when packed in polyolefin shrink film. A higher percentage weight loss in the present study could be due to the use of GG based active film used for packaging that possess higher WVTR than thin film of polyolefin or cling film.

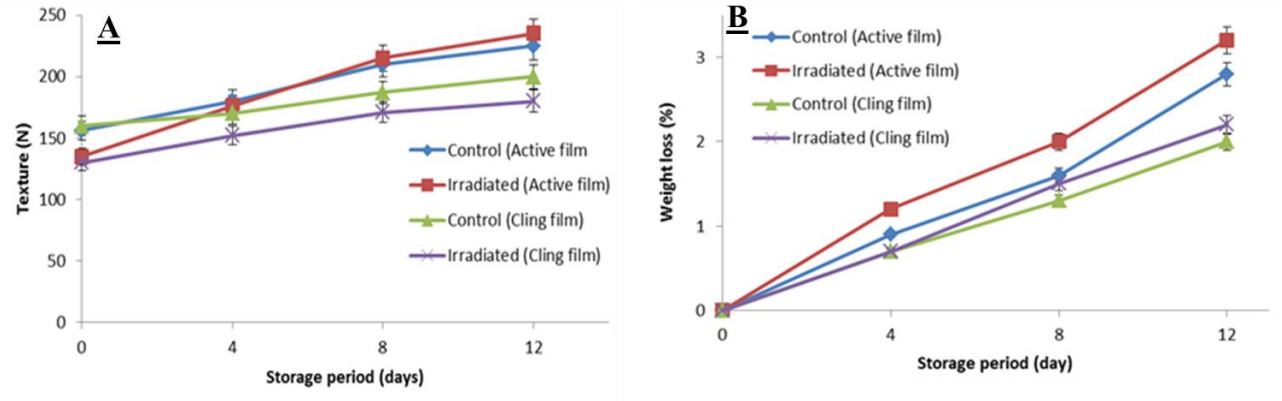

Figure 38: Effect of irradiation and storage period on (A) Texture of minimally processed pomegranate arils (B) Moisture loss of minimally processed pomegranate arils.

3.4.5.7 Effect of irradiation on pH and total soluble sugar in pomegranate juice

Total soluble sugar (TSS) represents the amount of dissolved sugars in the fruit and it is an indicator of sweetness level in a fruit [226]. Gamma irradiation was found to bring no significant ($p < 0.05$) change in TSS content, however, with storage TSS increased slightly in both control and irradiated samples packed in either of the film (Table 47). Active film wrapped 2 kGy irradiated arils had TSS of 16 ± 1 °Brix at day 0 which increased to a value of 19 ± 1 °Brix at the end of day 12. The breakdown of polysaccharides into water soluble sugars during storage might be the reason for the increase in the sugar content. There was a decrease in pH for irradiated and non-irradiated samples, over the storage period (Table 47). Irradiated samples when packed in active films had a pH of 3.9 ± 0.1 at day 0 which decreased to 3.6 ± 0.1 at the end of 12 day storage period. During storage of fresh fruits, senescence is facilitated by the breakdown of sugars through fermentation processes by microbes into alcohol and carbon dioxide

that contribute to reduced pH of the samples. The increase in acidity is an indication of spoilage and the presence of microbes like yeast. Irradiation dose of 2 kGy was effective for preserving the quality of pomegranate arils samples packed in cling or active film as indicated by the relatively low acidity recorded over the storage period. Similar results were obtained by Owureku-Asare et al. (2014) [227] for minimally processed pineapple.

Table 47: Effect of storage and irradiation on pH and Total soluble sugar (TSS) of arils juice (A) Active film (B) Cling film.

A

Days	TSS (°Brix)		pH	
	Control	Irradiated	Control	Irradiated
0	16 ± 1^{b}	16 ± 1^{b}	3.8 ± 0.2^{a}	3.9 ± 0.1^{a}
4	18 ± 1^{ab}	17 ± 1^{ab}	3.7 ± 0.3^{ab}	3.8 ± 0.2^{ab}
8	19 ± 1^{a}	18 ± 1^{ab}	3.6 ± 0.2^{ab}	3.7 ± 0.2^{ab}
12	20 ± 1^{a}	19 ± 1^{a}	3.4 ± 0.1^{b}	3.6 ± 0.1^{b}

B

Days	TSS (°Brix)		pH	
	Control	Irradiated	Control	Irradiated
0	17 ± 1^{b}	17 ± 1^{b}	3.8 ± 0.2^{a}	3.8 ± 0.1^{a}
4	19 ± 1^{ab}	18 ± 1^{ab}	3.6 ± 0.3^{ab}	3.7 ± 0.2^{ab}
8	20 ± 1^{a}	19 ± 1^{ab}	3.5 ± 0.2^{ab}	3.6 ± 0.2^{ab}
12	21 ± 1^{a}	20 ± 1^{a}	3.3 ± 0.1^{b}	3.5 ± 0.1^{b}

Any two means in the same column followed by the same letter are not significantly ($p > 0.05$) different.

3.4.5.8 Antioxidant activity

Minimally processed fresh cut fruits and vegetables are known to possess significant antioxidant activity. However, processing and storage may deteriorate the inherent antioxidant activity of the food product. Therefore estimation of processing and storage effect on antioxidant activity forms an important parameter for the development of minimally processed food product from nutritional view point.

The DPPH test usually provides basic information on the ability to scavenge free radicals. DPPH activity of control sample at zero days was found to be 876 ± 44 mg trolox equivalent/liter of arils juice (Figure 39A), similar results was obtained by Piljac-Žegarac

et al. (2009) [228]. No significant ($p < 0.05$) difference was observed in DPPH radical scavenging activity during entire storage period for both the packaging materials. However, irradiated samples for both the packaging materials demonstrated significantly ($p < 0.05$) higher antioxidant properties as compared to their corresponding controls. Immediately after irradiation antioxidant activity increased to 989 ± 77 mg TE/L. Irradiation induced free radicals may act as stress signals and initiate stress responses in fruits thus consequentially increase antioxidant activity [229].

Further, effect of irradiation, types of packaging and storage on the Fe^{3+}-reducing powers of pomegranate arils was investigated since reducing power of a compound may serve as an indicator of its potential antioxidant activity. Reducing capacity of control pomegranate juice packed in either of the packaging film was found to be 1.96 ± 0.1 mg trolox equivalent/liter (Figure 39B), similar results were obtained by Elfalleh et al. [230]. No significant ($p < 0.05$) difference was seen in reducing power values for pomegranate juice with packaging film, radiation treatment and storage time.

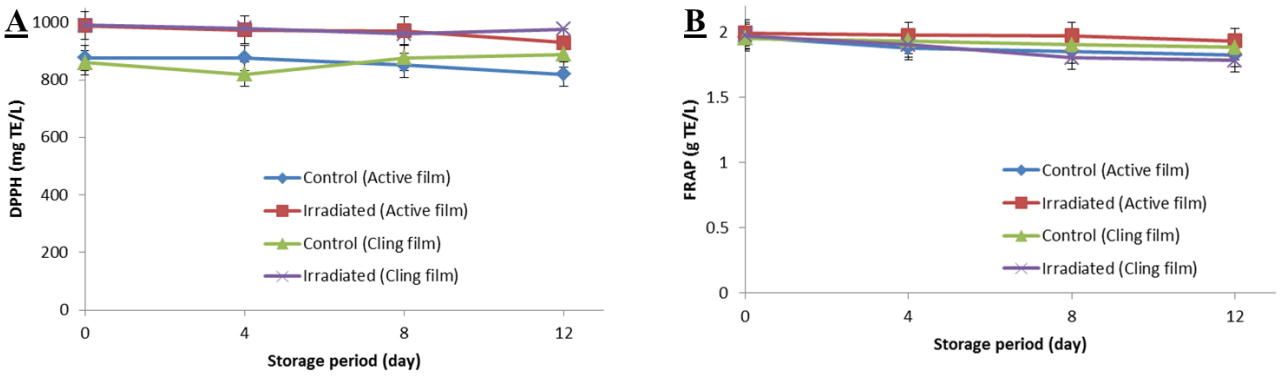

Figure 39: Effect of irradiation and storage on (A) DPPH radical scavenging activity of pomegranate juice (B) Reducing potential of pomegranate juice.

Antioxidant activities were thus found to be maintained in irradiated pomegranate arils throughout the storage period irrespective of packaging used. Cao et al. (1996) [231] have earlier reported that phenolics and ascorbic acid are some of the major antioxidants in fruits and vegetables. Fan et al. (2003) [229] have also obtained a positive correlation between phenolic content and antioxidant activity in iceberg lettuce exposed to radiation doses. Anthocyanins are also known to have strong antioxidant activity. Thus the effect of radiation processing on the anthocyanins, phenolics, flavonoids and vitamin C was further investigated.

3.4.5.9 Total anthocyanins, phenolics, flavanoids and vitamin C content of pomegranate juice

Phenolics, flavonoids and vitamin C form important nutritional constituents of vegetables. Anthocyanins are responsible for imparting the characteristic red color of pomegranate juice [232]. Thus preserving these compounds in fruits and vegetable is essential for maintaining their quality.

Total anthocyanins content of control pomegranate juice was found to be 50 ± 3 mg/L when either of the packaging was used (Figure 40), whereas, Valero et al. (2014) [233] reported a value of 29.50 ± 2.59 mg/L. Difference in the observed values could be due to different pomegranate variety used. Immediately after irradiation a significant ($p < 0.05$) reduction in total anthocyanins content was observed for both the packaging materials. At day 0 anthocyanins content decrease to a value of 43 ± 3 mg/L immediately after irradiation of active film wrapped samples. This might be attributed to radiation induced

degradation of anthocyanins. Alighourchi et al. (2008) [234] also demonstrated significant ($p < 0.05$) reduction in individual and total anthocyanins content of pomegranate juice after irradiation. However, with storage and types of packaging film used there was no significant ($p < 0.05$) change in total anthocyanins content (Figure 40).

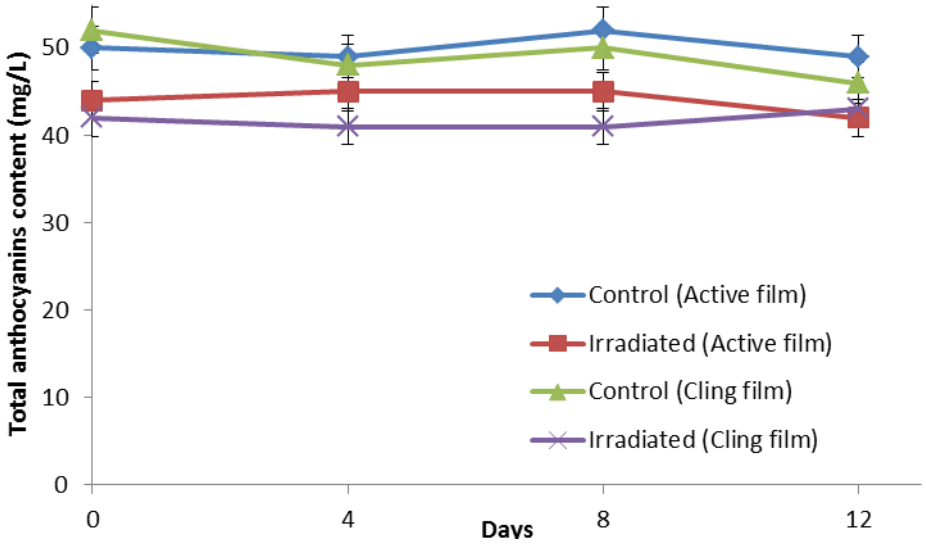

Figure 40: Effect of irradiation and storage on total anthocyanins content of pomegranate juice.

Total phenolic and flavanoid content of control juice at day 0 was 1541 ± 91 mg GAE/L and 613 ± 31 mg QE/L respectively irrespective of packaging used (Figure 41 A & B). In the present study no changes in total phenolic and flavanoid content was noted as a result of irradiation. Storage and packaging also had no effect on the total phenolic content and flavonoids. Arvanitoyannis et al. (2009) [69] and Tripathi et al. (2013) [224] earlier reported that radiation induced increase in phenolic content of carrot, kale juice and ash

gourd respectively. Villavicencio et al. (2000) [235] on the other hand reported a radiation induced reduction in phenolic content at 10 kGy in Macacar bean.

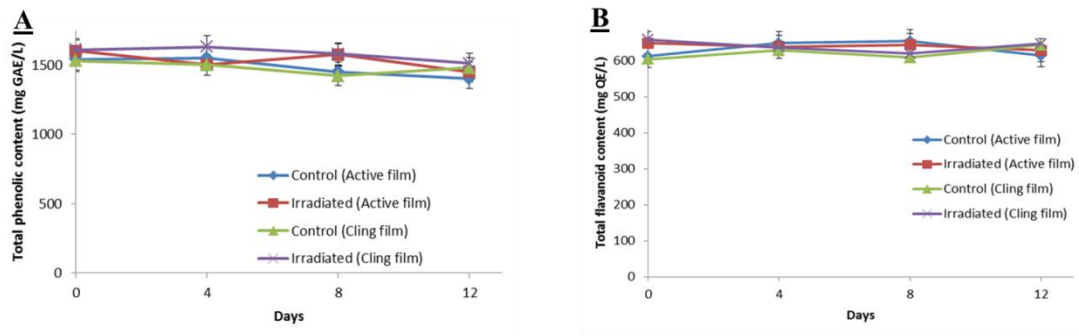

Figure 41: Effect of radiation treatment and storage period on total (A) Phenolic content of pomegranate juice (B) Flavanoid content of pomegranate juice.

Vitamin C is most sensitive vitamin being degraded rapidly on exposure to heat, light and oxygen. Therefore measuring the content of vitamin C in pomegranate juice could tell the effect of irradiation and storage on overall and individual vitamins content of arils. It acts as an antioxidant in the body by acting against oxidative stress and is also a cofactor in several key enzymatic reactions. In present study juice prepared from control pomegranate packed in either cling film or active film had 198 ± 11 mg/L of vitamin C at day 0 (Figure 42). The content of ascorbic acid was found to be unaffected by storage, packaging and radiation processing. A similar observation was observed by Tripathi et al. (2013) [224] in irradiated ash gourd. Thus the nutritional quality of pomegranate arils packed in active film or cling film with respect to its antioxidant activity, phenolic and flavonoid content and vitamin C status was maintained upon irradiation and during entire storage study.

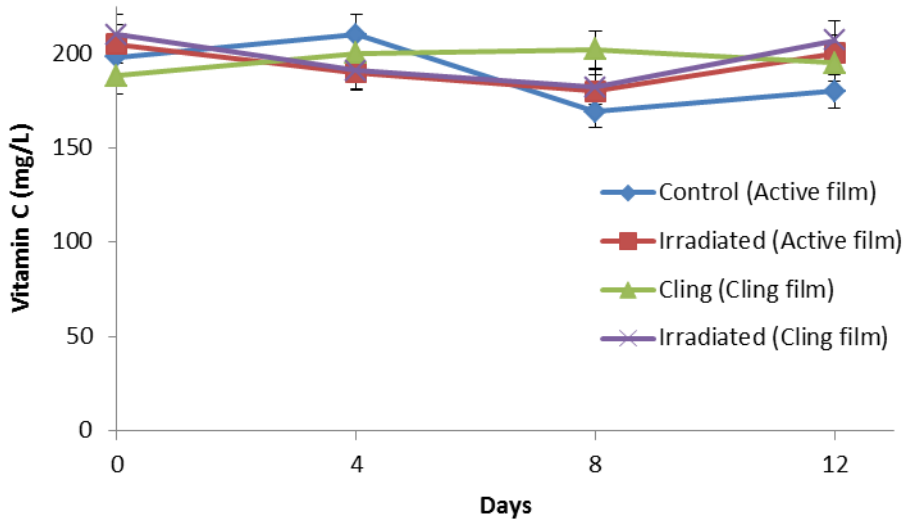

Figure 42: Effect of irradiation and storage on ascorbic acid content of pomegranate juice.

Above obtained results successfully demonstrate that film developed in present study performed better that commercial available cling film for shelf life extension of irradiated pomegranate arils. Radiation processed arils (2 kGy) had a shelf life of only 8 days when packaged in cling films as compared to 12 days for samples packed in active films. Samples packed in active films demonstrated similar sensory and biochemical characteristics when compared to samples packed in commercial cling films. Thus, GG based films could possibly provide suitable biodegradable alternative for non-biodegradable cling films.

3.4.6 Dip treatment of pomegranate arils for shelf life extension

Edible coatings are a type of packaging in which the packaging material is integrated on food surfaces as surface coatings. This imparts semi-permeability to the surface against

water vapor and gases and thereby extending the shelf life of coated product by creating modified atmosphere [236].

Pomegranate arils were dip treated in solution having 0.2% and 0.5% aqueous w/v pomace extract along with 0.5% guar gum prior to storage at 10 °C. Further microbiological, sensory and nutritional analysis of control and treated arils was done at an interval of two days for the entire storage period.

3.4.6.1 Microbial analysis

The effectiveness of dip treatment on the mesophillic count is shown in Figure 43A. It was observed that there was significant ($p < 0.05$) effect of dip coating on microbial counts immediately after treatment. Control arils had initial microbial count of 3.3 ± 0.17 cfu/g which reduced to 2.9 ± 0.15 cfu/g post dip treatment with 0.5% pomace extract solution. Similar results were reported by Mastromatteo et al. (2011) [237] when grape fruit seed extract was coated on kiwi fruit wherein the initial microbial load decreased from 2.48 cfu/g to 2 cfu/g. A 0.2% solution was however not found to be efficient in reducing the microbial load from the arils. Shelf life of control and 0.2% treated arils was 4 day. Mesophilic counts in control samples reached $>10^7$ cfu g^{-1} after storage of four days but remained less than $<10^6$ cfu g^{-1} even after storage of 6 days in 0.5% pomace treated samples. A 0.5% of pomace extract solution effectively prevented the growth of microbial population and this in turn increased the shelf life of arils up to 6 days (Figure 43 & 44). Similar result was obtained for yeast and mold counts (Figure 43B). Initial yeast and mold counts of control and 0.2% treated arils was 0.95 ± 0.1 cfu/g, however, for

0.5% treated arils it was 0.8 ± 0.1 cfu/g. After 6 days of storage fungal counts of control samples increased to 3.7 ± 0.25 cfu/g, however, for 0.5% dip treated arils it was 3.15 ± 0.15 cfu/g.

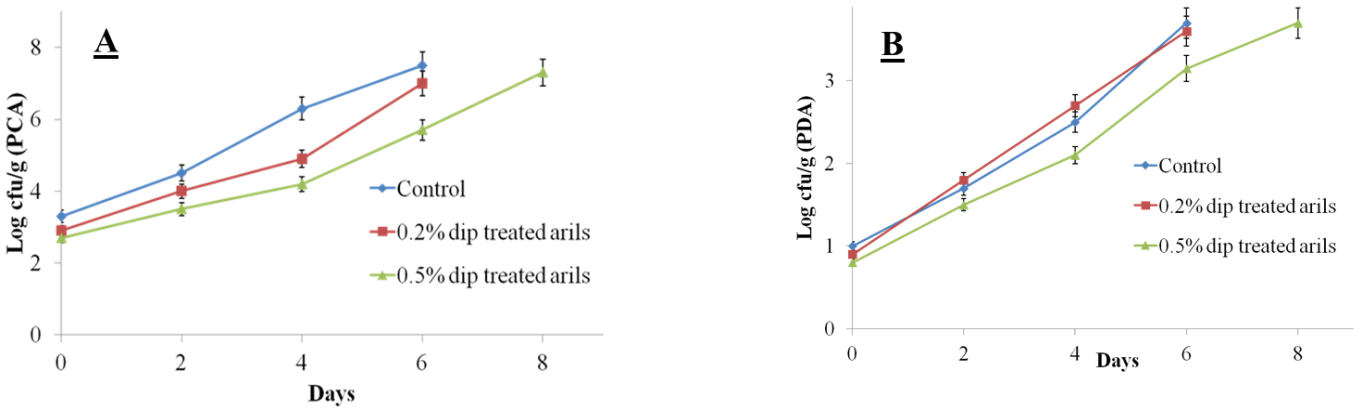

Figure 43: Effect of dip treatment of arils on its (A) Mesophilic count with storage (B) Yeast and mold count with storage.

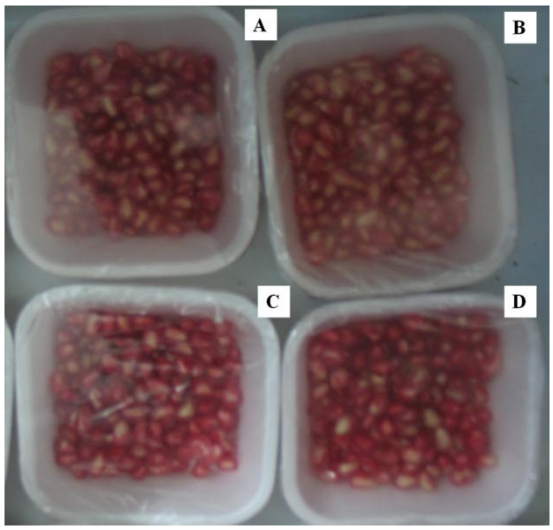

Figure 44: Images of post dip treatment and storage on arils (A) Control, day 0 (B) Control, day 6 (C) 0.5% treated arils, day 0 (D) 0.5% treated arils, day 6.

It can be concluded from result that 0.5% dip treatment efficiently reduced the microbial load thereby increasing the shelf life of minimally processed pomegranate arils up to 6 days. The 0.5% treated arils and the control samples were therefore further analyzed for their acceptability.

3.4.6.2 Sensory analysis

Sensory quality of control and 0.5% treated pomegranate arils were analyzed by hedonic testing. Scores obtained for the control and treated samples are given in table 48. Dip coating with grape pomace extract was found to impose no effect on sensory attributes of arils. The panelist could not detect any difference on appearance, aroma, taste and texture qualities between control and treated samples. No significant change ($p < 0.05$) was found in the sensory qualities of pomegranate arils due to dip treatment during entire storage period. Beyond storage period of 4 days control samples were microbiologically unacceptable and therefore the sensory analysis was not performed.

Table 48: Effect of dip treatment of arils on its sensory attributes.

Days	Dip treatment	Color	Texture	Taste	Aroma	Overall acceptability
0	Control	6.5 ± 0.8^a	6.6 ± 0.5^a	7.7 ± 0.6^a	6.0 ± 1.0^a	7.2 ± 0.7^a
	Treated	6.9 ± 0.6^a	6.7 ± 0.6^a	7.7 ± 1.0^a	6.5 ± 0.6^a	7.3 ± 0.9^a
2	Control	6.3 ± 0.6^a	6.3 ± 0.5^a	7.5 ± 0.3^a	6 ± 0.7^a	6.3 ± 0.7^a
	Treated	6.6 ± 0.8^a	6.5 ± 0.7^a	7.6 ± 0.8^a	6.1 ± 0.4^a	6.8 ± 0.9^a
4	Control	6.3 ± 0.7^a	6.4 ± 0.6^a	7.3 ± 0.9^a	5.9 ± 0.6^a	6.2 ± 0.8^a
	Treated	6.4 ± 0.7^a	6.3 ± 0.4^a	7.1 ± 0.7^a	6.0 ± 0.8^a	6.4 ± 1.0^a
6	Control	NA	NA	NA	NA	NA
	Treated	6.4 ± 0.6^a	6.1 ± 0.5^a	6.9 ± 0.7^a	5.8 ± 0.6^a	6.2 ± 0.7^a

Any two means in the same column followed by the same letter are not significantly ($p > 0.05$) different.

3.4.6.3 Color

Figure 45 represents the effect of dip treatment and storage on color of minimally processed pomegranate arils. L* values decreased significantly ($p < 0.05$) for control samples due to blackening of arils at tips. L* values at day 0 for control sample was 60 ± 5 and at the end of 6 days it reached to a value of 50 ± 4. However, for treated arils luminosity (L*) remained statistically ($p < 0.05$) unchanged during storage and the visual quality was found to be acceptable during the entire storage.

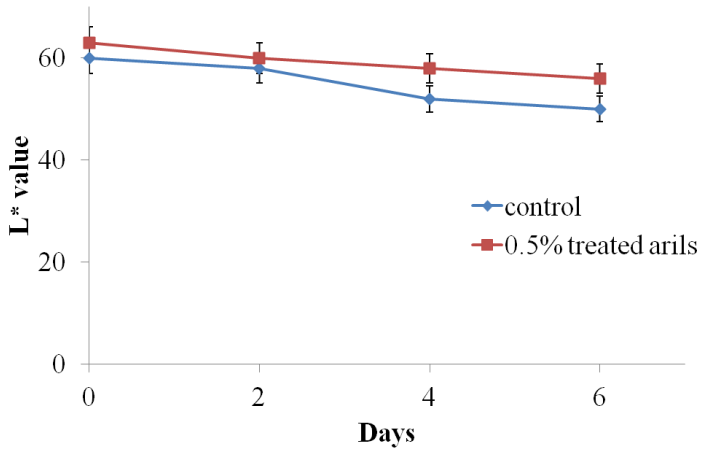

Figure 45: Effect of dip treatment on L* values of pomegranate arils.

3.4.6.4 Headspaces gases

Initial CO_2 and O_2 percentage of control samples were 1.8 ± 0.1% and 20.1 ± 1.9 % respectively. In present study the concentrations of CO_2 and O_2 did not change significantly ($p < 0.05$) among treatments over time inside the headspace of the packed tray (Figure 46). However, Martínez-Romero et al. (2013) [143] demonstrated significant increase in CO_2 concentration and decrease in O_2 concentration for *Aloe vera* gel coated

RTE pomegranate arils packed in air tight rigid polypropylene boxes. Difference in CO_2 and O_2 headspace gases observation in the present study and earlier report might be due to different permeability of the packaging used [143]. Similar report was published by Gil et al. (1996) [142] due to very high O_2 and CO_2 permeability of the oriented polypropylene film.

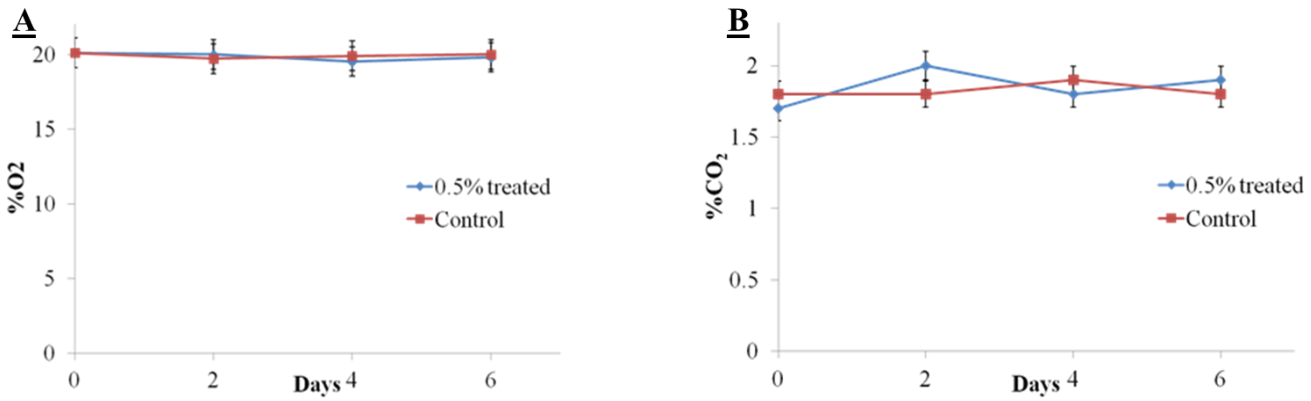

Figure 46: Effect of dip treatment on headspace gaseous composition of pomegranate arils (A) $\%O_2$ (B) $\%CO_2$.

3.4.6.5 Texture analysis

Figure 47A provides the firmness of both the control and dip treated (0.5%) samples. In control samples, the firmness increased from 178 ± 15 N at day 0 to 215 ± 19 N with storage period of 6 days. Similarly, firmness increased to 229 ± 18 N for samples subjected to dip treatment. Increased texture during storage was due to moisture loss of arils through the packaging. Similar result was earlier reported by us in section 3.4.5.5.

3.4.6.7 Moisture loss

Figure 47B shows the percentage of initial weight losses (%) of RTE pomegranate arils as affected by dip treatment and storage. Significant ($p < 0.05$) weight loss was observed in both the samples during storage and this was responsible for the increased firmness of arils (section 3.4.6.5). At the end of 6 days 2.9 ± 0.15 and 2.7 ± 0.13 % of moisture loss was observed for control and dip treated samples, respectively.

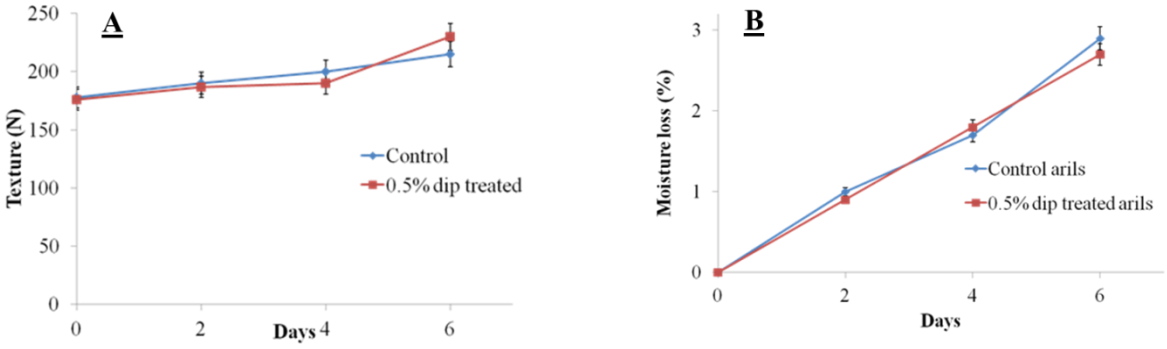

Figure 47: Effect of grape pomace extract dip treatment and storage period on (A) texture of minimally processed pomegranate arils (B) Moisture loss of minimally processed pomegranate arils.

3.4.6.8 Effect of edible coating on pH and total soluble sugar on juice

TSS of control and 0.5% dip coated arils was 17 ± 1 and 16 ± 1 °Brix respectively, and it was not significantly ($p < 0.05$) effected with storage (Table 49). At day 0, pH of control arils was 3.9 ± 0.1 and it remained constant with storage as well as with dip treatment (0.5%). However, earlier (section 3.4.5.7) TSS and pH of control arils were significantly

($p < 0.05$) effected with storage up to 12 days. Difference in observation might be due to shorter storage study of only 6 days in case of dip treatment.

Table 49: Effect of storage and irradiation on pH and Total Soluble Sugar of arils juice.

Days	TSS (°Brix)		pH	
	Control	Treated	Control	Treated
0	17 ± 1^a	16 ± 1^a	3.9 ± 0.2^a	3.8 ± 0.1^a
2	17 ± 1^a	16 ± 1^a	3.9 ± 0.3^a	3.8 ± 0.2^a
4	18 ± 1^a	17 ± 1^a	3.8 ± 0.2^a	3.7 ± 0.2^a
6	19 ± 1^a	18 ± 1^a	3.7 ± 0.1^a	3.6 ± 0.1^a

Any two means in the same column followed by the same letter are not significantly ($p > 0.05$) different.

3.4.6.9 Effect of dip treatment and storage on nutritional properties of minimally processed pomegranate arils

DPPH activity of control sample was found to be 891 ± 45 mg trolox equivalent/liter of arils juice (Figure 48A). DPPH radical scavenging activity of pomegranate arils was not significantly ($p < 0.05$) effected by dip treatment. Similar result was achieved by Oms-Oliu et al. (2008) [238] for polysaccharide based edible coatings of fresh-cut pears. Storage also had no effect on the DPPH radical scavenging activity in both control and dip treated samples (Figure 48A).

Reducing capacity of pomegranate juice was found to be 2.1 ± 0.1 mg trolox equivalent/liter (Figure 48B). No significant ($p < 0.05$) difference was noticed in reducing power values for pomegranate juice with dip treatment for entire storage period of 6 days. Antioxidant activities were thus found to be maintained in control and treated pomegranate arils during their entire shelf life.

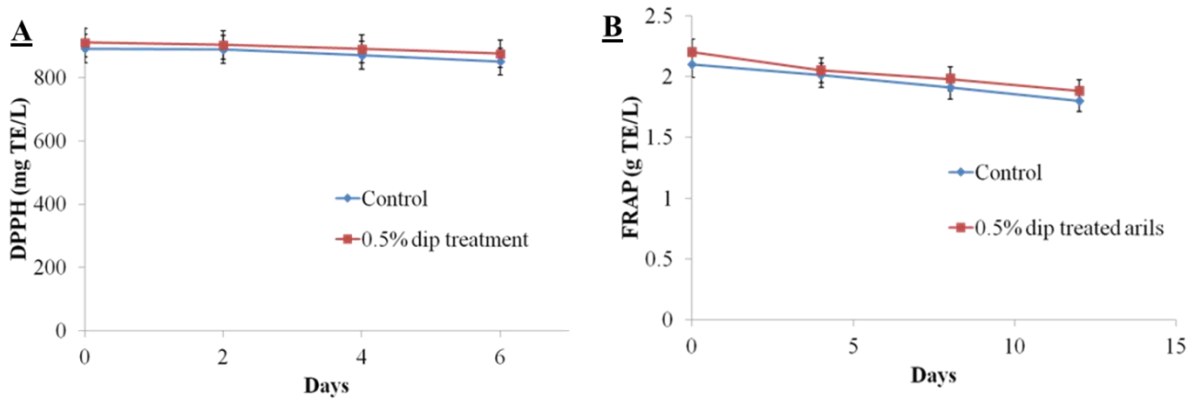

Figure 48: Effect of dip treatment and storage on (A) DPPH radical scavenging activity of pomegranate juice (B) Reducing potential of pomegranate juice.

Total anthocyanins content of control pomegranate juice was found to be 53 ± 3 mg/L (Figure 49). Dip treatment along with storage had no significant ($p < 0.05$) effect on total anthocyanins content.

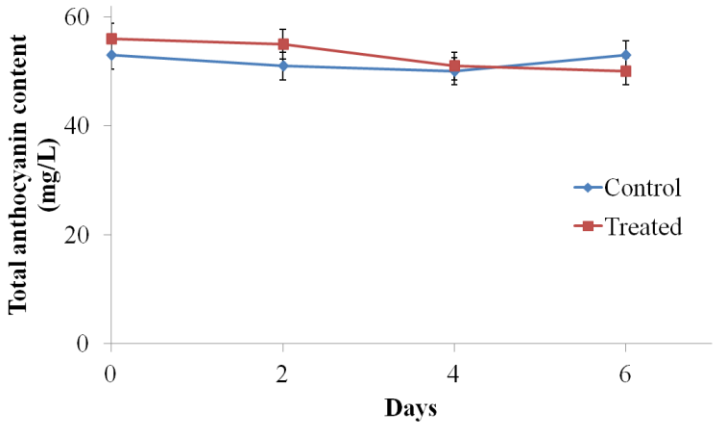

Figure 49: Effect of dip treatment and storage on total anthocyanins content of pomegranate juice.

Total phenolic content of control juice at day 0 was found to be 1480 ± 79 mg GAE/L while the total flavanoid content was estimated to be 633 ± 36 mg QE/L. No changes in the total phenolic and flavanoid content were noted as a result of dip treatment (Figure 50 A & B). Storage also had no effect on the total phenolic content and flavonoids. No effect on total phenolic content was also observed by Martínez-Romero et al. (2013) [143] between control RTE pomegranate arils and arils treated with *Aloe vera* gel.

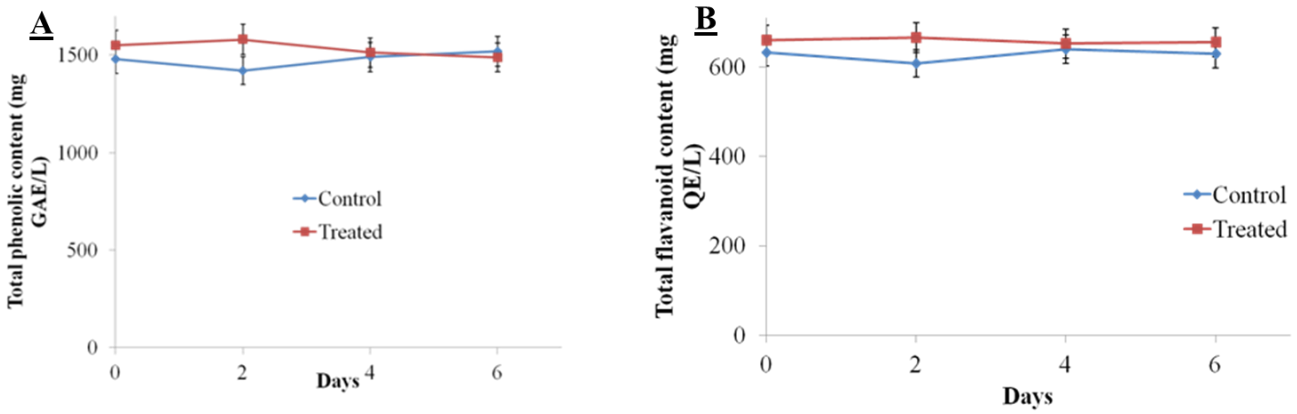

Figure 50: Effect of dip coating and storage on total (A) Phenolic content of pomegranate juice (B) Flavanoid content of pomegranate juice.

In present study juice prepared from control pomegranate had a vitamin C content of 180 ± 11 mg/L at day 0 (Figure 51). The content of ascorbic acid was found to be unaffected by storage and dip treatment. Thus the microbial and nutritional quality of pomegranate arils with respect to its antioxidant activity, phenolic and flavonoid content and vitamin C status was maintained upon dip treatment and during entire storage study of 6 days.

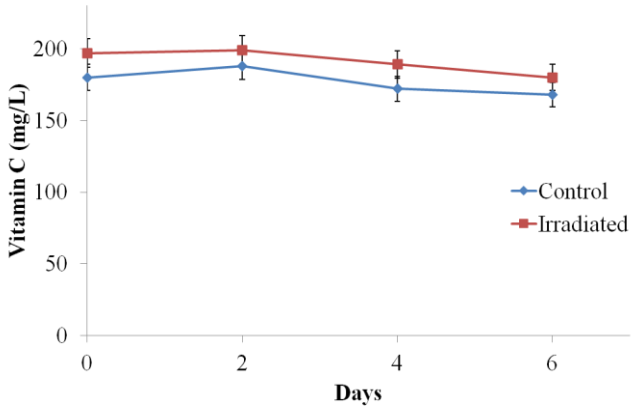

Figure 51: Effect of irradiation and storage on ascorbic acid content of pomegranate juice

Thus the efficacy of dip treatment of RTE pomegranate arils in aqueous GG solution containing grape pomace extract (0.5%) was clearly demonstrated for shelf life extension of arils up to 6 days.

4. Summary and Conclusions

Petroleum based packaging is a hazard to the environment owing to their non-biodegradability. Therefore attempt was made to develop GG based biodegradable film to counter the challenges of conventional film. Standardization of protocol for film formation was initially carried out. It was found that 1.5 g of GG, 0.6 g glycerol dissolved in 150 mL of distilled water and dried in glass plate (dimension 21 cm × 21 cm) at 80 °C for 8 h gave films with excellent mechanical properties. Purification of GG significantly improved film properties as compared to films prepared from unpurified GG. It was also observed that film formed from different viscosity grade GG had no effect on its mechanical and barrier properties. Further, moisture content as well as content of glycerol in film also influenced its percentage elongation. After optimization of film formation process effect of radiation treatment on the properties of GG film was investigated.

Radiation processing of GG resulted in decrease in molecular weight of GG as analyzed by Ostwald viscometer and gel permeation chromatography. No significant change was however, observed in mannose:galactose ratio of GG due to radiation processing. Irradiation of GG in powder form up to 500 Gy resulted in 32.6% increase in tensile strength of its films. SAXS studies demonstrated that partial ordering of the polymer chains at a low dose of 500 Gy resulted in an increase in tensile strength. At higher irradiation doses, a dose dependent decrease in tensile and puncture strength of films was observed. Films prepared from unirradiated GG and subjected to irradiation processing thereafter exhibited stability up to 25 kGy without significant loss in its mechanical and barrier properties. Thus, these films can be suitably employed for food irradiation

applications without loss of functionality. In conclusion, purification of GG combined with low dose irradiation can improve the mechanical properties of the films produced.

Further, nanocomposite films were prepared using GG incorporated with organically modified (cloisite 20A) and unmodified (nanofil 116) nanoclays for improved physical properties of film. Incorporation of either of the intercalated nanoclay up to 10% significantly improved the mechanical properties of nanocomposite as compared to the control films. Higher concentration of nanoclay (20%) resulted in sharp decline in mechanical properties due to formation of nanoclay clumps and cracks in the films. Nanofil 116 demonstrated better compatibility with GG as compared to closite 20A. Organic modification of cloisite 20A rendered it hydrophobic and incompatible with polar GG polymer. Irradiation of 2.5% nanofil 116 incorporated nanocomposite films resulted in increased Young's modulus due to radiation induced higher dispersion of clay in films up to 25 kGy. Further treatment at higher radiation doses resulted in a dose dependent decrease in mechanical properties of films because of radiation induced degradation. WVTR decreased significantly even on incorporation of small amount of nanoclay in GG based films due to increased tortuosity in path of water vapor diffusion through films. However, irradiation had no effect on WVTR of nano-composite films. Color co-ordinates of films significantly changed with incorporation of nanoclay. Nano composite films were darker, greener and yellower as compared to control. X-ray scattering analysis suggested that 0.56 nm and 1.35 nm increase in basal spacing of nanofil 116 and cloisite 20A, respectively, after 7 days of dispersion. This increase in basal spacing is responsible for intercalation of GG in interstitial spaces of nanoclays thus

resulting in better mechanical and water vapor barrier properties. FTIR analysis demonstrated no functional group transformation due to nanoclay incorporation or radiation processing. Thus the type and content of nanoclay incorporation during development of films had significant effect on the mechanical and barrier properties of GG based nano-composites.

Film prepared from 500 Gy irradiated GG powder demonstrated improved mechanical strength and nano-composite film having 2.5% of nanofil 116 also had excellent film properties. Interestingly film prepared from 500 Gy irradiated GG powder incorporated with 2.5% nanofil 116 showed poor film properties as compared to film prepared from control GG having 2.5% of nanofil 116. This might be due to radiation induced ordering of GG in nanometer scale which further interferes in intercalation of GG chains into nano scale basal spacing of nanofil 116. GG film incorporated with nanofil 116 demonstrated superior mechanical properties than closite 20A incorporated film.

An attempt was further made to develop film having properties comparable to commercial cling film. In this context mechanical and barrier properties of GG based films were improved by optimizing concentrations (w/w of GG) of various additives (beeswax (0-2.5%), tween 80 (0.5-1%), nanofil 116 (0-10%) and glycerol (0-40%)). A 5 level CCD was used for the optimization. Incorporation of beeswax (up to 1.25%) resulted in higher Young's modulus due to reduction in amount of water in films. At 0.63% of beeswax a significant reduction of WVTR of film was observed due to increased hydrophobicity as compared to film prepared without beeswax. Film having

0.63% of beeswax was as smooth and homogeneous as control GG film. However, at 1.25% of beeswax emulsion was visible and at 1.88% crystals formed. These crystals significantly reduced the mechanical and barrier properties of film. Tween 80 concentration dependent increase in tensile strength and percent elongation was observed as it aids in better compatibility between beeswax and polymeric film matrix. Higher content of emulsifier resulted in reduced tensile strength and Young's modulus of films. Up to 2.5% of nanoclay tensile strength and Young's modulus increases due to transfer of mechanical stress from polymeric chain to nanoclay sheets. Further increase in nanoclay concentration decreases the mechanical properties because of tactoid formation. Nanoclay also induces tortuous path in films which reduces the diffusion of water vapor through it. Glycerol concentration dependent increase in percent elongation and decrease in tensile strength, Young's modulus and WVTR was observed. Puncture strength was not affected by any additives. Optimized films demonstrated superior tensile strength and Young's modulus than cling film however WVTR of optimized film was 88.9 $g/m^2/d$ and that of cling film was 35 $g/m^2/d$. WVTR of GG based films further be reduced by incorporation of higher amount of beeswax.

An attempt was made to reduce the WVTR of the developed GG films to make it comparable with commercial cling films. In this regard beeswax irradiated at various doses was incorporated to determine its compatibility with GG. Effect of radiation on beeswax was also analyzed where in a dose dependent decrease in intrinsic viscosity of beeswax was observed at all doses. It was noted that the content of wax esters and alkenyl diacylglycerols decreased while that of, fatty alcohols and fatty acids increased with

radiation dose. Incorporation of control beeswax (0.5%) increased Young's modulus by 30% and decreased WVTR by 45% of GG films as compared to native GG films. Addition of control beeswax at higher concentration negatively affects the film properties. Loading of 1% of irradiated beeswax (50 kGy) improved Young's modulus by 80% and decreased WVTR by 58%. Thus it was demonstrated that a higher amount of beeswax could be added to in GG when the wax was irradiated thus improving film characteristics.

Optimization of concentration of additives such as irradiated beeswax (50 kGy), tween 80, nanofil 116 and glycerol at different concentrations was further attempted by RSM to improve the mechanical and barrier properties of GG based films. Optimized values obtained by RSM was 1.21% 50 kGy irradiated beeswax, 87.5% tween 80, 13.91% glycerol and nanofil 3.07%. Close agreement with the observed and predicted values and excellent mechanical and barrier properties of optimized film thus demonstrated the usefulness of RSM design for better film properties. However, optimized film still had 1.77 times higher WVTR than that of cling films. In order to further lower the WVTR thickness of optimized film was increased to 29 µm from 14 µm. This resulted in film having with WVTR of 39 ± 4 g/m^2/d that was comparable to cling film WVTR. However, the mechanical properties remain unaffected.

The film thus developed was further incorporated with grape pomace extract to convert it into active packaging. Being a wine industry waste, pomace is a cheap source of antimicrobial and antioxidants. It was observed that incorporation of pomace extract up to 5% (w/w of GG) resulted in no significant ($p < 0.05$) effect on the characteristics of RSM

optimized film. Furthermore films incorporated with pomace extract were stable up to a radiation dose of 5 kGy. Developed film (5% grape pomace extract w/w of GG) showed antimicrobial property against *S. aureus, S. typhimurium, E. coli and B. cereus*. Irradiation up to dose of 5 kGy did not affect antimicrobial property of the films. The developed active film was further applied for packaging of Ready to eat (RTE) pomegranate arils in order to extend its shelf life.

Shelf life of arils packed in active film was similar (4 days) to that of arils packed in cling film. However, 2kGy irradiated arils packed in active film had longer shelf life than that of arils packed in cling film at 10 °C. Microbial analysis showed 2 kGy irradiated arils packed in active film had shelf life of 12 days. This might be due to minimal chance of arils recontamination through active packaging than that of cling wrap. Sensory attributes were also acceptable for entire shelf life of minimally processed irradiated arils packed in active film. Irradiation along with storage and types of packaging used had no significant effect on antioxidant activity (DPPH and FRAP), total anthocyanins, phenolics, flavanoids and vitamin C content of pomegranate arils. Thus the efficacy of developed active film on extending the shelf life of minimally processed pomegranate arils over cling film by irradiation application was demonstrated here.

Aqueous GG based grape pomace extract containing edible coating was developed for shelf life extension of pomegranate arils. Microbial analysis showed 0.5% of extract containing GG solution increased the shelf life of arils up to 6 days. Sensory attributes of dip treated arils were acceptable during entire storage period. Edible coating also resulted

in no change in headspace gaseous composition of packed trays. Dip treatment along with storage had no significant effect on antioxidant activity (DPPH and FRAP), total anthocyanins, phenolics, flavanoids and vitamin C content of pomegranate juice. Thus the suitability of dip solution containing GG and grape pomace extract for extending the shelf life of pomegranate arils was successfully demonstrated.

Developed active standalone film had better mechanical strength and comparable WVTR to commercially available cling films. Effectiveness of active film for increasing the shelf life of pomegranate arils as compared to PVC based film was also demonstrated here. It is of future interest to evaluate the economic viability of developed film in comparison to currently available petroleum based commercial film for food packaging applications.

5. References

1. Cha, D. S., & Chinnan, M. S. (2004). Biopolymer-based antimicrobial packaging: a review. *Critical Reviews in Food Science and Nutrition*, 44(4), 223-237.

2. Kang, H. J., & Min, S. C. (2010). Potato peel-based biopolymer film development using high-pressure homogenization, irradiation, and ultrasound. *LWT-Food Science and Technology*, 43(6), 903-909.

3. Petersson, L., & Oksman, K. (2006). Biopolymer based nanocomposites: comparing layered silicates and microcrystalline cellulose as nanoreinforcement. *Composites Science and Technology*, 66(13), 2187-2196.

4. Kang, H. J., Jo, C., Lee, N. Y., Kwon, J. H., & Byun, M. W. (2005). A combination of gamma irradiation and $CaCl_2$ immersion for a pectin-based biodegradable film. *Carbohydrate Polymers*, 60(4), 547-551.

5. Avella, M., De Vlieger, J. J., Errico, M. E., Fischer, S., Vacca, P., & Volpe, M. G. (2005). Biodegradable starch/clay nanocomposite films for food packaging applications. *Food Chemistry*, 93(3), 467-474.

6. Soazo, M., Rubiolo, A. C., & Verdini, R. A. (2011). Effect of drying temperature and beeswax content on physical properties of whey protein emulsion films. *Food Hydrocolloids*, 25(5), 1251-1255.

7. Andrady, A. L., & Neal, M. A. (2009). Applications and societal benefits of plastics. *Philosophical Transactions of the Royal Society B: Biological Sciences*, 364(1526), 1977-1984.

8. Marsh, K., & Bugusu, B. (2007). Food packaging—roles, materials, and environmental issues. *Journal of Food Science*, 72(3), R39-R55.

9. Mody, A. S. (2000). Biodegradable polymer. *Popular Plastics and Packaging*, 12, 89-91.

10. Rhim, J. W., & Ng, P. K. (2007). Natural biopolymer-based nanocomposite films for packaging applications. *Critical Reviews in Food Science and Nutrition*, 47(4), 411-433.

11. *http://www.foodsafetynews.com/2014/07/study-175-hazardous-chemicals-legally-used-to-produce-food-packaging/#.VFJP8PmUdvI*

12. Harish Prashanth, K. V., & Tharanathan, R. N. (2007). Chitin/chitosan: modifications and their unlimited application potential—an overview. *Trends in Food Science & Technology*, 18(3), 117-131.

13. Gabor, D., & Tita, O. (2012). Biopolymers Used in Food Packaging: A. *Acta Universitatis Cibiniensis Series E: Food Technology*, 16(2), 3.

14. Hernandez-Izquierdo, V. M., & Krochta, J. M. (2008). Thermoplastic processing of proteins for film formation—a review. *Journal of Food Science*, 73(2), R30-R39.

15. Baldwin, E. A., Nisperos-Carriedo, M. O., & Baker, R. A. (1995). Use of edible coatings to preserve quality of lightly (and slightly) processed products. *Critical Reviews in Food Science & Nutrition*, 35(6), 509-524.

16. Krochta, J.M., Baldwin, E.A., & Nisperos-Carriedo, M. (1994). Edible coating and films to improve food quality. *Lancaster, USA: Technomic Publishing Company*, (379 p).

17. Zhang, H., & Mittal, G. (2010). Biodegradable protein-based films from plant resources: A review. *Environmental Progress & Sustainable Energy*, 29(2), 203-220.

18. Rhim, J. W., Gennadios, A., Weller, C. L., & Hanna, M. A. (2002). Sodium dodecyl sulfate treatment improves properties of cast films from soy protein isolate. *Industrial Crops and Products*, 15(3), 199-205.

19. Rhim, J. W., Mohanty, K. A., Singh, S. P., & Ng, P. K. (2006). Preparation and properties of biodegradable multilayer films based on soy protein isolate and poly (lactide). *Industrial & Engineering Chemistry Research*, 45(9), 3059-3066.

20. Mariniello, L., Di Pierro, P., Esposito, C., Sorrentino, A., Masi, P., & Porta, R. (2003). Preparation and mechanical properties of edible pectin–soy flour films obtained in the absence or presence of transglutaminase. *Journal of Biotechnology*, 102(2), 191-198.

21. Hernández-Muñoz, P., Villalobos, R., & Chiralt, A. (2004). Effect of thermal treatments on functional properties of edible films made from wheat gluten fractions. *Food Hydrocolloids*, 18(4), 647-654.

22. Micard, V., Belamri, R., Morel, M. H., & Guilbert, S. (2000). Properties of chemically and physically treated wheat gluten films. *Journal of Agricultural and Food Chemistry*, 48(7), 2948-2953.

23. Lee, S. L., Lee, M. S., & Song, K. B. (2005). Effect of gamma-irradiation on the physicochemical properties of gluten films. *Food Chemistry*, 92(4), 621-625.

24. Lens, J. P., De Graaf, L. A., Stevels, W. M., Dietz, C. H. J. T., Verhelst, K. C. S., Vereijken, J. M., & Kolster, P. (2003). Influence of processing and storage conditions on the mechanical and barrier properties of films cast from aqueous wheat gluten dispersions. *Industrial Crops and Products*, 17(2), 119-130.

25. Kim, S., Sessa, D. J., & Lawton, J. W. (2004). Characterization of zein modified with a mild cross-linking agent. *Industrial Crops and Products*, 20(3), 291-300.

26. Rhim, J. W., Gennadios, A., Fu, D., Weller, C. L., & Hanna, M. A. (1999). Properties of ultraviolet irradiated protein films. *LWT-Food Science and Technology*, 32(3), 129-133.

27. Wang, Y., Xiong, Y. L., Rentfrow, G. K., & Newman, M. C. (2013). Oxidation promotes cross-linking but impairs film-forming properties of whey proteins. *Journal of Food Engineering*, 115(1), 11-19.

28. Ramos, Ó. L., Silva, S. I., Soares, J. C., Fernandes, J. C., Poças, M. F., Pintado, M. E., & Malcata, F. X. (2012). Features and performance of edible films, obtained from whey protein isolate formulated with antimicrobial compounds. *Food Research International*, 45(1), 351-361.

29. Popović, S., Peričin, D., Vaštag, Ž., Lazić, V., & Popović, L. (2012). Pumpkin oil cake protein isolate films as potential gas barrier coating. *Journal of Food Engineering*, 110(3), 374-379.

30. Gómez-Guillén, M. C., Giménez, B., López-Caballero, M. A., & Montero, M. P. (2011). Functional and bioactive properties of collagen and gelatin from alternative sources: A review. *Food Hydrocolloids*, 25(8), 1813-1827.

31. Denavi, G. A., Pérez-Mateos, M., Añón, M. C., Montero, P., Mauri, A. N., & Gómez-Guillén, M. C. (2009). Structural and functional properties of soy protein isolate and cod gelatin blend films. *Food Hydrocolloids*, 23(8), 2094-2101.

32. Li, B., Kennedy, J. F., Jiang, Q. G., & Xie, B. J. (2006). Quick dissolvable, edible and heatsealable blend films based on konjac glucomannan–Gelatin. *Food Research International*, 39(5), 544-549.

33. Arvanitoyannis, I. S., Nakayama, A., & Aiba, S. I. (1998). Chitosan and gelatin based edible films: state diagrams, mechanical and permeation properties. *Carbohydrate Polymers*, 37(4), 371-382.

34. Andreuccetti, C., Carvalho, R. A., & Grosso, C. R. (2009). Effect of hydrophobic plasticizers on functional properties of gelatin-based films. *Food Research International*, 42(8), 1113-1121.

35. Haroun, A. A., Beherei, H. H., & El-Ghaffar, M. A. (2010). Preparation, characterization, and in vitro application of composite films based on gelatin and collagen from natural resources. *Journal of Applied Polymer Science*, 116(4), 2083-2094.

36. Bigi, A., Cojazzi, G., Panzavolta, S., Rubini, K., & Roveri, N. (2001). Mechanical and thermal properties of gelatin films at different degrees of glutaraldehyde crosslinking. *Biomaterials*, 22(8), 763-768.

37. De Carvalho, A. J. F., Curvelo, A. A. S., & Agnelli, J. A. M. (2001). A first insight on composites of thermoplastic starch and kaolin. *Carbohydrate Polymers*, 45(2), 189-194.

38. Tharanathan, R. N. (2003). Biodegradable films and composite coatings: past, present and future. *Trends in Food Science & Technology*, 14(3), 71-78.

39. Fishman, M.L., Friedman, R. B., & Huang, S.J. (Eds.) (1994). Polymers from agricultural coproducts. *ACS Symposium Series 575*. Washington, DC: American Chemical Society.

40. Fernandez-Saiz, P., Lagaron, J. M., Hernandez-Muñoz, P., & Ocio, M. J. (2008). Characterization of antimicrobial properties on the growth of *S. aureus* of novel renewable blends of gliadins and chitosan of interest in food packaging and coating applications. *International Journal of Food Microbiology*, 124(1), 13-20.

41. Kester, J. J., & Fennema, O. (1986). Edible films and coatings: A review. *J. Food Sci*., 40, 47-59.

42. Labuza, T. P., & Breene, W. M. (1989). Applications of "active packaging" for improvement of shelf-life and nutritional quality of fresh and extended shelf-life foods 1. *Journal of Food Processing and Preservation*, 13(1), 1-69.

43. Davis, D. H., Elson, C. M., & Hayes, E. R. (1989). N,O-Carboxylmethyl chitosan. A new water soluble chitin derivative. In. Chitin–chitosan. *Elsevier Applied Science, London, UK*, pp. 467-472.

44. Sittikijyothin, W., Torres, D., & Gonçalves, M. P. (2005). Modelling the rheological behaviour of galactomannan aqueous solutions. *Carbohydrate Polymers*, 59(3), 339-350.

45. Aydinli, M., & Tutas, M. (2000). Water sorption and water vapour permeability properties of polysaccharide (locust bean gum) based edible films. *LWT-Food Science and Technology*, 33(1), 63-67.

46. Aydinli, M., Tutas, M., & Bozdemir, O. A. (2004). Mechanical and light transmittance properties of locust bean gum based edible films. *Turkish Journal of Chemistry*, 28(3), 163-172.

47. Bozdemir, O. A., Tutas, M. (2003). Plasticiser effect on water vapour permeability properties of locust bean gum-based edible films. *Turkish Journal of Chemistry*, 27, 773–782.

48. Yadav, H. (2013). Guar Industry Outlook 2015 – NIAM *ccsniam.gov.in/GUAR_Booklet_03122013.pdf*.

49. Das, D., Ara, T., Dutta, S., & Mukherjee, A. (2011). New water resistant biomaterial biocide film based on guar gum. *Bioresource Technology*, 102(10), 5878-5883.

50. Mikkonen, K. S., Rita, H., Helén, H., Talja, R. A., Hyvönen, L., & Tenkanen, M. (2007). Effect of polysaccharide structure on mechanical and thermal properties of galactomannan-based films. *Biomacromolecules*, 8(10), 3198-3205.

51. Rao, M. S., Kanatt, S. R., Chawla, S. P., & Sharma, A. (2010). Chitosan and guar gum composite films: Preparation, physical, mechanical and antimicrobial properties. *Carbohydrate Polymers*, 82(4), 1243-1247.

52. Chen, S., & Nussinovitch, A. (2001). Permeability and roughness determinations of wax-hydrocolloid coatings, and their limitations in determining citrus fruit overall quality. *Food Hydrocolloids*, 15(2), 127-137.

53. Scott, G. (2000). 'Green'polymers. *Polymer degradation and stability*, 68(1), 1-7.

54. Debeaufort, F., Quezada-Gallo, J. A., & Voilley, A. (1998). Edible films and coatings: tomorrow's packagings: a review. *Critical Reviews in Food Science*, 38(4), 299-313.

55. Krochta, J. M., & De Mulder-Johnston, C. (1997). Edible and biodegradable polymer films: Challenges and opportunities. *Food Technology*, 51(2), 61–74.

56. Xiao, L., Wang, B., Yang, G., & Gauthier, M. (2012). Poly (Lactic Acid)-Based Biomaterials: Synthesis, Modification and Applications. *Biomedical Science, Engineering and Technology*, 11.

57. Sorrentino, A., Gorrasi, G., & Vittoria, V. (2007). Potential perspectives of bio-nanocomposites for food packaging applications. *Trends in Food Science & Technology*, 18(2), 84-95.

58. Damodaran, S. (1996). Amino acids, peptides, and proteins. *Food Science And Technology-New York-Marcel Dekker-*, 321-430.

59. Perez-gago, M. B., & Krochta, J. M. (2001). Denaturation time and temperature effects on solubility, tensile properties, and oxygen permeability of whey protein edible films. *Journal of Food Science*, 66(5), 705-710.

60. Liu, C. C., Tellez-Garay, A. M., & Castell-Perez, M. E. (2004). Physical and mechanical properties of peanut protein films. *LWT-Food Science and Technology*, 37(7), 731-738.

61. Pérez-Gago, M. B., Nadaud, P., & Krochta, J. M. (1999). Water Vapor Permeability, Solubility, and Tensile Properties of Heat-denatured versus Native Whey Protein Films. *Journal of Food Science*, 64(6), 1034-1037.

62. Kristo, E., Biliaderis, C. G., & Zampraka, A. (2007). Water vapour barrier and tensile properties of composite caseinate-pullulan films: Biopolymer composition effects and impact of beeswax lamination. *Food Chemistry*, 101(2), 753-764.

63. Liu, L., Liu, L., Liu, C. K., Fishman, M. L., & Hicks, K. B. (2007). Composite films from pectin and fish skin gelatin or soybean flour protein. *Journal of Agricultural and Food Chemistry*, 55(6), 2349-2355.

64. Lee, K. Y., Shim, J., & Lee, H. G. (2004). Mechanical properties of gellan and gelatin composite films. *Carbohydrate Polymers*, 56(2), 251-254.

65. Wang, L., Auty, M. A., & Kerry, J. P. (2010). Physical assessment of composite biodegradable films manufactured using whey protein isolate, gelatin and sodium alginate. *Journal of Food Engineering*, 96(2), 199-207.

66. Brandenburg, A. H., Weller, C. L., & Testin, R. F. (1993). Edible films and coatings from soy protein. *Journal of Food Science*, 58(5), 1086-1089.

67. Ustunol, Z., & Mert, B. (2004). Water Solubility, Mechanical, Barrier, and Thermal Properties of Cross-linked Whey Protein Isolate-based Films. *Journal of Food Science*, 69(3), FEP129-FEP133.

68. Avena-Bustillos, R. J., & Krochta, J. M. (1993). Water Vapor Permeability of Caseinate-Based Edible Films as Affected by pH, Calcium Crosslinking and Lipid Content. *Journal of Food Science*, 58(4), 904-907.

69. Arvanitoyannis, I. S., Stratakos, A. C., & Tsarouhas, P. (2009). Irradiation applications in vegetables and fruits: a review. *Critical Reviews in Food Science and Nutrition*, 49(5), 427-462.

70. Ikeda, N. (1976). Wholesomeness of irradiated foods.

71. Foods, I. (1989). Facts about Food Irradiation. *International Atomic Energy Agency.*

72. Niemira, B. A., & Fan, X. (2006). Low-dose irradiation of fresh and fresh-cut produce: safety, sensory and shelf life. *Food Irradiation Research and Technology*, 169-181.

73. Stoffers, N. H., Linssen, J. P., Franz, R., & Welle, F. (2004). Migration and sensory evaluation of irradiated polymers. *Radiation Physics and Chemistry*, 71(1), 205-208.

74. *http://www.fda.gov/Food/IngredientsPackagingLabeling/IrradiatedFoodPackaging/ucm081399.htm*.

75. Gennadios, A., Rhim, J. W., Handa, A., Weller, C. L., & Hanna, M. A. (1998). Ultraviolet radiation affects physical and molecular properties of soy protein films. *Journal of Food Science*, 63(2), 225-228.

76. Hwang, I. T., Jung, C. H., Kuk, I. S., Choi, J. H., & Nho, Y. C. (2010). Electron beam-induced crosslinking of poly (butylene adipate-co-terephthalate). *Nuclear Instruments and Methods in Physics Research Section B: Beam Interactions with Materials and Atoms*, 268(21), 3386-3389.

77. Kyung Kim, J., Jo, C., Jin Park, H., & Woo Byun, M. (2008). Effect of gamma irradiation on the physicochemical properties of a starch-based film. *Food Hydrocolloids*, 22(2), 248-254.

78. Sabato, S. F., Ouattara, B., Yu, H., D'aprano, G., Le Tien, C., Mateescu, M. A., & Lacroix, M. (2001). Mechanical and barrier properties of cross-linked soy and whey protein based films. *Journal of Agricultural and Food Chemistry*, 49(3), 1397-1403.

79. Schwartz, B. J. (2003). Conjugated polymers as molecular materials: How chain conformation and film morphology influence energy transfer and interchain interactions. *Annual Review of Physical Chemistry*, 54(1), 141-172.

80. Winokur, M. J., Skotheim, T. A., Elsenbaumer, R. L., & Reynolds, J. R. (1998). Handbook of conducting polymers. *New York, USA: Dekker*, 2nd edition, 707.

81. Vieira, M. G. A., da Silva, M. A., dos Santos, L. O., & Beppu, M. M. (2011). Natural-based plasticizers and biopolymer films: A review. *European Polymer Journal*, 47(3), 254-263.

82. Choi, J. S., & Park, W. H. (2004). Effect of biodegradable plasticizers on thermal and mechanical properties of poly (3-hydroxybutyrate). *Polymer testing*, 23(4), 455-460.

83. Cheng, L. H., Karim, A. A., & Seow, C. C. (2006). Effects of water-glycerol and water-sorbitol interactions on the physical properties of konjac glucomannan films. *Journal of Food Science*, 71(2), E62-E67.

84. Karbowiak, T., Hervet, H., Léger, L., Champion, D., Debeaufort, F., & Voilley, A. (2006). Effect of plasticizers (water and glycerol) on the diffusion of a small molecule in iota-carrageenan biopolymer films for edible coating application. *Biomacromolecules*, 7(6), 2011-2019.

85. Carvalho, R. A., Grosso, C. R. F., & Sobral, P. J. A. (2008). Effect of chemical treatment on the mechanical properties, water vapour permeability and sorption isotherms of gelatin-based films. *Packaging Technology and Science*, 21(3), 165-169.

86. Zhang, Y., & Han, J. H. (2006). Mechanical and thermal characteristics of pea starch films plasticized with monosaccharides and polyols. *Journal of food science*, 71(2), E109-E118.

87. Kristo, E., & Biliaderis, C. G. (2006). Water sorption and thermo-mechanical properties of water/sorbitol-plasticized composite biopolymer films: Caseinate–pullulan bilayers and blends. *Food Hydrocolloids*, 20(7), 1057-1071.

88. Bergo, P. V. A., Carvalho, R. A., Sobral, P. J. A., Dos Santos, R. M. C., Da Silva, F. B. R., Prison, J. M., ... & Habitante, A. M. Q. B. (2008). Physical properties of edible films based on cassava starch as affected by the plasticizer concentration. *Packaging Technology and Science*, 21(2), 85-89.

89. Suyatma, N. E., Tighzert, L., Copinet, A., & Coma, V. (2005). Effects of hydrophilic plasticizers on mechanical, thermal, and surface properties of chitosan films. *Journal of Agricultural and Food Chemistry*, 53(10), 3950-3957.

90. Bradley, E. L., Castle, L., & Chaudhry, Q. (2011). Applications of nanomaterials in food packaging with a consideration of opportunities for developing countries. *Trends in Food Science & Technology*, 22(11), 604-610.

91. Arora, A., & Padua, G. W. (2010). Review: nanocomposites in food packaging. *Journal of Food Science*, 75(1), R43-R49.

92. Sinha Ray, S., & Okamoto, M. (2003). Polymer/layered silicate nanocomposites: a review from preparation to processing. *Progress in Polymer Science*, 28(11), 1539-1641.

93. Pandey, P. (2013). Moving Forward Responsibly: Agribiotechnology to Agrinanotechnology in India. *Asian Biotechnology and Development Review*, 15(5), 81-101.

94. Lagaly, G. (1999). Introduction: from clay mineral-polymer interactions to clay mineral-polymer nanocomposites. *Applied Clay Science*, 15(1), 1–9.

95. McGlashan, S. A., & Halley, P. J. (2003). Preparation and characterisation of biodegradable starch-based nanocomposite materials. *Polymer International*, 52(11), 1767-1773.

96. Alavi, S., Thomas, S., Sandeep, K. P., Kalarikkal, N., Varghese, J., & Yaragalla, S. (Eds.). (2014). Polymers for Packaging Applications. *CRC Press*.

97. Pandey, J. K., Raghunatha Reddy, K., Pratheep Kumar, A., & Singh, R. P. (2005). An overview on the degradability of polymer nanocomposites. *Polymer Degradation and Stability*, 88(2), 234-250.

98. Almasi, H., Ghanbarzadeh, B., & Entezami, A. A. (2010). Physicochemical properties of starch–CMC–nanoclay biodegradable films. *International Journal of Biological Macromolecules*, 46(1), 1-5.

99. Gontard, N., Marchesseau, S., CUQ, J. L., & Guilbert, S. (1995). Water vapour permeability of edible bilayer films of wheat gluten and lipids. *International Journal of Food Science & Technology*, 30(1), 49-56.

100. Krochta, J. M. (2002). Proteins as raw materials for films and coatings: definitions, current status, and opportunities. *Protein-Based Films and Coatings*, 1-41.

101. Massoudi, R. (2009). Frequent use of certain candles produces unwanted chemicals. *http://www.scsu.edu/news_article.aspx?news_id=832*.

102. Lin, D., & Zhao, Y. (2007). Innovations in the development and application of edible coatings for fresh and minimally processed fruits and vegetables. *Comprehensive Reviews in Food Science and Food Safety*, 6(3), 60-75.

103. Soazo, M., Rubiolo, A. C., & Verdini, R. A. (2011). Effect of drying temperature and beeswax content on physical properties of whey protein emulsion films. *Food Hydrocolloids*, 25(5), 1251-1255.

104. Monedero, F. M., Fabra, M. J., Talens, P., & Chiralt, A. (2009). Effect of oleic acid–beeswax mixtures on mechanical, optical and water barrier properties of soy protein isolate based films. *Journal of Food Engineering*, 91(4), 509-515.

105. Han, J. H., Seo, G. H., Park, I. M., Kim, G. N., & Lee, D. S. (2006). Physical and mechanical properties of pea starch edible films containing beeswax emulsions. *Journal of Food Science*, 71(6), E290-E296.

106. Debeaufort, F., Martin-Polo, M., & Voilley, A. (1993). Polarity homogeneity and structure affect water vapor permeability of model edible films. *Journal of Food Science*, 58(2), 426-429.

107. Cheng, L. H., Abd Karim, A., & Seow, C. C. (2008). Characterisation of composite films made of konjac glucomannan (KGM), carboxymethyl cellulose (CMC) and lipid. *Food Chemistry*, 107(1), 411-418.

108. Debeaufort, F., & Voilley, A. (1995). Effect of surfactants and drying rate on barrier properties of emulsified edible films. *International Journal of Food Science & Technology*, 30(2), 183-190.

109. Maran, J. P., Sivakumar, V., Sridhar, R., & Thirugnanasambandham, K. (2013). Development of model for barrier and optical properties of tapioca starch based edible films. *Carbohydrate Polymers*, 92(2), 1335-1347.

110. Brandelero, R. P. H., Yamashita, F., & Grossmann, M. V. E. (2010). The effect of surfactant Tween 80 on the hydrophilicity, water vapor permeation, and the mechanical properties of cassava starch and poly (butylene adipate-co-terephthalate)(PBAT) blend films. *Carbohydrate Polymers*, 82(4), 1102-1109.

111. Brandelero, R. P. H., Grossmann, M. V., & Yamashita, F. (2012). Films of starch and poly (butylene adipate co-terephthalate) added of soybean oil (SO) and Tween 80. *Carbohydrate Polymers*, 90(4), 1452-1460.

112. Muscat, D., Adhikari, R., McKnight, S., Guo, Q., & Adhikari, B. (2013). The physicochemical characteristics and hydrophobicity of high amylose starch–glycerol films in the presence of three natural waxes. *Journal of Food Engineering*, 119(2), 205-219.

113. Andreuccetti, C., Carvalho, R. A., Galicia-García, T., Martínez-Bustos, F., & Grosso, C. R. (2011). Effect of surfactants on the functional properties of gelatin-based edible films. *Journal of Food Engineering*, 103(2), 129-136.

114. Peng, Y., Yin, L., & Li, Y. (2013). Combined effects of lemon essential oil and surfactants on physical and structural properties of chitosan films. *International Journal of Food Science & Technology*, 48(1), 44-50.

115. Rodríguez, M., Oses, J., Ziani, K., & Mate, J. I. (2006). Combined effect of plasticizers and surfactants on the physical properties of starch based edible films. *Food Research International*, 39(8), 840-846.

116. Chen, C. H., Kuo, W. S., & Lai, L. S. (2009). Effect of surfactants on water barrier and physical properties of tapioca starch/decolorized hsian-tsao leaf gum films. *Food Hydrocolloids*, 23(3), 714-721.

117. Chambi, H., & Grosso, G. (2011). Production and characterization of multicomponent films based on polysaccharides, gelatin and lipids: Effect of surfactants addition. *International Congress on Engineering and Food*, 11th conference.

118. Chao, Z., Yue, M., Xiaoyan, Z., & Dan, M. (2010). Development of Soybean Protein-Isolate Edible Films Incorporated with Beeswax, Span 20, and Glycerol. *Journal of Food Science*, 75(6), C493-C497.

119. Appendini, P., & Hotchkiss, J. H. (2002). Review of antimicrobial food packaging. *Innovative Food Science & Emerging Technologies*, 3(2), 113-126.

120. FAO Database (2012) at *http://faostat.fao. org*.

121. Sanhueza, L., Tello, M., Vivanco, M., Mendoza, L., & Wilkens, M. (2014). Relation between antibacterial activity against food transmitted pathogens and total phenolic compounds in grape pomace extracts from cabernet sauvignon and syrah varieties. *Advances in Microbiology*, 2014.

122. Lu, Y., & Yeap Foo, L. (1999). The polyphenol constituents of grape pomace. *Food Chemistry*, 65(1), 1-8.

123. Frankel, E. N. (1999). Food antioxidants and phytochemicals: present and future perspectives. *Lipid/Fett*, 101(12), 450-455.

124. Katsube, N., Iwashita, K., Tsushida, T., Yamaki, K., & Kobori, M. (2003). Induction of apoptosis in cancer cells by bilberry (Vaccinium myrtillus) and the anthocyanins. *Journal of Agricultural and Food Chemistry*, 51(1), 68-75.

125. Deng, Q., & Zhao, Y. (2011). Physicochemical, nutritional, and antimicrobial properties of wine grape (Cv. Merlot) pomace extract-based films. *Journal of food science*, 76(3), E309-E317.

126. Corrales, M., Han, J. H., & Tauscher, B. (2009). Antimicrobial properties of grape seed extracts and their effectiveness after incorporation into pea starch films. *International Journal of Food Science & Technology*, 44(2), 425-433.

127. Cerruti, P., Santagata, G., Gomez d'Ayala, G., Ambrogi, V., Carfagna, C., Malinconico, M., & Persico, P. (2011). Effect of a natural polyphenolic extract on the

properties of a biodegradable starch-based polymer. *Polymer Degradation and Stability*, 96(5), 839-846.

128. Deng, Q. (2011). Chemical composition of dietary fiber and polyphenols of wine grape pomace skins and development of wine grape (cv. Merlot) pomace extract based films.

129. Hunter, J. S. (1959). Determination of optimum operating conditions by experimental methods. *Industrial Quality Control*, 15, 6–12.

130. Li, Y. X., Peng, J., Lui, W. B., & Lin, J. (2009). Effects of glycerol and ethylene–acrylic acid on composition optimization of PVOH/starch-blended biodegradable resin using response surface methodology. *Journal of Applied Polymer Science*, 114(5), 2915-2921.

131. Rafieian, F., Shahedi, M., Keramat, J., & Simonsen, J. (2014). Thermomechanical and Morphological Properties of Nanocomposite Films from Wheat Gluten Matrix and Cellulose Nanofibrils. *Journal of Food Science*, 79(1), N100-N107.

132. Espitia, P. J. P., Soares, N. D. F. F., Teófilo, R. F., Coimbra, J. S. D. R., Vitor, D. M., Batista, R. A., ... & Medeiros, E. A. A. (2013). Physical–mechanical and antimicrobial properties of nanocomposite films with pediocin and ZnO nanoparticles. *Carbohydrate Polymers*, 94(1), 199-208.

133. Srinivasa, P. C., Ravi, R., & Tharanathan, R. N. (2007). Effect of storage conditions on the tensile properties of eco-friendly chitosan films by response surface methodology. *Journal of Food Engineering*, 80(1), 184-189.

134. Wang, L., Liu, L., Holmes, J., Huang, J., Kerry, J. F., & Kerry, J. P. (2008). Effect of pH and addition of corn oil on the properties of whey protein isolate-based films using response surface methodology. *International Journal of Food Science & Technology*, 43(5), 787-796.

135. Chen, Y. D., Peng, J., & Lui, W. B. (2009). Composition optimization of poly (vinyl alcohol)-/cornstarch-blended biodegradable composite using response surface methodology. *Journal of Applied Polymer Science*, 113(1), 258-264.

136. Schmidt, V. C. R., Porto, L. M., Laurindo, J. B., & Menegalli, F. C. (2013). Water vapor barrier and mechanical properties of starch films containing stearic acid. *Industrial Crops and Products*, 41, 227-234.

137. Chillo, S., Flores, S., Mastromatteo, M., Conte, A., Gerschenson, L., & Del Nobile, M. A. (2008). Influence of glycerol and chitosan on tapioca starch-based edible film properties. *Journal of Food Engineering*, 88(2), 159-168.

138. Denavi, G., Tapia-Blácido, D. R., Añón, M. C., Sobral, P. J. A., Mauri, A. N., & Menegalli, F. C. (2009). Effects of drying conditions on some physical properties of soy protein films. *Journal of Food Engineering*, 90(3), 341-349.

139. Guilbert, S., Gontard, N., & Gorris, L. G. (1996). Prolongation of the shelf-life of perishable food products using biodegradable films and coatings. *LWT-Food Science and Technology*, 29(1), 10-17.

140. Dhall, R. K. (2013). Advances in edible coatings for fresh fruits and vegetables: a review. *Critical reviews in Food Science and Nutrition*, 53(5), 435-450.

141. Chandra, R., Babu, K. D., Jadhav, V. T., & Teixeira da Silva, J. A. (2010). Origin, History and Domestication of Pomegranate. *Fruit, Vegetable and Cereal Science and Biotechnology*, 4 (Special Issue 2), 1-6.

142. Gil, M. I., Martínez, J. A., & Artés, F. (1996). Minimally processed pomegranate seeds. *LWT-Food Science and Technology*, 29(8), 708-713.

143. Martínez-Romero, D., Castillo, S., Guillén, F., Díaz-Mula, H. M., Zapata, P. J., Valero, D., & Serrano, M. (2013). *Aloe vera* gel coating maintains quality and safety of ready-to-eat pomegranate arils. *Postharvest Biology and Technology*, 86, 107-112.

144. Ghasemnezhad, M., Zareh, S., Rassa, M., & Sajedi, R. H. (2013). Effect of chitosan coating on maintenance of aril quality, microbial population and PPO activity of pomegranate (Punica granatum L. cv. Tarom) at cold storage temperature. *Journal of the Science of Food and Agriculture*, 93(2), 368-374.

145. Oz, A. T., & Ulukanli, Z. (2012). Application of edible starch-based coating including glycerol plus oleum nigella on arils from long-stored whole pomegranate fruits. *Journal of Food Processing and Preservation*, 36(1), 81-95.

146. Salama, M. I., Ayaad, H. M., Aboul-Anean, H. E., & Fahmy, H. M. (2012). Effect of edible coating as a carrier of essential oils and ultraviolet light (UV-C) on improving quality of minimally processed Manfalouty pomegranate. *Research Journal of Agriculture & Biological Sciences,* 8(2), 315-324.

147. Ergun, M., & Ergun, N. (2009). Maintaining quality of minimally processed pomegranate arils by honey treatments. *British Food Journal*, 111(4), 396-406.

148. Vega, M. P., Lima, E. L., & Pinto, J. C. (2001). In-line monitoring of weight average molecular weight in solution polymerizations using intrinsic viscosity measurements. *Polymer*, 42(8), 3909-3914.

149. Beer, M. U., Wood, P. J., & Weisz, J. (1999). A simple and rapid method for evaluation of Mark–Houwink–Sakurada constants of linear random coil polysaccharides using molecular weight and intrinsic viscosity determined by high performance size exclusion chromatography: application to guar galactomannan. *Carbohydrate Polymers*, 39(4), 377-380.

150. Kasai, N., & Kakudo, M. (2005). X-ray diffraction by macromolecules. *Springer*, 80, 504.

151. Gunstone, F. D., Harwood, J. L., & Padley, F. B. (1994). The Lipid Handbook. *CRC Press*, 2nd edition, 234.

152. Jacobson, J. L. (2006). Introduction to wine laboratory practices and procedures. *New York: Springer,* chapter-6.

153. Paixão, N., Perestrelo, R., Marques, J. C., & Câmara, J. S. (2007). Relationship between antioxidant capacity and total phenolic content of red, rosé and white wines. *Food Chemistry*, 105(1), 204-214.

154. Luximon-Ramma, A., Bahorun, T., Soobrattee, M. A., & Aruoma, O. I. (2002). Antioxidant activities of phenolic, proanthocyanidin, and flavonoid components in extracts of Cassia fistula. *Journal of Agricultural and Food Chemistry*, 50(18), 5042-5047.

155. Garrido, J., & Borges, F. (2011). Wine and grape polyphenols—A chemical perspective. *Food Research International*, 44(10), 3134-3148.

156. Association of Official Analytical Chemists (AOAC). (1990). Official Methods of Analysis, *Arlington, VA,* 15th edition.

157. Chien, P. J., Sheu, F., & Yang, F. H. (2007). Effects of edible chitosan coating on quality and shelf life of sliced mango fruit. *Journal of Food Engineering*, 78(1), 225-229.

158. Saroj, S. D., Shashidhar, R., Pandey, M., Dhokane, V., Hajare, S., Sharma, A., & Bandekar, J. R. (2006). Effectiveness of radiation processing in elimination of Salmonella Typhimurium and Listeria monocytogenes from sprouts. *Journal of Food Protection®*, 69(8), 1858-1864.

159. López-Rubira, V., Conesa, A., Allende, A., & Artés, F. (2005). Shelf life and overall quality of minimally processed pomegranate arils modified atmosphere packaged and treated with UV-C. *Postharvest Biology and Technology*, 37(2), 174-185.

160. Ayhan, Z., & Eştürk, O. (2009). Overall quality and shelf life of minimally processed and modified atmosphere packaged "Ready-to-Eat" pomegranate arils. *Journal of food science*, 74(5), C399-C405.

161. Cunha, P. L., Paula, R., & Feitosa, J. (2007). Purification of guar gum for biological applications. *International Journal of Biological Macromolecules*, 41(3), 324-331.

162. Handa, A., Gennadios, A., Froning, G. W., Kuroda, N., & Hanna, M. A. (1999). Tensile, solubility, and electrophoretic properties of egg white films as affected by surface sulfhydryl groups. *Journal of Food Science*, 64(1), 82-85.

163. Caner, C., Vergano, P. J., & Wiles, J. L. (1998). Chitosan film mechanical and permeation properties as affected by acid, plasticizer, and storage. *Journal of Food Science*, 63(6), 1049-1053.

164. Rachtanapun, P., & Wongchaiya, P. (2012). Effect of relative humidity on mechanical properties of blended chitosan-methylcellulose film. *Chiang Mai Journal of Science*, 39(1), 133-137.

165. Carvalho, O. T., Avérous, L., & Tadini, C. C. (2011, May). Mechanical properties of cassava starch-based nano-biocomposites. *In 11th International Congress on Engineering and Food, Athens*, Greece, 111-112.

166. Jumel, K., Harding, S. E., & Mitchell, J. R. (1996). Effect of gamma irradiation on the macromolecular integrity of guar gum. *Carbohydrate Research*, 282(2), 223-236.

167. Gupta, S., Shah, B., Sanyal, B., Variyar, P. S., & Sharma, A. (2009). Role of initial apparent viscosity and moisture content on post irradiation rheological properties of guar gum. *Food Hydrocolloids*, 23(7), 1785-1791.

168. Cunha, P. L., Castro, R. R., Rocha, F. A., de Paula, R., & Feitosa, J. (2005). Low viscosity hydrogel of guar gum: Preparation and physicochemical characterization. *International Journal of Biological Macromolecules*, 37(1), 99-104.

169. Zhai, M., Yoshii, F., & Kume, T. (2003). Radiation modification of starch-based plastic sheets. *Carbohydrate Polymers*, 52(3), 311-317.

170. Jo, C., Kang, H., Lee, N. Y., Kwon, J. H., & Byun, M. W. (2005). Pectin-and gelatin-based film: effect of gamma irradiation on the mechanical properties and biodegradation. *Radiation Physics and Chemistry*, 72(6), 745-750.

171. Byun, E. H., Kim, J. H., Sung, N. Y., Choi, J. I., Lim, S. T., Kim, K. H., ... & Lee, J. W. (2008). Effects of gamma irradiation on the physical and structural properties of *β*-glucan. *Radiation Physics and Chemistry*, 77(6), 781-786.

172. Pedersen, J. S. (1994). Determination of size distribution from small-angle scattering data for systems with effective hard-sphere interactions. *Journal of Applied Crystallography*, 27(4), 595-608.

173. Parvin, F., Khan, M. A., Saadat, A. H. M., Khan, M. A. H., Islam, J. M., Ahmed, M., & Gafur, M. A. (2011). Preparation and characterization of gamma irradiated sugar

containing starch/poly (vinyl alcohol)-based blend films. *Journal of Polymers and the Environment*, 19(4), 1013-1022.

174. Rhim, J. W., Hong, S. I., Park, H. M., & Ng, P. K. (2006). Preparation and characterization of chitosan-based nanocomposite films with antimicrobial activity. *Journal of Agricultural and Food Chemistry*, 54(16), 5814-5822.

175. Tong, X., Zhao, H., Tang, T., Feng, Z., & Huang, B. (2002). Preparation and characterization of poly (ethyl acrylate)/bentonite nanocomposites by in situ emulsion polymerization. *Journal of Polymer Science Part A: Polymer Chemistry*, 40(11), 1706-1711.

176. Ibrahim, S. M. (2011). Characterization, mechanical, and thermal properties of gamma irradiated starch films reinforced with mineral clay. *Journal of Applied Polymer Science*, 119(2), 685-692.

177. Kampeerapappun, P., Aht-ong, D., Pentrakoon, D., & Srikulkit, K. (2007). Preparation of cassava starch/montmorillonite composite film. *Carbohydrate Polymers*, 67(2), 155-163.

178. Mangiacapra, P., Gorrasi, G., Sorrentino, A., & Vittoria, V. (2006). Biodegradable nanocomposites obtained by ball milling of pectin and montmorillonites. *Carbohydrate Polymers*, 64(4), 516-523.

179. Rhim, J. W. (2011). Effect of clay contents on mechanical and water vapor barrier properties of agar-based nanocomposite films. *Carbohydrate Polymers*, 86(2), 691-699.

180. Chang, J. H., An, Y. U., & Sur, G. S. (2003). Poly (lactic acid) nanocomposites with various organoclays. I. Thermomechanical properties, morphology, and gas permeability. *Journal of Polymer Science Part B: Polymer Physics*, 41(1), 94-103.

181. Hussain, F., Chen, J., & Hojjati, M. (2007). Epoxy-silicate nanocomposites: cure monitoring and characterization. *Materials Science and Engineering: A*, 445, 467-476.

182. Yasmin, A., Abot, J. L., & Daniel, I. M. (2003). Processing of clay/epoxy nanocomposites by shear mixing. *Scripta Materialia*, 49(1), 81-86.

183. Nascimento, T. A., Calado, V., & Carvalho, C. W. P. (2012). Development and characterization of flexible film based on starch and passion fruit mesocarp flour with nanoparticles. *Food Research International*, 49(1), 588-595.

184. Chrissafis, K., Antoniadis, G., Paraskevopoulos, K. M., Vassiliou, A., & Bikiaris, D. N. (2007). Comparative study of the effect of different nanoparticles on the mechanical properties and thermal degradation mechanism of in situ prepared poly (ε-caprolactone) nanocomposites. *Composites Science and Technology*, 67(10), 2165-2174.

185. Kumar, P., Sandeep, K. P., Alavi, S., Truong, V. D., & Gorga, R. E. (2010). Effect of type and content of modified montmorillonite on the structure and properties of Bio-Nanocomposite films based on soy protein isolate and montmorillonite. *Journal of Food Science*, 75(5), N46-N56.

186. Walley, P., Zhang, Y., & Evans, J. R. G. (2012). Self-assembly of montmorillonite platelets during drying. *Bioinspiration & Biomimetics*, 7(4), 046004.

187. Zaidi, L., Bruzaud, S., Kaci, M., Bourmaud, A., Gautier, N., & Grohens, Y. (2013). The effects of gamma-irradiation on the morphology and properties of polylactide/Cloisite 30B nanocomposites. *Polymer Degradation and Stability*, 98(1), 348-355.

188. Dadbin, S., Naimian, F., & Akhavan, A. (2011). Poly (lactic acid)/layered silicate nanocomposite films: morphology, mechanical properties, and effects of γ-radiation. *Journal of Applied Polymer Science*, 122(1), 142-149.

189. Touati, N., Kaci, M., Ahouari, H., Bruzaud, S., & Grohens, Y. (2007). The Effect of γ-Irradiation on the Structure and Properties of Poly (propylene)/Clay Nanocomposites. *Macromolecular Materials and Engineering*, 292(12), 1271-1279.

190. Qin, H., Zhang, S., Liu, H., Xie, S., Yang, M., & Shen, D. (2005). Photo-oxidative degradation of polypropylene/montmorillonite nanocomposites. *Polymer*, 46(9), 3149-3156.

191. Bharadwaj, R. K. (2001). Modeling the barrier properties of polymer-layered silicate nanocomposites. *Macromolecules*, 34(26), 9189-9192.

192. Chiou, B. S., Wood, D., Yee, E., Imam, S. H., Glenn, G. M., & Orts, W. J. (2007). Extruded starch–nanoclay nanocomposites: Effects of glycerol and nanoclay concentration. *Polymer Engineering & Science*, 47(11), 1898-1904.

193. Navarro-Tarazaga, M. L., Sothornvit, R., & Pérez-Gago, M. B. (2008). Effect of plasticizer type and amount on hydroxypropil methylcellulose-beeswax edible film

properties and postharvest quality of coated plums (cv. Angeleno). *Journal of Agricultural and Food Chemistry*, 56, 9502-9509.

194. Lo, Y. L. (2003). Relationships between the hydrophilic–lipophilic balance values of pharmaceutical excipients and their multidrug resistance modulating effect in Caco-2 cells and rat intestines. *Journal of Controlled Release*, 90(1), 37-48.

195. Remington, J. P. (2006). Remington: The science and practice of pharmacy (Vol. 1). D. B. Troy, & P. Beringer (Eds.). *Lippincott Williams & Wilkins*, 332.

196. Mali, S., Grossmann, M. V. E., García, M. A., Martino, M. N., & Zaritzky, N. E. (2006). Effects of controlled storage on thermal, mechanical and barrier properties of plasticized films from different starch sources. *Journal of Food Engineering*, 75(4), 453-460.

197. Han, J. H., Seo, G. H., Park, I. M., Kim, G. N., & Lee, D. S. (2006). Physical and mechanical properties of pea starch edible films containing beeswax emulsions. *Journal of Food Science*, 71(6), E290-E296.

198. Senna, M. M., Salmieri, S., El-Naggar, A. W., Safrany, A., & Lacroix, M. (2010). Improving the compatibility of zein/poly (vinyl alcohol) blends by gamma irradiation and graft copolymerization of acrylic acid. *Journal of Agricultural and Food Chemistry*, 58(7), 4470-4476.

199. Baggio, A., Gallina, A., Dainese, N., Manzinello, C., Mutinelli, F., Serra, G., ... & Sangiorgi, E. (2005). Gamma radiation: a sanitating treatment of afb-contaminated

beekeeping equipment gamma radiation sanitation in beekeeping management. *Apimondia J*, 40, 22-27.

200. Pérez-Gago, M. B., & Krochta, J. M. (2001). Lipid particle size effect on water vapor permeability and mechanical properties of whey protein/beeswax emulsion films. *Journal of Agricultural and Food Chemistry*, 49(2), 996-1002.

201. Banerjee, A., Variyar, P. S., Chatterjee, S., & Sharma, A. (2014). Effect of post harvest radiation processing and storage on the volatile oil composition and glucosinolate profile of cabbage. *Food Chemistry*, 151, 22-30.

202. McHugh, T. H., & Krochta, J. M. (1994). Water vapor permeability properties of edible whey protein-lipid emulsion films. *Journal of the American Oil Chemists' Society*, 71(3), 307-312.

203. Callegarin, F., Gallo, J. A. Q., Debeaufort, F., & Voilley, A. (1997). Lipids and biopackaging. *Journal of the American Oil Chemists' Society*, 74(10), 1183-1192.

204. Villalobos, R., Hernández-Muñoz, P., & Chiralt, A. (2006). Effect of surfactants on water sorption and barrier properties of hydroxypropyl methylcellulose films. *Food Hydrocolloids*, 20(4), 502-509.

205. Andreuccetti, C., Carvalho, R. A., Galicia-García, T., Martínez-Bustos, F., & Grosso, C. R. (2011). Effect of surfactants on the functional properties of gelatin-based edible films. *Journal of Food Engineering*, 103(2), 129-136.

206. Soppirnath, K. S., & Aminabhavi, T. M. (2002). Water transport and drug release study from cross-linked polyacrylamide grafted guar gum hydrogel microspheres for the controlled release application. *European Journal of Pharmaceutics and Biopharmaceutics*, 53(1), 87-98.

207. Tunç, S., & Duman, O. (2010). Preparation and characterization of biodegradable methyl cellulose/montmorillonite nanocomposite films. *Applied Clay Science*, 48(3), 414-424.

208. Sousa, E. C., Uchôa-Thomaz, A. M. A., Carioca, J. O. B., Morais, S. M. D., Lima, A. D., Martins, C. G., ... & Rodrigues, L. L. (2014). Chemical composition and bioactive compounds of grape pomace (Vitis vinifera L.), Benitaka variety, grown in the semiarid region of Northeast Brazil. *Food Science and Technology (Campinas)*, 34(1), 135-142.

209. Butkhup, L., Chowtivannakul, S., Gaensakoo, R., Prathepha, P., & Samappito, S. (2010). Study of the phenolic composition of Shiraz red grape cultivar (Vitis vinifera L.) cultivated in north-eastern Thailand and its antioxidant and antimicrobial activity. *South African Journal for Enology & Viticulture*, 31(2), 89.

210. Rockenbach, I. I., Rodrigues, E., Gonzaga, L. V., Caliari, V., Genovese, M. I., Gonçalves, A. E. D. S. S., & Fett, R. (2011). Phenolic compounds content and antioxidant activity in pomace from selected red grapes (*Vitis vinifera L.* and *Vitis labrusca L.*) widely produced in Brazil. *Food Chemistry*, 127(1), 174-179.

211. Naznin, M., Abedin, M. Z., Khan, M. A., & Gafur, M. A. (2012). Influence of *Acacia catechu* extracts and urea and gamma irradiation on the mechanical properties of starch/PVA-based material. *International Scholarly Research Notices, 2012*.

212. Moradi, M., Tajik, H., Razavi Rohani, S. M., Oromiehie, A. R., Malekinejad, H., Aliakbarlu, J., & Hadian, M. (2012). Characterization of antioxidant chitosan film incorporated with *Zataria multiflora* Boiss essential oil and grape seed extract. *LWT-Food Science and Technology*, 46(2), 477-484.

213. Bernhard, K., Schrempf, H., & Goebel, W. (1978). Bacteriocin and antibiotic resistance plasmids in *Bacillus cereus* and *Bacillus subtilis*. *Journal of Bacteriology*, 133(2), 897-903.

214. Han, J., Castell-Perez, M. E., & Moreira, R. G. (2007). The influence of electron beam irradiation of antimicrobial-coated LDPE/polyamide films on antimicrobial activity and film properties. *LWT-Food Science and Technology*, 40(9), 1545-1554.

215. Prakash, A., Guner, A. R., Caporaso, F., & Foley, D. M. (2000). Effects of low-dose gamma irradiation on the shelf life and quality characteristics of cut romaine lettuce packaged under modified atmosphere. *Journal of Food Science*, 65(3), 549-553.

216. Farkas, J., Saray, T., Mohacsi-Farkas, C., Horti, K., & Andrassy, E. (1997). Effects of low-dose gamma radiation on shelf-life and microbiological safety of pre-cut/prepared vegetables. *Advances in Food Sciences*, 19(3-4), 111-119.

217. Khattak, A. B., Bibi, N., Chaudry, M. A., Khan, M., Khan, M., & Qureshi, M. J. (2005). Shelf life extension of minimally processed cabbage and cucumber through gamma irradiation. *Journal of Food Protection®*, 68(1), 105-110.

218. Reij, M. W., & Den Aantrekker, E. D. (2004). Recontamination as a source of pathogens in processed foods. *International Journal of Food Microbiology*, 91(1), 1-11.

219. Agarwal, S. R., & Sreenivasan, A. (1973). Packaging aspects of irradiated flesh foods: Present status A review. *International Journal of Food Science & Technology*, 8(1), 27-37.

220. SCHULZ, G.L. (1969). Research and Development Associates, *Activities Rept*, 22, 97.

221. Hotchkiss, J. H. (1997). Food-packaging interactions influencing quality and safety. *Food Additives & Contaminants*, 14(6-7), 601-607.

222. Sanchez-Mata, M. C., Camara, M., & Dıez-Marques, C. (2003). Extending shelf-life and nutritive value of green beans (*Phaseolus vulgaris* L.), by controlled atmosphere storage: macronutrients. *Food Chemistry*, 80(3), 309-315.

223. Zagory, D. (1999). Effects of post-processing handling and packaging on microbial populations. *Postharvest Biology and Technology*, 15(3), 313-321.

224. Tripathi, J., Chatterjee, S., Vaishnav, J., Variyar, P. S., & Sharma, A. (2013). Gamma irradiation increases storability and shelf life of minimally processed ready-to-

cook (RTC) ash gourd (*Benincasa hispida*) cubes. *Postharvest Biology and Technology*, 76, 17-25.

225. Hamid, N. A., El-Dawla, E. A., & Nasr, I. S. (2012). Effects of Shrink Film Wrapping and Irradiation on Storage Quality of Leconte Pears (Pyrus communis L.).

226. Bartholomew, D. P., Paull, R. E., & Rohrbach, K. G. (Eds.). (2002). *The pineapple: botany, production, and uses.* CABI.

227. Owureku-Asare, M., Adu-Gyamfi A., Agyei-Amponsah J.,… (2014). Effect of Gamma Irradiation Treatment and Storage on Physico-chemical, Microbial and Sensory Quality of Minimally Processed Pineapple (*Ananas comosus*). *British Journal of Applied Science & Technology*, 4(19), 2752-2761.

228. Piljac-Žegarac, J., Valek, L., Martinez, S., & Belščak, A. (2009). Fluctuations in the phenolic content and antioxidant capacity of dark fruit juices in refrigerated storage. *Food Chemistry*, 113(2), 394-400.

229. Fan, X., Toivonen, P. M., Rajkowski, K. T., & Sokorai, K. J. (2003). Warm water treatment in combination with modified atmosphere packaging reduces undesirable effects of irradiation on the quality of fresh-cut iceberg lettuce. *Journal of agricultural and food chemistry*, 51(5), 1231-1236.

230. Elfalleh, W., Yahia, Y., & Ferchichi, A. Main pomegranate phytochemicals and their contribution to the antioxidant potencies of pomegranate juice.

231. Cao, G., Sofic, E., & Prior, R. L. (1996). Antioxidant capacity of tea and common vegetables. *Journal of Agricultural and Food Chemistry*, 44(11), 3426-3431.

232. Vegara, S., Martí, N., Mena, P., Saura, D., & Valero, M. (2013). Effect of pasteurization process and storage on color and shelf-life of pomegranate juices. *LWT-Food Science and Technology*, 54(2), 592-596.

233. Valero, M., Vegara, S., Martí, N., & Saura, D. (2014). Clarification of pomegranate juice at industrial scale. *Journal of Food Process Technology*, 5(324), 2.

234. Alighourchi, H., Barzegar, M., & Abbasi, S. (2008). Effect of gamma irradiation on the stability of anthocyanins and shelf-life of various pomegranate juices. *Food Chemistry*, 110(4), 1036-1040.

235. Villavicencio, A. L. C., Mancini-Filho, J., Delincée, H., & Greiner, R. (2000). Effect of irradiation on anti-nutrients (total phenolics, tannins and phytate) in Brazilian beans. *Radiation Physics and Chemistry*, 57(3), 289-293.

236. Kasapis, S., Norton, I. T., & Johan, B. (Eds.). (2009). *Modern biopolymer science: bridging the divide between fundamental treatise and industrial application*. Academic Press, page-308.

237. Mastromatteo, M., Mastromatteo, M., Conte, A., & Del Nobile, M. A. (2011). Combined effect of active coating and MAP to prolong the shelf life of minimally processed kiwifruit (*Actinidia deliciosa* cv. Hayward). *Food Research International*, 44(5), 1224-1230.

238. Oms-Oliu, G., Soliva-Fortuny, R., & Martín-Belloso, O. (2008). Edible coatings with antibrowning agents to maintain sensory quality and antioxidant properties of fresh-cut pears. *Postharvest Biology and Technology*, 50(1), 87-94.

List of publication arising from the thesis

1. Journal

A. Published:

1. Saurabh, C. K., Gupta, S., Bahadur, J., Mazumder, S., Variyar, P. S., & Sharma, A. (2013). Radiation dose dependent change in physiochemical, mechanical and barrier properties of guar gum based films. Carbohydrate polymers, 98(2), 1610-1617.

2. Saurabh, C. K., Gupta, S., Bahadur, J., Mazumder, S., Variyar, P. S., & Sharma, A. (2015). Mechanical and barrier properties of guar gum based nano-composite films. Carbohydrate polymers, 124, 77-84.

3. Gupta, S., Saurabh, C. K., Variyar, P. S., & Sharma, A. (2015). Comparative analysis of dietary fiber activities of enzymatic and gamma depolymerized guar gum. Food Hydrocolloids, 48, 149-154.

B. Communicated:

1. Saurabh, C. K., Gupta, S., Bahadur, J., Mazumder, S., Variyar, P. S., & Sharma, A. Improving mechanical & barrier properties of guar gum based biodegradable films: Optimization of additives by Response Surface Methodology.

C. Manuscript under preparation

1. Saurabh, C. K., Gupta, S., Variyar, P. S., & Sharma, A. Shelf life extension of minimally processed pomegranate arils packed in guar gum based active films by gamma irradiation.

2. Saurabh, C. K., Gupta, S., Variyar, P. S., & Sharma, A. Shelf life extension of minimally processed pomegranate arils by dip coating.

2. Conferences

A. Impact of radiation processing on mechanical and barrier properties of guar gum based packaging films.XXI ICFOST.

B. Effect of nanoclay on mechanical and barrier properties of guar gum based biodegradable film. XXII ICFOST.

Carbohydrate Polymers 98 (2013) 1610–1617

Contents lists available at ScienceDirect

Carbohydrate Polymers

journal homepage: www.elsevier.com/locate/carbpol

Radiation dose dependent change in physiochemical, mechanical and barrier properties of guar gum based films

Chaturbhuj K. Saurabh[a,1], Sumit Gupta[a,1], Jitendra Bahadur[b], S. Mazumder[b], Prasad S. Variyar[a,*], Arun Sharma[a]

[a] Food Technology Division, Bhabha Atomic Research Centre, Trombay, Mumbai 400 085, India
[b] Solid State Physics Division, Bhabha Atomic Research Centre, Trombay, Mumbai 400 085, India

ARTICLE INFO

Article history:
Received 7 November 2012
Received in revised form 3 July 2013
Accepted 18 July 2013
Available online xxx

Keywords:
Guar gum
Irradiation
Mechanical properties
Biodegradable film
Small angle X-ray scattering

ABSTRACT

Mechanical and water vapor barrier properties of biodegradable films prepared from radiation processed guar gum were investigated. Films prepared from GG irradiated up to 500 Gy demonstrated significantly higher tensile strength as compared to non-irradiated control films. This improvement in tensile strength observed was demonstrated to be due to the ordering of polymer structures as confirmed by small angle X-ray scattering analysis. Exposure to doses higher than 500 Gy, however, resulted in a dose dependent decrease in tensile strength. A dose dependent decrease in puncture strength with no significant differences in the percent elongation was also observed at all the doses studied. Water vapor barrier properties of films improved up to 15% due to radiation processing. Radiation processing at lower doses for improving mechanical and barrier properties of guar based packaging films is demonstrated here for the first time.

1. Introduction

In the past twenty years, the production and use of plastics in the world has increased enormously to about 200 million tons per year. Packaging constitutes the largest market for plastics, amounting to over 12 million tons per year (Rhim and Perry, 2007). Increasing demand for synthetic packaging materials has put tremendous pressure on the environment because of their poor biodegradability and non-renewability (Ghasemlou, Khodaiyan, Oromiehie, & Yarmand, 2011). This has lead to a search for packaging materials that are biodegradable as well as recyclable (Mangiacapra, Gorrasi, Sorrentino, & Vittoria, 2006). One of the alternatives is the development of packaging material from biopolymers (i.e. protein, polysaccharide and lipid) that are biodegradable, non-toxic and derived from completely renewable resources. Among the biopolymers, polysaccharides are the most widely used for preparation of packaging films.

Widely studied polysaccharides for edible or biodegradable films are: starch, chitosan, carrageenan, and galactomannans. In packaging industry galactomannan is used as edible coating because it forms very thick aqueous solution at low concentration (Cerqueira et al., 2011), is an excellent emulsifier and non-toxic (Cerqueira, Lima, Teixeira, Moreira, & Vicente, 2009). Guar gum (GG) is a type of galactomannan, derived from endosperm of an annual legume plant *Cyamopsis tetragonoloba*. India accounts for 80 percent of world production of GG. It is a hetropolysaccharide of a mannose (i.e. (1-4)-linked β-D-mannopyranose) backbone with galactose side groups ((1-6)-linked α-D-galactopyranose) (Aydinli, Tutas, & Bozdemir, 2004; Das, Ara, Dutta, & Mukherjee, 2011; Martins, Cerqueira, Souza, Carmo, & Vicente, 2010). It is mainly used in paper, food and pharmaceutical industries (Chudzikowski, 1971).

Major limitations in the use of biopolymers as packaging materials are their relatively poor mechanical and barrier properties such as tensile strength and water vapor transmission rate as compared to their non-biodegradable counterparts (Cha and Chinnan, 2004; Kang and Min, 2010; Petersson and Oksman, 2006). This has resulted in a greater focus on improving the properties of these polymers to match the commercially available packaging material. Various chemical and physical methods have been used for improving biopolymer film properties. Among the physical methods, addition of plasticizer for improving mechanical properties of biodegradable films has been extensively reported. This increases the percentage elongation of films by forming hydrogen bond with the polymer and reducing polymeric interactions. Polysaccharide based films are commonly plasticized with polyols such as glycerol (Garcia, Ribba, Dufresn, Aranguren, & Goyanes, 2011).

* Corresponding author at: Food Flavor and Aroma Chemistry Section, Food Technology Division, BARC, Mumbai 400 085, India. Tel.: +91 22 25590560; fax: +91 22 25505151.
E-mail address: pvariyar@barc.gov.in (P.S. Variyar).
[1] These authors are contributed equally.

0144-8617/$ – see front matter © 2013 Elsevier Ltd. All rights reserved.
http://dx.doi.org/10.1016/j.carbpol.2013.07.041

Among the chemical methods, chemical modification of guar galactomannan with benzamide for preparation of water resistant films has been recently reported (Das et al., 2011). Mikkonen et al. (2007) used enzymatic depolymerization for improving mechanical properties of GG film. Gamma irradiation has been widely used for the improvement of mechanical properties of pectin (Kang, Jo, Lee, Kwon, & Byun, 2005), starch (Kim, Jo, Park, & Byun, 2008) and calcium caseinate edible films (Vachon et al., 2000). Use of gamma irradiation for GG depolymerization has been previously reported (Gupta, Shah, Sanyal, Variyar & Sharma, 2009). There are several advantages associated with gamma irradiation such as convenience, eco friendly nature of the process (Hwang, Jung, Kuk, Choi, & Nho, 2010) and short processing time.

Physical treatments such as gamma irradiation could possibly change conformations of polymers in solution. Several investigations have shown that the conformation and morphology of polymer chains affect the physical properties of the polymer. Polymer chain conformation and chain correlation can be estimated by small angle X-ray scattering (SAXS) (Winokur, Skotheim, Elsenbaumer, & Reynolds, 1998). SAXS arises from the fluctuations of electron density in a mesoscopic length scale (1–100 nm) in a specimen and hence scattering profile contains the information about the size/size distribution and shape of the inhomogeneities (Glatter and Kratky, 1982).

To the best of our knowledge, no reports exist till date on the assessment of the effects of gamma irradiation on mechanical and barrier properties of GG based films. The main objective of this work was to study the effect of irradiation on physiochemical properties of GG and to determine the impact of these properties on the mechanical and barrier properties of films prepared from the irradiated GG.

2. Materials and methods

2.1. Purification of GG

Purification of guar gum was carried out as per procedure detailed earlier by Jumel, Harding, and Mitchell (1996). In brief, 2.5 g of GG (Merck India ltd.) was dissolved in 250 ml of distilled water by using shear mixer (Omni mixer, Sorvall, USA) at speed 2 for 2 min. Solution obtained was kept overnight on magnetic stirrer at room temperature (25 ± 2 °C). Resulting solution was centrifuged at 9000 rpm for 30 min for removal of insoluble impurities. Ethanol was added to supernatant in the proportion of 2:1 and resulting mixture was kept overnight for precipitation of GG. The precipitate obtained was freeze dried to obtain dry purified GG powder. Yield obtained by above purification procedure was 60%.

2.2. Irradiation of GG

Purified GG as dried powder was exposed to gamma radiation processing using a ^{60}Co gamma irradiator having dose rate of 4.1 kGy/hr (GC-5000, BRIT, India) at room temperature. GG was subjected to a dose of (0.25, 0.5. 0.75, 1, 5, 10, 25 and 50 kGy). In addition, films prepared from control unirradiated GG were subjected to gamma radiation to a dose of (1, 5, 10, 25, 50 and 100 kGy) after 7 days of conditioning.

2.3. Viscosity average molecular weight analysis by Ostwald viscometer

Viscosity average molecular weight of GG post irradiation was measured using Ostwald's viscometer at constant temperature of 24 ± 1 °C. 0.1% w/v aqueous solution was prepared from control and irradiated GG and specific viscosity (η_{sp}) was obtained using following Eq. (1):

$$[\eta_{sp}] = \frac{(t - t_0)}{t_0} \quad (1)$$

where t = flow time of a polymer solution through viscometer; t_0 = flow time of the pure solvent through the same viscometer.

Intrinsic viscosity (η) was then calculated from η_{sp} using following Eq. (2):

$$[\eta] = \frac{[\eta_{sp}]}{c} \quad (2)$$

where c = polymer concentration.

Viscosity-average molecular weight (M_v) was calculated from η (Eq. (3)) (Vega, Lima, & Pinto, 2001).

$$[\eta] = KM_v^a \quad (3)$$

where K and a are the parameters that depend on the solvent-polymer pair. The a and K values used for guar galactomannan were 0.72 and 5.13×10^{-4}, respectively (Beer, Wood, & Weisz, 1999).

2.4. Molecular weight and polydispersity index analysis by gel permeation chromatography

Number average molecular weight (M_n), weight average molecular weight (M_w) and polydispersity index (PDI) (M_w/M_n) were determined by gel permeation chromatography (GPC) using a column (300 mm length × 4.6 mm I.D.), 5u Biobasic SEC-1000, Thermo Scientific, UK). The HPLC system (Ultimate 3000, Dionex Corporation, Germany) having differential refractive index detector (RI-101, Shodex Corporation, USA) was used. The mobile phase was deionized water (Millipore, Bedford, MA) and the flow rate was fixed at 0.6 mL/min. All GG samples were injected (20 μL) as their aqueous solutions at concentrations of 0.2% (w/v) which were centrifuged at 12,000 rpm for 15 min prior to analysis. The column was calibrated using pullulan standards (Fluka Analytical, St. Louis, USA) ranging from molecular weights of 6000 to 2,560,000 Da. Pullulan standards were analyzed using similar HPLC conditions described above.

Number average molecular weight (M_n) was calculated by following Eq. (4):

$$M_n = \sum \left(\frac{N_i}{\sum N_i} \times M_i \right) \quad (4)$$

where N_i = detector response at a particular time

$$\sum N_i = \text{Total detector response}$$

M_i = Molecular weight at given time.

Weight average molecular weight was calculated by following Eq. (5):

$$M_w = \sum \left(\frac{A_i \times M_i}{\sum A_i} \right) \quad (5)$$

where $A_i = N_i \times M_i$

Based on M_n and M_w, PDI was calculated using equation given below:

$$\text{PDI} = \frac{M_w}{M_n} \quad (6)$$

2.5. Determination of mannose to galactose ratio of GG by HPLC

Control and irradiated GG samples were hydrolyzed by 1 N sulphuric acid at 90 °C for 5 h. After hydrolysis samples were neutralized using barium hydroxide and barium sulfate precipitates

thus formed were removed by centrifugation at 12,000 rpm for 10 min. Supernatants were freeze dried and dried powder obtained was dissolved (1% w/v) in 70:30::acetonitrile:water and filtered through 45 μm filter prior to analysis. Samples were then analyzed using HPLC system (Quaternary gradient pump, PU-2089 plus, Jasco, Japan) equipped with High Q silica base amino column (Hi Q SIL NH_2, KYA TECH Corporation, Japan) with column dimension (4.6 mm I.D. × 250 mm L) and refractive index detector (RI-2031 plus, Jasco, Japan). All samples were analyzed by ChromPass software (Jasco, Japan). The mobile phase was 80:20::acetonitrile:water with a flow rate of 1 ml min^{-1}. 100 μL of all GG samples were injected. Standard curves for both galactose and mannose were made from 0.25 mg to 1 mg using similar HPLC conditions described above. Linear regression equations for both standards were then obtained. In hydrolyzed GG samples, galactose and mannose content was calculated using linear regression equations obtained above and G/M ratio was then obtained.

2.6. Preparation of GG films

1.5 g of GG was added into 150 mL water along with 0.5 mL of glycerol (40% w/w of GG) as plasticizer and kept overnight at room temperature (25 ± 2 °C) on magnetic stirrer. Solution thus obtained was centrifuged at 3000 rpm for 15 min for the removal of air bubbles. 150 ml of solution was poured and spread evenly onto surface of glass plate (21 cm × 21 cm), having removable boundary of insulating tape. Plates were then kept in oven at 80 °C for 8 h for drying. Dried GG films were conditioned at 50% relative humidity at room temperature (25 ± 2 °C) for 7 days. After conditioning films were pealed and subjected to physical and mechanical analysis. In another set of experiment, films were also prepared from unpurified native guar gum in the same manner as above.

2.7. Physical and mechanical properties of GG films

GG films were cut into strips of dimension 2 cm × 15 cm. Micrometer (103–131, Mitutoyo, Japan) was used to determine film thickness. Measurements were randomly taken at three different locations on each film strip. The mean value of thickness of each strip was used in calculations for the tensile strength, puncture strength and % elongation of same strip. Mechanical properties of films were analyzed using a Texture analyzer (TA.HD Plus, Stable Micro Systems). The American Society of Testing and Materials (ASTM) standard method D882-10 was used to measure the tensile strength (TS), Young's modulus and percent elongation at break (% E) of films. Puncture strength of films (5 cm × 2 cm) were determined by 2 mm needle probe having test speed of 30 mm/min. Water vapor transmission rate (WVTR) of GG films were determined by using round cups having 100 mL volume capacities and having 120 cm^2 area of mouth. It was filled with 60 mL of distilled water and sealed with GG film using adhesive tapes and assembly was kept in desiccators at 25 ± 2 °C. 100% RH gradient was used and maintained by using excess of H_2SO_4. The mass of water lost from the cup was monitored as a function of time, and the WVTR was calculated from the steady-state region. Color of films were determined using a colorimeter (CM-3600d Konica Minolta sensing Inc., Japan) by measuring L^*, a^* and b^* values. Instrument was calibrated using a white tile supplied along with the equipment. Source used was D65 with observer set at 10 degrees. Opacity is a measure of the extent of light passing through any material. Opacity of films was determined using Hunter lab method, as the relationship between reflectance of each sample on black standard and the reflectance on white standard using Eq. (7) as given below:

$$\text{Opacity} = (Y_b/Y_w) \times 100 \quad (7)$$

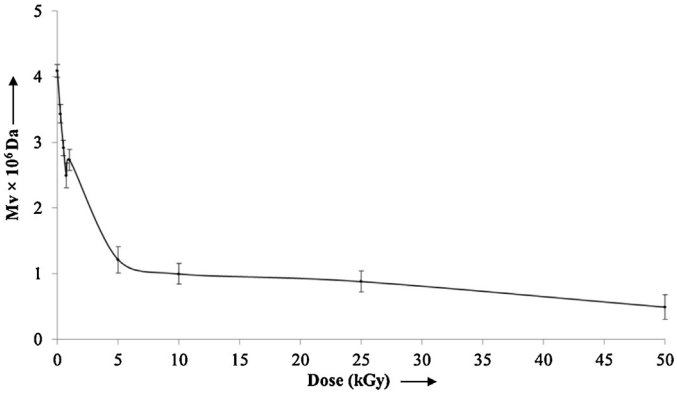

Fig. 1. Effect of gamma irradiation on viscosity average molecular weight (M_v) of GG.

All measurements were carried out in triplicates at room temperature 25 ± 2 °C and 50% relative humidity.

2.8. Small angle X-rays scattering measurements

SAXS measurements were performed on the aqueous solution of the control, 500 Gy and 50 kGy dose treated polymer at a lab based SAXS setup using CuKα source. Size of the incident photon beam on the sample was 0.4 mm diameter. The SAXS detector was mounted at a sample-to-detector distance of 1.07 m, corresponding to a q-range of 0.1–2.5 nm^{-1}. The magnitude of the scattering wave vector, q equals:

$$q = 2 \sin\theta/\lambda = q/2\pi \quad (8)$$

where 2θ is the scattering angle and λ = 0.154 nm the used wavelength.

2.9. FTIR analysis of guar gum films

Spectra of guar gum films were scanned in the range of 4000–600 cm^{-1} on a FTIR (FT/IR 4100, Jasco) spectrometer. ATR assembly was used for obtaining FTIR spectra. Films were directly pressed on ATR assembly and spectra were recorded. 40 scans were taken for each film sample.

2.10. Statistical analysis

DSAASTAT ver. 1.101 by Andrea Onofri was used for statistical analysis of data. Three samples were taken for every treatment and each sample was further analyzed in triplicates. Data was analyzed by Analysis of variance (ANOVA) and multiple comparisons of means were carried out using Duncan's multiple range test.

3. Result and discussion

3.1. Effect of gamma irradiation on physio-chemical properties of GG

Control GG had an intrinsic viscosity (η_{sp}) of 2.95 and viscosity average molecular weight (M_v) of 4.09 × 10^6 Da. Radiation processing resulted in significant ($p < 0.05$) reduction in viscosity average molecular weight (M_v) of GG (Fig. 1). Reduction in M_v due to irradiation was in a non-linear dose dependent manner. GG irradiation resulted in rapid decrease in M_v up to 2 kGy followed by a much slower decrease at higher doses. M_v of GG reduced to 1.5 × 10^6 Da and 4.9 × 10^5 Da at 2 and 50 kGy, respectively (Fig. 1). Similar results were also obtained by Jumel et al. (1996) during irradiation processing of GG.

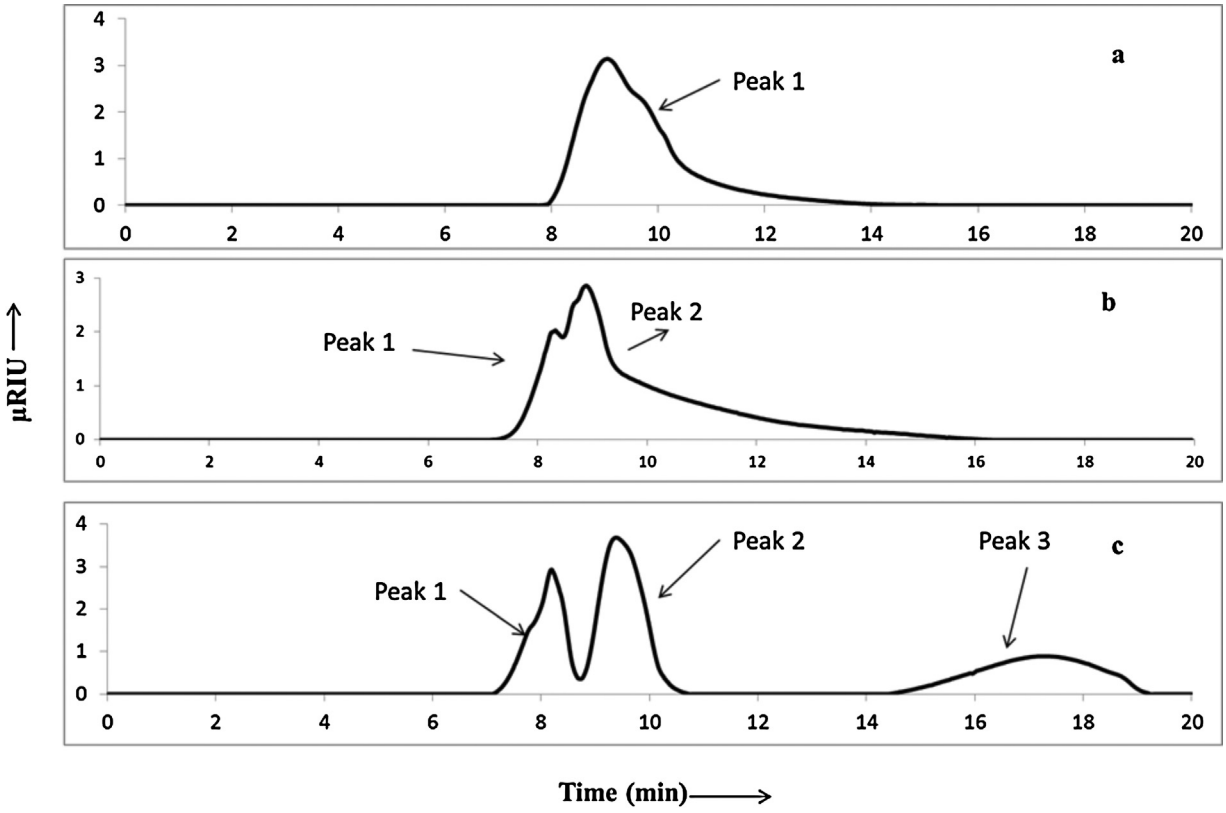

Fig. 2. A representative gel permeation chromatogram (GPC) of GG samples: (a) control unirradiated GG; (b) GG irradiated to a dose of 1 kGy; (c) GG irradiated to a dose of 50 kGy.

GG samples were further analyzed using gel permeation chromatography (GPC) for evaluation of weight average molecular weight (M_w). GPC chromatogram for the control GG showed a single peak corresponding to M_w of 4×10^6 Da (Fig. 2a). In earlier studies on guar gum M_w was reported to be 2.7×10^6 Da by Jumel et al. (1996). Hence results obtained are in accordance with published data. Two peaks (Peaks 1 and 2) were observed in GPC chromatograms at doses up to 1 kGy for GG irradiation (Fig. 2b). Peaks 1 and 2 had M_w of 4×10^6 and 2.5×10^6 Da, respectively. M_w of these peaks was comparable to that of control GG. At low doses (up to 1 kGy) of irradiation a disruption of supramolecular structures of GG polymer rather than depolymerization as reported by Jumel et al. (1996) could possibly explain the two peaks observed in GPC chromatograms. A third peak (Peak 3) having a M_w 2×10^5 Da was also observed in GPC chromatograms beyond the irradiation dose of 1 kGy (Fig. 2c). Appearance of this peak in the chromatogram could be attributed to the formation of depolymerized polymer as a result of gamma radiation. Radiation processing up to a dose of 5 kGy resulted in significant ($p < 0.05$) increase in relative area of peak 2 with corresponding decrease in area of peak 1. However, beyond radiation dose of 5 kGy a significant ($p < 0.05$) dose dependent increase in relative area percent of peak 3 with a decrease in Peaks 1 and 2 was observed (Fig. 3). Results from both viscosity as well as gel permeation chromatography suggested a gradual degradation of GG during irradiation. Similar results for radiation induced degradation of GG were earlier reported by Gupta et al. (2009).

Polydispersity index (PDI), which is a measure of molecular weight distribution of any polymer sample, was also calculated for control and irradiated GG samples. A radiation dose dependent increase in PDI of GG samples was observed (Fig. 4). PDI of control GG was 1.05 which increased to 1.16 at 1 kGy and 1.29 at 50 kGy for irradiated GG (Fig. 4). Jumel et al. (1996) have also reported a wide molecular weight distribution of irradiated GG samples as compared to non-irradiated controls. Increase in PDI with irradiation dose could possibly be explained by random phenomenon of radiation induced degradation of GG polymer.

M/G ratio of control GG was found to be 1.6:1 which is in accordance with results reported previously by Cunha, Castro, Rocha, Paula, and Feitosa (2005). No statistically significant ($p < 0.05$) differences were observed in M/G ratio of GG samples due to radiation processing in the present study. M/G ratio of galac-

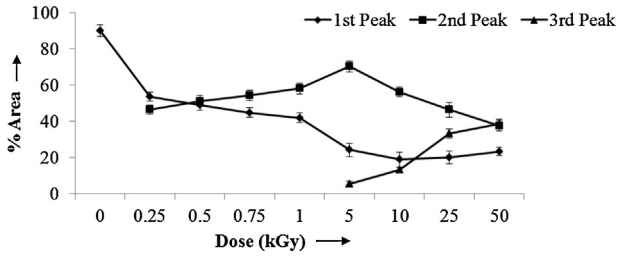

Fig. 3. Variation of relative percent area of peaks observed in gel permeation chromatography (GPC) of GG with radiation dose.

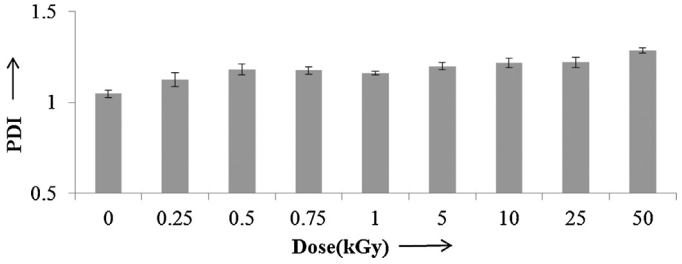

Fig. 4. Effect of gamma irradiation on polydispersity index (PDI) of GG.

Table 1
Effect of gamma irradiation on mechanical and barrier properties and color co-ordinates of guar gum films. Films prepared from irradiated guar gum.

Dose (kGy)	Tensile strength (MPa)	Young's Modulus (MPa)	Puncture strength (N)	% Elongation	Water vapor transmission rate ($gm/m^2/day$)	L^* (Black to white)	a^* (Green to magenta)	b^*(Blue to yellow)	Opacity (%)
0	60.5 ± 8.7^{bc}	162 ± 23^{a}	2.3 ± 0.2^{a}	13.9 ± 4.5^{b}	190 ± 10^{ab}	97.7 ± 0.8^{a}	0.8 ± 0.2^{c}	1 ± 0.1^{d}	12.9 ± 0.2^{d}
0.25	71.4 ± 10.6^{ab}	151 ± 39^{a}	1.93 ± 0.2^{b}	22.8 ± 3.8^{a}	186.9 ± 8.3^{abc}	94.4 ± 0.8^{d}	2.3 ± 0.3^{a}	1.9 ± 0.2^{f}	15.2 ± 0.5^{a}
0.5	80.2 ± 13.9^{a}	158 ± 16^{a}	1.8 ± 0.2^{b}	18.6 ± 1.9^{ab}	192.5 ± 12^{ab}	94.4 ± 0.9^{d}	1.6 ± 0.3^{b}	1.7 ± 0.2^{f}	13.4 ± 0.5^{cd}
0.75	58.6 ± 7.8^{bc}	149 ± 11^{a}	1.69 ± 0.1^{b}	19.4 ± 2.5^{ab}	195.7 ± 12^{ab}	96.1 ± 0.7^{bc}	0.1 ± 0.01^{ef}	$0.2 \pm .04^{b}$	13.3 ± 0.5^{cd}
1	55 ± 6.2^{c}	154 ± 19^{a}	1.6 ± 0.3^{b}	14.7 ± 1.2^{b}	184 ± 7.5^{abc}	97.2 ± 0.6^{ab}	$.03 \pm .02^{ef}$	$0.3 \pm .04^{b}$	12.9 ± 0.3^{d}
5	26.7 ± 5.3^{d}	65 ± 19^{b}	1.7 ± 0.3^{b}	18.4 ± 2.4^{ab}	170 ± 4.4^{cd}	98.3 ± 0.8^{a}	0.2 ± 0.1^{de}	0.7 ± 0.1^{c}	13.2 ± 0.7^{cd}
10	22.4 ± 3.8^{de}	63 ± 11^{b}	1.2 ± 0.1^{c}	19.1 ± 3.3^{ab}	175.6 ± 8^{bcd}	94.8 ± 0.7^{cd}	0.1 ± 0.04^{f}	0.9 ± 0.04^{a}	14.3 ± 0.3^{b}
25	19.32 ± 4.5^{de}	49 ± 12^{b}	1.0 ± 0.2^{c}	16.1 ± 1.6^{b}	177.5 ± 9^{bcd}	96 ± 0.7^{bc}	0.42 ± 0.04^{d}	0.8 ± 0.1^{c}	13.9 ± 0.3^{bc}
50	7.8 ± 2.5^{e}	35 ± 11^{b}	0.8 ± 0.2^{c}	7.8 ± 2.5^{c}	160.6 ± 5.2^{d}	96.1 ± 0.6^{bc}	0.7 ± 0.2^{c}	1.4 ± 0.1^{e}	13.8 ± 0.4^{bc}

Any two means in the same column followed by the same letter are not significantly ($p > 0.05$) different.

tomannans significantly affects the mechanical properties of the films. For example, films prepared from the locust bean gum (M/G ratio of approximately 3.33) were stronger and more flexible than films prepared from control GG (M/G ratio of approximately 1.67) (Mikkonen et al., 2007).

3.2. Effect of radiation on mechanical properties of GG based films

GG films were prepared from control and irradiated samples in powder form. Films prepared from unirradiated unpurified GG demonstrated thickness of 13.66 ± 3.3 μm, tensile strength of 6 ± 1.1 MPa and Young's modulus of 63 ± 12 MPa. While that from purified GG demonstrated an improved tensile strength of 60.5 ± 8.7 MPa and Young's modulus of 162 ± 23 MPa with thickness of 14.33 ± 2.3 μm. In a previous study on GG based films the tensile strength of control GG plasticized with 40% glycerol (w/w of GG) was reported to be 12 MPa (Mikkonen et al., 2007). Films prepared from other galactomannans such as locust bean gum were reported to have a tensile strength of 35 MPa (Aydinli et al., 2004). A substantial improvement in tensile strength and Young's modulus of films observed here might be due to the additional purification step followed in this study, which leads to removal of insoluble impurities from GG. Impurities mainly consisted of high molecular weight macromolecules, proteins and arabinose and glucose residues (Cunha, Paula, & Feitosa, 2007). This could lead to a uniform and compact packing of GG polymer chains in the films prepared, resulting in increased tensile strength. Thus, all further work was performed on purified GG. However, no statistically significant effect of purification was observed on film thickness.

Radiation processing had a significant ($p < 0.05$) effect on the tensile strength of GG films. Interestingly, an increase in tensile strength to 80.2 ± 13.9 MPa up to a dose of 500 Gy with dose dependent decrease, thereafter, was observed (Table 1). The tensile strength of GG films reduced to 7.8 ± 2.5 MPa at a dose of 50 kGy. Kim et al. (2008) reported an increase in tensile strength by 27.5% of starch and locust bean gum combination films at irradiation dose of 3 kGy. An increased tensile strength for starch based plastics sheets at irradiation dose of 30–70 kGy with a dose dependent decrease at higher doses (>70 kGy) was also reported by Zhai, Yoshii, and Kume (2003). For pectin-based films, an increase in tensile strength by 31.2% at a dose of 10 kGy with a decrease at higher doses was reported earlier (Jo, Kang, Lee, Kwon, & Byun, 2005). Improved tensile strength due to irradiation in previous studies was attributed to radiation induced cross-linking of polymers, while reduction in tensile strength at higher doses was reported to have occurred due to radiation induced degradation of polymers (Byun et al., 2008). An increase in tensile strength of GG based films due to enzymatic depolymerization because of increased solubility and better orientation of short chain polymer was previously reported (Mikkonen et al., 2007). Surprisingly, no increase in tensile strength was observed due to radiation induced depolymerization in the present study. This might be due to the fact that radiation depolymerization resulted in different molecular weight distributions as compared to enzymatic depolymerization. In the present study, a dose dependent increase in PDI was observed thus suggesting a wide molecular weight distribution of irradiated GG samples. Further, even at a high radiation dose of 50 kGy presence of higher Mw fractions was demonstrated by GPC studies (Fig. 2c). Due to the presence of higher Mw fractions and wide molecular weight distribution, a restriction in the ordering of polymer chains is expected that could possibly decrease tensile strength. Interestingly, at a lower irradiation dose of 500 Gy 32.6 percent increase in tensile strength was observed (Table 1). These changes could possibly be due to conformational change in GG particle structure, which was further confirmed by SAXS.

Young's modulus is a measure of stiffness of any sample. Films prepared with irradiated GG demonstrated no statistically significant ($p < 0.05$) difference in Young's modulus up to a dose of 1 kGy. However, a dose dependent decrease was noted thereafter (Table 1). A decrease in Young's modulus signifies a reduction in stiffness of films i.e. films prepared become more amenable to deformation.

GG films prepared from control samples were also directly subjected to irradiation processing and its impact on their tensile strength is shown in Table 2. No significant ($p < 0.05$) impact on tensile strength and Young's modulus was observed due to radiation processing up to a dose of 25 kGy and 50 kGy, respectively. Beyond these doses the tensile strength and Young's modulus showed a dose dependent decrease (Table 2). This decrease was however lesser when films were directly irradiated compared to films prepared from irradiated GG.

Effect of radiation on puncture strength of films was also evaluated. Puncture strength of control GG films was 2.3 ± 0.2 N. A radiation dose dependent decrease in puncture strength of GG films was observed. The puncture strength reduced to 1.2 ± 0.1 N at 10 kGy, and thereafter to 0.8 ± 0.2 N at 50 kGy (Table 1). Films prepared from control GG and subjected to irradiation processing demonstrated no significant change in puncture strength up to a dose of 10 kGy; however it decreased to 1.6 ± 0.3 N and 0.9 ± 0.1 N at 25 kGy and 100 kGy, respectively (Table 2).

Percent elongation indicates the flexibility of films. The films prepared from non-irradiated GG demonstrated 13.9 ± 4.5 percent elongation. In a previous study on GG films (Mikkonen et al., 2007), percent elongation was observed to be 40 percent. In the present study, GG was purified to remove all insoluble impurities before film preparation. This might have resulted in decreased percent elongation. No trend was observed on the percent elongation of films prepared from irradiated GG and for GG films subjected directly to irradiation (Tables 1 and 2). Similar results were also found for percent elongation by Zhai et al. (2003), for irradiation of

Table 2
Effect of irradiation on mechanical and barrier properties and color co-ordinates of guar gum films. Films prepared from control guar gum and irradiated thereafter.

Dose (kGy)	Tensile strength (MPa)	Young's modulus (MPa)	Puncture strength (N)	% Elongation	Water vapor transmission rate (gm/m^2/day)	L^* (Black to white)	a^* (Green to magenta)	b^*(Blue to yellow)	Opacity (%)
0	60.5 ± 8.7^{a}	162 ± 23^{a}	2.3 ± 0.2^{a}	13.9 ± 4.5^{ab}	190 ± 10^{a}	97.2 ± 0.6^{a}	0.6 ± 0.2^{a}	1.1 ± 0.2^{f}	12.9 ± 0.2^{d}
1	51.9 ± 1.1^{a}	158 ± 33^{a}	2.1 ± 0.1^{a}	12 ± 3.9^{ab}	190.8 ± 11.1^{a}	95 ± 0.6^{b}	$.02 \pm .01^{e}$	0.3 ± 0.1^{c}	13.8 ± 0.4^{ab}
5	55.9 ± 4.5^{a}	177 ± 36^{a}	2.3 ± 0.2^{a}	12.3 ± 5.5^{ab}	188.3 ± 8^{a}	94.7 ± 0.4^{b}	0.4 ± 0.1^{bc}	0.7 ± 0.1^{e}	13.3 ± 0.3^{cd}
10	51.8 ± 5.2^{a}	148 ± 25^{ab}	2 ± 0.3^{ab}	15 ± 0.9^{ab}	185.6 ± 6.2^{ab}	94.8 ± 0.8^{b}	0.2 ± 0.1^{de}	$.04 \pm .02^{d}$	13.5 ± 0.2^{bc}
25	58.5 ± 3.8^{a}	166 ± 29^{a}	1.6 ± 0.3^{bc}	18.5 ± 5.1^{a}	192.9 ± 3.8^{a}	93.7 ± 0.4^{bc}	0.3 ± 0.1^{cd}	$0.3 \pm .01^{c}$	14.2 ± 0.3^{a}
50	43.1 ± 1.2^{b}	151 ± 29^{ab}	1.4 ± 0.3^{c}	9.3 ± 1.7^{b}	183.9 ± 4.7^{ab}	93 ± 0.4^{c}	0.5 ± 0.1^{ab}	$.01 \pm .01^{d}$	13.2 ± 0.1^{cd}
100	40.9 ± 5.3^{b}	101 ± 20^{b}	0.9 ± 0.1^{d}	17.5 ± 3.6^{a}	181 ± 6.5^{ab}	93.3 ± 1^{c}	0.7 ± 0.1^{g}	3.1 ± 0.2^{a}	14.1 ± 0.2^{a}

Any two means in the same column followed by the same letter are not significantly ($p > 0.05$) different.

starch based plastic film. Thus, our results are in concurrence with earlier studies.

3.3. Characterization of guar gum by small angle X-ray scattering (SAXS)

Conformation of unirradiated and irradiated (500 Gy and 50 kGy) GG was analyzed by small angle X-ray scattering. The SAXS profiles for the control and different dose treated polymer are shown in Fig. 5. In the present case, the interpretation the SAXS scattering data is based on the analysis of the scattering curve, which showed the dependence of the scattering intensity, I, on the scattering wave vector q. The scattered intensity as a function of q for the three solutions (Fig. 5), shows a power law behavior [$I(q) \sim q^{-d}$]. The slope of the linear region in $\log I(q)$ vs. $\log q$ plot gives the value of the exponent d, the dimensionality of the scattering object. Typically, the exponent $d = 2$ is exhibited by Gaussian chains in case of polymer. The scattering curve for the control polymer and 50 kGy treated polymer show a q^{-2} dependence in the experimental q range. However, for the 500 Gy dose treated polymer, in addition to the q^{-2} dependence a prominent peak at high q is also observed (Fig. 5). This prominent peak probably arises due to correlations of short length scales, with the inter-chain correlation length, $\xi = 2\pi/q^*$(where q^* is the peak position). The peak position was found to be 1.74 nm^{-1}.The correlation length ξ was calculated as 3.6 nm. The scattering profile for control and 50 kGy treated polymer is modeled by assuming Gaussian coiled chain, the formula used for (Eq. (9)):

$$Igc(q) = \frac{2\left[\exp(-q^2R_g^2) - 1 + q^2R_g^2\right]}{q^4R_g^4} \quad (9)$$

where R_g is the typical chain length of the polymer.

To account the ordering of the polymer treated up to 500 Gy, a hard sphere structure factor $S(\varphi, r_{hs})$ (Pedersen, 1994) was taken into account where φ is the local packing fraction of the polymer and $2r_{hs}$ is the typical correlation length. The scattering intensity for the 500 Gy treated polymer can be written as:

$$I(q) = Igc(q) \times S(\varphi, r_{hs}) \quad (10)$$

It is evident from Fig. 5 that above discussed model fit the data quite satisfactorily. The typical chain length R_g for all the specimens was found to be ~ 20 nm. The correlation length $2r_{hs}$ was found to be 3.2 nm which is approximately same as that estimated from the peak position (ξ). The local packing fraction of the chain is found to be 0.22. Thus, it is clear from the SAXS analysis the conformation of the GG polymer chain do not undergo modification under different radiation doses under present probed length scale. However, for lower dose of 500 Gy, the ordering of the chains occurs with typical correlation length of 3.6 nm and local packing fraction of 0.22. Thus, the possibility of ordering of chains resulting in better orientation of GG polymers during film formation and increased tensile strength at lower dose up to 500 Gy is suggested.

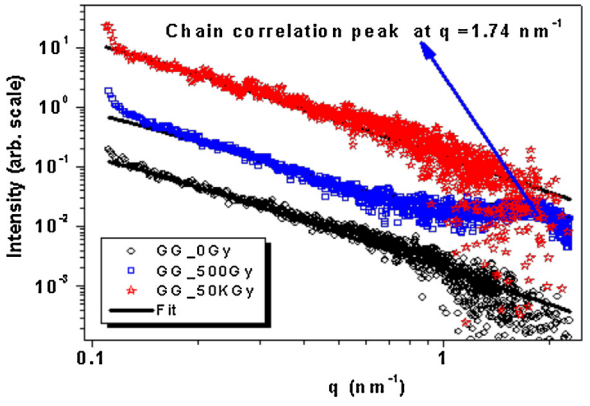

Fig. 5. The small angle X-ray scattering (SAXS) profiles of the control and irradiated (500 Gy, 50 kGy) GG.

3.4. Effect of radiation on water vapor transmission rate of guar gum based films

WVTR of control GG films was 190 ± 10 gm/m^2/day. Aydinli et al. (2004) found water vapor transmittance rate for locust bean gum plasticized with PEG 200 and PEG 1000 to be 251 gm/m^2/day and 136 gm/m^2/day, respectively. Radiation significantly ($p < 0.05$) affected WVTR of films. Films made from irradiated GG powder had WVTR of 160.6 ± 5.2 gm/m^2/day at 50 kGy (Table 1). Thus, an enhanced barrier to water vapor was noted in GG films prepared from GG powder irradiated at higher doses with no significant effect at doses less than 1 kGy. No significant effect of radiation was observed on the WVTR of films prepared from non-irradiated GG and subjected to irradiation processing thereafter (Table 2). These results are in good agreement with Kim et al. (2008) who concluded that radiation treatment of biomaterials may result in more compact structure (because of lower molecular weight fragments) and could help natural polymers to overcome their hydrophilic character.

3.5. Color and opacity of guar gum films

Values for color coordinates i.e. L^*, a^* and b^* are shown in Tables 1 and 2. No significant ($p < 0.05$) differences were obtained in L^* values for films prepared with irradiated guar gum. Films prepared with GG irradiated at lower doses up to 500 Gy demonstrated slightly higher a^* values as compared to control films indicating increased redness of films. However at higher doses beyond 500 Gy a^* values were comparable to that of control. No statistical significant ($p < 0.05$) difference was obtained in b^* values for films prepared with irradiated GG. For films prepared with control GG and subjected to radiation processing thereafter a significant dose dependent reduction in L^* values were observed indicating

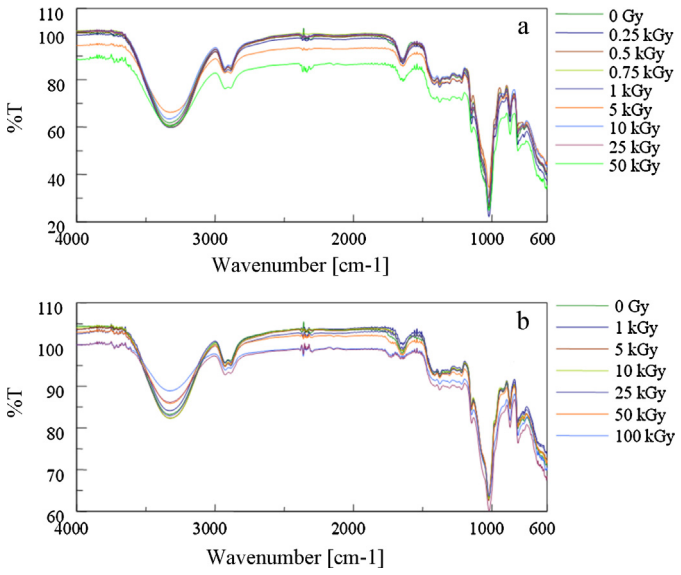

Fig. 6. FTIR profiles of GG films: (a) films prepared from irradiated GG; (b) control GG films then subjected to irradiation.

increased darkness of films. At very high doses of 100 kGy increased b^* values were observed. Increase in b^* values indicate increase yellowness of films. Jo et al. (2005) also reported similar results for irradiated pectin and gelatin based films i.e. with dose decrease in L^* and a^* values and increase in b^* values.

Opacity indicates degree to which light is not allowed to pass through. Opacity of packaging films is important as it affect the packaged products visibility to consumers. A significantly higher opacity was observed in films prepared with irradiated GG as well as films subjected to radiation processing after preparation, as compared to control samples. Observed increase in opacity might be due to increased darkness or redness in irradiated samples. Although, significant variance was observed instrumentally in color and opacity of samples after irradiation visual differences were negligible to be discerned by naked eye.

3.6. FTIR analysis of films

To compare the changes in chemical structure of control and gamma irradiated guar gum films, FTIR spectra was recorded. Fig. 6 shows FTIR spectra of control as well as irradiated gaur gum films. IR spectra of films prepared with irradiated GG and films subjected to radiation processing after preparation were superimposable with control films. Gupta et al. (2009) reported no change in FTIR spectrum of control and irradiated guar gum. Above results suggests that during radiation processing there are no major functional group transformations but only random free radical chain scission in GG due to irradiation.

4. Conclusion

Radiation processing of GG resulted in decrease in molecular weight of GG as analyzed by Ostwald viscometer and gel permeation chromatography. No significant change was observed in mannose:galactose ratio of GG due to radiation processing. Enhanced tensile strength of GG films was observed in the present study as compared to reported values in literature due to the purification procedure followed. Irradiation of GG in powder form up to 500 Gy resulted in 32.6% increase in tensile strength of its films. SAXS studies demonstrated that partial ordering of the polymer chains at a low dose of 500 Gy resulted in an increase in tensile strength. A dose dependent decrease in tensile and puncture strength of films was observed. Films prepared from unirradiated GG and subjected to irradiation processing thereafter exhibited stability up to 25 kGy without significant loss in its mechanical and barrier properties. Thus, these films can be suitably employed for food irradiation applications without loss of functionality. In conclusion, purification of GG combined with low dose irradiation can improve the mechanical properties of the films produced by it.

References

Aydinli, M., Tutas, M., & Bozdemir, O. A. (2004). Mechanical and light transmittance properties of locust bean gum based edible films. *Turkish Journal of Chemistry*, *28*, 163–171.

Beer, M. U., Wood, P. J., & Weisz, J. (1999). A simple and rapid method for evaluation of Mark–Houwink–Sakurada constants of linear random coil polysaccharides using molecular weight and intrinsic viscosity determined by high performance size exclusion chromatography: Application to guar galactomannan. *Carbohydrate Polymers*, *39*, 377–380.

Byun, E. H., Kim, J. H., Sung, N. Y., Choi, J. I., Lim, S. T., Kim, K. H., Yook, H. S., Byun, M. W., & Lee, J. W. (2008). Effects of gamma irradiation on the physical and structural properties of β-glucan. *Radiation Physics and Chemistry*, *77*, 781–786.

Cerqueira, M. A., Lima, A. M., Teixeira, J. A., Moreira, R. A., & Vicente, A. A. (2009). Suitability of novel galactomannans as edible coatings for tropical fruits. *Journal of Food Engineering*, *94*, 372–378.

Cerqueira, M. A., Bourbon, A. I., Pinheiro, A. C., Martins, J. T., Souza, B. W. S., Teixeira, J. A., & Vicente, A. A. (2011). Galactomannans use in the development of edible films/coatings for food applications. *Trends in Food Science & Technology*, *22*, 662–671.

Cha, D. S., & Chinnan, M. S. (2004). Biopolymer-based antimicrobial packaging: A Review. *Critical Reviews in Food Science and Nutrition*, *44*, 223–237.

Chudzikowski, R. J. (1971). Guar gum and its applications. *Journal of the Society of Cosmetic Chemists*, *22*, 43–60.

Cunha, P. L. R., Castro, R. R., Rocha, F. A. C., Paula, R. C. M., & Feitosa, J. P. A. (2005). Low viscosity hydrogel of guar gum: Preparation and physicochemical characterization. *International Journal of Biological Macromolecules*, *37*, 99–104.

Cunha, P. L. R., Paula, R. C. M., & Feitosa, J. P. A. (2007). Purification of guar gum for biological applications. *International Journal of Biological Macromolecules*, *41*, 324–331.

Das, D., Ara, T., Dutta, S., & Mukherjee, A. (2011). New water resistant biomaterial biocide film based on guar gum. *Bioresource Technology*, *102*, 5878–5883.

Garcia, N. L., Ribba, L., Dufresn, A., Aranguren, M., & Goyanes, S. (2011). Effect of glycerol on the morphology of nanocomposites made from thermoplastic starch and starch nanocrystals. *Carbohydrate Polymers*, *84*, 203–210.

Ghasemlou, M., Khodaiyan, F., Oromiehie, A., & Yarmand, M. S. (2011). Development and characterization of a new biodegradable edible film made from kefiran, an exopolysaccharide obtained from kefir grains. *Food Chemistry*, *127*, 1496–1502.

Glatter, O., & Kratky, O. (1982). *Small angle X-ray scattering*. London: Academic Press.

Gupta, S., Shah, B., Sanyal, B., Variyar, P. S., & Sharma, A. (2009). Role of initial apparent viscosity and moisture content on post irradiation rheological properties of guar gum. *Food Hydrocolloids*, *23*, 1785–1791.

Hwang, I. T., Jung, C. H., Kuk, I. S., Choi, J. H., & Nho, Y. C. (2010). Electron beam-induced crosslinking of poly(butylene adipate-co-terephthalate). *Nuclear Instruments and Methods in Physics Research Section B: Beam Interactions with Materials and Atoms*, *268*, 3386–3389.

Jo, C., Kang, H., Lee, N. Y., Kwon, J. H., & Byun, M. W. (2005). Pectin- and gelatin-based film: Effect of gamma irradiation on the mechanical properties and biodegradation. *Radiation Physics and Chemistry*, *72*, 745–750.

Jumel, K., Harding, S. E., & Mitchell, J. R. (1996). Effect of gamma irradiation on the macromolecular integrity of guar gum. *Carbohydrate Research*, *282*, 223–236.

Kang, H. J., Jo, C., Lee, N. Y., Kwon, J. H., & Byun, M. W. (2005). A combination of gamma irradiation and $CaCl_2$ immersion for a pectin-based biodegradable film. *Carbohydrate Polymers*, *60*, 547–551.

Kang, H. J., & Min, S. C. (2010). Potato peel-based biopolymer film development using high-pressure homogenization, irradiation, and ultrasound. *LWT – Food Science and Technology*, *43*, 903–909.

Kim, J. K., Jo, C., Park, H. J., & Byun, M. W. (2008). Effect of gamma irradiation on the physicochemical properties of a starch-based film. *Food Hydrocolloids*, *22*, 248–254.

Mangiacapra, P., Gorrasi, G., Sorrentino, A., & Vittoria, V. (2006). Biodegradable nanocomposites obtained by ball milling of pectin and montmorillonites. *Carbohydrate Polymers*, *64*, 516–523.

Martins, J. T., Cerqueira, M. A., Souza, B. W., Carmo, A. M., & Vicente, A. A. (2010). Shelf life extension of ricotta cheese using coatings of galactomannans from nonconventional sources incorporating nisin against listeria monocytogenes. *Journal of Agriculture and Food Chemistry*, *58*, 1884–1891.

Mikkonen, K. S., Rita, H., Helen, H., Talja, R., Hyvonen, A., & Tenkanen, L. M. (2007). Effect of polysaccharide structure on mechanical and thermal properties of galactomannan-based films. *Biomacromolecules*, *8*, 3198–3205.

Pedersen, J. S. (1994). Determination of size distribution from small-angle scattering data for systems with effective hard-sphere interactions. *Journal of Applied Crystallography*, *27*, 595–608.

Petersson, L., & Oksman, K. (2006). Biopolymer based nanocomposites: Comparing layered silicates and microcrystalline cellulose as nanoreinforcement. *Composites Science and Technology*, *66*, 2187–2196.

Rhim, J. W., & Perry, K. W. Ng. (2007). Natural biopolymer-based nanocomposite films for packaging applications. *Critical Reviews in Food Science and Nutrition*, *47*, 411–433.

Vachon, C., Yu, H. L., Yefsah, R., Alain, R., Gelais, D. S., & Lacroix, M. (2000). Mechanical and structural properties of milk protein edible films cross-linked by heating and gamma-irradiation. *Journal of Agriculture and Food Chemistry*, *48*, 3202–3209.

Vega, M. P., Lima, E. L., & Pinto, J. C. (2001). In-line monitoring of weight average molecular weight in solution polymerizations using intrinsic viscosity measurements. *Polymer*, *42*, 3909–3914.

Winokur, M. J., Skotheim, T. A., Elsenbaumer, R. L., & Reynolds, J. R. (1998). *Handbook of conducting polymers* (2nd edition, pp. 707). New York, USA: Dekker.

Zhai, M., Yoshii, F., & Kume, T. (2003). Radiation modification of starch-based plastic sheets. *Carbohydrate Polymers*, *52*, 311–317.

Carbohydrate Polymers 124 (2015) 77–84

Contents lists available at ScienceDirect

Carbohydrate Polymers

journal homepage: www.elsevier.com/locate/carbpol

Mechanical and barrier properties of guar gum based nano-composite films

Chaturbhuj K. Saurabh[a,1], Sumit Gupta[a,1], Jitendra Bahadur[b], S. Mazumder[b], Prasad S. Variyar[a,*], Arun Sharma[a]

[a] Food Technology Division, Bhabha Atomic Research Centre, Trombay, Mumbai 400 085, India
[b] Solid State Physics Division, Bhabha Atomic Research Centre, Trombay, Mumbai 400 085, India

ARTICLE INFO

Article history:
Received 10 January 2014
Received in revised form
18 November 2014
Accepted 3 February 2015
Available online 12 February 2015

Keywords:
Guar gum
Nanoclay
Biodegradable film
Irradiation
X-ray scattering

ABSTRACT

Guar gum based nano-composite films were prepared using organically modified (cloisite 20A) and unmodified (nanofil 116) nanoclays. Effect of nanoclay incorporation on mechanical strength, water vapor barrier property, chromatic characteristics and opacity of films was evaluated. Nano-composites were characterized using X-ray scattering, FTIR and scanning electron microscopy. A nanoclay concentration dependent increase in mechanical strength and reduction in water vapor transmission rate was observed. Films containing nanofil 116 (2.5% w/w guar gum) and closite 20A (10% w/w guar gum) demonstrated a 102% and 41% higher tensile strength, respectively, as compared to the control. Lower tensile strength of cloisite 20A films as compared to nanofil 116 films was due to its incompatibility with guar gum. X-ray scattering analysis revealed that interstitial spacing between nanofil 116 and cloisite 20A sheets increased due to intercalation by guar gum polymer. This resulted in improved mechanical and barrier properties of nano-composites compared to control.

1. Introduction

Conventional packaging materials are derived from non-renewable petroleum resources and their disposal is of prime concern because of non-biodegradability and non-economical recycling procedures (Garcia, Rubio, & Lagaron, 2010). Therefore, it is of interest to overcome the disadvantage of petrochemical based plastics by developing biodegradable packaging material from natural sources such as polysaccharides, proteins and lipids. However, relatively poor mechanical and barrier properties of biopolymers as compared to petroleum based packaging materials limit their commercialization. One possible approach for the improving mechanical and barrier characteristics of biopolymer films is to make nano-hybrid composite films by mixing with inorganic nano size clays (Avella et al., 2005; Rhim, Hong, Park, & Perry, 2006; Rhim, Hong, & Ha, 2009).

Among the inorganic nano size clays, Montmorillonite (MMT) has been extensively used for preparation of polymer nano-composites. MMT consists of inorganic layered silicates several hundred nanometers long having layer spacing of few nanometers. Hundreds of such layered platelets are stacked into particles or tactoids (Arora & Padua, 2010). These layered silicates significantly affect the properties of nano-composite films. The size range of nanoclay is around 100 nm in one or more dimensions (Bradley, Castle, & Chaudhry, 2011). Due to its nano scale size it interacts with matter at the atomic, molecular, or macromolecular level (Almasi, Ghanbarzadeh, & Entezami, 2010). Intercalation and exfoliation are two approaches that are widely used for the dispersion of nanoclay in polymeric matrices. Intercalation results in moderate penetration of polymeric chain into nanoclay basal spacing resulting in slight expansion of interlayer spaces without disturbing the shape of layered stack. In exfoliation the layered structure loses its shape and forms single sheet that behaves likes a homogenous mixture within the polymeric solution (Uhl, Davuluri, Wong, & Webster, 2004; Arora & Padua, 2010).

For development of renewable source based biodegradable packaging material guar gum (GG) can be a potential candidate because of its long polymeric chain, high molecular weight and wide availability as compared to other biopolymers. India accounts for 80% of world production of GG. It is a galactomannan with mannose to galactose ratio of 1.6 and is derived from endosperm of an annual legume plant *Cyamopsis tetragonoloba* (Cunha, Castro,

* Corresponding author. Tel.: +91 22 25590560; fax: +91 22 25505151.
E-mail addresses: pvariyar@barc.gov.in, prasadpsv@rediffmail.com (P.S. Variyar).
[1] These authors contributed equally.

http://dx.doi.org/10.1016/j.carbpol.2015.02.004
0144-8617/

Rocha, Paula, & Feitosa, 2005). It consists of mannose backbone linked by (1–4) β-D-mannopyranose with galactose as a side group linked by (1–6) α-D-galactopyranose (Fernandes, Goncalves, & Doublier, 1993). Very few reports exist on GG based biodegradable packaging film. Das, Ara, Dutta, and Mukherjee (2011) developed a water resistance biocide film by intrinsically modifying GG into GG benzamide. Enzymatic depolymerization was also previously reported to improve mechanical properties of GG based films (Mikkonen et al., 2007).

Gamma irradiation has proved to be a convenient tool for inducing cross-links between polymer and nanoclay of the nanocomposite films resulting in improved functional properties of biobased films (Xu et al., 2012). Gamma radiation after interacting with biopolymers leads to the formation of very reactive intermediates such as excited states, ions, and free radicals (Khan et al., 2010). The presence of clay stimulated the formation of such radicals from biopolymer and also sustained the life of radicals longer which resulted in high efficiency of cross-linking in the nanocomposite (Ibrahim, 2011). We had earlier demonstrated that low doses of gamma radiation (≥500 Gy) resulted in improved mechanical properties of GG films due to the ordering of polymer structures as confirmed by small angle X-ray scattering analysis (Saurabh et al., 2013). Other reports suggest that gamma radiation improved films characteristics by inducing cross linking of polymeric chains (Kang, Jo, Lee, Kwon, & Byun, 2005; Kim, Jo, Park, & Byun, 2008). However, to the best of our knowledge no reports exists till date on the combined effect of gamma irradiation and incorporation of nanoclays on the mechanical and barrier properties of GG based biodegradable films. In the present work two types of commonly used nanoclays i.e. nanofil 116 and cloisite 20A were incorporated into GG films and its mechanical and barrier properties were subsequently analyzed. The effect of gamma irradiation on the physical properties of the films thus prepared was also evaluated.

2. Materials and methods

2.1. Purification of GG

Purification of GG was carried out as per procedure described earlier by Jumel, Harding, and Mitchell (1996). In brief, 2.5 g of GG (Merck India ltd.) was dissolved in 250 mL of distilled water by using shear mixer (Omni mixer, Sorvall, USA) at speed 2 for 2 min. Solution obtained was kept overnight at room temperature (25 ± 2 °C) on magnetic stirrer. Resulting solution was centrifuged for 30 min at 9000 rpm for removal of insoluble impurities. Ethanol in the proportion of 2:1 was added to the supernatant and resulting mixture was kept overnight for precipitation of GG. The precipitate obtained was freeze dried to obtain dry purified GG powder. A 60% yield was obtained by above purification procedure.

2.2. Dispersion of nanoclay

Cloisite 20A is a natural MMT modified with a quaternary ammonium salt while nanofil 116 is an inorganic nano-dispersible layered silicate based on a refined natural bentonite. Both the clays were obtained as a gift sample from Southern Clay Products, Inc., US. Rockwood Additives Ltd., UK. Different dilutions of aqueous nanoclay suspensions (0.01, 0.025, 0.05, 0.075, 0.1 and 0.2% w/v of distilled water) were prepared and then separately kept on magnetic stirrer for 7 days at low temperature (5 ± 0.5 °C) to avoid microbial contamination. After 7 days of mixing, obtained nanoclay suspension was centrifuged at 4000 rpm for 10 min at 10 °C to pellet out nanoclay tactoids.

2.3. Preparation of nano-composite films

Purified GG was added to different dilutions of dispersed nanoclays suspension (150 mL) prepared as detailed above to make 1% w/v aqueous solution. Thus the amount of nanoclay on w/w basis with respect to GG was 1, 2.5, 5, 7.5, 10 and 20%. Glycerol (0.6 g i.e. 40% w/w of GG) was added as plasticizer and mixture obtained was kept overnight at room temperature (25 ± 2 °C) on magnetic stirrer for intercalation of polymer in nanoclay sheets. Solution thus obtained was centrifuged at 3000 rpm for 15 min for the removal of air bubbles. 150 mL of solution was poured and spread evenly onto surface of glass plate (21 cm × 21 cm), having removable boundary of insulating tape. For drying, plates were then kept in oven for 8 h at 80 °C. Dried nano-composite films were conditioned at 50% relative humidity at room temperature (25 ± 2 °C) for 7 days. After conditioning films were peeled and subjected to physical and mechanical analysis.

2.4. Irradiation of nano-composite film

GG based films incorporated with 2.5% nanofil 116 or 10% cloisite 20A were subjected to gamma irradiation (1, 5, 10, 25, 50 and 100 kGy) at room temperature in ^{60}Co gamma irradiator (GC-5000, BRIT, India, dose rate 3.6 kGy/h). The treated films were conditioned as mentioned above (Section 2.3) prior to analysis of their physical and barrier properties.

2.5. Physical and mechanical properties of nano-composite films

Films were cut into strips of dimension 2 cm × 15 cm. Film thickness was determined by using micrometer (103–131, Mitutoyo, Japan). Measurements were randomly taken at three different locations on each film strip. The lowest value of thickness of each strip was used in calculations for the tensile strength and Young's modulus of the same strip. Mechanical properties i.e. tensile strength, Young's modulus, puncture strength and percent elongation of films were analyzed using a texture analyzer (TA. HD. Plus, Stable Micro Systems). The American Society of Testing and Materials (ASTM) standard method D882-10 was used to measure the tensile strength, Young's modulus and percent elongation at break (% E) of films. Puncture strength of films (5 cm × 2 cm) were determined by 2 mm needle probe having pre test speed of 10 mm/s and test speed of 0.5 mm/s. Water vapor transmission rate (WVTR) of films were determined by using round cups having 100 mL volume capacity and 120 cm^2 mouth area. The cup was filled with 60 mL of distilled water and sealed with films prepared using adhesive tapes. This assembly was kept in desiccators at 25 ± 2 °C and 87% relative humidity. The mass of water lost from the cup was monitored as a function of time, and the WVTR was calculated when steady-state was achieved. Color of films were determined using a colorimeter (CM-3600d Konica Minolta sensing Inc., Japan) by measuring L^*, a^* and b^* values. Instrument was calibrated using a white tile supplied along with the equipment. Source used was D65 with observer set at 10°. Opacity of films was determined using Hunter lab method, as the relationship between reflectance of each sample on black standard and the reflectance on white standard using the following equation:

$$\text{Opacity} = \left(Y_b/Y_w\right) \times 100 \quad (1)$$

All measurements were carried out in triplicates at room temperature 25 ± 2 °C and 50% relative humidity.

2.6. X-rays scattering measurements

SAXS (Small angle X-rays scattering) measurements were performed on the cloisite 20A composite films (films were 4 times

Table 1
Physical properties of GG based nanofil 116 composites.

Nanofil116 (w/w GG) (%)	Tensile strength (MPa)	Young's modulus (GPa)	Puncture strength (N)	% Elongation	WVTR ($g/m^2/d$)	L^*	a^*	b^*	Opacity (%)
0	56 ± 7^{b}	0.2 ± 0.1^{f}	1.8 ± 0.3^{a}	17 ± 5.5^{a}	170 ± 23^{a}	98.7 ± 0.6^{a}	0.6 ± 0.2^{a}	1.1 ± 0.2^{bc}	12.9 ± 0.2^{cd}
1	56 ± 12^{b}	0.6 ± 0.4^{d}	1.5 ± 0.3^{ab}	15 ± 4.5^{a}	153 ± 21^{ab}	98 ± 0.3^{a}	-0.5 ± 0.1^{b}	0.8 ± 0.1^{c}	12.1 ± 0.6^{d}
2.5	113 ± 20^{a}	11 ± 0.8^{a}	1.6 ± 0.3^{ab}	11 ± 3^{a}	128 ± 19^{bc}	97.9 ± 0.7^{a}	-0.6 ± 0.1^{b}	1 ± 0.1^{bc}	12.4 ± 0.7^{cd}
5	91 ± 13^{a}	9.5 ± 0.8^{b}	1.7 ± 0.3^{ab}	18 ± 4^{a}	112 ± 10^{c}	95.3 ± 0.8^{b}	-1.2 ± 0.2^{c}	1.3 ± 0.2^{b}	12.4 ± 0.9^{cd}
7.5	98 ± 17^{a}	9.7 ± 0.2^{b}	1.7 ± 0.2^{a}	13 ± 3^{a}	104 ± 16^{c}	94.8 ± 0.9^{b}	-1.5 ± 0.3^{c}	1.4 ± 0.2^{b}	13.5 ± 0.8^{bc}
10	94 ± 14^{a}	7.5 ± 0.5^{c}	1.9 ± 0.3^{a}	16 ± 5.5^{a}	102 ± 13^{c}	90.6 ± 0.6^{c}	-2.2 ± 0.3^{d}	1.9 ± 0.3^{a}	14.5 ± 0.4^{ab}
20	36 ± 9^{b}	1.7 ± 0.3^{e}	1.2 ± 0.3^{b}	13 ± 3^{a}	109 ± 12^{c}	89.7 ± 0.5^{c}	-2.4 ± 0.3^{d}	2.1 ± 0.4^{a}	14.8 ± 1^{a}

Any two means in the same column followed by the same letter are not significantly ($p > 0.05$) different.

folded) and powder cloisite 20A at a lab based SAXS setup using Cu$K\alpha$ source. The size of incident photon beam on the sample was 0.4 mm diameter. The SAXS detector was mounted at a sample to detector distance of 1.07 m, corresponding to a q-range of 0.1–2.5 nm^{-1}. The magnitude of the scattering wave vector, q equals:

$$q = 2\sin\theta/\lambda = q/2\pi \quad (2)$$

where 2θ is the scattering angle and $\lambda = 0.154$ nm the used wavelength of X-ray beam.

Interlayer distance (d or d-spacing) between clay layers can be estimated from:

$$d = 2\pi/q \quad (3)$$

X-ray powder diffraction (XRD) measurements were performed on nanofil 116 powder and nanofil 116 composite films (films were 4 times folded). XRD patterns were obtained on a Philips PW-1820 powder diffractometer using Cu$K\alpha$ radiation. The X-ray tube rating was maintained at 30 kV and 20 mA. The goniometer was calibrated for correct zero position using silicon standard. Interlayer distance between clay layers can be estimated from Bragg's equation (Kasai & Kakudo, 2005):

$$d = \lambda/\left(2\sin(\theta)\right) \quad (4)$$

2.7. Field emission gun–scanning electron microscopes (FEG–SEM)

The surface morphology of films was analyzed by FEG–SEM. The scanning electron micrographs were taken with a JSM-7600F instrument (Joel, Japan). A sputter coater was used to pre coat conductive gold onto the films surface before observing the microstructure at 25 kV.

2.8. FTIR analysis of nano-composite films

Spectra of films were scanned in the range of 4000–600 cm^{-1} on a FTIR (FT/IR 4100, Jasco) spectrometer. ATR assembly was used for obtaining FTIR spectra. Films were directly pressed on ATR assembly and spectra were recorded. 40 scans were taken for each film sample.

2.9. Statistical analysis

DSAASTAT ver. 1.101 by Andrea Onofri was used for statistical analysis of data. Three samples were taken for every treatment and each sample was further analyzed in triplicate. Data was analyzed by Analysis of variance (ANOVA) and multiple comparisons of means were carried out using Duncan's multiple range test.

3. Results and discussion

3.1. Effect of type and concentration of nanoclay on tensile strength and Young's modulus of nano-composites

Thickness of native GG films was found to be 15.2 ± 2.3 μm. No significant ($p < 0.05$) effect was observed on thickness of films due to addition of nanoclays. Rhim et al. (2006) also reported no significant change in thickness between chitosan based nano-composite film and neat chitosan film.

Tensile strength is the maximum stress that a material can withstand while being stretched or pulled before failing or breaking. Rigidity of the film is indicated by Young's modulus or modulus of elasticity, and higher the modulus, the more rigid is the film. A significant ($p < 0.05$) concentration dependent increase in tensile strength and Young's modulus as compared to control GG films was observed due to incorporation of both nanoclays (Tables 1 and 2). Nano-composites prepared by incorporating nanofil 116 demonstrated highest tensile strength and Young's modulus at a concentration of 2.5%, while the best mechanical properties for cloisite 20A containing films was observed at a concentration of 10%. Nanofil 116 incorporation (2.5%) resulted in films with tensile strength of 113 ± 20 MPa and Young's modulus of 11 ± 0.8 GPa (Table 1) while the values for these mechanical properties for cloisite 20A (10%) containing films were 79 ± 8 MPa and 1.8 ± 0.2 GPa, respectively (Table 2). Control films had a tensile strength of 56 ± 7 MPa and Young's modulus of 0.2 ± 0.1 GPa (Table 1). This observed improvement in mechanical properties of nano composites could be due to the nano level interactions of clay with the polymer matrix resulting in greater possibility of energy transfer from polymer to clay layered silicates (Pandey, Raghunatha, Pratheep, & Singh, 2005). Improved mechanical properties of biodegradable films by formation of clay nano-composites were previously reported for several polymers such as polyethyl acrylate (Tong, Zhao, Tang, Feng, & Huang, 2002), starch (Ibrahim, 2011; Avella et al., 2005; Kampeerapappun, Aht-ong, Pentrakoon, & Srikulkit, 2007), pectin (Mangiacapra, Gorrasi, Sorrentino, & Vittoria, 2006) and agar (Rhim, 2011). Thus our results are in agreement with already published literature data.

Incorporation of either of the nanoclay beyond concentration of 10% in films resulted in a significant ($p < 0.05$) reduction in mechanical properties as compared to control films (Tables 1 and 2). Negative impact of clay loading in films at higher concentration (>10%) is mainly attributed to agglomeration of clay particles resulting in formation of stacked clays without complete dispersion through the polymer matrix. This leads to non-homogenous distribution of clay in the film thus forming cracks and reduction in mechanical strength (Chang, An, & Sur, 2003).

In the present study, the maximum increase in tensile strength as compared to control film was 102% for 2.5% nanofil 116 films and 41% for 10% cloisite containing films (Tables 1 and 2). Whereas, in previous studies a 31.5% increase for agar based 10% cloisite Na^+ clay nano-composite films (Rhim, 2011) and 88% increase for

Table 2
Physical properties of GG based cloisite 20A composites.

Cloisite 20A (w/wGG) (%)	Tensile strength (MPa)	Young's modulus (GPa)	Puncture strength (N)	% Elongation	WVTR (g/m^2/d)	L^*	a^*	b^*	Opacity (%)
0	56 ± 7^{c}	0.2 ± 0.1^{d}	1.8 ± 0.3^{a}	17 ± 5.5^{a}	170 ± 23^{a}	98.7 ± 0.6^{a}	0.6 ± 0.2^{a}	1.1 ± 0.2^{bc}	12.9 ± 0.2^{bc}
1	53 ± 11^{c}	0.6 ± 0.1^{c}	1.4 ± 0.2^{ab}	16 ± 3.5^{a}	157 ± 10^{a}	98.9 ± 0.3^{a}	-0.2 ± 0.1^{b}	0.9 ± 0.1^{c}	12.3 ± 0.4^{c}
2.5	62 ± 10^{bc}	0.7 ± 0.1^{c}	1.6 ± 0.1^{ab}	16 ± 5^{a}	132 ± 10^{b}	98.4 ± 0.7^{a}	-0.7 ± 0.2^{c}	1 ± 0.1^{bc}	12.6 ± 0.7^{c}
5	67 ± 12^{abc}	1.2 ± 0.3^{b}	1.7 ± 0.3^{ab}	13.5 ± 5^{a}	125 ± 9^{b}	95.7 ± 0.8^{b}	-0.9 ± 0.2^{cd}	1.1 ± 0.2^{bc}	12.8 ± 0.9^{c}
7.5	77 ± 8^{ab}	1.5 ± 0.2^{b}	1.8 ± 0.1^{a}	17 ± 3.5^{a}	121 ± 9^{b}	94.2 ± 0.6^{c}	-1.2 ± 0.3^{d}	1.3 ± 0.2^{b}	13.4 ± 0.7^{abc}
10	79 ± 8^{a}	1.8 ± 0.2^{a}	1.6 ± 0.2^{ab}	16 ± 3^{a}	124 ± 9^{b}	91.8 ± 0.6^{d}	-1.9 ± 0.3^{e}	1.7 ± 0.3^{a}	14.1 ± 0.7^{ab}
20	25 ± 2^{d}	1.2 ± 0.1^{b}	1.2 ± 0.3^{b}	21.5 ± 4.5^{a}	129 ± 8^{b}	90.9 ± 0.9^{d}	-2.3 ± 0.2^{e}	1.9 ± 0.1^{a}	14.6 ± 0.9^{a}

Any two means in the same column followed by the same letter are not significantly ($p > 0.05$) different.

3% pectin based natural MMT films (Mangiacapra et al., 2006) was reported. Thus, in the present study a higher improvement in tensile strength as compared to previous reports was observed especially in case of nanofil 116 (natural MMT). This might be due to the better compatibility between GG and nanofil 116. Another reason for observed results is that in present work mild treatment (stirring for seven days) for intercalation was given. However, in previous studies (Rhim, 2011; Mangiacapra et al., 2006) high shear mixing and ultrasonication was used. It is known that parallel sheet of nanoclay can break under high shear mixing as well as ultrasound (Hussain, Chen, & Hojjati, 2007; Yasmin, Abot, & Daniel, 2003). This could lead to the reduction in aspect ratio of nanoclay that negatively affects the mechanical properties of films.

It was also observed that mechanical properties of films prepared by incorporating nanofil 116 at concentrations of 2.5% and above were significantly ($p < 0.05$) superior as compared to films prepared with cloisite 20A (Tables 1 and 2) at similar concentrations. This might be due to the hydrophobic nature of the two tallow groups of cloisite 20A resulting in its uneven dispersion in hydrophilic GG polymeric matrices compared to nanofil 116. Mangiacapra et al. (2006) have also demonstrated better physical properties of apple peel pectin based nano-composites employing hydrophilic natural sodium MMT in comparison to organically (hydrophobic) modified clay.

3.2. Effect of type and concentration of nanoclay on puncture strength and percent elongation of nano-composite films

Puncture strength of nano-composite films were measured to determine the force required to penetrate the films. Puncture strength of control film was 1.8 ± 0.3 N. Nanoclay concentration (up to 10%) had no significant ($p < 0.05$) effect on the puncture strength (Tables 1 and 2). However, significant ($p < 0.05$) reduction (33%) in puncture strength as compared to control was observed in films incorporated with 20% of either nanoclays (Tables 1 and 2). Reduction in puncture strength at higher concentration (>10%) might be due to agglomeration of nanoclays. Few studies have been conducted in the past to determine the effect of nanoclay concentration on puncture strength of films. Nascimento, Calado, and Carvalho (2012) also found that addition of organoclay reduced the puncture strength of mesocarp flour of passion fruit (*Passiflora edulis*) based films.

Flexibility of a film is measured by elongation at break and it is defined as the ability of the film to deform before breaking. Control films had percent elongation of 17 ± 5.5. No significant change ($p < 0.05$) was observed in percent elongation of the films due to incorporation of nanoclays (Tables 1 and 2). Chrissafis, Antoniadis, Paraskevopoulos, Vassiliou, and Bikiaris (2007) reported only 8% increase in percent elongation when cloisite 20A was added in poly ε-caprolactone film due to plasticizing effect of the MMT's organic modifier. Thus results presented in this study are in agreement with previous reports.

3.3. X-ray scattering

SAXS patterns of cloisite 20A powder and GG-cloisite 20A (2.5%, 10%, and 20% w/w GG) nano-composite films are shown in Fig. 1A. Cloisite 20A powder showed a signature peak at q of 2.48. The d-spacing of cloisite 20A corresponding to this peak was calculated to be 2.53 nm. This was slightly higher than the reported d-spacing value of 2.48 nm (Kumar, Sandeep, Alavi, Truong, & Gorga, 2010). After seven days of intercalation the d-spacing of all cloisite 20A composite was 3.88 nm. XRD patterns of nanofil 116 powder and GG-nanofil 116 (2.5%, 10%, and 20% w/w GG) nano-composite films are shown in Fig. 1B. Nanofil 116 powder showed a diffraction peak at a 2θ angle of 7.06°. The d-spacing of nanofil 116 corresponding to the diffraction peak was calculated to be 1.25 nm. This was in agreement with the d-spacing value of 1.25 nm as reported earlier (Walley, Zhang, & Evans, 2012). After seven days of dispersion a 2θ angle of 4.8 corresponding to a d-spacing of 1.81 nm was noted for nanofil 116 composite. Thus, it is evident from the above results that basal spacing in nanoclays increased after seven days of stirring. Increased basal spacing resulted in a greater intercalation of nanoclays by GG polymer thus resulting in increased mechanical properties of nano-composites as compared to control. Similar results were also observed by Rhim (2011) for agar based cloisite Na^+clay composite films. In spite of higher basal spacing of cloisite 20A than nanofil 116, mechanical properties of cloisite 20A composite films were inferior to nanofil 116 containing films. This

Table 3
Effect of irradiation on physical properties of GG based 2.5% nanofil 116 composites.

Dose (kGy)	Tensile strength (MPa)	Young's modulus (GPa)	Puncture strength (N)	% Elongation	WVTR (g/m^2/d)	L^*	a^*	b^*	Opacity (%)
0	113 ± 20^{a}	11 ± 0.8^{b}	1.6 ± 0.3^{ab}	11 ± 3^{a}	128 ± 19^{a}	97.9 ± 0.7^{a}	-0.6 ± 0.1^{a}	1 ± 0.1^{e}	12.4 ± 0.7^{b}
1	108 ± 13^{a}	12 ± 1^{b}	1.7 ± 0.1^{a}	15 ± 2^{a}	132 ± 10^{a}	97.3 ± 0.7^{a}	-0.7 ± 0.1^{a}	1.2 ± 0.1^{e}	12.4 ± 0.7^{b}
5	98 ± 10^{a}	13.3 ± 0.7^{ab}	1.4 ± 0.2^{abc}	14.5 ± 4.5^{a}	115 ± 13^{a}	97 ± 0.6^{a}	-1.3 ± 0.2^{b}	1.4 ± 0.1^{d}	12.6 ± 0.7^{b}
10	94 ± 11^{a}	14.1 ± 3.8^{ab}	1.5 ± 0.3^{ab}	13.5 ± 2^{a}	113 ± 13^{a}	96.8 ± 0.8^{ab}	-1.8 ± 0.3^{c}	2.4 ± 0.3^{c}	12.9 ± 0.6^{b}
25	91 ± 10^{a}	15.3 ± 1^{a}	1.3 ± 0.1^{bc}	13 ± 3.5^{a}	108 ± 15^{a}	95.7 ± 0.7^{bc}	-2.1 ± 0.2^{c}	3.8 ± 0.3^{b}	13.4 ± 0.4^{b}
50	40 ± 6^{b}	6 ± 1.1^{c}	1.1 ± 0.1^{cd}	12 ± 2^{a}	124 ± 12^{a}	95 ± 0.5^{cd}	-2.6 ± 0.4^{d}	4.3 ± 0.5^{ab}	14.2 ± 0.2^{a}
100	32 ± 3^{b}	5 ± 1.1^{c}	0.9 ± 0.1^{d}	11 ± 2^{a}	121 ± 9^{a}	94.3 ± 0.9^{d}	-3.4 ± 0.4^{e}	5.4 ± 1^{a}	14.7 ± 0.3^{a}

Any two means in the same column followed by the same letter are not significantly ($p > 0.05$) different.

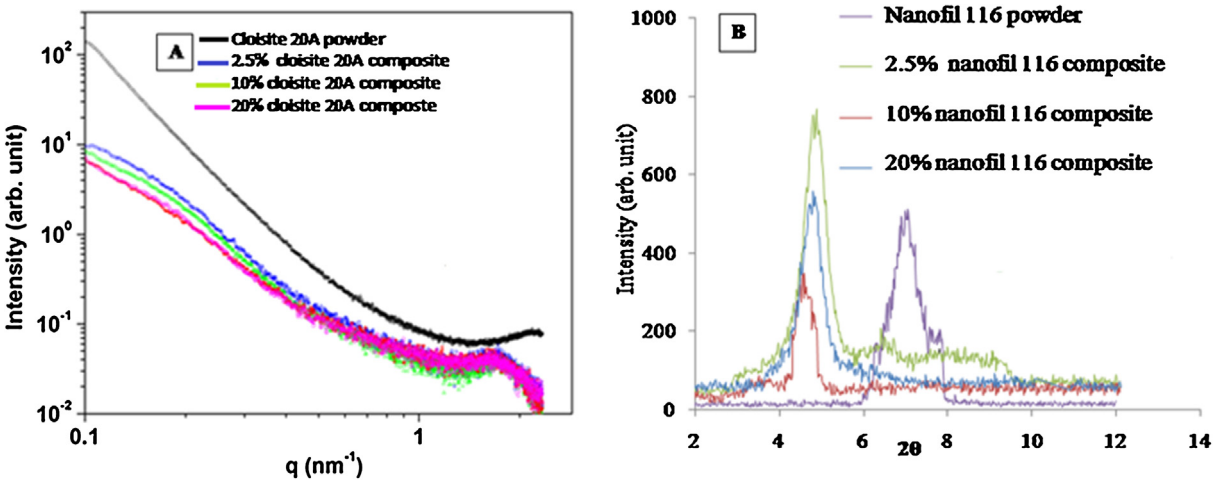

Fig. 1. X-ray scattering profiles: (A) SAXS patterns of cloisite 20A powder and GG-cloisite 20A nano-composites; (B) XRD patterns of nanofil 116 powder and GG-nanofil 116 nano-composites.

might be due to the organophilic modification of closite 20A which renders in incompatible with hydrophilic GG.

3.4. Effect of irradiation on mechanical properties of nano-composite films

In present study, maximum tensile strength and Young's modulus was observed for nano-composites prepared with 2.5% nanofil 116 and 10% cloisite 20A. Thus, further work on radiation processing of nano-composites was performed on these films only. Tensile strength of nanofil 116 composite films showed resistance against radiation up to 25 kGy with a dose dependent significant ($p < 0.05$) decrease thereafter (Table 3). Whereas, films incorporated with cloisite 20A were found to be more radiation sensitive and unstable beyond a dose of 5 kGy (Table 4). We had earlier demonstrated that GG films were stable up to a radiation dose of 25 kGy (Saurabh et al., 2013). Interestingly, an increase in Young's modulus of nanofil 116 composite films was observed due to radiation processing up to a dose of 25 kGy with a dose dependent decrease thereafter (Table 3). Young's modulus increased from 11 ± 0.8 GPa in the control to 15.3 ± 1 GPa at 25 kGy which however reduced to 5 ± 1.1 GPa at 100 kGy. Observed improvement in Young's modulus might be due to the radiation induced improvement in dispersion of nanoclay in polymer matrices as reported earlier for polylactide based nano-composite films by Zaidi et al. (2013). Surprisingly, for cloisite 20A films no significant ($p < 0.05$) change in Young's modulus was observed up to a dose of 100 kGy. In earlier study on radiation processing of GG films no significant effect on Young's modulus was observed (Saurabh et al., 2013). No effect of radiation processing on percent elongation was observed for nanofil 116 containing films. Puncture strength demonstrated stability up to radiation dose of 10 kGy with dose dependent decrease thereafter (Table 3). In case of cloisite 20A containing films a reduction in percent elongation beyond 50 kGy was observed while its puncture strength remained stable only up to 5 kGy (Table 4).

It could be clearly inferred from above results that radiation stability of various mechanical properties of nanofil 116 containing films are better as compared to cloisite 20A films. In previous work on radiation treatment of starch and unmodified MMT it was observed that clay particles stimulated the formation of radicals and also sustained life of radicals longer which favored crosslinking between starch molecules. Radiation processing of starch-unmodified MMT nano-composites led to increased gel formation thus confirming crosslinking. Starch based nano-composites were stable under radiation up to a dose of 30 kGy with degradation observed thereafter (Ibrahim, 2011). Similarly, radiation processing (30 kGy) resulted in increased film strength of polylactic acid and MMT nanocomposites (Dabdin, Naimian, & Akhavan, 2011).

However, in several literatures increased rate of degradation due to radiation processing of nano-composites prepared with organically modified clay (OMMT) are reported as compared to pristine polymer. Touati, Kaci, Ahouari, Bruzaud, and Grohens (2007) reported that polypropylene (PP)/OMMT nano-composites undergo much faster degradation as compared to pristine PP due to radiation processing. These authors suggested that organically modified clay particles acts as an oxidation catalysts leading to degradation of polymer. Similar result was observed by Qin et al. (2005), rate of photo-oxidative degradation of PP/MMT nano-composites was much faster than that of pure PP when exposed to ultraviolet radiation.

This can again be concluded that unmodified clay nano-composites (prepared using nanofil 116) demonstrated significantly better radiation stability as compared to those prepared with organically modified clay (cloisite 20A). Organically modified clay particles (cloisite 20A) might have produced significantly higher number of carbon centered radicals due to radiation processing as compared to unmodified clay (nanofil 116) leading to greater degradation of GG polymer. To best of our knowledge no reports are available on comparing effect of modified and unmodified clays on polymers during radiation processing. Therefore, direct literature comparisons could not be obtained.

3.5. WVTR of nano-composite films

WVTR of nano-composites prepared with either of nanoclays demonstrated a significant ($p < 0.05$) decrease as compared to control up to concentrations of 2.5% (Tables 1 and 2). However, no further reduction in WVTR at higher concentrations (>2.5%) was observed. WVTR demonstrated a reduction from 170 ± 23 g/m^2/day in control films to 128 ± 19 and 132 ± 10 g/m^2/day for 2.5% nanofil 116 and cloisite 20A films, respectively (Tables 1 and 2). Irradiation of nano-composite films had no significant ($p < 0.05$) effect on its WVTR (Tables 3 and 4). It is known that the layered structure of nanoclays obstruct transmission of water vapor through the film matrix and thus delay the diffusion of water vapor due to tortuosity (Bharadwaj, 2001). Thus, an optimum concentration of 2.5% nanofil 116 yielded a nano-composite film that had a lower WVTR besides highest tensile strength and Young's modulus among both

Table 4
Effect of irradiation on physical properties of GG based 10% cloisite 20A composites.

Dose (kGy)	Tensile strength (MPa)	Young's modulus (GPa)	Puncture strength (N)	% elongation	WVTR (g/m^2/d)	L^*	a^*	b^*	Opacity (%)
0	79 ± 8^{a}	1.8 ± 0.2^{a}	1.6 ± 0.2^{a}	32 ± 6^{a}	124 ± 9^{a}	91.8 ± 0.6^{a}	-1.9 ± 0.3^{a}	1.7 ± 0.3^{e}	14.1 ± 0.7^{c}
1	76 ± 11^{a}	1.9 ± 0.2^{a}	1.6 ± 0.3^{a}	29 ± 7^{a}	116 ± 9^{a}	91.6 ± 0.3^{ab}	-2.2 ± 0.7^{a}	2.1 ± 0.5^{e}	14 ± 0.6^{c}
5	64 ± 8^{a}	1.7 ± 0.2^{a}	1.5 ± 0.2^{ab}	33 ± 5^{a}	115 ± 14^{a}	91 ± 0.4^{abc}	-2.8 ± 0.5^{ab}	2.9 ± 0.7^{de}	14.6 ± 0.3^{bc}
10	46 ± 10^{b}	2.4 ± 0.4^{a}	1.2 ± 0.1^{bc}	24 ± 7^{ab}	112 ± 7^{a}	90.6 ± 0.2^{bc}	-3.6 ± 0.4^{bc}	3.9 ± 0.8^{cd}	14.8 ± 0.8^{bc}
25	32 ± 7^{bc}	1.7 ± 0.1^{a}	1 ± 0.2^{c}	34 ± 12^{a}	116 ± 8^{a}	90.1 ± 0.9^{cd}	-4.7 ± 0.6^{c}	5.1 ± 0.6^{c}	15.3 ± 0.9^{abc}
50	23 ± 10^{cd}	2 ± 0.4^{a}	0.5 ± 0.1^{d}	24 ± 7^{ab}	113 ± 13^{a}	89.4 ± 0.7^{d}	-5.9 ± 0.8^{d}	6.8 ± 1^{b}	15.9 ± 1^{ab}
100	15 ± 6^{d}	2.1 ± 0.1^{a}	0.4 ± 0.1^{d}	11 ± 2^{b}	113 ± 7^{a}	$89.2 \pm .6^{d}$	-7.3 ± 1^{e}	8.5 ± 1^{a}	16.3 ± 0.5^{a}

Any two means in the same column followed by the same letter are not significantly ($p > 0.05$) different.

clays studied. Inaptness of cloisite 20A with GG could explain the higher WVTR of films containing cloisite 20A as compared to nanofil 116.

3.6. FEG–SEM

In order to understand microstructure of films FEG–SEM analysis was carried out. Surface morphology of control GG films was observed to be homogeneous and smooth (Fig. 2A). As observed from results obtained in present study best mechanical properties were obtained at a concentration of 2.5% and 10% for nanofil 116 and cloisite 20A, respectively. Furthermore, addition of either of the clays up to 10% resulted in films having better mechanical properties than control films. However, higher concentration of nanoclay (20%) resulted in decreased mechanical properties of nano-composite films (Tables 1 and 2). FEG–SEM analysis showed that at lower concentration of 2.5% nanofil 116 containing films had homogeneous and smooth surface like control film (Fig. 2B). However, surface morphology of cloisite 20A (10%) containing films was not smooth and few nanoclay clumps were clearly observed (Fig. 2C).

At higher concentration of 20% presence of large amount of nanoclay clumps in nanofil 116 and cloisite 20A films can be clearly seen (Fig. 2D and E). This agglomeration of clay particles at higher concentrations resulted in reduced mechanical strength of nanocomposites. It was also observed that at a concentration of 20%, cloisite 20A containing films had large clumps and patches as compared to nanofil 116 incorporated films (Fig. 2D and E). This further proves incompatibility of organomodified clay (closite 20A) with the GG. Better mechanical properties of nanofil 116 composite films as compared to cloisite 20A composite films observed in present study could thus be explained.

3.7. Color and opacity

Values for color coordinates of GG based nano-composite films are shown in Tables 1–4. L^*, a^* and b^* values of control films was 98.7 ± 0.6, 0.6 ± 0.2 and 1.1 ± 0.2, respectively. It was observed that L^* and a^* values reduces significantly ($p < 0.05$) on nanoclay concentration dependent manner. However, a concentration dependent increase in b^* values was observed. Reduction in L^* and a^* values indicates increased darkness and greenness of the films,

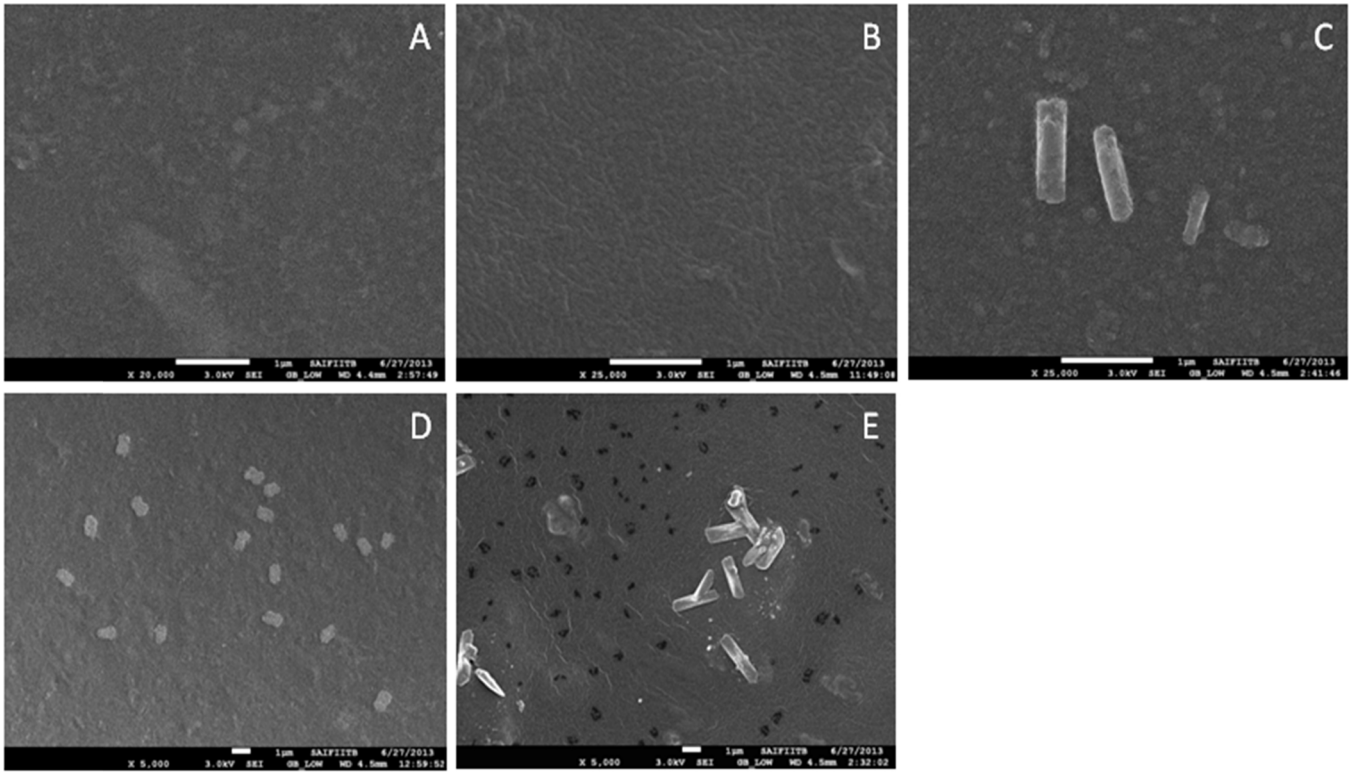

Fig. 2. FEG–SEM images of GG based films: (A) control GG film; (B) 2.5% nanofil 116 composite; (C) 10% cloisite 20A composite; (D) 20% nanofil 116 composite; (E) 20% cloisite 20A composite.

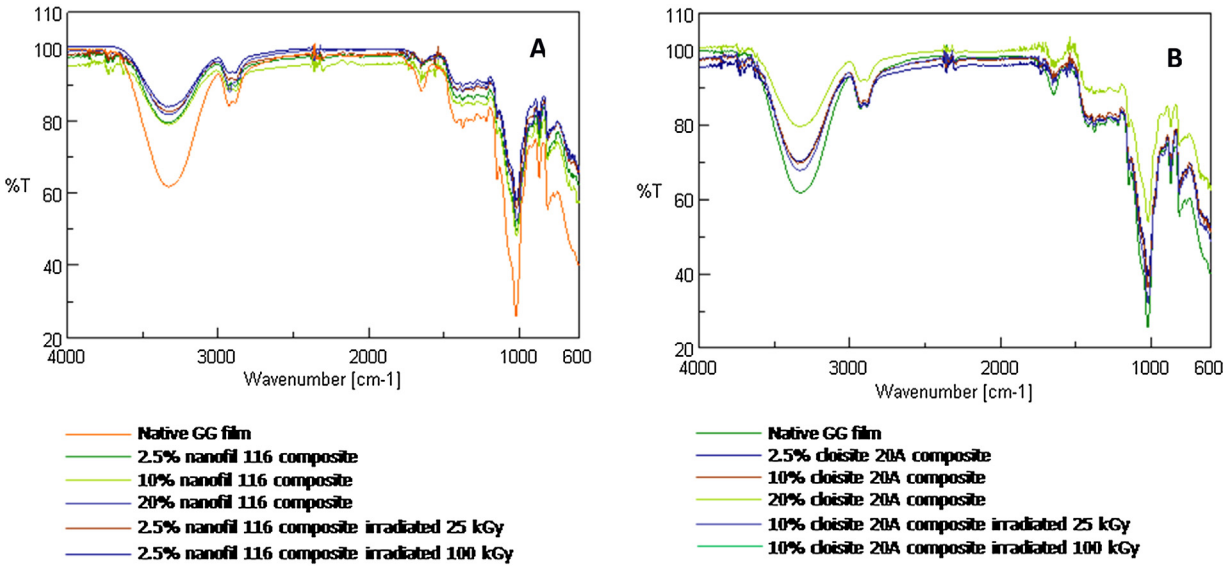

Fig. 3. FTIR spectra: (A) control GG films, and irradiated and non-irradiated GG-nanofil 116 nano-composite films; (B) control GG films, and irradiated and non-irradiated GG-cloisite 20A nano-composite films.

respectively, while increase in b^* values signify increased yellowness of films. Similar results were also observed for chitosan based nano-composite films by Rhim et al. (2006).

Radiation dose dependent decrease in L^* and a^* values with corresponding increase in b^* values was also observed for nano-composite films (Tables 3 and 4). We had earlier demonstrated similar results for films prepared with only GG (Saurabh et al., 2013). Thus, results obtained in present study are in accordance with already published literature data.

Opacity of any substance is a measure of the degree to which light is not allowed to pass through it. Opacity of packaging films is important as it affects the visibility of the packaged product to consumers. Nanoclay concentration or radiation dose dependent increase in opacity was observed in GG based nano-composite films (Tables 1–4). Opacity of control GG film was 12.9 ± 0.2 which increased to 14.8 ± 1 and 14.6 ± 0.9 for 20% nanofil 116 and cloisite 20A containing film, respectively (Tables 1 and 2). Observed increase in opacity might be due to increased darkness or color of the GG based films. Although, significant ($p < 0.05$) variance was observed instrumentally in color and opacity of samples after incorporation of nanoclay visual differences were negligible to be discerned by naked eye.

3.8. FTIR

Change in chemical structure of control (without nanaoclays), irradiated and non-irradiated nano-composite GG films was determined by comparison of FTIR spectra. A superimposable FTIR spectrum of control as well as nano-composite GG films was obtained suggesting that addition of nanoclays or radiation processing had no major functional group transformations but only random free radical chain scission in GG due to irradiation (Fig. 3A and B). Small shifts in peak due to phosphorous stretching (P—O—P) in plane bands between 1025 cm^{-1} to 870 cm^{-1} could be observed in nano-composite films due to presence of nanoclays.

4. Conclusions

In this study nano-composite films were prepared using GG polymer incorporated with organically modified (cloisite 20A) and unmodified (nanofil 116) nanoclays. Incorporation of either of the intercalated nanoclay up to 10% significantly improved the mechanical properties of nano-composite as compared to control films. Higher concentration of nanoclay (20%) resulted in sharp decline in mechanical properties due to formation of nanoclay clumps and cracks in the films. Nanofil 116 demonstrated better compatibility with GG as compared to closite 20A. Organic modification of cloisite 20A rendered it hydrophobic and incompatible with polar GG polymer. Irradiation of 2.5% nanofil 116 films resulted in increased Young's modulus of nano-composite due to radiation induced higher dispersion of clay in films up to 25 kGy. Further irradiation treatment resulted in dose dependent decrease in mechanical properties of films because of radiation induced degradation. WVTR decreases significantly even with incorporation of small amount of nanoclay in GG based films due to increased tortuosity in path of water vapor diffusion through films. However, irradiation had no effect on WVTR of nano-composite films. Color co-ordinates of films significantly changed with incorporation of nanoclay. Nano composite films were darker, greener and yellower as compared to control. X-ray scattering analysis suggested that 0.56 nm and 1.35 nm increase in basal spacing of nanofil 116 and cloisite 20A, respectively, after 7 days of dispersion. This increase in basal spacing is responsible for intercalation of GG in interstitial spaces of nanoclays thus resulting in better mechanical and water vapor barrier properties. FTIR analysis demonstrated no functional group transformation due to nanoclay incorporation or radiation processing. Thus the type and content of nanoclay incorporation during development of films had significant effect on the mechanical and barrier properties of GG based nano-composites.

Acknowledgment

We are thankful to SAIF, IIT Bombay for allowing us to use FEG–SEM facility.

References

Almasi, H., Ghanbarzadeh, B., & Entezami, A. A. (2010). Physicochemical properties of starch–CMC–nanoclay biodegradable films. *International Journal of Biological Macromolecules*, *46*(1), 1–5.

Arora, A., & Padua, G. W. (2010). Review: Nanocomposites in food packaging. *Journal of Food Science*, *75*(1), R43–R49.

Avella, M., De Vlieger, J. J., Errico, M. E., Fischer, S., Vacca, P., & Volpe, M. G. (2005). Biodegradable starch/clay nanocomposite films for food packaging applications. *Food Chemistry*, *93*(3), 467–474.

Bharadwaj, R. K. (2001). Modeling the barrier properties of polymer-layered silicate nanocomposites. *Macromolecules*, *34*(26), 9189–9192.

Bradley, E. L., Castle, L., & Chaudhry, Q. (2011). Applications of nanomaterials in food packaging with a consideration of opportunities for developing countries. *Trends in Food Science & Technology*, *22*(11), 604–610.

Chang, J. H., An, Y. U., & Sur, G. S. (2003). Poly(lactic acid) nanocomposites with various organoclays. I. Thermomechanical properties, morphology, and gas permeability. *Journal of Polymer Science, B: Polymer Physics*, *41*(1), 94–103.

Chrissafis, K., Antoniadis, G., Paraskevopoulos, K. M., Vassiliou, A., & Bikiaris, D. N. (2007). Comparative study of the effect of different nanoparticles on the mechanical properties and thermal degradation mechanism of in situ prepared poly (ε-caprolactone) nanocomposites. *Composites Science and Technology*, *67*(10), 2165–2174.

Cunha, P. L., Castro, R. R., Rocha, F. A., de Paula, R., & Feitosa, J. (2005). Low viscosity hydrogel of guar gum: Preparation and physicochemical characterization. *International Journal of Biological Macromolecules*, *37*(1), 99–104.

Dadbin, S., Naimian, F., & Akhavan, A. (2011). Poly(lactic acid)/layered silicate nanocomposite films: Morphology, mechanical properties, and effects of γ-radiation. *Journal of Applied Polymer Science*, *122*(1), 142–149.

Das, D., Ara, T., Dutta, S., & Mukherjee, A. (2011). New water resistant biomaterial biocide film based on guar gum. *Bioresource Technology*, *102*(10), 5878–5883.

Fernandes, P. B., Goncalves, M. P., & Doublier, J. L. (1993). Influence of locust bean gum on the rheological properties of kappa-carrageenan systems in the vicinity of the gel point. *Carbohydrate Polymers*, *22*(2), 99–106.

Hussain, F., Chen, J., & Hojjati, M. (2007). Epoxy-silicate nanocomposites: Cure monitoring and characterization. *Materials Science and Engineering: A*, *445*, 467–476.

Ibrahim, S. M. (2011). Characterization, mechanical, and thermal properties of gamma irradiated starch films reinforced with mineral clay. *Journal of Applied Polymer Science*, *119*(2), 685–692.

Jumel, K., Harding, S. E., & Mitchell, J. R. (1996). Effect of gamma irradiation on the macromolecular integrity of guar gum. *Carbohydrate Research*, *282*(2), 223–236.

Kampeerapappun, P., Aht-ong, D., Pentrakoon, D., & Srikulkit, K. (2007). Preparation of cassava starch/montmorillonite composite film. *Carbohydrate Polymers*, *67*(2), 155–163.

Kang, H. J., Jo, C., Lee, N. Y., Kwon, J. H., & Byun, M. W. (2005). A combination of gamma irradiation and $CaCl_2$ immersion for a pectin-based biodegradable film. *Carbohydrate Polymers*, *60*(4), 547–551.

Kasai, N., & Kakudo, M. (2005). *X-ray diffraction by macromolecules* (Vol. 80) Amsterdam: Springer.

Khan, R. A., Salmieri, S., Dussault, D., Uribe-Calderon, J., Kamal, M. R., Safrany, A., et al. (2010). Production and properties of nanocellulose-reinforced methylcellulose-based biodegradable films. *Journal of Agricultural and Food Chemistry*, *58*(13), 7878–7885.

Kumar, P., Sandeep, K. P., Alavi, S., Truong, V. D., & Gorga, R. E. (2010). Effect of type and content of modified montmorillonite on the structure and properties of bionanocomposite films based on soy protein isolate and montmorillonite. *Journal of Food Science*, *75*(5), N46–N56.

Kyung Kim, J., Jo, C., Jin Park, H., & Woo Byun, M. (2008). Effect of gamma irradiation on the physicochemical properties of a starch-based film. *Food Hydrocolloids*, *22*(2), 248–254.

Mangiacapra, P., Gorrasi, G., Sorrentino, A., & Vittoria, V. (2006). Biodegradable nanocomposites obtained by ball milling of pectin and montmorillonites. *Carbohydrate Polymers*, *64*(4), 516–523.

Mikkonen, K. S., Rita, H., Helén, H., Talja, R. A., Hyvönen, L., & Tenkanen, M. (2007). Effect of polysaccharide structure on mechanical and thermal properties of galactomannan-based films. *Biomacromolecules*, *8*(10), 3198–3205.

Nascimento, T. A., Calado, V., & Carvalho, C. W. P. (2012). Development and characterization of flexible film based on starch and passion fruit mesocarp flour with nanoparticles. *Food Research International*, *49*(1), 588–595.

Pandey, J. K., Raghunatha Reddy, K., Pratheep Kumar, A., & Singh, R. P. (2005). An overview on the degradability of polymer nanocomposites. *Polymer Degradation and Stability*, *88*(2), 234–250.

Qin, H., Zhang, S., Liu, H., Xie, S., Yang, M., & Shen, D. (2005). Photo-oxidative degradation of polypropylene/montmorillonite nanocomposites. *Polymer*, *46*(9), 3149–3156.

Rhim, J. W. (2011). Effect of clay contents on mechanical and water vapor barrier properties of agar-based nanocomposite films. *Carbohydrate Polymers*, *86*(2), 691–699.

Rhim, J. W., Hong, S. I., & Ha, C. S. (2009). Tensile, water vapor barrier and antimicrobial properties of PLA/nanoclay composite films. *LWT-Food Science and Technology*, *42*(2), 612–617.

Rhim, J. W., Hong, S. I., Park, H. M., & Ng, P. K. (2006). Preparation and characterization of chitosan-based nanocomposite films with antimicrobial activity. *Journal of Agricultural and Food Chemistry*, *54*(16), 5814–5822.

Sanchez-Garcia, M. D., Lopez-Rubio, A., & Lagaron, J. M. (2010). Natural micro and nanobiocomposites with enhanced barrier properties and novel functionalities for food biopackaging applications. *Trends in Food Science & Technology*, *21*(11), 528–536.

Saurabh, C. K., Gupta, S., Bahadur, J., Mazumder, S., Variyar, P. S., & Sharma, A. (2013). Radiation dose dependent change in physiochemical, mechanical and barrier properties of guar gum based films. *Carbohydrate Polymers*, *98*(2), 1610–1617.

Tong, X., Zhao, H., Tang, T., Feng, Z., & Huang, B. (2002). Preparation and characterization of poly(ethyl acrylate)/bentonite nanocomposites by in situ emulsion polymerization. *Journal of Polymer Science, A: Polymer Chemistry*, *40*(11), 1706–1711.

Touati, N., Kaci, M., Ahouari, H., Bruzaud, S., & Grohens, Y. (2007). The effect of γ-irradiation on the structure and properties of poly(propylene)/clay nanocomposites. *Macromolecular Materials and Engineering*, *292*(12), 1271–1279.

Uhl, F. M., Davuluri, S. P., Wong, S. C., & Webster, D. C. (2004). Organically modified montmorillonites in UV curable urethane acrylate films. *Polymer*, *45*(18), 6175–6187.

Walley, P., Zhang, Y., & Evans, J. R. G. (2012). Self-assembly of montmorillonite platelets during drying. *Bioinspiration & Biomimetics*, *7*(4), 046004.

Xu, W., Liu, B., Yang, H., Liu, K., Jia, S., & Chen, F. (2012). Effect of γ-irradiation on the physicochemical properties of mixed soy protein isolate/starch material. *African Journal of Biotechnology*, *11*(28), 7238–7246.

Yasmin, A., Abot, J. L., & Daniel, I. M. (2003). Processing of clay/epoxy nanocomposites by shear mixing. *Scripta Materialia*, *49*(1), 81–86.

Zaidi, L., Bruzaud, S., Kaci, M., Bourmaud, A., Gautier, N., & Grohens, Y. (2013). The effects of gamma-irradiation on the morphology and properties of polylactide/Cloisite 30B nanocomposites. *Polymer Degradation and Stability*, *98*(1), 348–355.

Food Hydrocolloids 48 (2015) 149–154

Contents lists available at ScienceDirect

Food Hydrocolloids

journal homepage: www.elsevier.com/locate/foodhyd

Comparative analysis of dietary fiber activities of enzymatic and gamma depolymerized guar gum

Sumit Gupta [1], Chaturbhuj K. Saurabh [1], Prasad S. Variyar*, Arun Sharma

Food Technology Division, Bhabha Atomic Research Centre, Mumbai, 400085, India

ARTICLE INFO

Article history:
Received 24 June 2014
Received in revised form
29 January 2015
Accepted 9 February 2015
Available online 26 February 2015

Keywords:
Guar gum
Radiation depolymerization
Dietary fiber
Enzyme hydrolyzed

ABSTRACT

Gamma radiation depolymerized guar gum (RDGG) and partially enzymatically hydrolyzed guar gum (PHGG) were compared for their intrinsic viscosity (η), molecular weight distribution, proximate composition, mannose to galactose (M/G) ratio, glucose and bile acid dialysis retardation index (GDRI & BDRI) and production of short chain fatty acids (SCFA) during model intestinal fermentation. RDGG had a higher η value (37.90 ml/g) compared to PHGG (28.58 ml/g). PHGG had one peak with M_w of 12 kDa, while RDGG showed three peaks (M_w 1323.9 kDa, 614.02 kDa and 38.38 kDa) when subjected to gel permeation chromatography. Both RDGG and PHGG had similar proximate composition and M/G ratio. RDGG demonstrated higher GDRI and BDRI of 21.74% and 56.63% while PHGG had values of 12.74% and 0% respectively. Similar contents of SCFA were obtained using either RDGG or PHGG as carbon source. RDGG thus demonstrated improved physiological properties compared to enzyme hydrolyzed counterpart in *in vitro* assays.

1. Introduction

Dietary fibers are considered as an important nutritive component of human health and include wide variety of carbohydrates such as gums, pectin, lignin, cellulose, hemicellulose and resistant starch. Water soluble dietary fibers have received much attention in recent times due to their various physiological functions (Yoon, Chu, & Juneja, 2008).

Guar gum, one of the most promising soluble type of dietary fiber is a polygalactomannan derived from seeds of legume plant, *Cyamopsis tetragonalobus*. It is widely used as thickener in food products such as sauces, syrups, ice cream, instant foods, beverages, confectionaries and baked goods (Dogan, Kayacier, & Ic, 2007; Miyazawa & Funazukuri, 2006). Structurally, it is a galactomannan with a backbone of mannose units linked together by β-D-(1-4)-glycosidic linkage. Galactose units are linked to every alternate mannose units by α-1, 6 linkages on both sides of this backbone thus exhibiting a mannose to galactose ratio of 2:1 (Yoon et al., 2008). Molecular weight of guar gum is in range of 2000–3000 kDa and it provides extremely high viscosities in aqueous solutions even at low concentrations.

A WHO study group has recommended a daily intake of about 37 g total dietary fiber. The FASEB (Federation of American Societies for Experimental Biology) expert panel has recommended a daily intake of 20–35 g/day total dietary fiber from foods for the healthy, adult population of the USA (Burton-Freeman, 2000). Whereas, the American Diabetes Association has recommended a fiber intake of 40–50 g/day (American Diabetes Association, 1998). Guar gum in its native form is not suitable for use as a dietary fiber because it results in the liquid products with high viscosity when added to enteral formulas or liquid supplements at physiologically effective concentrations (Patrick, Gohman, Marx, DeLegge, & Greenberg, 1998). Moreover, high viscosity of guar gum is a limiting factor in its incorporation in foods at levels greater than 1 percent. Foods with physiologically relevant quantities of viscous fibers have very low consumer acceptability and have a slimy mouth feel and also cause tooth packing (Roberts, 2011). In addition, due to its high viscosity guar gum decreases the protein efficacy, lipid utilization and adsorption of nutrients by interfering with the digestion. It also results in slow gastric emptying (Yoon et al., 2008). Therefore, it needs to be depolymerized in order to be used as dietary fiber.

Physiological properties of guar gum can be improved by the controlled partial enzymatic hydrolysis by using β-endo-mannase

* Corresponding author. Food flavor and aroma chemistry section. Food Technology Division, BARC, Mumbai 85, India. Tel.: +91 22 25590560; fax: +91 22 25505151.
E-mail address: pvariyar@barc.gov.in (P.S. Variyar).
[1] These authors contributed equally.

http://dx.doi.org/10.1016/j.foodhyd.2015.02.013
0268-005X/

which is one of the most popular techniques. Endo-β-D-mannase hydrolyzes guar gum by selectively cutting mannose backbone-chain, leaving galactosyl groups intact. Partially hydrolyzed guar gum (PHGG) is one hundredth of original length of polymer and has an average molecular weight of 20 kDa. PHGG is GRAS (Generally recognized as safe) water soluble white powder which is odorless, tasteless, gives transparent solutions and is widely used as soluble type of dietary fiber since 1974 (Yoon et al., 2008). Its intake shows physiological effects such as increasing defecating frequency, reducing serum cholesterol and glucose concentration and production of short chain fatty acids (SCFA) resulting in lowering of pH of feces (Miyazawa & Funazukuri, 2006).

Use of gamma radiation could provide cheap and easy alternative to enzymatic hydrolysis of guar gum. There are numerous reports available in literature on γ-irradiation induced depolymerization of guar gum (Dogan et al., 2007; Gupta, Shah, Sanyal, Variyar, & Sharma, 2009; Jumel, Harding, & Mitchell, 1996). γ-irradiation can degrade guar gum by direct deposition of energy on polymer backbone or by hydroxyl (•OH) radical mediated reaction. Jumel et al. (1996) reported that molecular mass and viscosity of guar gum decreased with no significant changes in gross conformation during irradiation. However, radiation depolymerized guar gum (RDGG) has different molecular weight distribution from that of enzymatic hydrolyzed gum. This might lead to different physiological properties of radiation treated guar gum. To the best of our knowledge there are no reports on inter-comparison of gamma and enzymatic hydrolyzed guar gum for physiological functions. Use of bile acid dialysis retardation index (BDRI) and glucose dialysis retardation index (GDRI) to assess effect of dietary fiber on bile acids uptake in small intestine and jejunal nutrient absorption respectively was previously described by Adiotomre, Eastwood, Edwards, and Brydon (1990). Here, an attempt has been made to compare physiological functions of radiation and enzymatic hydrolyzed guar by different *in vitro* assays such as BDRI, GDRI and model intestinal fermentation.

2. Materials and methods

2.1. Materials

Guar gum sample of unknown molecular weight was obtained from Merck India Ltd. and partially enzymatically hydrolyzed guar gum (PHGG) (Sunfiber®) was provided by Taiyo Lucid Pvt. Ltd., Mumbai, India. H_2SO_4, acetonitrile and phenol were purchased from Merck India Ltd., India. $FeCl_3$, Na_2S, mannose, sodium taurocholate, $MnCl_2$, $CoCl_2$, soya trypticase broth and resazurine dye were procured from Himedia Lab Pvt. Ltd., India. Cysteine hydrochloride, $Ba(OH)_2$ and KH_2PO_4 were purchased from S.D. Fine-Chem Ltd., Mumbai, India. $MgSO_4$ and Na_2HPO_4 were obtained from Thomas Baker Ltd., Mumbai, India. Galactose and sodium azide were procured from BDH chemicals, India. $CaCl_2$ used was obtained from Loba-Chemie, Mumbai, India.

2.2. Preparation of samples for irradiation

Guar gum was irradiated in both powder and solution form. For irradiation in solution form gum solutions were made as 1% (w/v) in distilled water. Guar gum was dispersed in water using high speed mixer (Omni mixer, SORVALL, U.S.A.) for five minutes. The solutions were then kept overnight at 25 °C for complete hydration.

2.3. Gamma irradiation of samples

In powder form guar gum samples were subjected to radiation dose of 10, 15, 20, 25, 50 and 90 kGy while in solution form gum samples were irradiated at 2, 2.5, 3, 3.5, 4, 4.5 and 5 kGy. Irradiation was carried out at ambient temperature using a Co-60 gamma irradiator (GC-5000, BRIT, India). Dose rate as calculated by Fricke's dosimeter was 6.7 kGy/h with dose uniformity ratio of 1.13.

2.4. Purification of guar gum samples

Purification of guar gum was essentially carried out according to the procedure described earlier (Cunha, de Paula, & Feitosa, 2007). In brief, after irradiation in powder form guar gum was made to a 1% (w/v) aqueous solution and hydrated overnight. Samples irradiated in solution form were used as such. Solutions were centrifuged at 12800 g at 25 °C for 25 min. Twice the volume of distilled ethanol was added to the supernatant and the mixture was kept overnight for precipitation of polysaccharide. Solution was again centrifuged at 2050 *g* for 25 min at 25 °C. Purified guar gum was collected as pellet and was then freeze dried. Flakes obtained after drying were ground in pestle mortar and resulting free flowing white powder was stored in air tight bottles till further use.

2.5. Intrinsic viscosity

Intrinsic viscosity (η) of guar gum was calculated as per the procedure described earlier (Wang, Ellis, & Ross-Murphy, 2000). In brief, relative viscosity (η_r) was measured using a capillary viscometer from which specific viscosity (η_{sp}) was calculated:

$$\eta_{sp} = \eta_r - 1 \tag{1}$$

Further, η was determined from η_{sp} using Eq. (2):

$$\eta = \frac{\sqrt{1 + 1.4\eta sp} - 1}{0.7\ C} \tag{2}$$

Where, *C* is concentration of polymer solutions. All measurements were carried out at concentration of 0.1% w/v galactomannan.

2.6. Gel permeation chromatography (GPC)

GPC was carried out to calculate weight average molecular weight (M_w) for guar gum samples. Guar gum samples were analyzed by GPC column (BioBasic Sec-1000 column (300 mm × 7.8 mm 5 μm particle size) Thermo scientific) using HPLC (Ulitmate 3000, Dionex corporation) equipped with autosampler (Ultimate 3000 autosampler, Dionex Corporation, Germany) and refractive index detector (RH01, Shodex). Aqueous solutions of guar gum (0.2%) were injected (20 μl) using the autosampler and the data was acquired from the RI detector. Deionized water (Milli Q system, U.K.) was used as solvent system at a flow rate of 0.6 ml/min. Time vs. detector response data was exported into spreadsheet software (Excel 2007). Pullulan standards (10 kDa–25000 kDa, Fluka, U.S.A.) were also injected in similar conditions. Data of log (M_w, pullulan standards) vs. retention time (Rt) was plotted to obtain a straight line and a linear regression equation was calculated. Molecular weight of guar gum was calculated using linear regression equation obtained for pullulan standards and from the following equation with the Mark-Houwink-Sakurada constants reported for guar gum and pullulan (Miyazawa & Funazukuri, 2006).

$$M_g = 0.67M_p^{0.97} \tag{3}$$

Weight average molecular weight was calculated by following equation:

$$M_w = \sum\left(\frac{Ai \times Mi}{\sum Ai}\right) \quad (4)$$

Where N_i = detector response at a particular time

M_i = Molecular weight at given time

$A_i = N_i \times M_i$

2.7. Glucose dialysis retardation index

GDRI for both commercial PHGG and RDGG sample were estimated according to previously detailed procedure (Adiotomre et al., 1990). 0.2 g of each fiber was dissolved in 6 ml aqueous solution containing 0.1% sodium azide and hydrated overnight. 36 mg of glucose was then dissolved in this solution. Resulting solution was filled in dialysis bag of 10 cm length. Dialysis bags used were previously soaked in 0.1% sodium azide solution. 6 ml sodium azide solution with glucose alone was used for control. Each bag was tied and suspended in 100 ml of 0.1% sodium azide solution and placed in stirred bath at 37 °C for 60 min. At 30 and 60 min, 2 ml of dialysate was analyzed for glucose by phenol-sulphuric acid method (DuBois, Gilles, Hamilton, Rebers, & Smith, 1956). In brief, to 500 μl dialysate equal volume of 5% phenol solution was added followed by 5 ml of H_2SO_4. Samples were allowed to cool for 30 min and O.D. was measured at 490 nm. Similar procedure was followed for standard glucose solutions of known concentrations (0.5%–0.04%). Amount of glucose present in samples were calculated using linear regression equation. All analysis was performed in triplicate. GDRI was then determined using Eq. (5):

$$GDRI = 100 - \left[\frac{\text{Total glucose diffused from sac containing fiber} \times 100}{\text{Total glucose diffused from sac with no fiber present}}\right] \quad (5)$$

2.8. Bile acid dialysis retardation index

The assay was carried out according to procedure already reported (Adiotomre et al., 1990) and was similar to that followed for glucose dialysis retardation index (GDRI). Phosphate buffer (pH 7) containing 0.1% sodium azide and 15 mM taurocholic acid was used alone (control) or with addition of 0.2 g of fibers. Both fibers were hydrated overnight in phosphate buffer. Dialysis bags after filling with 6 ml of buffered taurocholic acid solutions were placed in 100 ml phosphate buffer with 0.1% sodium azide. 2 ml of dialysate were removed at 30 and 60 min and analyzed for taurocholic acid by spectrophotometric assay (Fini & Zuman, 1993). In brief, 1 ml of dialysate was taken in test tubes to which 4 ml of sulphuric acid was added. Test tubes were then incubated in water bath at 70 °C for 30 min. Samples were allowed to cool for 30 min and O.D. was taken at 388 nm. Standard curve was prepared using known amounts of taurocholic acid per assay (20 μg–200 μg). Amount of taurocholic acid present in dialysates was calculated using a linear regression equation. Each analysis was performed in triplicates. BDRI was calculated using Eq. (6)

$$BDRI = 100 - \left[\frac{\text{Total taurocholic acid diffused from sac containing fiber} \times 100}{\text{Total taurocholic acid diffuced from sac with no fiber present}}\right] \quad (6)$$

2.9. Fermentation studies

Effect of depolymerization method on production of short chain fatty acids (SCFA) was evaluated. Hydrolyzed guar gum samples were fermented *in vitro* in a batch system under strict anaerobic conditions using rat feces as inoculums. Procedure followed was as described earlier by Goni & Martin-Carron (1998). Media used for fermentation contained: 2.5 g peptone water, 125 μl micromineral solution, 250 ml buffer solution, 250 ml macromineral solution, 1.25 ml resazurine solution (0.1% w/v), 33.5 ml reducing solution and 40 ml NaOH solution (1 M) per liter of distilled water. Finally, CO_2 gas was passed through media to make it reducing which was confirmed by change of color from light pink to blue due to presence of resazurine dye. Media prepared was sterilized by autoclaving.

Micromineral solution was prepared by dissolving 132 g $CaCl_2.2H_2O$, 100 g $MnCl_2.4H_2O$, 10 g $CoCl_2.6H_2O$ and 80 g $FeCl_3.6H_2O$ per liter of distilled water. Macromineral solution had 5.7 g Na_2HPO_4, 6.2 g KH_2PO_4 and 0.6 g $MgSO_4.7H_2O$ per liter of distilled water. Reducing solution was made by adding 6.25 g cysteine hydrochloride and 6.25 g $Na_2S.9H_2O$ in 33.5 ml distilled water. Inoculum was prepared by using fecal contents of male wistar rats with an average body weight of 170 g. Rat feces were weighed and added to a sterile flask containing sterilized media to give a 10% w/v inoculum. The inoculum was mixed for ten minutes and filtered (0.5 mm mesh) before use.

Fermentation was carried out in 40 ml serum bottles (Supelco, U.S.A.). In each bottle 16 ml of media was added along with 200 mg carbon source (RDGG and PHGG). 4 ml of inoculum was then added and bottles were closed. Air was then sucked from headspace using an air tight syringe with hypodermic needle. Six control bottles were also kept. Three contained no carbon source (-ve control) while, three had glucose (+ve control) as easily fermentable carbon source. Tubes were incubated at 37 °C for 72 h. Fermentation was stopped by adding 1 ml of concentrated HCl and fermentation media was centrifuged at 18500 g for 20 min to remove cells. Supernatant was extracted thrice with 10 ml double distilled diethyl ether. 45 μg of 2-octanol was used as an internal standard. Ether extract was then dried over anhydrous sodium sulfate and concentrated with gentle stream of nitrogen to less than 100 μl volume and analyzed with GC/MS.

GC/MS analysis was carried out on a GC/MS equipment (Shimadzu Corporation, Kyoto, Japan) equipped with a GC-17A gas chromatograph having capillary column (DB-5, JSW scientific, 0.33 μm I.D. and 30 m length). All injections were done in split mode (split ratio 1) with injection volume of 1.5 μl and carrier gas flow rate of 1.2 ml/min. Column was programmed as 35 °C initial temperature with a hold time of 10 min. Temperature was then raised at rate of 4 °C/min to 150 °C. It was then increased at a rate of

5 °C/min to 200 °C with a hold time of 1 min. Finally it was increased to 280 °C at the rate of 15 °C/min. GC was held at final temperature for 15 min. The operating conditions for MS were: ionization voltage, 70 ev; electron multiplier voltage, 1 kV. Samples were analyzed in scan mode in the mass range of m z^{-1} 50–600. All compounds were identified by comparing their retention indices and mass spectra to that of standard compounds in WILEY/NIST libraries of the instrument as well as from literature data. Quantification was done by internal standard method and results are expressed in μg (fatty acids produced) g^{-1} of carbon source used.

3. Results and discussion

3.1. Radiation processing of guar gum

3.1.1. Intrinsic viscosity (η)

Intrinsic viscosity is a measure of hydrodynamic volume occupied by isolated polymer molecule in solution (Khouryieh, Herald, Aramouni, & Alavi, 2007). The value of η depends on the shape of the molecule and is related to its molar mass (Jumel et al., 1996). The η of control guar gum sample was estimated to be 1250 ml/g while commercial PHGG had η of 28.58 ml/g. Effect of radiation processing carried out in powder and solution form on η of guar gum is shown in Fig. 1A and B, respectively. During irradiation in powder form rapid decrease up to a dose of 25 kGy was observed beyond which a moderate but significant ($p < 0.05$) decrease was noted (Fig. 1A). The η of guar gum reduced to 156.85 ml/g at radiation dose of 50 kGy. In the solution form a rapid decrease in η up to dose of 2.5 kGy and a slow decrease thereafter was observed (Fig. 1B). Radiation dose of 5 kGy to guar gum in solution form resulted in η of 37.9 ml/g. Radiation dose dependent breakdown of guar gum has been previously reported (Dogan et al., 2007; Gupta et al., 2009; Jumel et al., 1996). Guar gum irradiated in solution form demonstrated greater degradation of η as compared to gum irradiated in powder form. Rapid degradation of polymer when irradiated in solution form could be attributed to the formation of highly reactive •OH radical from water radiolysis that can abstract hydrogen from polymer chain. This gives rise to polymer free radical which is unstable and has little probability of encountering another radical in dilute solution and thus undergoes degradation into smaller molecular weight fractions (Gupta et al., 2009). Intrinsic viscosity (η) of guar gum irradiated (5 kGy) in solution form was comparable with η of PHGG. Guar gum irradiated (5 kGy) in solution form demonstrated η of 37.9 ml/g while PHGG had η of 28.58 ml/g. Thus for inter comparison with commercial PHGG, guar gum subjected to radiation dose of 5 kGy in solution form (RDGG) was used.

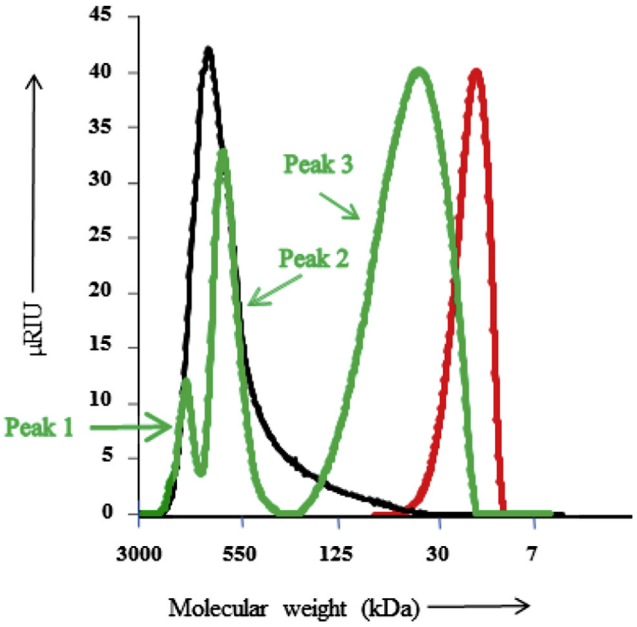

Fig. 2. Gel permeation chromatography (GPC) profiles of guar gum samples. GPC profile of unirradiated (control) guar gum (▬); GPC profile of commercial enzyme hydrolyzed guar gum (PHGG) (▬); Guar gum sample irradiated in aqueous solution (1% w/v) at dose of 5 kGy (▬).

3.2. Intercomparison of radiation depolymerized guar gum (RDGG) and PHGG

3.2.1. Gel permeation chromatography (GPC)

Gel permeation chromatography (GPC) was carried out to study the effect of radiation processing on weight average molecular weight (M_w) and molecular weight distribution (MWD) of gum samples. Control guar gum had M_w of 1187.69 kDa while PHGG demonstrated M_w value of 12 kDa. Only one peak was observed in GPC profile of control and PHGG samples, whereas, interestingly, in the samples subjected to radiation processing (5 kGy, solution form, RDGG) three different peaks were observed (Fig. 2). We had earlier demonstrated that peak 1 and 2 corresponds to native polymer while peak 3 is depolymerized fraction (Saurabh et al., 2013).

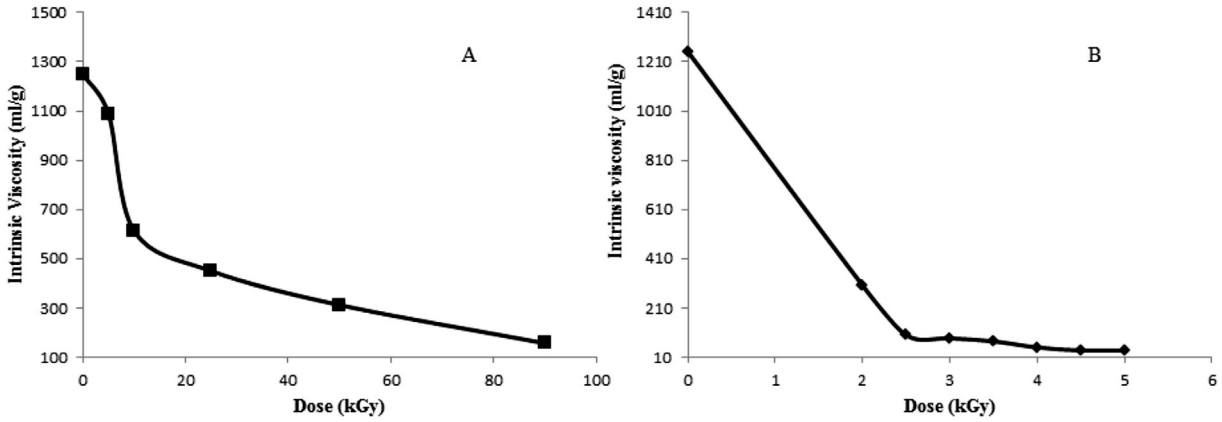

Fig. 1. Variation of intrinsic viscosity (η) of guar gum samples with irradiation dose. (A) Guar gum samples irradiated in dried powder form and (B) Guar gum samples irradiated in aqueous solution (1% w/v).

Radiation induced disruption of supramolecular structures of GG polymer as reported by Jumel et al. (1996) could possibly explain the two high Mw peaks (peak 1 and 2) observed in GPC chromatograms of RDGG. Observance of low Mw peak (peak 3) in the chromatogram of RDGG could be attributed to the formation of depolymerized polymer as a result of gamma radiation.

Variation of M_w of all three peaks and their percent area with dose is shown in Fig. 3A and B, respectively. M_w of all three peaks demonstrated a dose dependent decrease. M_w of peak 1 reduced from 1778.36 kDa to 1323.9 kDa, peak 2 decreased from 1187.69 kDa to 614.027 kDa while peak 3 decreased from 127.92 kDa to 38.38 kDa upon radiation dose of 5 kGy. Decrease in amount of peak 1 and 2 with corresponding increase in peak 3 in dose dependent manner was observed. At a dose of 5 kGy amount of peak 1 was only 4.08% while content of peak 2 and 3 was 18.07% and 77.59% respectively. The decrease in content of higher molecular weight fractions with corresponding increase in low molecular weight fraction was observed in radiation dose dependent manner. However, these results suggest that radiation depolymerized guar gum had higher M_w fractions (peak 1: 1323.9 kDa, peak 2: 614 kDa) along with depolymerized low M_w (peak 3: 38.38 kDa) fraction, while PHGG demonstrated only one peak in GPC profile.

3.2.2. Glucose dialysis retardation index (GDRI) and bile acid dialysis retardation index (BDRI)

GDRI of both PHGG and RDGG product was compared to judge efficacy of radiation depolymerization as a possible replacement of enzyme hydrolysis. GDRI was determined for both the samples at 30 min and 60 min. Results are shown in Table 1. RDGG demonstrated significantly higher ($p < 0.05$) GDRI than that of PHGG. PHGG had a GDRI of 12.74% at 60 min while the corresponding value for RDGG was 21.74%. Adiotomre et al. (1990) have earlier reported GDRI of guar gum to be 43%. They had evaluated guar gum sample having molecular weight of 250 kDa. Lower values obtained in present study might be due to lesser molecular weight of guar gum samples used. BDRI was estimated to evaluate the effects of depolymerized samples on bile acid metabolism in small intestine. BDRI was determined for both the products at 60 min. RDGG demonstrated a BDRI of 56.63% at 60 min while PHGG had a BDRI of 0%. Surprisingly, PHGG did not demonstrated bile acid uptake retardation. In previous reports, BDRI of native guar gum was demonstrated to have a value of 41% (Adiotomre et al., 1990).

RDGG demonstrated significantly ($p < 0.05$) higher values for both GDRI and BDRI as compared to PHGG. This phenomenon can be explained on the fact that in RDGG higher molecular weight fractions are also present apart from low M_w fraction (Fig. 2) while no high molecular weight fractions were present in PHGG (Fig. 2). It was previously demonstrated by Mikkonnen et al., 2009 that reduced degree of polymerization of guar gum resulted in decreased emulsion stability. High M_w fractions might provide better emulsification ability to RDGG resulting in better BDRI and GDRI. These results suggest that RDGG due to presence of higher molecular weight fractions could provide better prevention of glucose and bile acid uptake in intestine as compared to PHGG. However, results obtained must be corroborated with *in vivo* experiments.

Table 1
Glucose dialysis retardation index (GDRI) and Bile acid dialysis retardation index (BDRI) of radiation depolymerized guar gum (RDGG) and commercial enzyme partially hydrolyzed guar gum (PHGG) after 30 and 60 min of dialysis.

Sample	GDRI (%)		BDRI (%)	
	30 min	60 min	30 min	60 min
RDGG	21.9 ± 2.1	21.7 ± 2.2	Nil	56.6 ± 3.9
PHGG	13.5 ± 1.8	12.7 ± 1.9	Nil	Nil

3.2.3. Production of short chain fatty acids (SCFA)

Physico-chemical properties of fiber may have an effect on amount and ratio of SCFA produced. Table 2 shows amount of total and individual SCFA produced when RDGG and PHGG was used as carbon source during *in vitro* fermentation experiment. Highest amount of total SCFA were produced when glucose was used as a carbon source. No statistically significant difference ($p < 0.05$) was observed in total SCFA content between RDGG and PHGG as carbon source (Table 2). However, significant differences were observed in content of individual fatty acids.

Significantly ($p < 0.05$) higher contents of acetic, propionic and heptanoic acid were observed when RDGG was used as carbon source. However, higher production of butanoic, 2-methylbutanoic and pentanoic acid were obtained in samples having PHGG as carbon source. Content of isobutyric, isovaleric and hexanoic acid was found to be similar for both fibers. Acetic, butyric and propionic acids are major SCFA produced on fermentation of dietary fibers. It was observed that when RDGG was used as carbon source acetic and propionic acid formed were 132.4 ± 18.2 μg/g and 27 ± 5 μg/g of carbon source while use of PHGG produced only 87.2 ± 1 5.8 μg/g and 14.2 ± 6 μg/g, respectively. Stewart and Slavin (2006) analyzed

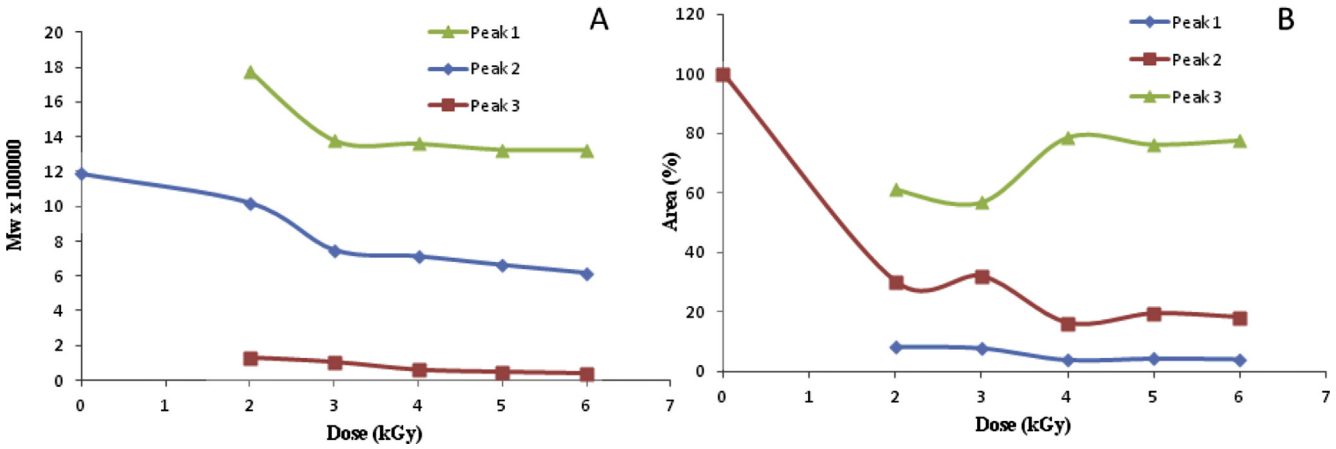

Fig. 3. Variation of weight average molecular weight (Mw) and relative area of three peaks obtained in Gel permeation chromatography profile of control and irradiated guar gum samples. (A) Variation of Mw of guar gum samples irradiated in aqueous solution form (1% w/v); (B) Relative area of all peaks obtained for guar gum irradiated in aqueous solution form (1% w/v).

Table 2
Amount of various short chain fatty acids produced during fermentation using different carbon sources. Values of fatty acids represented as μg $g^{-1}$of carbon source used.

Fatty acid	Glucose	Negative control	RDGG	PHGG
Total SCFA[a]	589.6 ± 116.2a	52.8 ± 15.4c	288 ± 60b	335 ± 78b
Acetic acid	173.4 ± 24a	16.6 ± 0.8c	132.4 ± 18.2a	87.2 ± 15.8b
Propanoic acid	69.2 ± 12a	7 ± 3c	27 ± 5b	14.2 ± 6c
Isobutyric acid	22.4 ± 7a	6 ± 2c	18 ± 6ab	11.2 ± 5bc
Butyric acid	182.6 ± 42a	12.6 ± 5c	55.2 ± 15b	132.8 ± 30.4a
Isovaleric acid	56.4 ± 14a	4.4 ± 2c	19.4 ± 6b	31 ± 9b
2-methyl butanoic acid	27.2 ± 6.2a	0.6 ± 0.4d	4.2 ± 2c	16 ± 4b
Pentanoic acid	31.8 ± 6a	3 ± 1.2c	8.8 ± 3b	27.2 ± 5a
Hexanoic acid	23.2 ± 4.2a	2.6 ± 1c	19.6 ± 3ab	13.8 ± 4b
Heptanoc acid	3.8 ± 0.8a	0 ± 0c	3.4 ± 1a	1.6 ± 0.4b

Values with different online letters in a same row are statistically significantly different ($p < 0.05$).
[a] Short chain fatty acid.

effect of different Mw of guar gum on SCFA production during *in vitro* fermentation. These researchers reported significantly higher production of acetic and propionic acid when higher Mw (400 kDa) guar gum was used as carbon source as compared to lower Mw (15 kDa) guar gum. In the RDGG higher Mw fractions apart from lower Mw fractions are also present whereas PHGG has only low Mw fractions. This might be the reason for observed higher production of acetic and propionic acid when RDGG was used as carbon source. Thus, our results are in accordance with already published literature data.

Surprisingly, a higher content of butyric acid (132.8 ± 30.4 μg/g) using PHGG was observed as compared to 55.2 ± 15 μg/g obtained using RDGG. Stewart and Slavin (2006) reported higher butyrate production when 400 kDa guar gum was used but lower butyrate production when 1100 kDa GG was used as compared to depolymerized product of 15 kDa. Thus they reported that butyrate production is not entirely positively correlated with Mw of guar gum. Since, RDGG had higher Mw fractions of 1323.9 and 614 kDa which might have resulted in lower butyrate production as compared to PHGG.

Acetic acid reduces serum fatty acid levels while propionate had previously been reported to control glycemia resulting in lower blood glucose levels. Butyric acid is major source of energy for colonic mucosa, prevents colonic mucosal atrophy and plays a role in preventing colon cancer by inducing apoptosis in cancerous cells (Tungland & Meyer, 2002). Stewart and Slavin (2006) had earlier reported M_w of guar gum can influence fatty acid profile during fermentation. RDGG had different M_w distribution as compared to PHGG which could possibly have led to different fatty acid profile. However, there are no previous studies on fermentation of RDGG and therefore no literature comparisons could be made.

4. Conclusions

In conclusion, irradiation of guar gum in solution form resulted in greater reduction of its intrinsic viscosity as compared to guar gum irradiated in powder form. Further, guar gum irradiated in solution form demonstrated lower M_w and higher content of depolymerized fractions in GPC studies. Both, RDGG and PHGG had similar proximate composition and mannose to galactose ratio. When compared for biological activities RDGG demonstrated higher values of GDRI and BDRI as compared to PHGG. Further, RDGG had similar production of total SCFA during *in vitro* fermentation. In present study, RDGG has demonstrated better activities in i*n vitro* assays. These results suggest feasibility of using gamma radiation for preparing depolymerized guar gum for dietary fiber applications. Further work in this direction would be to identify if these differences in activities can possibly result better physiological effects in humans.

References

Adiotomre, J., Eastwood, M. A., Edwards, C. A., & Brydon, W. G. (1990). Dietary fiber: in vitro methods that anticipate nutrition and metabolic activity in humans. *The American Journal of Clinical Nutrition, 52*(1), 128–134.

American Diabetes Association. (1998). Nutrition recommendations and principles for people with diabetes mellitus. *Diabetes Care, 21*(Suppl. 1), S32–S35.

Burton-Freeman, B. (2000). Dietary fiber and energy regulation. *The Journal of Nutrition, 130*(2), 272S–275S.

Cunha, P. L. R., de Paula, R. C. M., & Feitosa, J. P. A. (2007). Purification of guar gum for biological applications. *International Journal of Biological Macromolecules, 41*(3), 324–331.

Dogan, M., Kayacier, A., & Ic, E. (2007). Rheological characteristics of some food hydrocolloids processed with gamma irradiation. *Food Hydrocolloids, 21*(3), 392–396.

DuBois, M., Gilles, K. A., Hamilton, J. K., Rebers, P. A., & Smith, F. (1956). Colorimetric method for determination of sugars and related substances. *Analytical Chemistry, 28*(3), 350–356.

Fini, A., & Zuman, P. (1993). Spectrophotometric determination of bile acids; an evaluation. *Collection of Czechoslovak Chemical Communications, 58*(1), 53–61.

Goni, I., & Martin-Carron, N. (1998). In vitro fermentation and hydration properties of commercial dietary fiber-rich supplements. *Nutrition Research, 18*(6), 1077–1089.

Gupta, S., Shah, B., Sanyal, B., Variyar, P. S., & Sharma, A. (2009). Role of initial apparent viscosity and moisture content on post irradiation rheological properties of guar gum. *Food Hydrocolloids, 23*(7), 1785–1791.

Jumel, K., Harding, S. E., & Mitchell, J. R. (1996). Effect of gamma radiation on macromolecular integrity of guar gum. *Carbohydrate Research, 282*(2), 223–236.

Khouryieh, H. A., Herald, T. J., Aramouni, F., & Alavi, S. (2007). Intrinsic viscosity and viscoelastic properties of xanthan/guar mixtures in dilute solutions: effect of salt concentration on the polymer interactions. *Food Research International, 40*(7), 883–893.

Mikkonen, K. S., Tenkanen, M., Cooke, P., Xu, C., Rita, H., Willfor, S., et al. (2009). .Mannans as stabilizers of oil-in-water beverage emulsions. *LWT-Food Science and Technology, 42*(4), 849–855.

Miyazawa, T., & Funazukuri, T. (2006). Noncatalytic hydrolysis of guar gum under hydrothermal conditions. *Carbohydrate Research, 341*(7), 870–877.

Patrick, P. G., Gohman, S. M., Marx, S. C., DeLegge, M. H., & Greenberg, N. A. (1998). Effect of supplements of partially hydrolyzed guar gum on the occurrence of constipation and use of laxative agents. *Journal of the American Dietetic Association, 98*(8), 912–914.

Roberts, K. T. (2011). The physiological and rheological effects of foods supplemented with guar gum. *Food Research International, 44*(5), 1109–1114.

Saurabh, C. K., Gupta, S., Bahadur, J., Mazumder, S., Variyar, P. S., & Sharma, A. (2013). Radiation dose dependent change in physiochemical, mechanical and barrier properties of guar gum based films. *Carbohydrate Polymers, 98*(2), 1610–1617.

Stewart, M. L., & Slavin, J. L. (2006). Molecular weight of guar gum affects short-chain fatty acid profile in model intestinal fermentation. *Molecular Nutrition and Food Research, 50*(10), 971–976.

Tungland, B. C., & Meyer, D. (2002). Nondigestible Oligo- and polysaccharides (Dietary fiber): their physiology and role in human health and food. *Comprehensive Reviews in Food Science and Food Safety, 1*(3), 90–109.

Wang, Q., Ellis, P. R., & Ross-Murphy, S. B. (2000). The stability of guar gum in an aqueous system under acidic conditions. *Food Hydrocolloids, 14*(2), 129–134.

Yoon, S.-J., Chu, D.-C., & Juneja, L. R. (2008). Chemical and physical properties, safety and application of partially hydrolyzed guar gum as dietary fiber. *Journal of Clinical Biochemistry and Nutrition, 42*(1), 1–7.